Trophic role of Protozooplankton in northern marine ecosystems

Riisgaard, Karen

Publication date:
2014

Document Version
Publisher's PDF, also known as Version of record

Trophic Role of Protozooplankton in Northern Marine Ecosystems

PhD Thesis

Karen Riisgaard

EURO-BASIN
BASIN SCALE ANALYSIS, SYNTHESIS AND INTEGRATION

DTU Aqua
National Institute of Aquatic Resources

Trophic Role of Protozooplankton in Northern Marine Ecosystems

Ph.D. Thesis

By

Karen Riisgaard

Supervisor: Prof. Torkel Gissel Nielsen
Co-supervisor: Prof. Michael St. John

National Institute of Aquatic Resources
Technical University of Denmark (DTU-Aqua)

CONTENT

1. ABSTRACT

Protozooplankton are the major grazers on phytoplankton in the global ocean, but many questions related to their trophic role remain unanswered in particular for northern marine ecosystems. In the present thesis, protozooplankton communities were evaluated with special emphasis on factors, such as elevated temperature, water column stratification, pH and copepod predation, regulating their biomass, growth- and grazing rates. In addition, it was investigated what role protozooplankton have for the phytoplankton bloom dynamics at present and in a predicted warmer future. The studies were done through a combination of field observations and experiments conducted at four localities within the sub-Arctic and Arctic waters. The Ph.D. thesis is based on 6 scientific papers (Paper I-VI) dispersed on these four localities:

1) In the high Arctic North East Water Polynya, heterotrophic dinoflagellates and ciliates doubled their growth rates when the temperature was increased from -1.7 to 5 ^{o}C. Despite this, most protozooplankton were found in association with the highest phytoplankton concentration: i.e. in the marginal ice zones where the temperature was below the freezing point (Paper I).
2) In waters between Iceland and Norway, succession and population dynamics of autotrophic and heterotrophic microbes including protozooplankton were followed prior to the spring bloom in relation to deep ocean convection. A decrease in abundance of small sized phytoplankton relative to larger diatoms was explained by a strong top-down control by protozooplankton. The data further suggests that deep ocean convection control the protozooplankton community prior to the bloom, which may induce or accelerate the onset of the phytoplankton spring bloom (Paper II & III).
3) In the Arctic Disko Bay, pH was documented to increase from 7.5 to 8.5 due to CO_2 uptake from phytoplankton as the bloom developed. Microcosm experiments demonstrated that most protists were unaffected by the seasonal changes in pH, even during the massive phytoplankton spring bloom (Paper IV).
4) In a sub-Arctic fjord, field data indicated that the protozooplankton succession was regulated by copepod grazing during most of the productive season and that the protozooplankton provide an essential food source for the copepod populations. In addition the protozooplankton >20 µm were significantly herbivores on the small sized phytoplankton grazing. The importance of protozooplankton as grazers increased over a transect going from open-ocean to the inner part of the fjord (Paper V & VI).

In conclusion, protozooplankton contributed significantly to the area-specific biomass at all investigated sub-Arctic and Arctic localities with a tendency towards high protozooplankton concentrations in the upper water column of stratified waters. Future climate changes are expected to increase water column stratification which will lead to reduced phytoplankton size and increase the importance of protozooplankton as grazers that are especially suited for consuming small cells. This will shift the relative importance of larger metazoan grazers (e.g. copepods) towards protozooplankton.

2. DANSK RESUMÉ

Dyreplankton bestående af éncellede organismer (protozooplankton, Figur 1) er nogle af de vigtigste græssere af havets mikroskopiske planktonalger (fytoplanktonet), men mange spørgsmål vedrørende deres betydning i havets fødekæder er ubesvarede. Dette gælder især protozooplanktonet i de nordligste farvande. I denne phd-afhandling er den økologiske betydning af protozooplankton blevet vurderet med særlig vægt på betydende faktorer for protozooplanktonets vækst, fødeindtag og samlede biomasse, herunder især temperatur, lagdeling af vandsøjlen, pH og prædation fra vandlopper. Ydermere er protozooplanktonets betydning for forårsopblomstringen i dag og i en forventet varmere fremtid blevet vurderet. De samlede studier er baseret på feltobservationer i kombination med eksperimenter foretaget i subarktiske og arktiske farvande (Figur 2). Nærværende phd-afhandling er baseret på 6 videnskabelige tidsskriftartikler (Paper I-VI) fordelt på disse 4 områder:

1) I et arktisk område med åbent vand omgivet af is (North East Water Polynya) fordoblede heterotrofe dinoflagellater og ciliater deres vækstrater, når temperaturen blev øget fra -1.7 ^{o}C til 5 ^{o}C. Trods denne temperaturafhængighed blev de højeste biomasser af protozooplankton fundet i forbindelse med den højeste fødekoncentration: dvs. i israndszonerne, hvor temperaturen var under frysepunktet (Paper I).

2) Farvandene mellem Island og Norge (subarctic-Atlantic) er karakteriseret ved at være stærkt opblandede i vintermånederne. I disse vande blev successionen og populations-dynamikkerne af autotrofe og heterotrofe mikrober undersøgt frem mod forårsopblomstringen. En nedgang i antallet af små fytoplanktonceller i forhold til de større kiselalger blev forklaret af et højt græsningstryk udøvet af protozooplanktonet. Microcosm-forsøg med fraktioneret vand understøttede denne hypotese, og peger herudover på at en stærkt opblandet vandsøjle kontrollerer protozooplanktonsamfundet inden forårsopblomstringen, hvilket kan være med til at inducere eller accelerere forårsopblomstringen (Paper II & III).

3) I den arktiske Diskobugt blev det dokumenteret, at pH steg fra 7.5 til 8.5 pga. CO_2-optagelse i fytoplanktonet under forårsopblomstringen. Microcosm-forsøg demonstrerede, at de fleste protister var upåvirkede af de sæsonmæssige udsving i pH, selv under den massive forårsopblomstring. Teoretisk kan pH dog spille en rolle for protozooplanktonet, hvis pH stiger til mere end 8.5, som f.eks. kan være tilfældet i havis eller i israndszoner (Paper IV).

4) I en subarktisk fjord (Godthåbsfjord) indikerede feltobservationer at successionen af protozooplankton blev reguleret at græsning fra vandlopper gennem det meste af den produktive sæson, og at protozooplanktonet udgør en vigtig fødekilde for vandlopperne. Herudover blev det påvist, at protozooplankton > 20 µm er vigtige græssere på fytoplankton og græsser >100 % af den daglige primærproduktion og at protozooplanktont betydning som græssere steg over en gradient fra åbent hav til de inderste dele af fjorden (Paper V & VI).

Overordnet kan konkluderes, at protozooplanktonet bidrager væsentligt til planktonbiomassen på de fire undersøgte arktiske- og sub-arktiske lokaliteter. Desuden er der tendens til øgede koncentrationer af protozoolankton i de øverste vandlag i områder med temperatur- og saltholdigheds-springlag. Resultaterne antyder, at forventede fremtidige højere havtemperaturer vil øge den økologiske betydning af protozooplanktonet. En øget springlagsdannelse vil føre til en reduktion i størrelsen af planktonalgerne og dermed en øgning i koncentrationen af protozooplanktonet, som er specialiseret i at græsse netop små algeceller. Det vil medføre en forskydning i den relative økologiske betydning af det større meso-zooplankton (eksempelvis vandlopper), som ikke kan frafiltrere og æde de helt små planktonalger.

3. PREPHASE AND LIST OF PAPERS

This thesis was submitted as part of the requirements to fulfill the Doctor of Philosophy Degree (PhD) at the Technical University of Denmark (DTU). The presented research was conducted between May 2011 and October 2014, primarily at the National Institute of Aquatic Resources (DTU Aqua) in Charlottenlund, Denmark. The thesis was supervised by Profs.Torkel Gissel Nielsen and Michael St. John. Data were collected during field campaigns in coastal waters of Greenland and the North Atlantic. Data from the North East Water were collected during a cruise in 1993 and was provided for the thesis by Torkel Gissel Nielsen. The research was funded by the European Union Seventh Framework Programme project EURO-BASIN (ENV.2010.2.2.1-1) under grant agreement n° 264933, ERC grant Microbial Network Organisation **(**MINOS 250254).

The thesis is based on following list of papers:

I. Riisgaard K, Bjørnsen PK, Nielsen TG. Trophic role of high Arctic heterotrophic dinoflagellates and ciliates in the North East Water (NEW) Polynya. *To be submitted to Climate Change Biol*

II. Paulsen ML, Riisgaard K, Thingstad FT, St. John M, Nielsen TG. Pico- and nanophytoplankton support an active microbial food web prior to the North Atlantic spring bloom. *Submitted Aquat Microb Ecol*

III. Riisgaard K, Paulsen ML, St. John M, Nielsen TG. The North Atlantic heterotrophic protist community: Trophic links and their role in the food web. *Submitted Aquat Microb Ecol*

IV. Riisgaard K, Hansen PJ, Nielsen TG. Effect of increased pH on Arctic spring bloom dynamics *Submitted Mar Ecol Prog Ser*

V. Riisgaard K, Kjellerup S, Swalethorp R, Juul-Pedersen T, Nielsen TG (2014) Trophic role and top down control of a subarctic protozooplankton community. Mar Ecol Prog Ser. 500:67-82

VI. Calbet A, Riisgaard K, Saiz E, Zamora S, Stedmon C, Nielsen TG (2011) Phytoplankton growth and microzooplankton grazing along a sub-Arctic fjord (Godthåbsfjord, West Greenland). Mar Eco Prog. Ser. 442: 11-22

4. INTRODUCTION

4.1. Protozooplankton – definition and ecological role

We tend to overlook little things and especially little things that live where the weather is cold and harsh. The sub-Arctic Atlantic and adjacent Arctic waters have been exploited for centuries and are today recognised as some of the most productive waters in the global ocean (Field et al. 1998). Copepods of the genus *Calanus* are key players in sub-Arctic and Arctic waters (Conover 1988) since they are major grazers on the phytoplankton and efficiently transfer energy to the higher trophic levels such as seabirds, fish and marine mammals. However, within the last decade it has become clear that this classical food web does not capture all essential trophic pathways. Among these is the energy going through tiny single celled heterotrophic eukaryotes also termed "protozooplankton" (Sieburth 1977). Despite their negligible size, this diverse group adds an important twist to the classical energy pathway and deserve more attention in the cold marine ecosystems of the northern hemisphere.

The protozooplankton have shown to be abundant and productive in marine ecosystems all over the world (Landry and Calbet 2004), playing a substantial role in the cycling of elements in the water column (Fig. 1). In this sense, they are major grazers on the phytoplankton (Calbet and Landry 2004; Schmoker et al. 2013) and preferred prey items for many copepods (Saiz and Calbet 2010). In addition they are key components of the microbial loop (Azam et al. 1983; Sherr and Sherr 2002), since dissolved organic material (DOC) is incorporated into bacteria that are grazed by bacteria-consuming protozooplankton. DOC is inaccessible to most marine organisms, but through the microbial loop, energy is transferred to the classical linear food chain by metazoan predation on the protozooplankton. The energy loss at each trophic level is in the order of 10-20 % (Ryther 1969). Thus although protozooplankton transfer energy up the food web most energy is respired before reaching the higher trophic levels, and the microbial loop is thus mainly believed to be important in terms of regenerating nutrients (Williams and Le 2000).
The protozooplankton is a paraphyletic grade of pelagic protists which are all capable of ingesting food particles through phagotrophy or osmotrophy (see Box 1). The ability to take up food particles is the ancient form of nutrition (before photosynthesis) and has been demonstrated in most branches of the protist family tree (Sherr and Sherr 2002). Accordingly, protozooplankton includes a wide span of taxa with different sizes, morphology and feeding behaviour. The protozooplankton is dominated by heterotrophic nanoflagellates, dinoflagellates (Dinophyta) and ciliates (Ciliophora). Most attention has been given to dinoflagellates and ciliates since they are relatively large (10-150 µm) protists and highly abundant in most marine ecosystems. The smaller heterotrophic nanoflagellates include choanoflagellates, non-pigmented crysomonads, kinetoplastids and bicoecids (Fenchel 1982; Sherr and Sherr 2002), but are typically not distinguished. While some protozooplankton species are strictly heterotrophic, a large number are mixotrophic (Stoecker et al. 2009; Hansen 2011; Johnson 2011; see Box 1) and gain energy and/or nutrients from a combination of phagotrophy and photosysthesis. Mixotrophy

is especially widespread among protists in oligotrophic waters, but recent studies indicate that many, if not most flagellated autotrophs are in fact mixotrophs (Flynn et al. 2012).
The feeding behaviour and prey preference of protozooplankton is just as diverse as their morphology and includes all from bacteria to large chain forming diatoms, metazoan eggs and large aggregates of organic material (marine snow) (reviewed by Sherr and Sherr 2002). Heterotrophic nanoflagellates are primary bacterivorous (Fenchel 1982; Sanders et al. 1992; Boenigk and Arndt 2002) although they are also known to graze on picoeukaryotes (Christaki et al. 2001, 2005). Ciliates are mainly known to prey on nano-sized particles (Jonsson 1986; Fenchel 1987), whereas heterotrophic dinoflagellates primarily prey on larger plankton such as chain-forming diatoms, ciliates or even larger prey items like copepod fecal pellets (Bockstahler and Coats 1993; Jacobson and Anderson 1996; Jakobsen and Hansen 1997; Smalley et al. 1999; Sherr and Sherr 2007; Poulsen and Iversen 2008).

The ability of protozooplankton to take up food particles within this large size spectrum allows them to compete with the preferred food items (diatoms) of many metazoans (e.g. copepods) and at the same time to graze on the nanoplankton, which is too small for metazoans to exploit. In addition, protozooplankton benefits by a large growth potential and a short generation time and are thus, in contrast to metazoans, able to react quickly to changing environmental conditions.

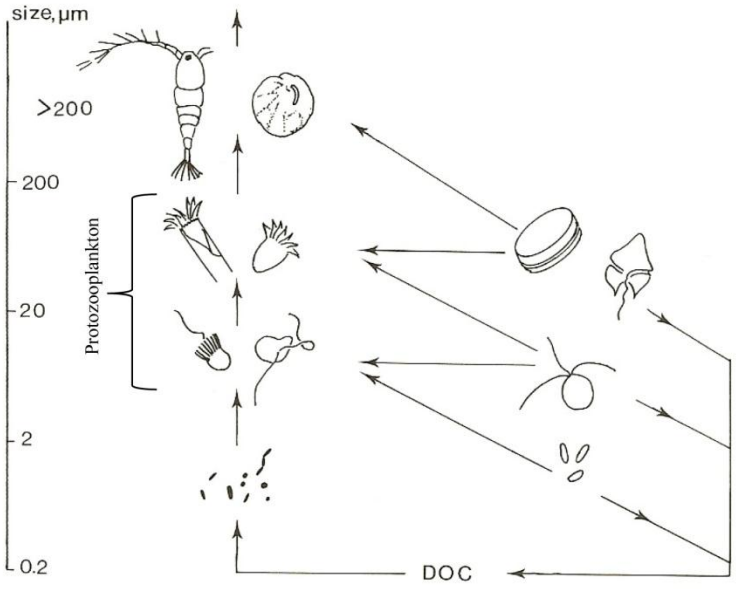

Fig 1. A scematic diagram of the planktonic food web grouped after organisms function and size. Trophic interactions are indicated by arrows. Autotrophic organisms are to the right and serve as food for protozooplankton and metazooplankton. All groups excrete dissolved organic matter (DOC) which is used as substrate for the heterotrophic bacteria. Note the two major trophic pathways: the "microbial loop" (DOC→bacteria→protoplankton) and the "linear classical food chain" (micro-autotrophs→metazoans). From Fenchel (1987), with inserted Tuborg-bracket showing the protozooplankton.

Classification of plankton

Most commonly used plankton classifications used for microbial plankton:

1. Size

Size groups are a simple and widely used way to separate plankton. The logarithmic size classes (Sieburth et al. 1978) based on equatorial spherical diameter (ESD) are:

- ***Femtoplankton*** (0.02-0.2 µm): viruses.
- ***Picoplankton*** (0.2-2 µm): autotrophic bacteria (cyanobacteria), heterotrophic bacteria and eukaryotic autotrophic flagellates.
- ***Nanoplankton*** (2-20 µm)*: heterotrophic and autotrophic flagellates.
- ***Microplankton*** (20-200 µm)*: large phytoplankton species (e.g. diatoms), dinoflagellates, ciliates, small metazoans (e.g. small copepod species, metazoan larvae and metazoan eggs).
- ***Mesoplankton*** (200-2000 µm) include primarily metazooplankton such as copepods (e.g. *Calanus* spp.), but protozooplankton and phytoplankton are also found within this group.

*The logarithmic size intervals are not always suitable for protozooplankton since those larger than 15 µm require different quantification methods than those smaller than 15 µm. In present work we also separate protozooplankton as **nanoflagellelates** (2-15 µm) and **microflagellates (**= microzooplankton**)** (15-200 µm) (Boenigk and Arndt 2002).

2. Trophic mode

Microbes gain energy from two basic ways: ***autotrophy*** (the organism gain energy from light and water) or ***heterotrophy*** (the organism gain energy from taking up organic matter).

Many protozoans are strictly heterotrophic, but a large part obtains energy by ***mixotrophy***: a combination of autotrophy and heterotrophy. Most often mixotrophy is a way for autotrophs to acquire a certain growth factor (e.g. nutrients), but it may also be a way to gain extra energy when food and/or light is scarce.

3. Nutritious mode

Organisms that are able to take up particulate organic matter through engulfment are termed ***phagotrophs.*** Organisms that can take up dissolved organics or inorganic nutrients over the cell membrane are termed ***osmotrophs.*** Typically, phagotrophs are e.g. herbivore or bacterivore ciliates, dinoflagellates or nanoflagellates, while typically osmotrophs are heterotrophic nanoflagellates consuming DOC (Jürgens and Massana 2008).

4.2. Seasonal cycle of northern marine ecosystems

The northern marine environment differs from those at lower latitudes by having lower temperatures and a strong seasonality in light. The sun irradiance defines the productive season, which is initiated by small-sized phytoplankton and progress into a bloom dominated by larger phytoplankton species: i.e. diatoms and occasionally *Phaeoystis pouchetii* (Degerlund and Eilertsen 2009). The bloom which is short and pronounced have attracted marine researchers attention for decades and intensive studies have been conducted during this short period: e.g. the North Atlantic spring bloom experiments (NABE) (Ducklow and Harris 1993) or field campaigns at the West Greenland shelf (Madsen et al. 2001; Aberle et al. 2007; Dünweber et al. 2010) where some of the strongest blooms in the sub-Arctic and Arctic region are known to occur (Harrison et al. 2013).

In the northern hemisphere the bloom plays an important role for structuring the entire food web since the annual primary production (90-400 g C m^{-2} yr^{-1}) is heavily weighted by the primary production during the spring bloom with rates averaging 2-3 g C m^{-2} d^{-1} (Harrison et al. 2013). The bloom is thus important in terms of feeding the higher trophic levels and in the drawdown of CO_2 from the atmosphere (Boyd and Newton 1995). The bloom typically terminates a few weeks later as nutrients become depleted in the Arctic coastal waters (Dünweber et al. 2010) or as the phytoplankton become controlled by grazers as is often the case in the open ocean (Dale 1999). The collapse is rapid, which is partly explained by higher sinking rates of diatoms as they become senescent in nutrient limited waters (Smetacek 1985; Passow 1991).

In high Arctic coastal waters the productive season is initiated when the sea ice breaks up, but the productive season starts earlier and continues for a longer period at lower latitudes along with the increasing day length and absence of sea-ice cover (Harrison et al. 2013). Copepods of the genus *Calanus* dominate the zooplankton during the spring bloom, but after spawning and refilling their lipid and wax-ester reserves (after a months or two), they migrate to the near-bottom waters where they stay until the next season (Conover 1988; Diel and Tande 1992; Madsen et al. 2001). When *Calanus* have resigned from the surface waters, the grazing pressure on the smaller plankton organisms is reduced and a diverse protozooplankton community is established (Levinsen et al. 2000; Seuthe et al. 2011).Thus, during the summer period, heterotrophic dinoflagellates and ciliates take over as dominating grazers on the phytoplankton. As the sun irradiance decrease in the autumn, the protozooplankton reduce in number along with the decreasing phytoplankton biomass. However, a small protozooplankton population remains in the upper water masses during winter (Levinsen et al. 2000), where they are sustained by the microbial loop (Vaqué et al. 2008; Iversen and Seuthe 2011). They are thus ready to exploit the phytoplankton as soon as the productive season once again is initiated.

4.3. Impact of climate changes on sub-Arctic and Arctic plankton communities

Seasonality obviously controls the annual plankton dynamics of high latitude ecosystems, but changes also occur on decadal scale and in this regard, climate changes become important.

The most visible impact of climate changes in the northern hemisphere is the shrinking summer sea-ice cover, which is a major controlling factor for the plankton succession. Over the period 1979 to 2012 has decreased with a rate of ca. 9-12 % per decade with an accelerating trend (Stocker et al. 2013). Climate models predict that the Arctic sea ice cover will continue to shrink during the 21st century, as the global mean surface temperature rises, and projections suggest that 43 to 94 % of the Arctic perennial (multi-year) sea-ice cover will be gone by 2100 (Stocker et al. 2013). A reduced sea-ice cover will allow sunlight to penetrate into the pelagic for a longer period and hereby expand the productive season in large parts of Arctic. An extended productive season may result in a succession pattern more similar to those found in temperate marine ecosystems, where both phytoplankton and protozooplankton have a bimodal succession pattern, with one peak in spring and another in the autumn (Levinsen and Nielsen 2002).

Stratification of the water column is another controlling factor for the plankton communities. Increasing surface temperature and higher input of freshwater from glacial melt-water runoff and precipitation will lead to a more stable water column due to a stronger vertical temperature-salinity gradient, particular in fjords and coastal regions. Water column stability also results in lower annual primary production since the nutrient depleted surface waters are separated from the nutrient rich bottom waters. In addition, grazing pressure may be higher in stratified waters, where the chance of predator-prey encounter is high. In essence this means that long term stratification bias the food web towards dominance of the microbial food web relative to the classical food chain (Cushing 1989).

Finally, a warmer climate will also have direct impact on ectothermic organisms, like plankton. Metabolism and enzyme processes are directly influenced by temperature and higher temperatures will increase speed up grazing- and respiration rates. An ultimate consequence of this is that a larger fraction of the phytoplankton production will be grazed by protozooplankton and thus mineralized in the surface waters, rather than channelled up the pelagic food web or sink to the deep waters and/or seabed to be eaten by the benthos.

4. OBJECTIVES OF THE THESIS

Despite the prominent role of protozooplankton in northern marine ecosystems, quantitative and qualitative studies of this plankton group are scarce. Likewise, it is unknown how a future warmer climate will impact the seasonal succession of the protozooplankton communities and what implications this has for the spring bloom dynamics.

The aim of the present thesis is to point out important factors regulating the protozooplankton community and to resolve what trophic role this plankton group has in regulating bloom dynamics in different sub-Arctic and Arctic marine ecosystems. The field data was collected in the Disko Bay, the Godthåbsfjord (Southwest Greenland), in the Greenland Sea (North East Water Polynya) and in the sub-Arctic North Atlantic Ocean (Iceland Basin, Norwegian Sea and Shetland Shelf). A number of experiments with different aims were conducted within these four locations. The thesis is divided into four major chapters based on the four specific objectives, each consisting of 1-2 papers.

The specific objectives were the following:

- To estimate how temperature in the low end of the temperature scale (-1.8 to 5 ^{o}C) affects protozooplankton growth rates and to study the protozooplankton community in a habitat characterized by cold temperatures (Paper I).

- To study how mixed layer depth in the sub-Arctic Atlantic affects microbial components prior to the bloom and to quantify the importance of protozooplankton as grazers within the deep convective layer (Paper II and III).

- To investigate if pH fluctuations during the Arctic spring bloom is an important factor regulating protozooplankton growth rate and evaluate the importance of pH for phytoplankton bloom dynamics (Paper IV).

- To evaluate how protozooplankton respond to the fluctuating copepod community in a sub-Arctic fjord and to quantify protozooplankton grazing impact along a glacier-to-open ocean transect. In addition, to discuss how the protozooplankton dynamics the in the sub-Arctic fjord differ from those at higher latitudes (Paper V and VI).

5. STUDY LOCALITIES

The studies were conducted at four localities within the sub-Arctic and Arctic region (Fig. 2). The localities represent four different ecosystems and differ in hydrography, temperature, phytoplankton succession and seasonality.

Fig. 2. The four study areas: North East Water (NEW) Polynya (Paper I), the sub-Arctic Atlantic (Paper II and III), Disko Bay (Paper IV) and Godthåbsfjord (Paper V and VI).

6.1. North East Water Polynya (NE Greenland)

Polynyas are large open-water regions in otherwise ice-covered polar ocean which tend to reoccur from year to year. The productive season in polynyas is usually 3-5 months but despite this, polynyas belong to some of the World's most productive marine habitats (Tremblay and Smith 2007; Harrison et al. 2013). High accumulations of birds and marine mammals occur in association with polynyas (Stirling 1997; Heide-Jørgensen et al. 2013) and they are accordingly of high ecological interest. Paper I is based on a study in the North East Water (NEW) polynya is located on the continental shelf of NW Greenland (~80 ^{o}N). A land fast ice-barrier at its southern distribution prevent ice from entering the polynya by creating an anticyclonic eddy in the area (Schneider and Budéus 1994). In the 1990's the NEW polynya was the second largest polynya in the Arctic, but the disappearance of the ice-barrier allowed ice to enter the polynya and its size decreased in the late 1990's. Today the entire area is covered with ice throughout the year (Barber and Massom 2007), but the absence of sea-ice makes polynyas ideal for studying how specific Arctic locations will respond to reductions in sea-ice cover.

5.2. Sub-Arctic North Atlantic

The focus area here referred to as "the sub-Arctic Atlantic" includes three sampling stations: Iceland Basin Station, Norwegian Basin Station and the Shetland Shelf Station (Fig. 2). The area is characterized by warm Atlantic water coming from south. In winter, before the spring bloom peaks, the water column is characterized by high turbulent mixing and deep convection (Backhaus et al. 1999), and the mixed layer may consequently be extremely deep reaching up to 1000 m (de Boyer Montégut et al. 2004). The three stations present different hydrological regimes within the sub-Arctic Atlantic (Fig. 2). St. 1 was chosen as focus station since this station had a persistent mixed layer reaching 500-600 m depth. Paper II includes data from all three sampling stations, whereas paper III focuses on the deep mixed station located in the Iceland Basin.

5.3. Disko Bay (West Greenland)

Disko Bay (~69 ^{o}N) is an inlet of the Baffin Bay located at the continental shelf of West Greenland. The productive season is controlled by the sea-ice, which usually covers the Bay 2-5 months a year. The bay is characterized by an intense phytoplankton bloom in spring (Nielsen and Hansen 1995) which is central for the high biodiversity in the bay. Since 1996 (Madsen et al. 2001) regular field monitoring have been conducted in the Disko Bay (close to Qeqertarsuauq) from Arctic Station (Copenhagen University) in spring, using a 250-300 m deep sampling station. The continuous monitoring of plankton succession makes this station unique in terms of background data. Data presented in paper IV are based on data obtained from the above mentioned sampling station in the Disko Bay, but all papers refer to studies from this station, due to the unique field dataset.

5.4. Godthåbthåbsfjord (SW Greenland)

The Godthåbsfjord is a sub-Arctic fjord system located next to Nuuk, Greenland. It is one of the largest fjord systems in Greenland, harbouring large populations of capelin and Atlantic cod (Smidt 1979; Storr-Paulsen et al. 2004; Bergstrøm and Vilhajalmsson 2008). In contrast to high Arctic systems where copepods of the genus *Calanus* tend to dominate (Digby 1953; Nielsen and Hansen 1995; Rysgaard et al. 1999; Iversen and Seuthe 2011), non-*Calanus* species such as *Pseudocalanus* spp., *Microsetella* spp., *Oithona* spp. and *Metridia longa* (Arendt et al. 2010; Tang et al. 2011) dominante in the Godthåbsfjord. Paper V is based on data collected in a side-branch to the Godthåbsfjord; Kapisigdtlit Fjord. Paper VI is based on experimental data obtained along a glacier-to-open sea transect in the fjord.

6. SUMMARY

At all investigated localities, protozooplankton contributed significantly to the area-specific plankton biomass. Temperature, water column stratification, prey availability, pH and grazing by copepods were identified as factors influencing the protozooplankton growth and abundance. A brief summary of major findings is given in the following.

7.1. Temperature dependency

Paper I examine how temperatures in the low end of the temperature scale (-2 to 5 ^{o}C) affect growth rates of heterotrophic dinoflagellates and ciliates. A growth experiment with two dinoflagellate species and two ciliate species revealed that growth decreased with a rate similar to what would be expected for heterotrophic dinoflagellates and ciliates found in temperate waters. The experiment was accompanied by field data collected in the high-Arctic North East Water Polynya, which indicated that the protozooplankton community was controlled by their phytoplankton prey rather than temperature. Consequently, protozooplankton peaked in the cold marginal ice-zones where phytoplankton biomass was highest, rather than in the warmer open waters with lower phytoplankton biomass.

7.2. Impact of deep convection on the microbial food web

Paper II and paper III present data obtained through a comprehensive field campaign in the sub-Arctic North Atlantic Ocean. The region is one of the most intensively studied areas in the global ocean. However, only few plankton studies have been conducted in the deep basins during winter, where the water column is characterized by a deep (600-1000 m) convective layer (Backhaus et al. 2003). In combination, the two papers evaluate the importance of deep winter mixing for regulating the plankton communities.

Paper II presents data collected prior to the spring bloom during repeated visits to stations in the the deep Icelandic and the Norwegian Basins and the shallow Shetland Shelf. The succession and dynamics of autotrophic and heterotrophic microbes was followed during a six-week period prior to the spring bloom. The phytoplankton was initially dominated by picophytoplankton and small nanophytoplankton, but their contribution relative to larger species decreased towards the end of the study period at all stations.

Paper III present data obtained through three fractionated microcosm experiments, conducted with water collected in the deep convective layer of the Iceland Basin. The experiments demonstrated that heterotrophic protists consumed bacteria, phytoplankton (pico- and nanophytoplankton) and heterotrophic nanoflagellates (HNF). The data suggests that

heterotrophic nanoflagellates are major grazers early in the productive season, whereas ciliates and dinoflagellates become more important as the bloom develops.

The conclusion of the two papers is that a reduced encounter between microzooplankton and phytoplankton during deep convection could explain part of the apparent build up in phytoplankton biomass. However, the reduced encounter also lead to a reduced top-down control of heterotrophic nanoflagellates, resulting in biased grazing towards smaller phytoplankton species, thus favoring larger fast growing diatoms that are resistant to nano-sized grazers.

7.3. Elevated pH as a controlling factor

Paper IV assess how an expected increase in primary production in the Arctic coastal waters affects pH and what impact temporary elevations in pH has on the heterotrophic protist communities. Field observations documented an increase in pH from 7.5 to 8.5 during the phytoplankton spring bloom in Disko Bay, West Greenland. Microcosm experiments demonstrated that the most pronounced effect of elevated pH was found for heterotrophic protists, which were significantly affected at pH 9.0, whereas diatoms proved to be more robust. The results demonstrate that most protists are unaffected by seasonal changes in pH, even during the massive phytoplankton spring bloom. However, pH could theoretically play a role in regulating species succession in sea-ice brine channels or marginal ice-zones where pH is known to be extremely elevated.

7.4. Protozooplankton as prey and as grazers in a sub-Arctic fjord

Paper V and VI present data on seasonal succession (March to August) and grazing potential of the protozooplankton within the Godthåbsfjord, SW Greenland. In Paper V, a grazing experiment with the copepod *Metridia longa* feeding on a natural plankton assemblage, demonstrated that *M. longa* efficiently cleared protozooplankton cells in the size range 10 to 60 µm. In combination with field data this indicates that the protozooplankton succession is regulated by copepod grazing during most of the season and that the protozooplankton provide an essential source of nutrition for the copepod populations. Paper VI documents that the protozooplankton were significant herbivores on small sized phytoplankton (<10 µm). Size-fractionated dilution experiments revealed that the grazing community were composed by protozooplankton >20 µm grazing >100 % of primary production per day in the inner parts of the fjord, whereas grazing impact on the phytoplankton communities were insignificant in the open-ocean and at the mouth of the fjord. The presented data from the two papers suggest that protozooplankton are an important intermediate link between the phytoplankton and the copepods in the Godthåbsfjord and that changes in hydrography towards more stratified melt-water influenced waters will benefit the protozooplankton communities.

7. REFLECTIONS ON THE METHODS

Estimates of protozooplankton growth and grazing impact are central if we want to understand their role in the marine food web. Reliable rates are difficult to obtain since the protozooplankton is this extremely diverse group of organism with very different trophic functions. In the present thesis several approaches were applied to capture some major tendencies and in the following pros and cons of the different methods are discussed.

Growth rate is equal to cell division rate (unless sexual reproduction occur) and in the present studies growth rates of protozooplankton were estimated from changes in cell abundance over time in incubations where grazing mortality was close to zero. In the field grazing mortality is hard to remove entirely, but it can be minimized by screening the natural plankton through different size fractions hereby removing metazoan grazers. Growth rates of protozooplankton were obtained by screening natural protozooplankton assemblages and incubating them under various conditions (Paper I, III and IV). Growth rates from short time incubations of protozooplankton are however difficult to obtain since the protozooplankton are fragile and therefore may experience higher mortality during the first couple of days. In cold waters, where the growth rates are low, it also requires several days to have data points enough to make sure that the cells grow exponentially. However, long-time incubations may result in trophic cascades and a few species will end up dominating the plankton community. If growth rates should only be estimated for a few selected species (e.g. Paper I and IV) cascades may not be a problem. However, if it is desired to use the obtained growth rates to estimate community production rates, I will recommend that the time is spend on obtaining solid biomass estimates of protozooplankton community and then convert these biomasses into production rates from existing models. In Paper I a temperature-depended growth model was generated from growth rates estimated from experiments assuming food saturation. In Paper V, a prey-density dependent model (Hansen et al. 1997) was applied for estimating protozooplankton growth and grazing rates. The later type of model does not assume prey saturation, but assumes that the protozooplankton community only feed on phytoplankton.

Grazing rate is the other major parameter for evaluating marine food webs and in this context the dilution technique has been highly valuable (Landry and Hassett 1982; Landry and Calbet 2004). Since the method was invented more than 1500 dilution experiments have been conducted (Schmoker et al. 2013). The technique (used in Paper VI) is based on reductions in encounter rate between predator and prey by considerably diluting the natural plankton community with particle free water, hereby providing estimates of phytoplankton growth and phytoplankton grazing mortality. The technique relies on several assumptions (Landry and Hassett 1982), that may not always be achieved (reviewed by Calbet & Saiz 2013). The most important assumptions being that 1) the grazers must not be food satiated, 2) changes in phytoplankton density must be exponential and 3) the phytoplankton growth rate is not affected by the dilution. Artifacts from dilution are the major reason why grazing rates obtained by the dilution technique are not always reliable. Trophic cascades are important artifacts, and are not always taken into consideration.

Dilution of nutrient limited communities may e.g. also result in higher growth rates in the diluted samples relative to the undiluted samples. Nutrient unlimited growth can be ensured by running experimental and control bottles with and without added nutrients. When applying the dilution technique to high chlorophyll waters, you have to make sure that the dilution series are of a magnitude that ensures that the protozooplankton community is not food satiated. However, if the phytoplankton growth is limited by nutrients or if the dilution causes other artifacts such as trophic cascades, other techniques should be used.

An alternative method for estimating protozoan grazing potential is the fractionation technique (Verity et al. 1993; Solic and Krstulovic 1994; Christaki et al. 2001, Paper III). The technique assumes that predators and prey can be separated by size and that the community essentially can be predator-free by size-screening the community. Growth- and mortality rates of the prey are estimated by the difference in prey growth rates in samples with predators (non-screened) and in samples without predators (screened). This technique has implications during e.g. the diatom bloom since diatoms are of the same size as their major protist grazers (dinoflagellates), but when the water is dominated by single cells, grazing estimates are close to those obtained by the dilution technique (Christaki et al. 2001). The technique was used in Paper III since the community was dilute and composed of mainly single celled phytoplankton species that are more easily separated from their grazers. Furthermore, we wanted to estimate the magnitude of other predator-prey interactions, such as consumptions of other heterotrophic protists, which is not possible from the dilution technique.

In conclusion there is no all-around method for estimating growth and grazing impact by protozooplankton and it is therefore important to be confident with the system you are working with before manipulating it or before applying a model.

8. PERSPECTIVES AND CONCLUSION

Since the microbial-loop concept was invented (Pomeroy 1974; Azam et al. 1983), a great effort has been put into estimating protozooplankton herbivory and bacterivory in marine and freshwater systems (Fenchel 2008). Despite this, food web models predicting e.g. net primary production in the sub-Arctic and Arctic marine waters need improvements on the protozooplankton compartment (Slagstad et al. 2011). In particular the models need more development on temperature-dependent respiration, grazing and growth of the protozooplankton at low temperatures. The present Ph.D. thesis provides new insights into the trophic role of protozooplankton in sub-Arctic and Arctic marine environments and present data suited for implementing in food web models simulating high latitude marine ecosystems under a changing climate.

The new data suggests that protozooplankton will play a more prominent role in a predicted warmer future because: 1) they will have higher growth rates as the sea temperature increases, 2) more stratified waters will increase protozooplankton prey-encounter rate, and 3) a reduction in phytoplankton cell size can be expected which will favour protozooplankton as they are suited to consume small-sized cells. In this way more energy will flow through an active protozooplankton community rather than sink to the deep waters, or than channelled directly to the larger metazoan grazers (copepods). Since the phytoplankton size will be biased towards smaller cells, protozooplankton will also add an important trophic link between the small sized phytoplankton and the metazoans. These changes will all result in increased recycling of nutrients within the pelagic.

A reduced sea-ice cover and intensified water column stratification due to temperature increase will lead to a longer productive season and a less pulsed succession of the plankton communities. The phytoplankton spring bloom is expected to decrease its magnitude and large specialist copepod grazers like *Calanus* species will be challenged by the small generalist protozooplankton that reside in the surface waters year-round and profit of less pulsed conditions in a warmer climate. Thus, in contrast to many other marine organisms, protozooplankton face a bright future under a changing climate.

9. ACKNOWLEDGEMENTS

The outcome of this thesis was only made possible with help and collaboration with many people who I want to thank. Foremost, I would like to thank my advisors Prof. Torkel Gissel Nielsen and Prof. Michael St. John for providing me with the opportunity to complete my Ph.D. thesis at DTU Aqua, and especially to you Torkel for being the best supervisor I could ask for throughout the entire process. I have been inspired and impressed by your enthusiasm, energy and passion for science.

I feel lucky to have collaborated with so many wonderful people and I want to thank all of you. Especially thanks to Maria Lund Paulsen. If possible I would have made the entire thesis with you by my side. Your positive energy and bright thoughts are true gifts when collaborating with you. Thanks to Sanne Kjellerup and Rasmus Swalethorp for three hard but fun and inspiring months of field work in Nuuk. I admire your persistence and relaxed approach to the longest sampling programs I have been exposed to. I also want to thank Dr. Albert Calbert and Dr. Enric Saiz for teaching me the secrets behind the dilution technique, for three great weeks on board RV Dana and for being excellent sources of knowledge. Thanks to Dr. Susanne Menden-Deuer for hosting me at your lab and to you Amanda Burke for great technical logistics. Although my work did not result in useful data, I had a wonderful time in Rhode Island and I learned more than you would probably think. I am grateful to Prof. Per Juel Hansen for scientific input and inspiration. It has been a pleasure to collaborate with you and observe how everything just somehow gets better whenever you touch it. I owe a big thank to Birgit Søborg for technical logistics and for your blessed personality that makes weeks of chlorophyll filtration fun.

Also I want to thank the many people including co-authors who have read several parts of the thesis and given excellent critique and comments: Mette Agersted, Mie Sichlau Winding, Maria Lund Paulsen, Nis Sand Jacobsen, Rasmus Swalethorp, Francoise Morrison, Chris Daniels, Sanne Kjellerup, Jan Heuschele and my dad. Also a big thank to anonymous reviewers of the papers.

For the non-scientic part I want to thank my officemates through the years and colleagues at DTU-Aqua who turned three years as Ph.D.-student into the three fantastic years with Friday-beers, lots of coffee breaks, probably more hundred jogging tours, parties and long lunch breaks. I'm going to miss you! Last but not least I want to thank my husband Anders Koed Madsen and our little son Lauge, who made me remember what really matters in life.

9. LITERATURE CITED

Aberle, N., K. Lengfellner, and U. Sommer. 2007. Spring bloom succession, grazing impact and herbivore selectivity of ciliate communities in response to winter warming. Oecologia **150**: 668–681.

Arendt, K. E., T. G. Nielsen, S. Rysgaard, and K. Tonnesson. 2010. Differences in plankton community structure along the Godthabsfjord, from the Greenland Ice Sheet to offshore waters. Mar. Ecol. Prog. Ser. **401**: 49–62.

Azam, F., T. Fenchel, J. G. Field, J. S. Gray, L. A. Mayer-Reil, and F. Thingstad. 1983. The ecological role of water-column microbes in the sea. Mar. Ecol. Prog. Ser. **10**: 257–263.

Backhaus, J., E. Hegseth, H. Wehde, X. Irigoien, K. Hatten, and K. Logemann. 2003. Convection and primary production in winter. Mar. Ecol. Prog. Ser. **251**: 1–14.

Backhaus, J., H. Wehde, E. Hegseth, and J. Kämpf. 1999. Phyto-convection:the role of oceanic convection in primary production. Mar. Ecol. Prog. Ser. **189**: 77–92.

Barber, D. G., and R. A. Massom. 2007. The role of sea ice in Arctic and Antarctic polynyas, p. 1–54. *In* W.O. Smith and D.G. Barber [eds.], Polynyas -windows to the world. Elsevier Oceanography Series, 74.

Bergstrøm, B., and H. Vilhajalmsson. 2008. Cruise report and pre-liminary results of the acoustic/pelagic trawl survey off West Greenland for capelin and polar cod 2005. 341–352.

Bockstahler, K. R., and D. W. Coats. 1993. Spatial and temporal aspects of mixotrophy in Chesapeake Bay dinoflagellates. J. Euk. Microbiol. **40**: 49–60.

Boenigk, J., and H. Arndt. 2002. Bacterivory by heterotrophic flagellates: community structure and feeding strategies. Antonie Van Leeuwenhoek **81**: 465–80.

Boyd, P., and P. Newton. 1995. Evidence of the potential influence of planktonic community structure on the interannual variability of particulate organic carbon flux. Deep Sea Res. Part I Oceanogr. Res. Pap. **42**: 619–639.

De Boyer Montégut, C., G. Madec, A. S. Fischer, A. Lazar, and D. Iudicone. 2004. Mixed layer depth over the global ocean: An examination of profile data and a profile-based climatology. J. Geophys. Res. **109**: C12003.

Calbet, A., and M. R. Landry. 2004. Phytoplankton growth, microzooplankton grazing, and carbon cycling in marine systems. Limnol. Oceanogr. **49**: 51–57.

Calbet, A., and E. Saiz. 2013. Effects of trophic cascades in dilution grazing experiments: from artificial saturated feeding responses to positive slopes. J. Plankton Res. **35**: 1183–1191.

Christaki, U., A. Giannakourou, F. V. A. N. Wambeke, and G. Grégori. 2001. Nanoflagellate predation on auto- and heterotrophic picoplankton in the oligotrophic Mediterranean Sea. J. Plankton Res. **23**: 1297–1310.

Christaki, U., E. Vázquez-Domínguez, C. Courties, and P. Lebaron. 2005. Grazing impact of different heterotrophic nanoflagellates on eukaryotic (*Ostreococcus tauri*) and prokaryotic picoautotrophs (*Prochlorococcus* and *Synechococcus*). Environ. Microbiol. **7**: 1200–10.

Conover, R. J. 1988. Comparative life histories in the genera *Calanus* and *Neocalanus* in high latitudes of the northern hemisphere. Hydrobiologia **167/168**: 127–142.

Cushing, D. H. 1989. A difference in structure between ecosystems in strongly stratified waters and in those that are only weakly stratified. J. Plankton Res. **11**: 1 – 14.

Dale, T. 1999. Seasonal development of phytoplankton at a high latitude oceanic site. Sarsia **84**: 419–435.

Degerlund, M., and H. C. Eilertsen. 2009. Main Species Characteristics of Phytoplankton Spring Blooms in NE Atlantic and Arctic Waters (68–80° N). Estuaries and Coasts **33**: 242–269.

Diel, S., and K. Tande. 1992. Does the spawning of *Calanus finmarchicus* in high latitudes follow a reproducible pattern? Mar. Biol. **113**: 21–31.

Digby, P. S. B. 1953. Plankton production in scoresby Sound, East Greenland. Br. Ecol. Soc. **22**: 289–322.

Ducklow, H. W., and R. P. Harris. 1993. Introduction to the JGOFS North Atlantic bloom experiment. Deep Sea Res. Part II Top. Stud. Oceanogr. **40**: 1–8.

Dünweber, M., R. Swalethorp, S. Kjellerup, T. Nielsen, K. Arendt, M. Hjorth, K. Tönnesson, and E. Møller. 2010. Succession and fate of the spring diatom bloom in Disko Bay, western Greenland. Mar. Ecol. Prog. Ser. **419**: 11–29.

Fenchel, T. 1982. Ecology of heterotrophic microflagellates. IV. Quantitative occurrence and importance as bacterial consumers. Mar. Ecol. Prog. Ser. **9**: 35–42.

Fenchel, T. 1987. Ecology of protozoa, First. T.D. Brock [ed.]. Science Tech.

Fenchel, T. 2008. The microbial loop – 25 years later. J. Exp. Mar. Bio. Ecol. **366**: 99–103.

Field, C. B., M. J. Behrenfeld, J. Randerson, and F. P. 1998. Primary Production of the Biosphere: Integrating Terrestrial and Oceanic Components. Science (80-.). **281**: 237–240.

Flynn, K. J., D. K. Stoecker, A. Mitra, J. A. Raven, P. M. Glibert, P. J. Hansen, E. Graneli, and J. M. Burkholder. 2012. Misuse of the phytoplankton-zooplankton dichotomy: the need to assign organisms as mixotrophs within plankton functional types. J. Plankton Res. **35**: 3–11.

Hansen, P. J. 2011. The role of photosynthesis and food uptake for the growth of marine mixotrophic dinoflagellates. J. Eukaryot. Microbiol. **58**: 203–14.

Hansen, P. J., P. K. Bjørnsen, and B. W. Hansen. 1997. Zooplankton grazing and growth : scaling within the 2-2,000-µm body size range. Limnol. Oceanogr. **42**: 687–704.

Harrison, G. W., Y. K. Børsheim, W. K. W. Li, G. L. Maillet, P. Pepin, E. Sakshaug, M. D. Skogen, and P. A. Yeats. 2013. Phytoplankton production and growth regulation in the Subarctic North Atlantic: A comparative study of the Labrador Sea-Labrador/Newfoundland shelves and Barents/Norwegian/Greenland seas and shelves. Prog. Oceanogr. **114**: 26–45.

Heide-Jørgensen, P., L. M. Burt, R. G. Hansen, N. H. Nielsen, M. Rasmussen, S. Fossette, and H. Stern. 2013. The significance of the North Water Polynya to Arctic top predators. Ambio **42**: 596–610.

Iversen, K. R., and L. Seuthe. 2011. Seasonal microbial processes in a high-latitude fjord (Kongsfjorden, Svalbard): I. Heterotrophic bacteria, picoplankton and nanoflagellates. Polar Biol. **34**: 731–749.

Jacobson, D. M., and D. M. Anderson. 1996. Widespread phagocytosis of ciliates nd other protists by marine mixotrophic and heterotrophic thecate dinoflagellates. J. Phycol. **32**: 279–285.

Jakobsen, H., and P. Hansen. 1997. Prey size selection, grazing and growth response of the small heterotrophic dinoflagellate *Gymnodinium* sp. and the ciliate *Balanion comatum*--a comparative study. Mar. Ecol. Prog. Ser. **158**: 75–86.

Johnson, M. D. 2011. Acquired phototrophy in ciliates: a review of cellular interactions and structural adaptations. J. Eukaryot. Microbiol. **58**: 185–95.

Jonsson, P. 1986. Particle size selection, feeding rates and growth dynamics of marine planktonic oligotrichous ciliates (Ciliophora: Oligotrichina). Mar. Ecol. Prog. Ser. **33**: 265–277.

Jürgens, K., and R. Massana. 2008. Protistan grazing on marine bacterioplankton, p. 383–441. *In* D. Kirchman [ed.], Microbial Ecology of the Oceans. John Wiley & Sons, Inc.

Landry, M. R., and A. Calbet. 2004. Microzooplankton production in the oceans. ICES J. Mar. Sci. **61**: 501–507.

Landry, M. R., and R. P. Hassett. 1982. Estimating the grazing impact of marine micro-zooplankton. Mar. Biol. **67**: 283–288.

Levinsen, H., and T. G. Nielsen. 2002. The trophic role of marine pelagic ciliates and heterotrophic dinoflagellates in arctic and temperate coastal ecosystems: A cross-latitude comparison. Limnol. Oceanogr. **47**: 427–439.

Levinsen, H., T. Nielsen, and B. Hansen. 2000. Annual succession of marine pelagic protozoans in Disko Bay, West Greenland, with emphasis on winter dynamics. Mar. Ecol. Prog. Ser. **206**: 119–134.

Madsen, S., T. Nielsen, and B. Hansen. 2001. Annual population development and production by *Calanus finmarchicus*, *C. glacialis* and *C. hyperboreus* in Disko Bay, western Greenland. Mar. Biol. **139**: 75–93.

Nielsen, T. G., and B. Hansen. 1995. Plankton community structure and carbon cycling on the western coast of Greenland during and after the sedimentation of a diatom bloom. Mar. Ecol. Prog. Ser. **125**: 239–257.

Passow, U. 1991. Species-specific sedimentation and sinking velocities of diatoms. Mar. Biol. **108**: 449–455.

Pomeroy, L. R. 1974. The ocean's food web, a changing paradigm. BioScience. Bioscience **24**: 499–504.

Poulsen, L., and M. Iversen. 2008. Degradation of copepod fecal pellets: key role of protozooplankton. Mar. Ecol. Prog. Ser. **367**: 1–13.

Rysgaard, S., T. G. Nielsen, and B. W. Hansen. 1999. Seasonal variation in nutrients, pelagic primary production and grazing in a high-Arctic coastal marine ecosystem, Young Sound, Northeast Greenland. Mar. Ecol. Prog. Ser. **179**: 12–25.

Ryther, J. H. 1969. Photosynthesis and fish production in the sea. Sci. New Ser. **166**: 72–76.

Saiz, E., and A. Calbet. 2010. Copepod feeding in the ocean: scaling patterns, composition of their diet and the bias of estimates due to microzooplankton grazing during incubations. Hydrobiologia **666**: 181–196.

Sanders, R., D. Caron, and G. Berninger U. 1992. Relationships between bacteria and heterotrophic nanoplankton in marine and fresh waters: an inter-ecosystem comparison. Mar. Ecol. Prog. Ser. **86**: 1–14.

Schmoker, C., S. Hernandez-Leon, and A. Calbet. 2013. Microzooplankton grazing in the oceans: impacts, data variability, knowledge gaps and future directions. J. Plankton Res. **35**: 691–706.

Schneider, W., and G. Budéus. 1994. The North East Water polynya (Greenland Sea) I. A physical concept of its generation. Polar Biol. **14**: 1–9.

Seuthe, L., K. Rokkan Iversen, and F. Narcy. 2011. Microbial processes in a high-latitude fjord (Kongsfjorden, Svalbard): II. Ciliates and dinoflagellates. Polar Biol. **34**: 751–766.

Sherr, E. B., and B. F. Sherr. 2002. Significance of predation by protists in aquatic microbial food webs. Antonie Van Leeuwenhoek **81**: 293–308.

Sherr, E. B., and B. F. Sherr. 2007. Heterotrophic dinoflagellates: a significant component of microzooplankton biomass and major grazers of diatoms in the sea. Mar. Ecol. Prog. Ser. **352**: 187–197.

Sieburth, J. M. 1977. Handbook of microbiology, p. 3–7. *In* A.I. Laskin and H.A. Lechevalier [eds.], Handbook of microbiology. CRN.

Sieburth, J. M., V. Smetacek, and J. Lenz. 1978. Pelagic ecosystem structure -heterotrophic compartments of plankton and their relationship to plankton size fractions. Limnol. Oceanogr. **23**: 1256–1263.

Slagstad, D., I. H. Ellingsen, and P. Wassmann. 2011. Evaluating primary and secondary production in an Arctic Ocean void of summer sea ice: An experimental simulation approach. Prog. Oceanogr. **90**: 117–131.

Smalley, G. W., D. W. Coats, and E. J. Adam. 1999. A new method using flourescent microsperes to determine grazing on ciliates by the mixotrophic dinoflagellate *Ceratium furca*. Aquat. Microb. Ecol. **17**: 167–179.

Smetacek, V. S. 1985. Role of sinking in diatom life-history cycles: ecological, evolutionary and geological significance. Mar. Biol. **84**: 239–251.

Smidt, E. 1979. Annual cycles of primary production and of zooplankton at southwest Greenland. Greenl Biosci **1**: 1–56.

Solic, M., and N. Krstulovic. 1994. Role of predation in controlling bacterial and heterotrophic nanoflagellate standing stocks in the coastal Adriatic Sea : seasonal patterns. Mar. Ecol. Prog. Ser. **114**: 219–235.

Stirling, I. 1997. The importance of polynyas, ice edges, and leads to marine mammals and birds. J. Mar. Syst. **10**: 9–21.

Stocker, T. F., D. Qin, K.-G. Plattner, M. M. B. Tignor, S. K. Allen, J. Boschung, A. Nauels, Y. Xia, V. Bex, and P. M. Midgley. 2013. Climate Change 2013: The Physical Science Basis, Working group I contribution to the fifth assesment report of the intergovermental report on climate change.

Stoecker, D., M. Johnson, C. deVargas, and F. Not. 2009. Acquired phototrophy in aquatic protists. Aquat. Microb. Ecol. **57**: 279–310.

Storr-Paulsen, M., K. Wieland, H. Hovgard, and H. Ratz. 2004. Stock structure of Atlantic cod (*Gadus morhua*) in West Greenland waters: implications of transport and migration. ICES J Mar Sci **61**: 972−982.

Tang, K. W., T. G. Nielsen, P. Munk, J. Mortensen, and A. Others. 2011. Metazooplankton community structure, feeding rate estimates, and hydrography in a meltwater-influenced Greenlandic fjord. Mar. Ecol. Prog. Ser. **434**: 77–90.

Tremblay, J. E., and J. W. O. Smith. 2007. Primary production and nutrient dynamics in polynyas, p. 239–269. *In* J.W.O. Smith and D.G. Barber [eds.], Polynyas -windows to the world. Elsevier Oceanography Series, 74.

Vaqué, D., Ò. Guadayol, F. Peters, J. Felipe, L. Angel-Ripoll, R. Terrado, C. Lovejoy, and C. Pedrós-Alió. 2008. Seasonal changes in planktonic bacterivory rates under the ice-covered coastal Arctic Ocean. Limnol. Oceanogr. **53**: 2427–2438.

Verity, P. G., D. K. Stoecker, M. E. Sieracki, and J. R. Nelson. 1993. Grazing, growth and mortality of microzooplankton during the 1989 North Atlantic spring bloom at 47°N, 18°W. Deep Sea Res. Part I Oceanogr. Res. Pap. **40**: 1793–1814.

Williams, P. J., and B. Le. 2000. Heterotrophic bacteria and the dynamics of dissolved organic material, D.L. Kirchman [ed.].

Paper I

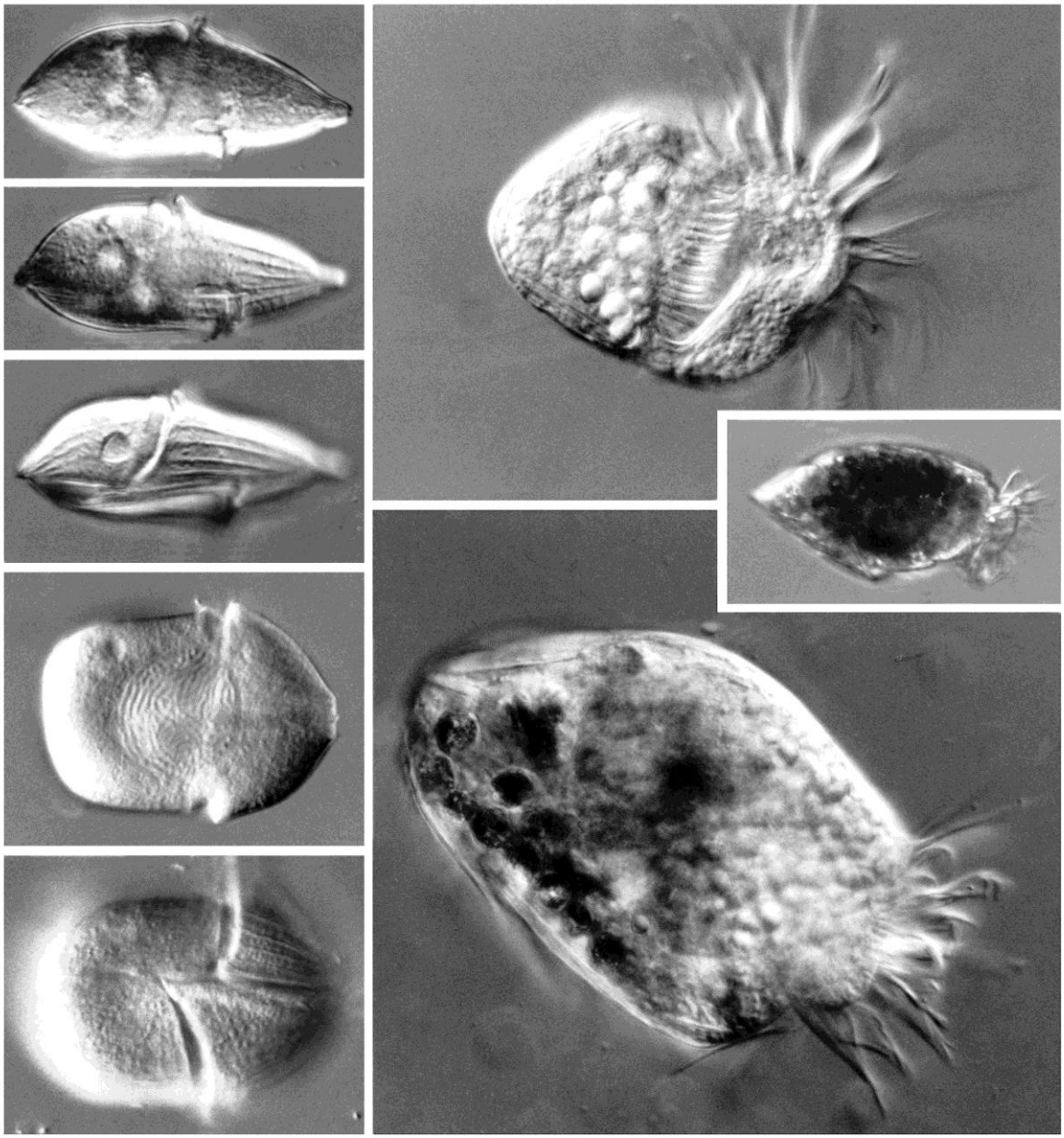

Dinoflagellates and ciliates from the NEW Polynya. Photo: Helge Abildhauge Thomsen

Growth potential of high Arctic heterotrophic dinoflagellates and ciliates in the North East Water (NEW) Polynya

Karen Riisgaard[1*], Peter Kofoed Bjørnsen[2], Nis Sand Jacobsen[1,4], Torkel Gissel Nielsen[1,3]

[1]National Institute of Aquatic Resources, DTU Aqua, Section for Oceanography and Climate, Kavalergården 6, 2920 Charlottenlund, Denmark.
[2]UNEP-DHI Centre, Agern Allé 5, 2970 Hørsholm, Denmark
[3]Greenland Climate Research Centre, Greenland Institute of Natural Resources, PO Box 570, 3900 Nuuk, Greenland
[4] Centre for Ocean Life, DTU Aqua, 2920 Charlottenlund, Denmark

ABSTRACT

Succession and growth potential of heterotrophic dinoflagellates and ciliates were studied in the Northeast Water (NEW) Polynya, North East Greenland. Biomass of protozooplankton (>10 µm) was dominated by gymnodoid dinoflagellates and oligotric ciliates and peaked together with the diatom dominated bloom at the ice edge. Growth rate of representative heterotrophic dinoflagellates and ciliates were measured in raw cultures at temperatures from -1.7 to 5^{o}C. The growth rates were in the range 0.13 to 0.43 d^{-1} and were positively correlated to temperature. The average Q_{10} was 3.8 ± 1.9 between -1.7 °C and 5 °C. A multivariate linear regression model correlating growth rate with temperature and cell volume was made with data combined from present study and growth rates from the literature. The highest abundance and biomass of heterotrohic dinoflagellates and ciliates were found in association with phytoplankton blooms in waters where the temperature was well below the freezing point. From the protozooplankton succession pattern we conclude that populations of heterotrophic dinoflagellates and ciliates are primarily controlled by their phytoplankton prey and predators and that temperature plays a minor role for succession of high Arctic ciliates and heterotrophic dinoflagellate populations.

KEY WORDS: NEW Polynya, heterotrophic protists, microzooplankton, growth rates, temperature

INTRODUCTION

Despite the prominent role of heterotrophic protists (protozooplankton) as grazers in the Arctic food web (Levinsen & Nielsen 2002), little is known about factors regulating their growth and abundance. Temperature is considered to the most important physical factors modulating growth of protozooplankton (Fenchel 1968, Finlay 1977, Müller & Geller 1993, Nielsen & Kiørboe 1994, Montagnes 1996, Weisse & Montagnes 1998, Levinsen & Nielsen 2002) and has been suggested as a major factor controlling protozooplankton in in the polar regions (Rose & Caron 2007). Metabolic processes (e.g. photosynthesis and growth) of polar autotrophic protists have been shown to double or triple when the temperature is increased 10 ^{o}C until until an optimum temperature level is reached (Montagnes et al. 2003). However, few studies have considered how hetetrotrophic protists respond to temperatures in the lower range of the scale (i.e. < 5 ^{o}C) (Lee & Fenchel 1972, Levinsen et al. 2000, Rose & Caron 2007). An exponential relationship between growth and increasing temperature has been documented for a number of temperate ciliates growing under food saturation in the temperature range 4 ^{o}C to 25 ^{o}C (Nielsen & Kiørboe 1994). For the other key group of arctic protozooplankton, the heteretrophic dinoflagellates, no temperature-growth rate relationships are available.

Polynyas are open-water areas within the polar ice packs that tend to re-occur at specific locations from year to year (Barber & Massom 2007). The sea surface temperature of polynyas is usually below the freezing point, but due to wind and ocean currents they stay ice-free wholly or partly of the year. Compared to the adjacent ice-covered waters, polynyas are areas of high productivity (Tremblay & Smith 2007) and thus important feeding and breeding habitats for top-predators such as seabirds and marine mammals including walruses, seals, whales and polar bears (Stirling 1997, Heide-Jørgensen et al. 2013). The polynya habitats are sensitive to climate changes and are as such objects for attention, but polynyas also provide us with key information on how ocean-atmospheric forcing and food-web structure may be changing in the Polar Regions under a future changing climate.

In Arctic polynyas the food web is centred around the short productive season (3-5 months) and especially the diatom bloom that develops just after the sea-ice breaks up or when the light returns in spring (Tremblay & Smith 2007). Copepods are the major metazoan herbivores in the Arctic polynyas during the summer grazing 10 to 55 % of the primary production in the NOW Polynya (Saunders et al. 2003) and on average 45 % of the primary production in the central NEW Polyna (Daly 1996). Appendicularians may however also contribute as substantial metazoan grazers in both the NOW Polynya (Acuña et al. 2002) and the NEW Polynya (Ashjian et al. 1995, 1997). In contrast to studies on metazoans few studies have considered the trophic role of protozooplankton in Arctic polynyas (Pesant et al. 1998, 2000), this despite documentation of high grazing capacities in Arctic waters elsewhere (Paranjape 1987; Verity et al. 2002; Levinsen & Nielsen 2002; Sherr et al. 2013).

The study was conducted in 1993 during a cruise in to the NEW Polynya, located from 79 to 81 °N on the continental shelf of North East Greenland. Of the 61 distinct reoccurring polynyas in the northern hemisphere, the NEW Polynya is one of the most intensively studied (Smith & Barber 2007). Throughout the 1990s the NEW Polynya was the largest recurrent polynya in the Arctic, but up through the first half of the 2000's the polynya gradually decreased in size and by 2007 it was almost non-existent (Barber & Massom 2007). Present study is from a cruise to the NEW polynya in 1993, when the polynya was close to its maximum size covering an area of ca. 44.000 km^2. The polynya remained open from approximately May to end of September (Bohm et al. 1997).

The aim of present study was to document the role of heterotrophic dinoflagellates and ciliates in the high Arctic marine systems and investigate their growth response to temperatures from -1.7 to 5 ^oC covering the range of water temperatures met in their Arctic environment.

MATERIAL & METHODS

Locality and sampling

Sampling and experiments were conducted in The North East Water (NEW) Polynya on the continental shelf of North East Greenland from May 22nd to August 2nd during leg I and II of the RV Polarstern Cruise in 1993 (cruises ARK IX/2 and 3), (Fig 1). The NEW Polynya is limited to the North, South and West by ice barriers and to the East by land associated with pack ice. A total transect of 10 stations were sampled once from July 4th to July 8th (80" 02'N, 16'23'W to 80" 33'N, 10'03'W) covering a wide range of ice cover, temperature and nutrient conditions. One time series station (st. 138) was sampled 6 times from May 25th to July 27th. On each location vertical profiles of temperature, salinity, chlorophyll *a* (Chl *a*) and nutrients were taken with a SeaBird CTD/Rosette equipped with Niskin bottles. Water for Chl *a* was filtered through Whatman GFF/F glass-fiber filters and size fractionated on 5 µm Poretic filters. All filters were extracted in 10 ml acetone in the dark. Concentrations of Chl *a* were determined on a Turner and converted to phytoplankton biomass (mg C m^{-3}) by using a carbon conversion factor of 42.7 (Juul-Pedersen et al. 2006).

Heterotrophic dinoflagellates and ciliates. The abundance of heterotrophic dinoflagellates and ciliates were estimates at 5 depths covering the upper 150 m. Heterotrophic nano-dinoflagellates (<20 µm) were estimated from samples fixed by 1 % glutaraldehyde and determined by epifluorescense microscopy on filters stained by proflavine (Haas 1982). The diameters of 100 cells per filter were measured, and biomass was calculated assuming spherical shape and a conversion factor of 0.12 pg C $µm^{-3}$ (Hansen et al. 1997). Micro-protozooplankton (>20 µm) were estimated from 250 ml subsamples fixed in Lugol's solution (1% final concentration). Samples were kept dark and cold until examination. All cells in two 50 ml Utermöhl chambers were counted using an inverted microscope. Plasma volumes were calculated using suitable geometric forms. Volumes were converted into biomass using a factor of 0.19 pg C um^{-3} for ciliates (Putt & Stoecker 1989)

and the equation: Log_{10} pg C $cell^{-1}$= -0.353 + 0.864 Log_{10} volume (μm^3) for heterotrophic dinoflagellates (Menden-Deuer & Lessard 2000).

Growth experiments

Sampling and laboratory analysis. The experiments were based on a raw culture established on June 8 1993 from Station 60 (Fig 1). Surface water was taken from 6.5 m depth using a SeaBird CTD/Rosette equipped with Niskin bottles. The sampler was carefully drained to a 2 l polycarbonate bottle at arrival on deck. Immediately after sampling, the water was brought to a cold container (2 °C). To remove larger predators and copepod eggs, water was reverse filtrated trough a 50 μm sieve and transferred into a 2 l polycarbonate bottle provided with B_1 medium (Hansen 1989). The bottle was mounted on a plankton wheel (1 rpm) and incubated in continuous light of 20 μE $m^{-2}s^{-1}$.

Experimental set-up. After four weeks of incubation on the plankton wheel (July 2nd) a dense phytoplankton population (dominated by diatoms and *Pyramimonas*) had developed as well as a community of ciliates and heterotrophic dinoflagellates. Two ciliate species; *Strombidium* sp. (small) and *Strombidium* sp. (large) respectively and two heterotrophic dinoflagellates species (*Gyrodinium spirale* and *Gymnodinium rubrum*) dominated in the culture and were chosen for the temperature experiments.

The raw culture was reverse filtered through a 80 μm sieve, diluted with 3.5 l 0.2 μm filtered surface water and 0.5 l B_1 medium. The diluted raw culture was distributed into 8 600 ml Nalgene polycarbonate bottles and incubated pair vice at 5 (4.93 ± 0.17), 2 (1.94 ± 0.24), 0 (0.01 ± 0.04) and -1.7 (-1.73 ± 0.13) °C. The temperature in the two "low temperature treatments" (-1.7 and 0 °C respectively) was kept constant by keeping the experimental bottles in 10 l plastic basins with 34 PSU water (-1.7 °C) or ice cold fresh water (0°C). The bottles incubated at 2 °C and 5 °C were kept in a 2 °C or 5 °C cooler respectively. To keep the plankton suspended, the bottles were rotated by hand every 3 h trough out the experiment.

Sampling. Every 3h temperature was measured and ice was added to adjust the temperature in the two low temperature treatments. The bottles were sampled every 48 h. A sub-sample of 100 ml was fixed in 1 % Lugol's solution and transferred to 50 ml Utermöhl chambers. All cells in two settling chamber were counted using an inverted microscope.

Specific growth rate (μ, d^{-1}) of dinoflagellates and ciliates was calculated according to the equation:

$$\mu = \frac{Ln\ N_1 - Ln\ N_0}{t_1 - t_0} \qquad \text{(eq. 1)}$$

where N_0 and N_1 are numbers of cells at time t_0 and t_1.

Production rate (g C m^{-2} d^{-1}) of heterotrophic dinoflagellates and ciliates was estimated from biomass and specific growth rates (μ).

The temperature coefficient Q_{10} was calculated from the power function (Van't Hoff 1984):

$$Q_{10} = (\mu_1/\mu_2)^{10/(t_1-t_2)}, \quad \text{(eq. 2)}$$

where μ_1 and μ_2 are growth rates at any pairs of temperature t_1 and t_2.Plasma volumes of the protists were calculated using geometric shapes: *Gyrodinium spirale*: two cones, *Gymnodinium rubrum* and *Strombidium* spp.: rotational ellipsoid.

To investigate the temperature dependence for protists growing within a broader temperature range (-1.7 to 25 ^{o}C), data on maximum growth rate (μ_{max}) of heterotrophic dinoflagellates and ciliates was compiled from the literature. The dataset included 28 species of heterotrophic dinoflagellates (24 studies, table 2) and four size-classes of ciliates (26 species or morphotypes) obtained from Nielsen & Kiørboe (1994). Temperature and cell volume have previously been identified as major controlling factors for estimating growth during prey saturation (Nielsen & Kiørboe 1994) and accordingly temperature and cell volume were investigated as variables for a temperature-body volume dependent growth correlation for heterotrophic dinoflagellates and ciliates.

The relationships between maximum growth rate and temperature-body volume were tested for significance using a multivariate linear model for heterotrophic dinoflagellate and ciliate respectively. The analysis was performed in R 3.01 using an F-test to determine if the slope was significantly different from 0. In both cases the model that explained most of the variation was achieved by log transforming the growth rate and the cell volume. The residuals were checked for normality using QQ-plots and one outlier was omitted from the heterotrophic dinoflagellate dataset. No interacting effects were found between temperature and cell size.

RESULTS

Horizontal and temporal development in ice, nitrate and chlorophyll

The ice cover along the transect was characterized by a thin ice cover from station 134 to 142 and open water from station 143-145 (Fig. 1). The surface water temperature (ca. 5 m depth) ranged from -1.7 to 1.9 °C from West to East of the transect, with highest temperature at station 144 (Fig. 2A). At the ice-covered stations (134-142) nitrate concentrations were high; > 2 µM , but were depleted at the most of the open water stations with a minimum of 0.02 µM at station 144 (Fig. 2A). Chl *a* maximum was found close to the surface (0.5-15 m) with maximum of 2 mg m^{-3} at the open water stations; st. 142-145 (Fig. 3A).

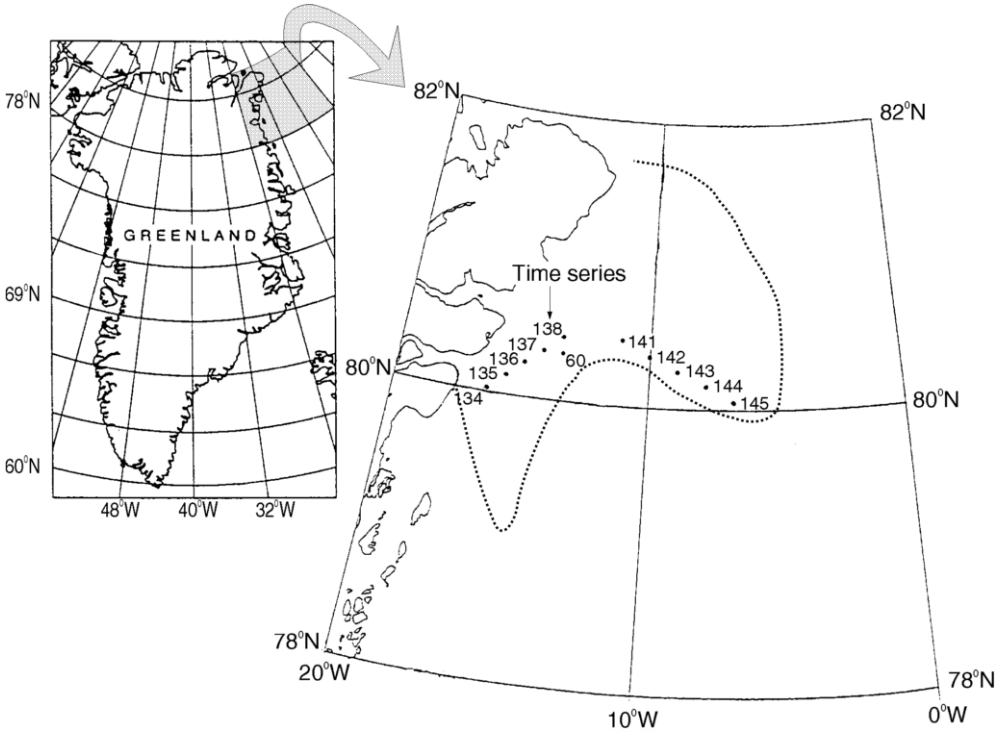

Fig. 1. Map of the sample area: The North East Water (NEW) Polynya located 79 °N at the North Eastern Greenland coast. The dotted line indicates the ice-edge: i.e. the eastern distribution of the polynya on July 5th. The experiments were based on a raw plankton sample collected at station 60.

The time series station was covered with ice until late June where the ice gradually broke up. Through the period May 28th to July 26th temperatures in the surface waters increased from -1.7 to 4.6 °C (Fig. 2B). Short after the ice broke up, a phytoplankton bloom developed with a peak on July 12th (Fig. 3B). As the phytoplankton bloom developed nitrate was depleted in the surface waters from >3 µM in late spring to <0.05 µM in July (Fig. 2B). Highest Chl *a* values was recorded sub-surface at 10-20 m depth (Fig. 3B).

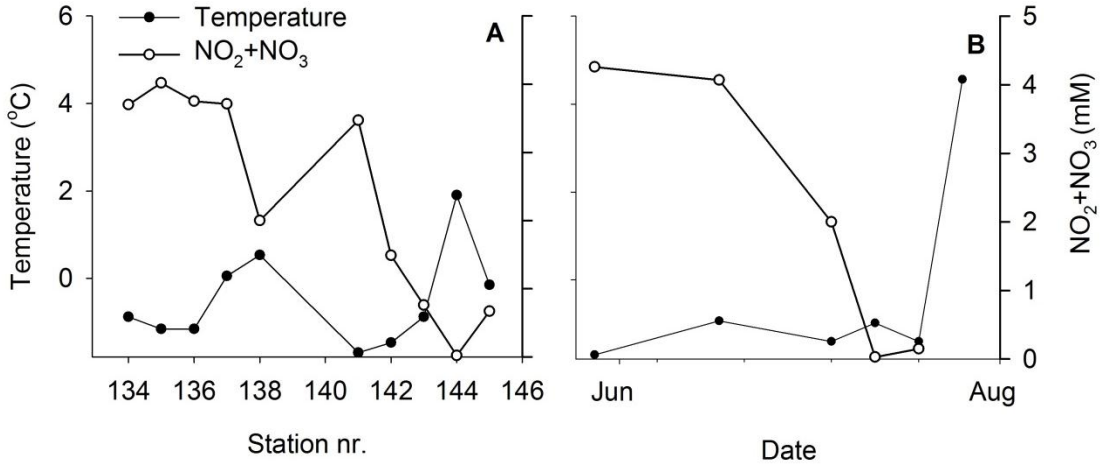

Fig. 2. (A) Horizontal and (B) temporal development in sea surface temperature (^{o}C) and sea surface NO_2 + NO_3 (mM).

Horizontal and temporal distribution of hetetrotrophic protists

At all stations, heterotrophic dinoflagellates and ciliates were found in the upper 50 m, with subsurface maxima at 10-20 m depth (Fig. 3C-F). Along the transect, heterotrophic micro-dinoflagellates and ciliates reached a maximum at station 143 with concentrations reaching 7 cells ml^{-1} and 4 cells ml^{-1} for heterotrohic dinoflagellates and ciliates respectively (Fig. 3C and E). At the time series station maximum concentrations of large micro-protozooplankton was reached July 12th reaching 3 cells ml^{-1} and 1 cell ml^{-1} for heterotrophic dinoflagellates and ciliates respectively (Fig. 3D and F). In all samples large (>10 µm) protozooplankton were dominated by naked gymnodioid heterotrophic dinoflagellates and naked oligotrich ciliates. The major dinoflagellate genera were *Gyrodinium*, *Gymnodinium* and *Amphedinium*. *Gyrodinium spirale* contributed with 2 to 43 % (9 % on average) of the biomass of the dinoflagellates >20 µm. The most abundant ciliate genera were *Strombidium* and *Strobilidium*.

The integrated phytoplankton biomass ranged from 0.1 to 1.6 g C m^{-2} along the transect and from 0.04 to 1.7 g C m^{-2} at the time series station (Fig. 4A-B). Along the transect, micro-protozooplankton biomass peaked in association with the phytoplankton bloom with a maximum of 0.8 g C m^{-2} (Fig. 4C). At the time series station dinoflagellates and ciliates reached a maximum two weeks later than the phytoplankton bloom with peak values of 0.5 g C m^{-2} (Fig 2D). Dinoflagellates dominated the protozooplankton biomass at all investigated stations where sea-ice was still present. When the ice-cover disappeared and the phytoplankton biomass increased to higher values (> 1 mg C m^{-2}), ciliates became the major contributor to the biomass. The biomass of heterotrophic nano-dinoflagellates was dominated by *Gymnodinium/Gyrodinium* species. Heterotrophic micro-dinoflagellates were dominated by 20-30 µm *Gymnodinium/Gyrodinium* species and >50 µm *Gyrodinium spirale*. The ciliate biomass was mostly made up by >50 µm *Strombidium* spp. Small heterotrophic dinoflagellates dominated both in numbers and biomass at most of the transect stations. However, when Chl *a* peaked at station 143, micro-protozooplankton

contributed with 49 % of the integrated (0-50 m) biomass of heterotrophic dinoflagellates and ciliates.

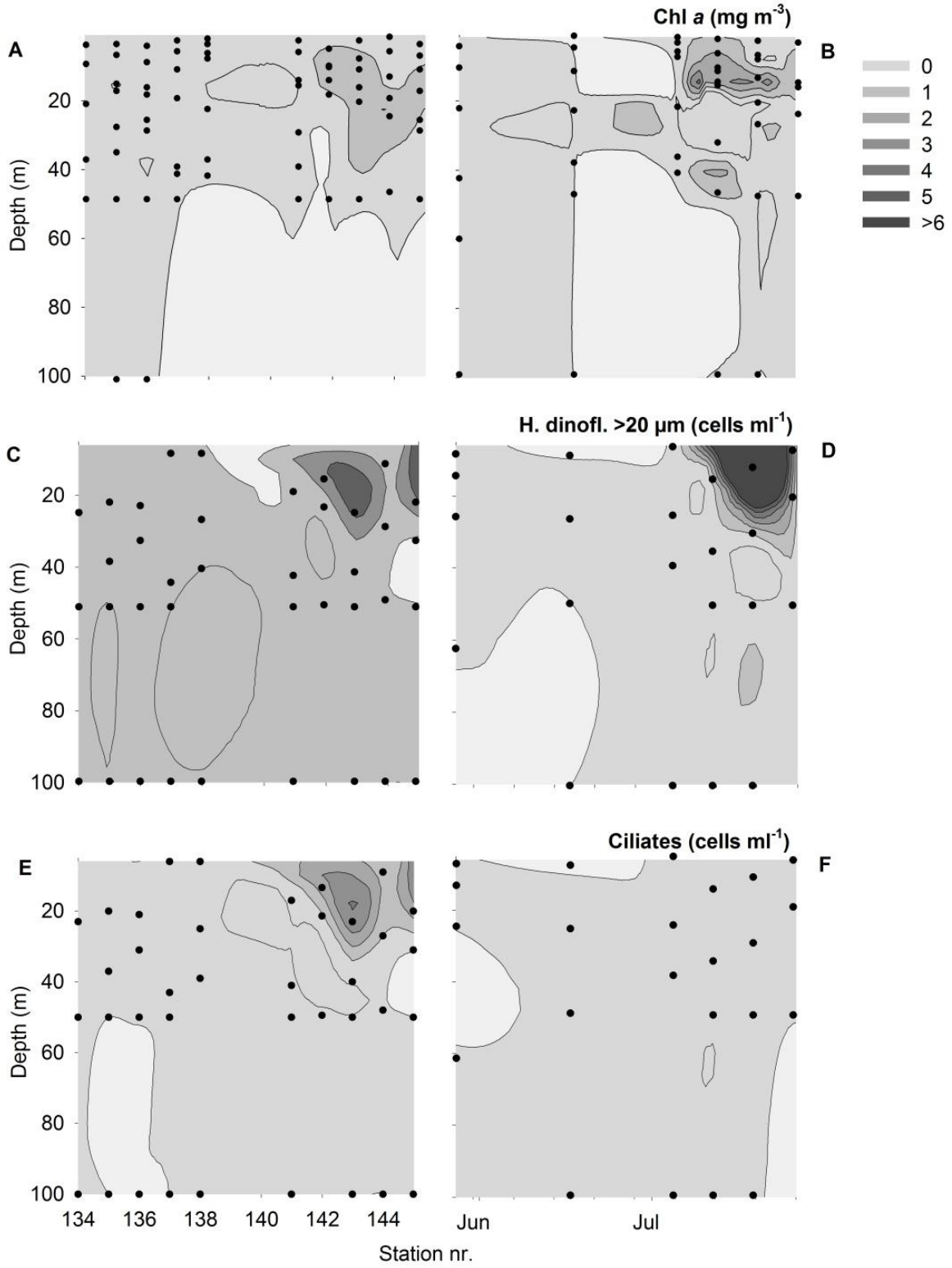

Fig. 3. Vertical distribution of Chl *a* (A-B), >20 µm heterotrophic dinoflagellates (H. dinofl.) (C-D) and > 20 µm

ciliates (E-F). Left panel: data from the transect stations. Right panel: data collected from May to July at the time series station. Values are only shown from the upper 100 m of the water column. Sampling depths are marked with: ●.

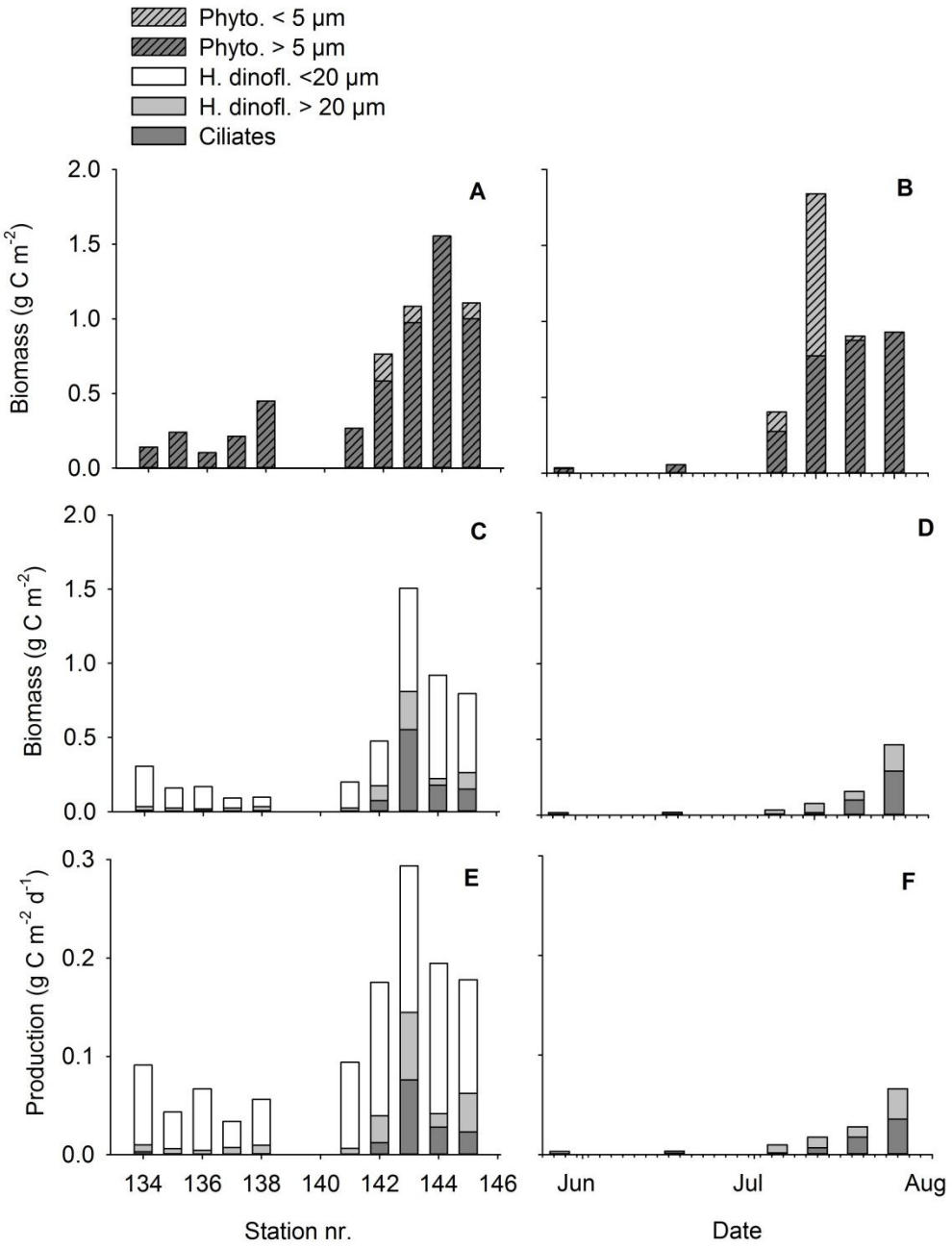

Fig. 4. Horizontal (left panel) and temporal (right panel) development A-B) phytoplankton (phyto.) biomass (g C m^{-2}), C-D) biomass of heterotrophic dinoflagellates (H. dinofl.) and ciliates (g C m^{-2}) E-F) production of heterotrophic dinoflagellates and ciliates (g C m^{-2} d^{-1}). Production rates of heterotrophic dinoflagellates and ciliates are estimated from *in situ* biomass and maximum potential growth rates calculated from Eq. 3 and Eq. 4. Values are integrated in the upper 50 m of the water column.

Growth rate in relation to temperature

The effect of temperature on growth rate (μ, d^{-1}) of heterotrophic dinoflagellates and ciliates was studied at four temperatures (-1.7, 0, 2 and 5 °C) using two heterotrophic dinoflagellate species; *Gyrodinium spirale* and *Gymnodinium rubrum*, and the two ciliate species; *Strombidium* sp. (small) and *Strombidium* sp. (large) (Fig. 5). Cell volumes are given in Table 1. Specific growth rates at the four temperatures were estimated using only data from the exponential phase of the growth curves (r^2 >0.80, $p < 0.05$, represented as solid lines in Fig. 6A-H and Fig. 7A-H). The growth rates of all four study organisms were positively correlated with temperature ($p < 0.01$, Fig. 8A-D). Q_{10} of the four species were on average 3.75 ± 1.93 between -1.7 and 5 °C (Table 1).

Tabel 1. Volume and Q_{10} values (± SD) of the heterotrophic dinoflagellate species; *Gyrodinium spirale* and *Gymnodinium rubrum* and the two ciliates *Strombidium* sp. (small) and *Strombidium* sp. (large).

	Volume ($10^3 \mu m^3$)	Q_{10} (-1.7 to 0 °C)	Q_{10} (0 to 2 °C)	Q_{10} (2 to 5 °C)	Q_{10} (-1.7 to 5 °C)
Gyrodinium spirale	18.3 ± 1.3	23.41 ± 12.52	1.82 ± 0.21	3.14 ± 0.87	6.85 ± 0.97
Gymnodinium rubrum	48.9 ± 3.1	2.65 ± 0.50	3.54 ± 0.86	1.62 ± 0.48	3.15 ± 0.64
Strombidium sp. (small)	67.8 ± 2.7	1.07 ± 0.02	2.99 ± 0.63	1.97 ± 0.12	2.10 ± 0.13
Strombidium sp. (large)	222.0 ± 9.1	3.52 ± 0.85	2.90 ± 0.60	1.71 ± 0.01	2.90 ± 0.16

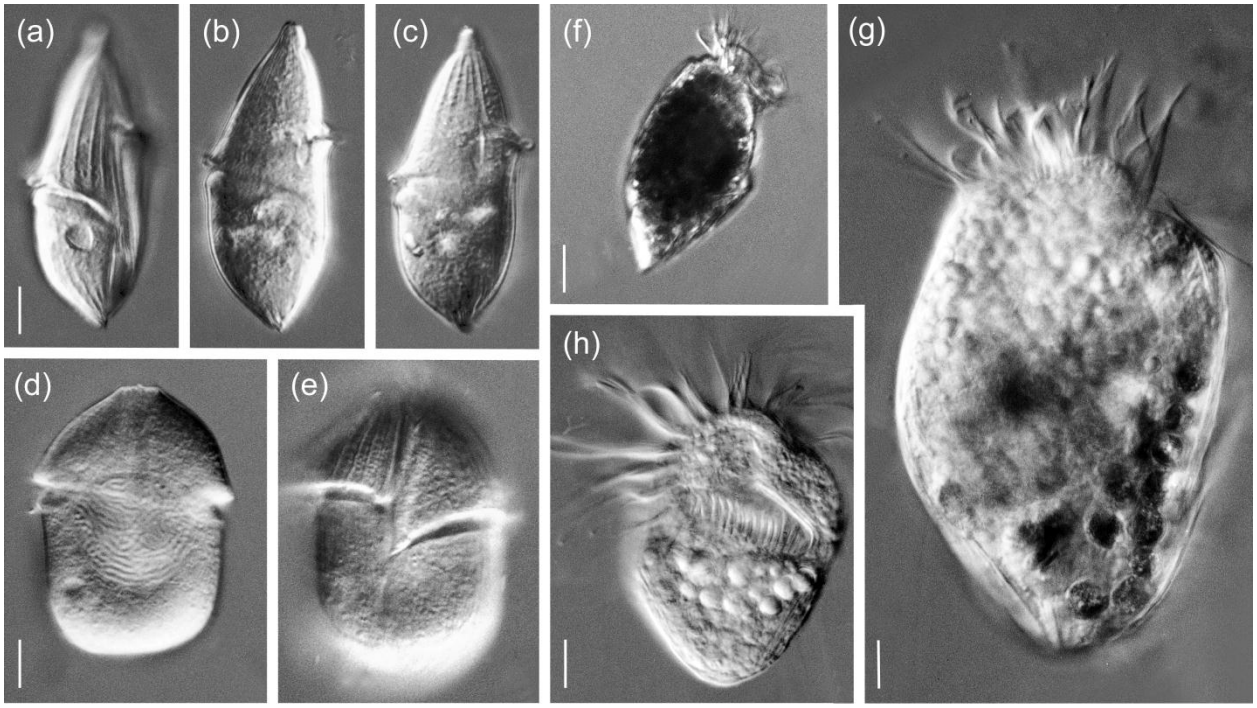

Fig. 5. (a-c) *Gyrodinium spirale* (d-e), *Gyrodinium rubrum*, (f-g) *Strombidium* sp. (large) and (h) *Strombidium* sp. (small).

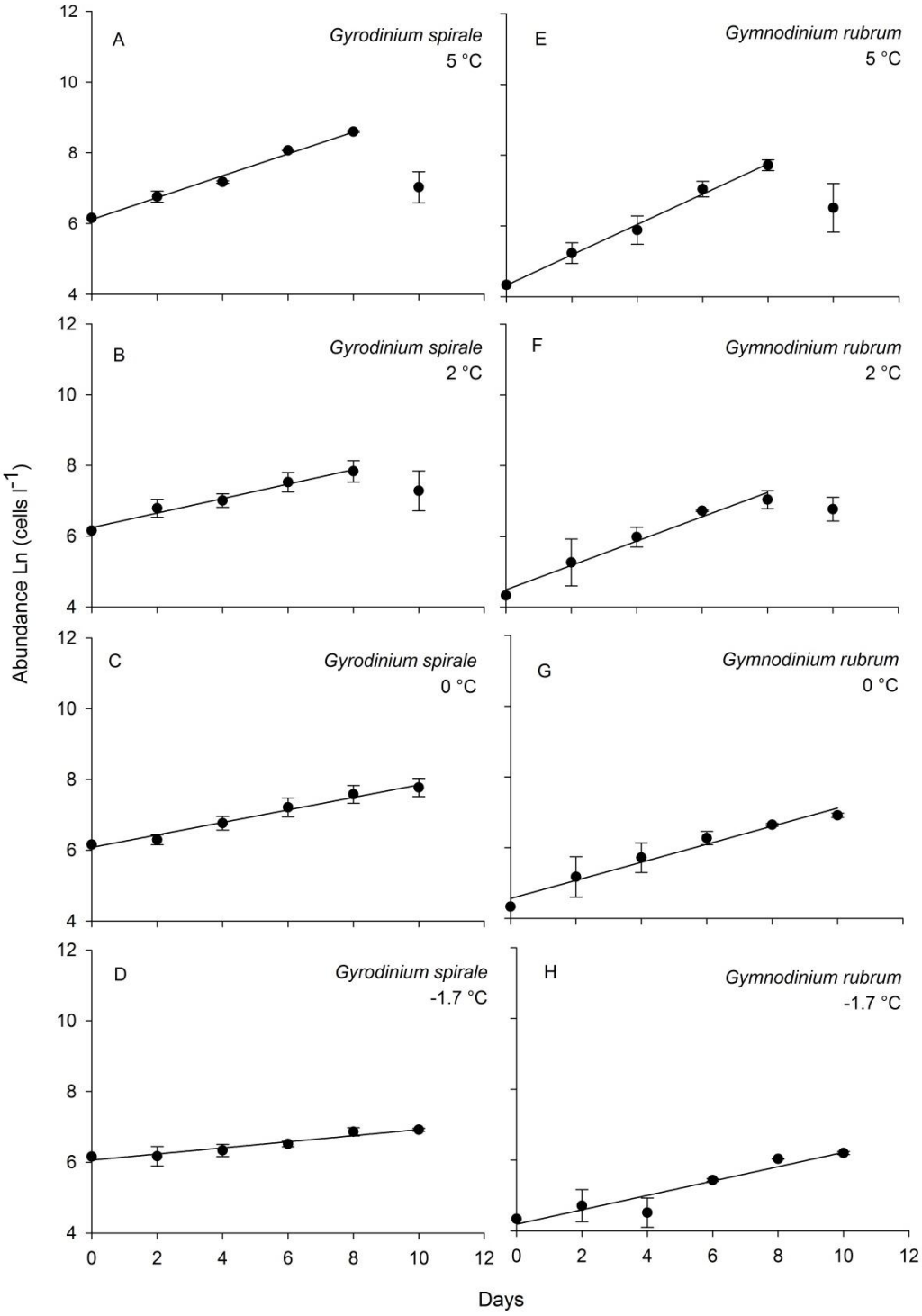

Fig. 6. Changes in cell numbers of *Gyrodinium spirale* (left panel) and *Gymnodinium rubrum* (right panel) in raw cultures at 5, 2, 0 and -1,8 °C. Data points represent treatment means ± SD (n = 2).

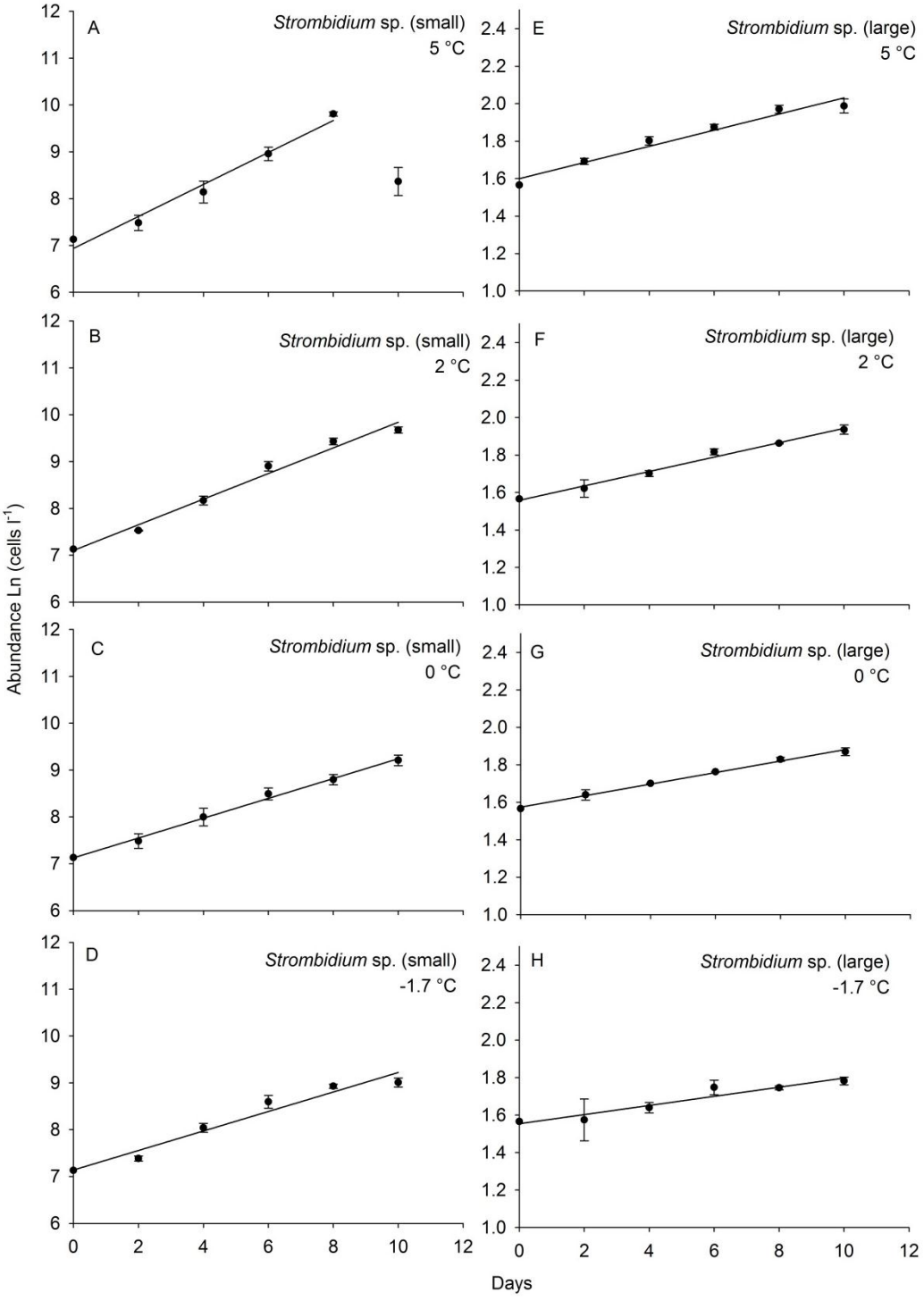

Fig. 7. Changes in cell numbers of *Strombidium* sp. 1 (left panel) and *Strombidium* sp. 2 (right panel) in raw cultures at 5, 2, 0 and -1.7 °C. Data points represent treatment means ± SD (n = 2).

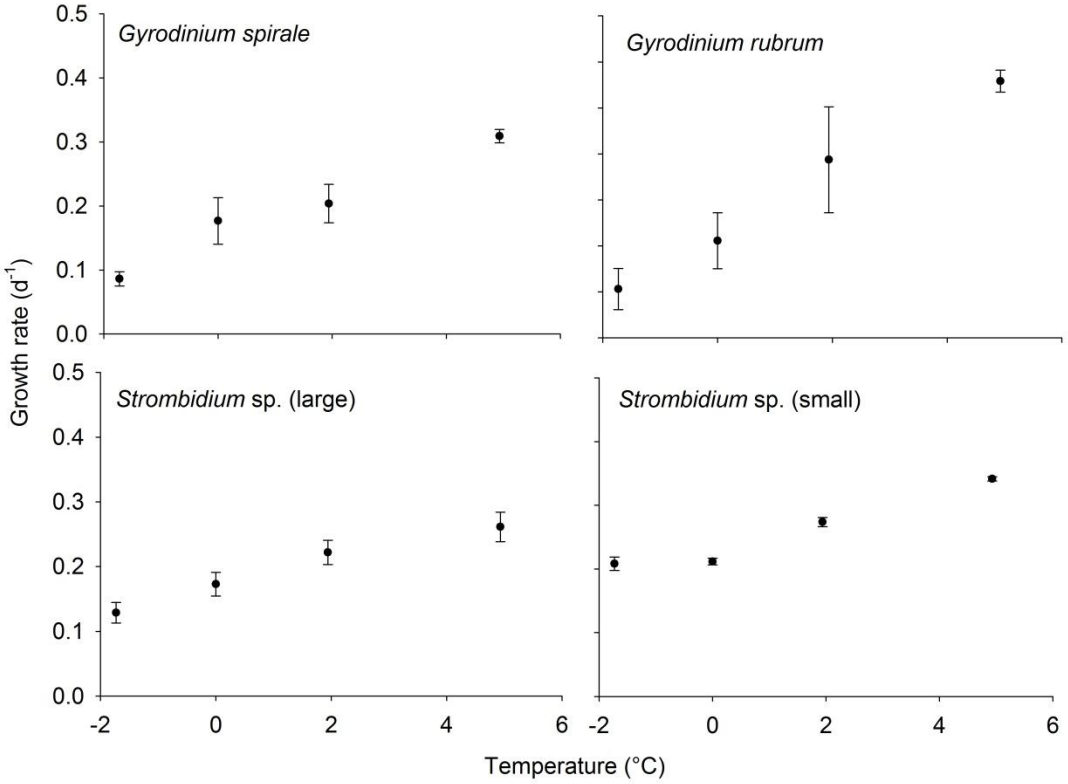

Fig. 8. Response of growth rate (μ, d^{-1}) to temperature (°C) of two heterotrophic dinoflagellate species (A-B) and two ciliate species (C-D). Data points represent mean ± SD (n = 2).

The multivariate linear regression showed that growth rates of heterotrophic dinoflagellates were highly correlated with temperature and log transformed body volume (eq. 3), explaining 71% of the variation ($p < 0.0001$ $r^2 = 0.71$). The same relationship was observed for ciliates, which explained 89% of the variation ($p < 0.0001$, $r^2 = 0.89$).

The strongest correlation was found between temperature and growth rate (μ, d^{-1}) for both heterotrophic dinoflagellates and ciliates (Fig. 9).

Heterotrophic dinoflagellates: $\text{Ln}\ \mu_{max} = 0.07\ T - 0.17\ \text{Ln}V - 0.09$, (eq. 3)

Ciliates: $\text{Ln}\ \mu_{max} = 0.095\ T - 0.13\ \text{Ln}V - 0.17$, (eq. 4)

Where T (^{o}C) is *in situ* temperature and V is cell body volume (μm^3).

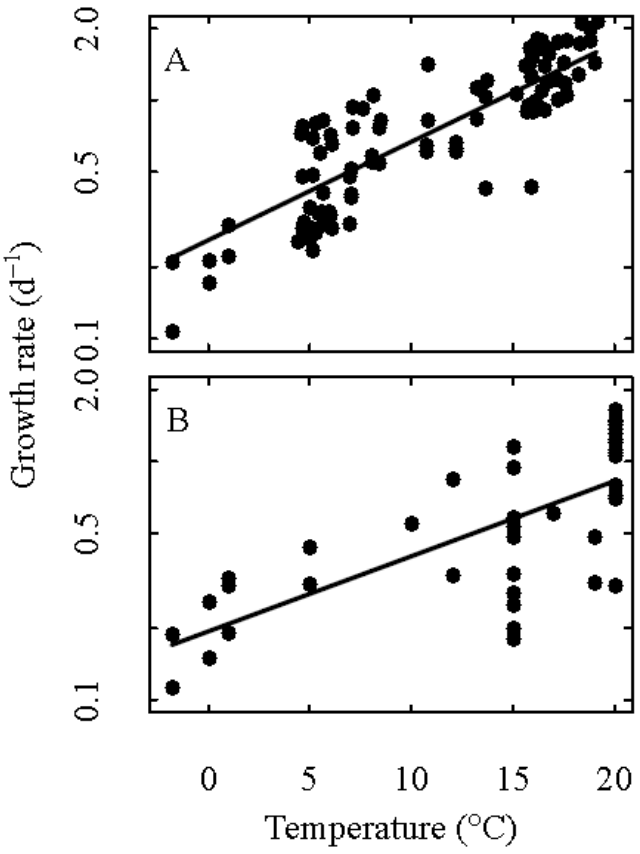

Fig. 9. Growth rates of (A) ciliates and (B) heterotrophic dinoflagellates as a function of temperature. Lines are predicted values according to Eq. 3 and Eq. 4, with cell volume modelled as the mean in the measurements.

Maximum potential community production of heterotrophic dinoflagellates and ciliates in the NEW Polynya was estimated from μ_{max} (Eq. 3 and 4) and the *in situ* biomass of heterotrophic dinoflagellates and ciliates assuming food saturation. Production of nano-protozooplankton averaged 0.09 ± 0.04 g C m^{-2} d^{-1} along the transect with dinoflagellates contribution the most (Fig. 4E-F). The production of micro-protozooplankton averaged 0.03 ± 0.04 mg C m^{-2} d^{-1} along the transect and 0.02 ± 0.02 mg C m^{-2} d^{-1} at the time series station. Note that the times series station do not include the heterotrophic nano-dinoflagellates.

Table 2. Maximum growth rate (μ_{max}) and body volume for heterotrophic dinoflagellates species grown at different temperatures.

Species	Growth rate (d^{-1})	Body volume (μm^3)	Temp. (^oC)	Source
Amphedinium	0.6	3150	15	Hansen (1992)
Diplopsalis lenticula	0.3	124788	15	Naustvoll (1998)
Gymnodinium	0.9	905	15	Jakobsen and Hansen (1997)
Gymnodinium sp.	0.3	1250	1	Bjørnsen and Kuparinen (1991)
Gymnodinium sp.	0.8	900	12	Strom (1991)
Gyrodinellum shiwhaense	1.0	1160	20	Jeong et al. (2011)
Gyrodinium dominans	0.5	10400	15	Hansen (1992)
Gyrodinium dominans	0.6	3300	17	Schmoker et al. (2011)
Gyrodinium hirobi	1.2	2758	20	Jacobsen and Anderson (1986)
Gyrodinium sp.	1.2	250	15	Hansen (1992)
Gyrodinium spirale	0.1	18300	-1.8	Present study
Gyrodinium spirale	0.1	18300	0	Present study
Gyrodinium spirale	0.2	18300	1	Present study
Gyrodinium spirale	0.3	18300	5	Present study
Gyrodinium spirale	0.5	18300	10	Present study
Gyrodinium spirale	0.5	11500	15	Hansen 1992
Gyrodinium spirale	0.8	134701	20	Kim and Jeong (2004)
Gyrodinium rubrum	0.2	48900	-1.8	Present study
Gyrodinium rubrum	0.3	48900	0	Present study
Gyrodinium rubrum	0.3	48900	1	Present study
Gyrodinium rubrum	0.4	48900	5	Present study
Luciella masanensis	1.5	10306	20	Jeong et al. (2007)
Oblea rotunda	0.7	6130	20	Strom and Buskey (1993)
Oxyrrhis marina	1.4	15902	20	Jeong et al. (2003)
Oxyrrhis marina	1.3	6300	20	Goldman and Dennett (1989)
Pfiesteria piscicida	1.5	15599	20	Jeong and Latz (1994)
Polykrikos kofoidii	1.1	344791	20	Jeong et al. (2001)
Protoperidinium conicum	1.1	399795	12	Menden-Deuer et al. (2005)
Protoperidinium crassipes	0.3	204000	19	Jeong and Latz (1994)
Protoperidinium divergens	0.5	119000	19	Jeong and Latz (1994)
Protoperidinium excentricum	0.3	192193	12	Menden-Deuer et al. (2005)
Protoperidinium hirobus	1.2	6400	20	Jacobson and Anderson (1993
Protoperidinium huberi	0.7	77952	20	Buskey et al. (1994)
Protoperidinium pallidum	0.3	423883	15	Naustvoll (2000)
Protoperidinium pellucidum	0.3	25300	15	Hansen (1992)
Protoperidinium pellucidum	0.7	197065	20	Buskey et al. (1994)
Protoperidinium spinifriferum	0.3	381704	20	Jacobsen and Anderson (1986)
Protoperininium bipes	1.4	1988	20	Jeong et al. (2004)
Protoperininium steinii	0.2	71936	15	Naustvoll (2000)
Protoperodinium vorax	1.1	38792	20	Siano and Montresor (2005)
Stoeckeria algicida	1.6	11249	20	Jeong et al. (2005)
Zygbikodinium divergens	0.2	523599	15	Naustvoll (2000)

DISCUSSION

Succession of heterotrophic dinoflagellates and ciliates in the NEW Polynya

Within the last decades the potential of protozooplankton as grazers (Paranjape 1987, Sherr et al. 1997, 2009, Verity et al. 2002) and as prey (Levinsen et al. 2000, Campbell et al. 2009) in Arctic ecosystems have been documented. The present study supports that high concentrations of heterotrophic dinoflagellates and ciliates are to be found even in high Arctic polynyas despite temperatures below 0^{o}C. The seasonal succession of heterotrophic dinoflagellates and ciliates followed the same pattern as in other high latitude waters such as the Young Sound and Kongsfjorden (79 ^{o}N) (Rysgaard et al. 1999, Seuthe et al. 2011) with peak abundances associated with the diatom dominated phytoplankton bloom in late summer. Along the transect, peak abundance was found in association with the ice edge where the average temperature were < 1 °C. This distribution pattern indicates that temperature only plays a minor role in regulating the heterotrophic dinoflagellates and ciliate communities in the NEW Polynya, and that these protists are rather controlled by their phytoplankton prey and possible by predators such as copepods.

Assuming a productive season of 75 days and average protozooplankton production rates obtained from present study, heterotrophic dinoflagellates and ciliates produce 1.6 g C m^{-2} yr^{-1} (contributing with 50 % each). These values are of the same magnitude as the Kongsfjord (Seuthe et al. 2011), where the annual production has been estimated to 0.4 and 0.5 g C m^{-2} yr^{-1} for ciliates and dinoflagellates respectively. The annual primary production (May to August 1992 and 1993) in the NEW Polynya is on average ~20 g C m^{-2} yr^{-1} (Smith Jr. 1995, Pesant et al. 1998, 2000). Kongsfjorden is located at same latitude as NEW Polynya, but due to inflow of warm Atlantic water the fjord stays ice-free for a longer period than the NEW Polynya. Despite this annual primary production in the Kongsfjord is similar to the NEW Polynya: ~30 g C m^{-2} yr^{-1} (Iversen & Seuthe 2011). Applying a literature value for gross growth efficiency of 33% (Hansen et al. 1997), maximum potential grazing by dinoflagellates and ciliates is estimated to 5.3 g C m^{-2} yr^{-1} in the NEW Polynya and 3.0 in the Kongsfjord. This is equivalent to 27 % and 10 % of the annual primary production at the two sites respectively. Thus despite a shorter productive season and notably colder waters, micro-protozooplankton may recycle a similar proportion of the primary production in the NEW Polynya as in the Kongsfjord or even higher. Although significant, this grazing impact by protozooplankton is low compared to the high productive Disko Bay, Midwest Greenland, where protozooplankton have been estimated to graze 55% of the annual primary production (Levinsen & Nielsen 2002). The estimate of primary production grazed by protozooplankton in the NEW Polynya does not consider heterotrophic nano-dinoflagellates. Also it does not consider other carbon sources than phytoplankton, such as copepod fecal pellets that are known to be degradated primarily by protozooplankton in temperate waters (Poulsen & Iversen 2008). Since copepod fecal pellet-production is high in the NEW Polynya (Daly 1996), these packages of food, could have made up a substantial part of the particular organic carbon (POC) consumed by protozooplankton.

Growth and temperature dependence

We here present the first study of growth rate of heterotrophic dinoflagellates and ciliates as a function of temperature in the range -1.7 to 5 °C. The maximum growth rate was found at 5 °C for all four species and was in the range 0.30-0.43 d^{-1}. At the two low temperature treatments (-1.7 °C and 0 °C) all four species were still growing close to maximum values predicted by Rose & Caron (2007) and near maximum rates (0.26 d^{-1}) obtained by Rose et al. (2013) at 0°C. Reductions in growth rates as a function of reduced temperature was thus within same magnitude as would have been expected in the higher end of the temperature scale (>5 °C and <20 °C) as suggested by Lee & Fenchel (1972).

Temperature dependency of protozooplankton is well documented (Fenchel 1968, Finlay 1977, Müller & Geller 1993, Nielsen & Kiørboe 1994, Montagnes 1996, Rose et al. 2013). In general the rate of change in growth with temperature can be described with the power function: $Q_{10}= (\mu_1/\mu_2)^{(10/(t1-t2)}$, where μ is the specific growth rate (d^{-1}) and t is the temperature (°C). Protozooplankton growing at their maximum rate have a Q_{10} between 1.5 and 4 (Hansen et al. 1997, Rose & Caron 2007), while higher Q_{10} values suggest temperature-limitation. The Q_{10} value derived from present study was on average 3.8 for the four investigated species between -1.7 °C and 5 °C (Table 1). This relatively low Q_{10} value indicates that although these Arctic species are growing under extreme temperature conditions, they grow within their maximum limits at the given temperature.

Several models have been used to predict maximum growth rate of heterotrophic dinoflagellates and ciliates (Montagnes. DJS et al. 1988, Müller & Geller 1993, Nielsen & Kiørboe 1994, Rose & Caron 2007), but none of these consider the temperature scale below 4 °C. Our data support an exponential relationship between body volume and growth rate and between temperature and growth rate for both heterotrophic dinoflagellates and ciliates in the temperature range -1.7 to 25 °C, which is comparable to the equation found for ciliates at temperatures in the range 4 to 25°C (Nielsen & Kiørboe 1994). Similar to the regression by Nielsen and Kiørboe (1994) the strongest correlations were found between temperature and growth rate.

Lee and Fenchel (1972) showed that ciliates isolated from the Southern Ocean had infinite survival between -2 and 10 °C, while ciliates isolated from temperate and tropical waters had infinite survival at higher temperatures. This indicates that polar heterotrophic dinoflagellates and ciliates have adapted to the permanently cold environment by achieving their maximum growth rate at a lower temperature than would be expected for similar species adapted to warmer waters at lower latitudes (Montagnes 1996, Weisse et al. 2001, Weisse et al. 2002). The equations presented here are expected to be valid only for protozooplankton subjected to the temperature range of which they have been adapted to.

Impact of higher temperatures on the Arctic marine food web

One of the most visible changes in the Arctic is the diminishing sea ice cover. Since the first satellite records in 1979 the perennial (summer minimum) sea ice extend has reduced with a rate of 9-12% per year (Comiso et al. 2008, Stocker et al. 2013). The trend is predicted to continue and the changes in sea ice cover are associated by major trophic changes. Brown and Arrigo (2013) observed that earlier sea-ice retreat in the Bering Sea resulted in relatively late phytoplankton blooms in open warmer waters (~3 °C) rather than earlier cold (<0.6 °C) ice edge related blooms. The expanded productive season has led to increases in primary production in the Arctic and the annual primary production is expected to increase even further in a future warmer Arctic (Stocker et al. 2013). The fate of this increased primary production in a warmer ocean is currently unknown. According to the most recent IPCC report, Arctic sea surface temperatures are projected to increase 3-5 ^{o}C by the end of the 21st century (Stocker et al. 2013) which will have major impact on the trophic dynamics: e.g. using the Q10 value 3.8 (present study), production of heterotrophic dinoflagellates and ciliates will increase with ~44% if the temperature is raised from -1.5 °C (mean *in situ* SST along the transect, present study) to 3 °C. Of course this back of an envelope calculation does not consider other changing parameters, but underlines the high growth potential of heterotrophic dinoflagellates and ciliates. Thus, although the annual primary production may increase, a larger fraction of the primary production will pass through a more active microbial food web rather than be channelled to higher trophic levels. Ecological models for predicting future gross primary production, net primary production and secondary production in Arctic marine waters are at present built on poor information on protozooplankton growth and grazing capacity (e.g. Slagstad et al. 2011). We hope that the present equations on protozooplankton temperature growth dependency will be used and provide an important brick in future food web models for northern ecosystems.

Acknowledgement: The authors wish to thank Alexandra C. Nielsen for logistic and technical support during the cruise and her effort in analyzing samples. We further acknowledge the captain and crew of R/V Polarstern.

LITTERATURE CITED

Acuña LJ, Deibel D, Saunders PA, Booth B, Hatfield E, Klein B, Mei Z, Rivkin R (2002) Phytoplankton ingestion by appendicularians in the North Water. Deep Sea Res II 49:5101–5115

Ashjian C, Smith S, Bignami F, Hopkins T, Lane L (1997) Distribution of zooplankton in the Northeast Water Polynya during summer 1992. J Mar Syst 10:279–298

Ashjian CJ, Smith SL, Lane PVZ (1995) The Northeast Water Polynya during summer 1992 : Distribution and aspects of secondary production of copepods. J Geophys Res 100:4371–4388

Barber DG, Massom RA (2007) The role of sea ice in Arctic and Antarctic polynyas. In: Smith WO, Barber DG (eds) Polynyas -windows to the world, first. Elsevier Oceanography Series, 74, Amsterdam, The Netherlands, p 1–54

Bjørnsen PK, Kuparinen J (1991) Growth and herbivory by heterotrophic dinoflagellates in the Southern Ocean, studied by microcosm experiments. Mar Biol 109:397–405

Bohm E, Hopkins TS, Minnett PJ (1997) Passive microwave observations of the Northeast Water Polynya interannual variability: 1978-1994. J Mar Syst 10:87–98

Brown ZW, Arrigo KR (2013) Sea ice impacts on spring bloom dynamics and net primary production in the Eastern Bering Sea. J Geophys Res 118:43–62

Buskey EJ, Coulter CJ, Brown SL (1994) Feeding, growth and bioluminescence of the heterotrophic dinoflagellate Protoperidinium huberi. Mar Biol 121:373–380

Campbell RG, Sherr EB, Ashjian CJ, Plourde S, Sherr BF, Hill V, Stockwell DA (2009) Mesozooplankton prey preference and grazing impact in the western Arctic Ocean. Deep Res Part II 56:1274–1289

Comiso JC, Parkinson CL, Gersten R, Stock L (2008) Accelerated decline in the Arctic sea ice cover. Geophys Res Lett 35:L01703

Daly KL (1996) Flux of particulate matter through copepods in the Northeast Water Polynya. J Mar Sys 10:319–342

Fenchel T (1968) The ecology of marine microbethos III. the reproductive potential of ciliates. Ophelia 5:123–136

Finlay BJ (1977) The dependence of reproductive rate on cell size and temperature in freshwater ciliated protozoa. Oecologia 30:75–81

Goldman JC, Dennett MR (1989) Dynamics of herbivorous grazing by the heterotrophic dinoflagellate Oxyrrhis marina. J Plankton Res 11:391–407

Haas LW (1982) Improved epifluorescence microscopy for observing planktonic micro-organisms. Ann Inst Ocean Paris 58:261–266

Hansen PJ (1989) The red tide dinoflagellate *Alexandrium tamarense*: effects on behaviour and growth of a tintinnid ciliate. Mar Ecol Prog Ser 53:105–116

Hansen PJ (1992) Prey size selection, feeding rates and growth dynamics of heterotrophic dinoflagellates with special emphasis on *Gyrodinium spirale*. Mar Biol 114:327–334

Hansen PJ, Bjørnsen PK, Hansen BW (1997) Zooplankton grazing and growth : scaling within the 2-2,000-µm body size range. Limnol Oceanogr 42:687–704

Heide-Jørgensen P, Burt LM, Hansen RG, Nielsen NH, Rasmussen M, Fossette S, Stern H (2013) The significance of the North Water Polynya to Arctic top predators. Ambio 42:596–610

Jacobsen DM, Anderson DM (1986) Thecate heterotrophic dinoflagellates: feeding behavior and mechanisms. J Phycol 22:249–258

Jacobson D, Anderson D (1993) Growth and grazing rates of Protoperidinium hirobi Abe, a thecate heterotrophic dinoflagellate. J Plankton Res 15:723–736

Jakobsen H, Hansen P (1997) Prey size selection, grazing and growth response of the small heterotrophic dinoflagellate *Gymnodinium* sp. and the ciliate *Balanion comatum*--a comparative study. Mar Ecol Prog Ser 158:75–86

Jeong HJ, Ha JH, Yoo YD, Park JY, Kim JH, Kang NS, Kim TH, Kim HS, Yih WH (2007) Feeding by the *Pfiesteria*-like heterotrophic dinoflagellate Luciella masanensis. J Eukaryot Microb 54:231–241

Jeong HJ, Kim JS, Kim JH, Kim ST, Seong CN, Kim TH, Song JY, Kim SK (2005) Feeding and grazing impact by the newly described heterotrophic dinoflagellate *Stoekeria algicida* on the harmful alga Heterosigma akashiwo. Mar Ecol Prog Ser 295:69–78

Jeong HJ, Kim SK, Kim JS, Kim ST, Yoo YD, Yoon JY (2001) Growth and grazing rates of the heterotrophic dinoflagellate Polykrikos kofoidii on the red-tide and toxic dinoflagellates. J Eukaryot Microbiol 48:298–308

Jeong HJ, Kim JS, Yoo YD, Kim ST, Kim TH, Park MG, Lee CH, Seong KA, Kang NS, Shim JH (2003) Feeding by the heterotrophic dinoflagellate *Oxyrrhis marina* on the red-tide raphidophyte Heterosigma akashiwo: a potential biological method to control red tides using mass-cultured grazers. J Eukaryot Microb 50:274–282

Jeong HJ, Latz MI (1994) Growth and grazing rates of the heterotrophic dinoflagellates *Protoperidinium* spp . on red tide dinoflagellates. Mar Ecol Prog Ser 106:173–185

Jeong HJ, Lee KH, Yoo Y Du, Kang NS, Lee K (2011) Feeding by the newly described, nematocyst-bearing heterotrophic dinoflagellate *Gyrodiniellum shiwhaense*. J Eukaryot Microbiol 58:511–24

Jeong H, Yoo Y, Kim S, Kang N (2004) Feeding by the heterotrophic dinoflagellate Protoperidinium bipes on the diatom *Skeletonema costatum*). Aquat Microb Ecol 36:171–179

Juul-Pedersen T, Nielsen TG, Michel C, Møller EF, Tiselius P, Thor P, Olesen M, Selander E, Gooding S (2006) Sedimentation following the spring bloom in Disko Bay, West Greenland, with special emphasis on the role of copepods. Mar Ecol Prog Ser 314:239–255

Kim J, Jeong H (2004) Feeding by the heterotrophic dinoflagellates *Gyrodinium dominans* and *G. spirale* on the red-tide dinoflagellate *Prorocentrum minimum*. Mar Ecol Prog Ser 280:85–94

Lee CC, Fenchel T (1972) Studies on ciliates associated with sea ice from Antarctica. Arch Protistenk Bd 114:237–244

Levinsen H, Nielsen TG (2002) The trophic role of marine pelagic ciliates and heterotrophic dinoflagellates in arctic and temperate coastal ecosystems: A cross-latitude comparison. Limnol Oceanogr 47:427–439

Levinsen H, Turner J, Nielsen T, Hansen B (2000) On the trophic coupling between protists and copepods in arctic marine ecosystems. Mar Ecol Prog Ser 204:65–77

Menden-Deuer S, Lessard E, Satterberg J, Grünbaum D (2005) Growth rates and starvation survival of three species of the pallium-feeding, thecate dinoflagellate genus *Protoperidinium*. Aquat Microb Ecol 41:145–152

Montagnes D (1996) Growth responses of planktonic ciliates in the genera *Strobilidium* and *Strombidium*. Mar Ecol Prog Ser 130:241–254

Montagnes DJS, Kimmance SA, Atkinson D (2003) Using Q10 : Can growth rates increase linearly with temperature ? Aquat Microb Ecol 32:307–313

Müller H, Geller W (1993) Maximum growth-rates of aquatic ciliated protozoa - the dependence on body size and temperature reconsidered. Arch Hydrobiol 126:315–327

Naustvoll L-J (1998) Growth and grazing by the thecate heterotrophic dinoflagellate *Diplopsalis lentiluca* (Diplopsalidaceae, Dinophyceae). Phycologia 37:1–9

Naustvoll L-J (2000) Prey size spectra and food preferences in thecate heterotrophic dinoflagellates. Phycologia 39:187–198

Nielsen TG, Kiørboe T (1994) Regulation of zooplankton biomass and production in a temperate, coastal ecosystem. 2. Ciliates. Limnol Oceanogr 39:1423–1423

Paranjape M (1987) Grazing by microzooplankton in the eastern Canadian arctic in summer 1983. Mar Ecol Prog Ser 40:239–246

Pesant S, Legendre L, Gosselin M, Ashjian C, Booth B, Fortier L (1998) Pathways of carbon cycling in the euphotic zone : the fate of large- sized phytoplankton in the Northeast Water Polynya. J Plankt re 20:1267–1291

Pesant S, Legendre L, Gosselin M, Bjornsen PK, Fortier L, Michaud J (2000) Pathways of carbon cycling in marine surface waters : the fate of small-sized phytoplankton in the Northeast Water Polynya. 22:779–801

Poulsen L, Iversen M (2008) Degradation of copepod fecal pellets: key role of protozooplankton. Mar Ecol Prog Ser 367:1–13

Rose JM, Caron DA (2007) Does low temperature constrain the growth rates of heterotrophic protists? Evidence and implications for algal blooms in cold waters. 52:886–895

Rysgaard S, Nielsen TG, Hansen BW (1999) Seasonal variation in nutrients, pelagic primary production and grazing in a high-Arctic coastal marine ecosystem, Young Sound, Northeast Greenland. Mar Ecol Prog Ser 179:12–25

Saunders P., Deibel D, Stevens C, Rivkin RB, Lee S., Klein B (2003) Copepod herbivory rate in a large arctic polynya and its relationship to seasonal and spatial variation in copepod and phytoplankton biomass. Mar Ecol Prog Ser 261:183–199

Schmoker C, Thor P, Hernández-León S, Hansen B (2011) Feeding, growth and metabolism of the marine heterotrophic dinoflagellate *Gyrodinium dominans*. Aquat Microb Ecol 65:65–73

Seuthe L, Rokkan Iversen K, Narcy F (2011) Microbial processes in a high-latitude fjord (Kongsfjorden, Svalbard): II. Ciliates and dinoflagellates. Polar Biol 34:751–766

Sherr EB, Sherr BF, Fessenden L (1997) Heterotrophic protists in the Central Arctic Ocean. Deep Sea Res Part II 44:1665–1682

Sherr EB, Sherr BF, Hartz AJ (2009) Microzooplankton grazing impact in the Western Arctic Ocean. Deep Sea Res Part II 56:1264–1273

Sherr EB, Sherr BF, Ross C (2013) Microzooplankton grazing impact in the Bering Sea during spring sea ice conditions. Deep Sea Res Part II Top Stud Oceanogr 94:57–67

Siano R, Montresor M (2005) Morphology , ultrastructure and feeding behaviour of *Protoperidinium vorax* sp. nov. (Dinophyceae, Peridiniales). Eur J Phycol 40:221–232

Slagstad D, Ellingsen IH, Wassmann P (2011) Evaluating primary and secondary production in an Arctic Ocean void of summer sea ice: An experimental simulation approach. Prog Oceanogr 90:117–131

Smith JWO, Barber DG (2007)Polynyas -windows to the World (JWO Smith and DG Barber, Eds.), first edit. Amsterdam, The Netherlands

Smith Jr. WO (1995) Primary productivity and new production in the Northeast Water. J Plankton Res 100:4357–4370

Stirling I (1997) The importance of polynyas, ice edges, and leads to marine mammals and birds. J Mar Syst 10:9–21

Stocker TF, Qin D, Plattner K-G, Tignor MMB, Allen SK, Boschung J, Nauels A, Xia Y, Bex V, Midgley PM (2013) Climate Change 2013: The Physical Science Basis, Working group I contribution to the fifth assesment report of the intergovermental report on climate change.

Strom SL (1991) Growth and grazing rates of the herbivorous dinoflagellate *Gymnodinium* sp. from the open subarctic Pacific Ocean. Mar Ecol Prog Ser 78:103–113

Strom SL, Buskey EJ (1993) Feeding , growth, and behavior of the thecate heterotrophic dinoflagellate *Oblea rutunda*. Limnol Oceanogr 38:965–977

Tremblay JE, Smith JWO (2007) Primary production and nutrient dynamics in polynyas. In: Smith JWO, Barber DG (eds) Polynyas -windows to the world, first. Elsevier Oceanography Series, 74, Amsterdam, The Netherlands, p 239–269

Van't Hoff JH (1984) Etudes de dynamique chimique. Muller, Amsterdam

Verity PG, Wassmann P, Frischer ME, Howard-Jones MH, Allen AE (2002) Grazing of phytoplankton by microzooplankton in the Barents Sea during early summer. J Mar Syst 38:109–123

Weisse T, Montagnes DJS (1998) Effect of temperature on inter- and intraspecific isolates of Urotricha (Prostomatida, Ciliophora). Aquat Microb Ecol 15:285–291

Paper II

Submitted to Aquatic Microbial Ecology

RV Meteor
Photo: Maria Lund Paulsen

Pico- and nanophytoplankton support an active microbial food web prior to the North Atlantic spring bloom

Maria Lund Paulsen[1,2*], Karen Riisgaard[2], T. Frede Thingstad[1], Mike St. John[2], Torkel Gissel Nielsen[2]

[1] Department of Biology, Marine Microbiology Department, University of Bergen, Norway
[2] National Institute of Aquatic Resources, DTU-Aqua, Section for Ocean Ecology & Climate, Denmark

ABSTRACT

In temperate, subpolar and polar marine systems, the classical perception is that diatoms initiate the spring bloom and thereby mark the beginning of the productive season. Contrary to this view, here we document an active microbial food web prior to the diatom bloom; a period with excess nutrients and deep convection of the water column. During repeated visits to stations in the deep Icelandic and the Norwegian Basins and the shallow Shetland Shelf (26 March to 29 April 2012), we investigated the succession and dynamics of autotrophic and heterotrophic microorganisms.

The major Chl *a* contribution in the early winter-spring transition was found in the fraction smaller than 10µm i.e. dominated by pico- and small nanophytoplankton. This fraction was further resolved by flow cytometry revealing an initial dominance in biomass of picoeukaryotes within the mixed layer with succession to small nanophytoplankton at all stations. We observed that the early production of the small phytoplankton was followed by a decrease in C:N ratio of the dissolved organic matter, an increase in heterotrophic prokaryote (bacteria) abundance and activity (indicated by the HNA:LNA bacteria ratio), and an increase in abundance and size of heterotrophic protists. The relative abundance of pico-sized phytoplankton decreased towards the end of the cruise at all stations, despite high nutrient concentrations and increasing day length. This decrease is hypothesised to be the result of top-down control by the fast growing population of heterotrophic protists. As a result the subsequent succession and nutrient depletion can be left to diatoms resistant to small grazers. We observed that the net-growth of phytoplankton towards the end of the study was driven by large phytoplankton (Chl *a* >50µm) at the deep mixed stations; Iceland Basin and Shetland Shelf, while large phytoplankton remained insignificant in the permanently stratified station in the Norwegian Basin. Accumulation of large phytoplankton was stimulated by deep mixing, while picophytoplankton was not, both physical and biological reasons for this development are disused herein.

KEY WORDS: Microbial food web, Pre-bloom, Deep mixing, Pico- and nanophytoplankton, Bacteria, Microzooplankton, Subarctic Atlantic

INTRODUCTION

Much of our conceptual understanding of the marine pelagic food web originates from the pioneer work of Sverdrup (1953), Cushing (1959) and Steele (1974). This understanding was based on coarse meshed samplers e.g. Continuous Plankton Recorder (CPR) surveys and vertical net hauls, and used to described the seasonality of northern marine ecosystems and inspired generations of marine researchers. However, little attention was paid to the role of microbial communities, in part due to the difficulty in sampling this component of the food web. With the advent of suitable techniques the microbial loop has been recognised to play a fundamental role in the flux of carbon and nutrients in marine ecosystems (Pomeroy 1974, Sorokin 1977, Azam et al. 1983). However, while the importance of the heterotrophic components of the microbial loop became recognised (Williams 1981), the role of the autotrophic microbial component in northern ecosystems, mainly the picophytoplankton, still received little attention. This lack of recognition was based on studies during the spring bloom where the relative abundance of picophytoplankton was low (Li et al. 1993) compared to oligotrophic subtropical waters (Agawin et al. 2000, Tremblay et al. 2009) where their dominance presumably is based on high affinity for mineral nutrients.

In addition, marine research in northern systems traditionally focused on the dynamics and fate of the spring diatom bloom because the new production of larger-celled species in this period was assumed to have a strong link to mesozooplankton and fish production (Sverdrup 1953, Steele 1974, Braarud & Nygaard 1978). The spring diatom bloom is however short term feature of the system with smaller phytoplankton and their associated grazers dominating for the majority of the year (Søndergaard et al. 1991, Joint et al. 1993, Sherr et al. 2003, Irigoien et al. 2005, Seuthe, Töpper, et al. 2011, Seuthe, Rokkan Iversen, et al. 2011).

In winter, before the spring bloom peaks, the water column is characterized by high turbulent mixing, deep convection (Backhaus et al., 1999) and low irradiance. During this period phytoplankton concentrations are dispersed (Li 1980) and the major mesozooplankton grazer, *Calanus finmarchicus* is in diapause at depth (Hirche 1996). The onset of the bloom is affected by several physical factors including a shoaling of deep convection (Taylor and Ferrari 2011), periods of 'critical' turbulence (Huisman 1999) eddy driven stratification (Mahadevan et al. 2012) and irradiance (i.e. the Critical depth model; Sverdrup 1953) which have been thoroughly described. Grazing by microzooplankton (MZP) has also been suggested to play a major role for the bloom development. Behrenfeld (2010) and Behrenfeld and Boss (2014) hypothesised that the increase in phytoplankton biomass in the North Atlantic during winter-spring-transition could be a result of a decoupling of the MZP grazers from their phytoplankton prey during mixed layer deepening (the Dilution-Recoupling Hypothesis). There has been controversy as to the mechanisms controlling the onset of the bloom resulting in a publication by Lindemann and St. John (2014) presenting a conceptual model of the interplay of these abiotic and biotic mechanisms. However, no attempt has been made to investigate the autotrophic planktonic community composition and dynamics in the subarctic Atlantic prior to the bloom.

Here we shift the focus from the diatom spring bloom to the microbial community found during the winter-spring transition and evaluate the relative contributions of pico- and

nanophytoplankton in the subarctic North Atlantic prior to the bloom. We investigate the succession of both autotrophic and heterotrophic plankton components, and evaluate a central assumption behind the hypothesis behind bloom formation in well mixed waters i.e. the decoupling of the heterotrophic protists from the phytoplankton community during deep mixing. Parallel to the *in situ* observations, which are presented here, an experimental approach was applied to study the microbial community in detail (e.g. estimation of growth and grazing rates) is presented in Riisgaard et al (Paper III).

MATERIAL & METHODS

Sampling site and hydrography

The study was conducted from 26 March to 29 April, 2012 during a cruise aboard the RV Meteor (cruise no. 87) coordinated by the University of Hamburg.. The study occupied three stations located in the subarctic North Atlantic, representing different hydrographical regimes: 2 stations on the edge of the deep basins (1300-1350 m) on either side of the Greenland-Scotland Ridge and one shallow station on the Shetland Shelf (160 m) (Fig. 1). Each station was revisited at 8-14 day intervals following a route circling the Faroe Islands. During each visit vertical profiles of temperature, salinity and PAR were performed using a CTD Sea Bird (SBE 9 plus) with an attached rosette of 10 L Niskin bottles.

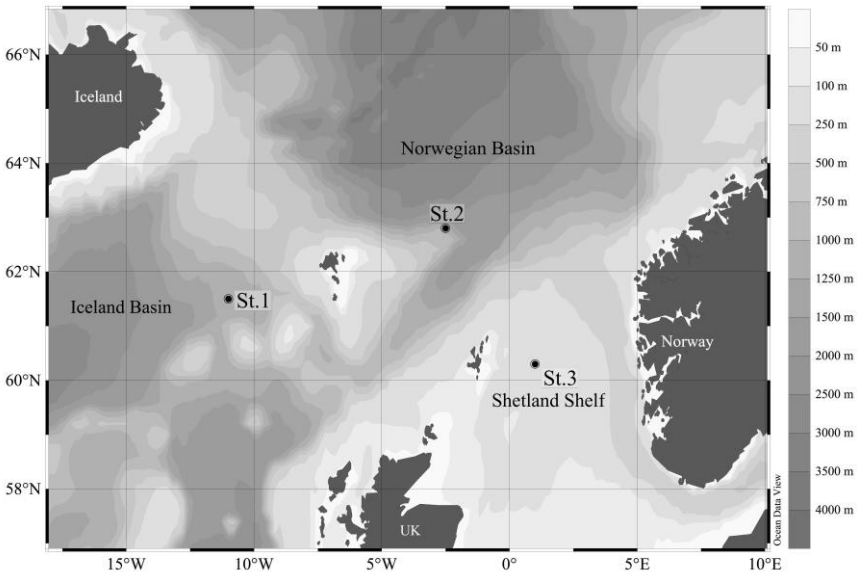

Fig. 1. Study area: (St.1) The 1350 m deep station in the Iceland Basin (61.5°N, 11°W), (St.2) the 1300 m deep station in the Norwegian Basin (62.8°N, 2.5°W) and (St.3) the 160 m deep station on the Shetland Shelf (60.3°N, 1°E).

Euphotic zone depth was defined as 0.1% of incident PAR measured at 5 m (Jerlov 1968) The depth of the mixed layer was identified as a decrease of 0.2°C from surface (10 m) temperatures (de Boyer Montégut et al. 2004), evaluated to be the most appropriate definition for high latitude regions where deep convection can occur.

Sampling depths were chosen based on water column structure, and covered the full water column, however with highest resolution within the mixed layer. During each visit to the stations, 3 CTD profiles were taken within a time frame of 20-36 h to capture the temporal dynamics. During these profiles, Niskin samples were collected to provide data on the abundance of microbial components, including: virus-like particles (thereafter referred to as virus), heterotrophic prokaryotes (Archaea and eubacteria, hereafter referred to as bacteria), small (<10 µm) phytoplankton, unidentified heterotrophic nanoflagellates (HNF), larger (>12 µm) ciliates and dinoflagellates (MZP) as well as Chlorophyll *a* (Chl *a*), nutrients, DOC and DON. The sampling of bacteria, viruses, small phytoplankton, and total Chl *a*, was about twice as frequent as sampling of the more analytically time-consuming fractionated Chl *a* and heterotrophic protists.

Nutrients, organic matter and Chl *a*

Nitrite and nitrate (N), phosphate (P) and silicate (Si) were measured on a Skalar Sanplus segmented-flow autoanalyser, following procedures outlined by Wood et al. (1967) for nitrate/nitrite Murphy and Riley (1962) for phosphate and Koroleff (1983) for the determination of silicic acid.

Total organic carbon (TOC) in unfiltered seawater was analyzed by high temperature combustion using a Shimadzu TOC-V_{CSH} (Dickson et al. 2007). Standardization was achieved using potassium hydrogen phthalate. Calibration was performed using deep seawater and low carbon reference waters as provided by the Hansell CRM Program and performed every sixth analysis to assess the day-to-day and instrument-to-instrument variability. The precision of TOC analyses was ~1 µmol kg^{-1} with a CV of 2-3%. Concentration of total nitrogen (TN) was determined simultaneously by high temperature combustion using a Shimadzu TNM1 attached to the Shimadzu TOC-V. Total organic nitrogen (TON) was calculated by subtracting inorganic N measured from parallel nutrient samples on board. As ammonium concentrations were low through out the cruise (0.18 µM ± 0.5, n = 400) (J. Jacob, unpublished) these were not included in the inorganic N pool..As in the DOC method, subsamples for TDN were manually injected into the combustion tube at 900°C. The resulting nitric oxide was then reacted with ozone with the resulting signal detected by a chemiluminescence instrument (Garside 1985). As the difference between TOC and dissolved organic carbon (DOC) is minor in northern systems when not in bloom situation (Anderson 2002), we use the term DOC in the following, equally for organic nitrogen; we use dissolved organic nitrogen (DON) instead of TON.

Chl *a* concentrations were determined from 100-1000 ml samples and size fractionated on Whatman GF/F filters (0.7 µm pore-size), 10 µm and 50 µm mesh filters, each fractionation treatment was triplicated. Filters were extracted in 96% ethanol for 12-24 h (Jespersen & Christoffersen 1987). Chl *a* concentrations were measured before and after addition of one drop of acid (1 M HCl) on a TD-700 Turner fluorometer calibrated against a Chl *a* standard.

Enumeration of bacteria, viruses and protists

Bacteria, viruses, small phytoplankton and HNF were enumerated using a FACS Calibur (Becton Dickinson, Oxford, UK) flow cytometer, with an air-cooled argon ion laser (488 nm, 15 mW) as the fluorescence excitation light source. Flow cytometry data were analysed using CellQuest software and the cell numbers were calculated using the instrument flow rate. For the enumeration of bacteria and viruses, 2 ml samples were fixed with glutaraldehyde (final conc. 0.5%) for 30 min in the dark at 4°C and thereafter flash-frozen in liquid nitrogen and stored in -80°C until further analysis, which was performed within 4 months. Samples were thawed and appropriate dilutions (5- and 10-fold) of fixed samples were prepared in 0.2-µm filtered TE buffer (Tris 10 mM, EDTA 1 mM, pH 8), stained with a green fluorescent nucleic-acid dye, SYBR Green I (Molecular Probes Inc., Eugene, Oregon), and kept for 10 min at +80°C in a water bath to provide optimal staining of viruses (Marie et al., 1999). Samples were counted for 1 min at a flow rate of ~30 µL min^{-1}. Heterotrophic prokaryotes (bacteria) and virus like particles (VLP) were discriminated on the basis of their side scatter and green fluorescence (Fig. 2A) following the approach of Marie et al. (1999). As reference, yellow-green fluorescent beads of 2-µm diameter (FluoSpheres® Carboxylate-Modified Microspheres, United Kingdom) were added. Bacteria are often found to group into two distinct clusters of high and low green fluorescence (Sherr et al. 2006; Huete-Stauffer and Morán 2012). As division was clear in current samples (Fig. 2B), the total bacteria counts were divided into low nucleic acid (LNA) and high nucleic acid (HNA) subgroups.

Small phytoplankton were preserved following the procedure used for bacterial samples, and analysed directly after thawing for 5 min at a flow rate of 60-70 µl min^{-1}. Groups were discriminated on the basis of their side-scatter light which is proportional to cell size, the pigments Chl *a* and phycoerythrin-emitting red and orange fluorescence, respectively, as in Larsen et al. (2004). Phytoplankton grouped into picoeukaryotes, *Synechococcus*, and small and large nanophytoplankton and mean red-fluorescence per cell within each group was recorded (Fig. 2C). The mean fluorescence per cell of each group was recorded using histogram plots.

Samples for HNF were fixed for 2 h with glutaraldehyde (final conc. 0.43%) at 4°C in the dark and thereafter preserved similar to the bacteria samples. Samples were stained with SYBR Green I for 2-4 h in the dark at 4°C and 0.5-µm yellow-green fluorescent beads were added as reference. Two ml undiluted samples were analysed for HNF, which were discriminated from phototrophic nanoflagellates in bivariate plots of the green fluorescence (from SYBRgreen) vs. red fluorescence (from Chl *a*) (Fig 2C), with minor modifications following the method of Zubkov et al. (2007). With this method we could not distinguish mixotrophic nanoflagellates.

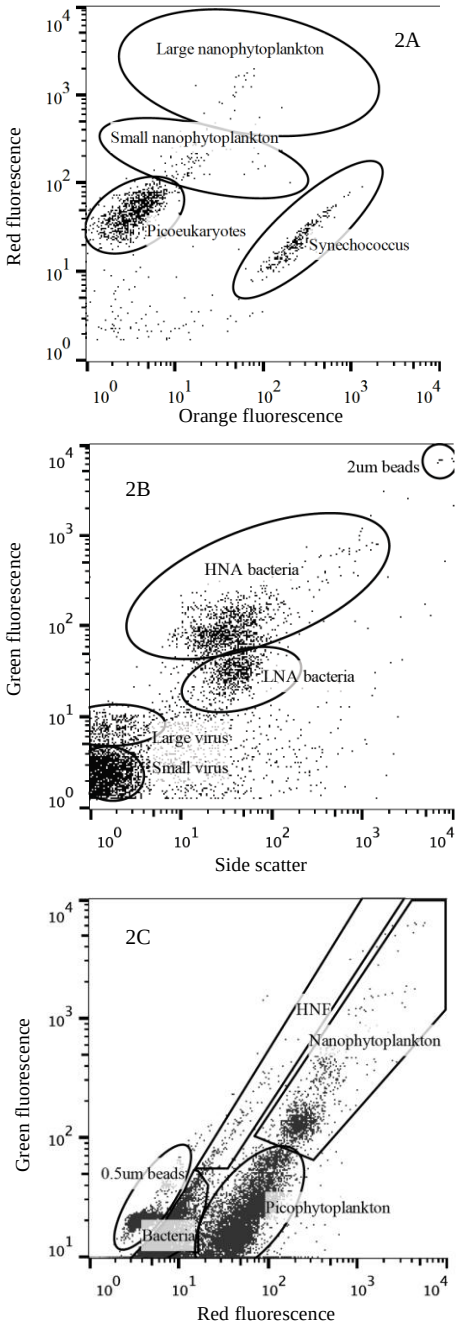

Fig. 2. Biparametric flow cytometry plots with the applied grouping of the different microbial groups. (A) the populations of autotrophic picoeukaryotes, *Synechococcus* and two size groups of autotrophic nanoflagellates distinguished on a plot of red fluorescence vs. orange fluorescence. (B) heterotrophic bacteria and viruses as distinguished on a plot of green fluorescence vs. side scatter. The group of high nuclei acid (HNA) bacteria express higher fluorescence than the low nuclei acid (LNA) bacteria. Two µm yellow-green reference fluorescent beads appear in the right upper corner of the plot. (C) heterotrophic nanoflagellates (HNF) are distinguished from nano-sized phototrophic protists on a plot of red fluorescence vs. green fluorescence. Bacteria and picophytoplankton are found at the bottom of the plot as well as 0.5 µm yellow-green fluorescent beads (see further explanation in the text).

For enumeration and sizing of lager protists water samples of 500 ml were gently decanted from the Niskin bottle through a silicon tube into brown glass bottles and fixed in acidic Lugol's solution (final conc. 3%) Samples for MZP were collected at fewer depths than for other samples (see sampling depths at each station Fig. 5) and kept cool and dark until analysis. In order to concentrate the samples, 500 ml sub-samples were allowed to settle for 48 h in tall cylinders (height and diameter) before the upper part of the sample was gently removed by decanting with a silicon tube leaving 100 ml in the cylinder. All or a minimum of 300 cells were counted.

Size and biomass estimation of protists

Dinoflagellates and ciliates were identified morphologically and divided into size classes covering 10 -µm ranges of equatorial spherical diameter (ESD) starting with 10-20 µm. ESD and cell volume are related by: $\pi/6 \times ESD^3$ = cell volume. Cell volumes were calculated using appropriate geometric shapes without including the membranelles. The bio-volumes were converted to carbon using the volume-to-carbon conversion factors given in Table 1. Qualitative observations of dominant micro-phytoplankton families and species were recorded in parallel.

The biomass of pico- and nanoflagellates was estimated based on literature conversion factors (Table 1). Size determinations of the various groups of phytoplankton (picoeukaryotes, *Synechococcus* and small and large nanophytoplankton) were performed by filtering parallel samples through 0.8, 1, 2, 5, 10-µm polycarbonate filters and counting the filtrate, hereby enumerating the percentage of each group within the given size interval, a method modified from Zubkov et al. (1998).

HNF size was estimated using epifluorescence microscopy. Samples (10 ml) were fixed with glutaraldehyde (final conc. = 1%) for 1 hr and stored at -80°C. The samples were filtered onto black polycarbonate filters (pore size 0.8 µm), stained with 4,6-diamidino-2-phenylin-dole dihydrochloride (DAPI) DNA-specific dye (Porter & Feig 1980), and analysed under a UV-microscope (x1000). To ensure the measured cells were heterotrophic, each cell was crosschecked for red auto-fluorescence. Diameters of 170 HNF were measured. For both HNF and groups of small phytoplankton the abundance within size intervals was converted to the weighted arithmetic averaged size and used for biomass estimation (Table 1).

Integrated values were calculated by trapezoid integration. When samples were not available from the exact mixed layer depth, a curve was fitted between the two neighbouring samples and the resulting curve equation used to estimate the value by the base of the mixed layer. The integrated biomass values (mg C m^{-2}) were converted to (mg C m^{-3}) by dividing with the depth of the mixed layer to enable comparison of the mean integrated biomass within the mixed layer between stations.

Table 1. Weighted arithmetic means of measured equivalent spherical diameter (ESD) within the size fractions chosen to represent small and large autotrophic nanoflagellates (ANF), heterotrophic nanoflagellates (HNF), picoeukaryotes and *Synechococcus* as well as the carbon conversion factors used to convert estimates of cell abundance to biomass (pg C $cell^{-1}$). Dinoflagellates and ciliates are estimated from biovolumes (V) of each individual and average ESD is therefore not presented. For smaller protist groups average ESD was measured; for HNF diameter was estimated by microscopy and for small phytoplankton the weighted arithmetic mean of the diameter was calculated from the abundance within different size intervals using filtration (see further explanation in the text). The biomass of viruses and bacteria are estimated using literature values.

Group	**Measured ESD (µm)**	**Carbon conversion fg C $µm^{-3}$**	**Conversion reference**	**Biomass pg C $cell^{-1}$**
Dino-flagelates		Log (pg C $cell^{-1}$) = -0.353 + 0.864 Log (V)	Menden-Deuer & Lessard 2000	
Aloricate ciliates		Log (pg C $cell^{-1}$) = -0.639 + 0.984 Log (V)	Putt & Stoecker 1989, modified by Menden-Deuer and Lessard 2000	
Loricate ciliates		Log (pg C $cell^{-1}$) = -0.168 + 0.841 Log (V)	Verity & Langdon 1984, Menden-Deuer & Lessard 2000	
Small ANF	4 ± 0.5	220	Booth 1988	7.140
Large ANF	9 ± 0.7	220	Booth, 1988	58.980
HNF	3.2 ± 0.3	220	Børsheim & Bratbak 1987	4.505
Picoeuk.	1.7 ± 0.4	220	Kana and Gilbert, 1987	0.581
Synecho.	1.1 ± 0.4	250	Booth, 1988	0.191
Bacteria			Lee & Fuhrman 1987	0.020

RESULTS

Physical regime

Weather during the cruise was generally windy causing mixing of the upper part of the water column in addition to the winter convection. The deep stations in the Iceland and Norwegian Basins were most stormy, and on several occasions winds reached Beaufort force 10 with sustained periods of Beaufort 8 and wave heights of 3-5 m. The day length increased from 11 to 16 h during the cruise.

Based on the water mass definitions of Blindheim and Østerhus (2005), the Iceland Basin consisted mostly of Atlantic Water (θ = 5-10.5°C, salinity = 35-35.05) reaching >1000 m, while Polar Overflow Water (θ <0.5°C, salinity = 34.88-34.93) was observed near the bottom on a few occasions. Deep convection or remnants thereof, was evident at the Iceland Basin down to ~ 600 m but reduced gradually to ~ 350 m during the study period (Fig. 3). In the Norwegian Basin the Atlantic Water was constrained to the upper 100 m while the major part of the water column (100-1300 m) consisted of cold Norwegian Sea Deep Water (θ <0.5°C, salinity = 34.9). Between the two water masses there was permanent stratification and the surface mixed layer reached a depth of ~50 m. The Shetland Shelf station was characterized by a uniform water mass of Atlantic Water mixed to the bottom and remained similar between visits. The dominating water masses at each of the three localities remained

consistent throughout the period. T-S diagrams revealed that the only major variations occurred in the Iceland Basin at 1200-1250 m due to an intrusion of intermediate water masses.

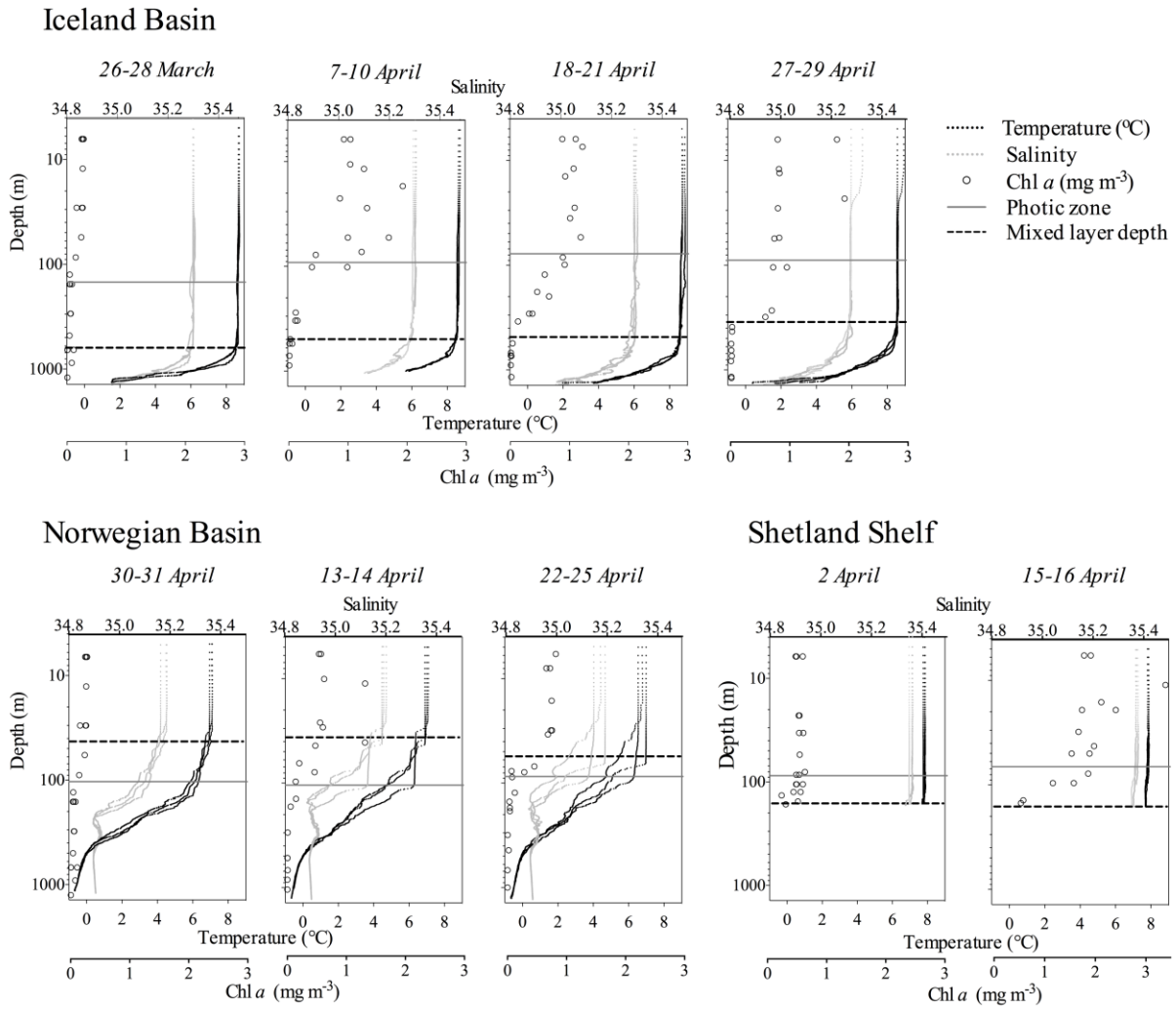

Fig. 3. Vertical profiles (n = 3) of temperature, salinity, total Chl *a* (sampled from the chosen sampling depths). All profiles were taken within 20-36 h (first visit to the left). Horizontal black dashed line indicates the mixed layer depth and the grey line mark the photic zone.

Changes in Chl *a*, nutrients and C:N ratio of organic matter

The integrated mean values of Chl *a* (mg m^{-3}) within the mixed layer at the three stations all showed a gradual increase during the cruise (Table 2, Fig. 3). Due to the on-going deep convection at the Iceland Basin and Shetland Shelf stations, a large fraction of Chl *a* was detrained i.e. mixed well below the photic zone (Fig. 3). The deep mixed stations showed the highest increase in Chl *a*; in the Iceland Basin from <0.1 to 0.7 mg m^{-3} during a 30 days period and over the Shetland Shelf from 0.5 to 1.4 mg m^{-3} during a 14 days period. The increase in Chl *a* at the mixed stations was mainly due to an increase in the >50 µm Chl *a* fraction (Fig. 4), which comprised up to 50% of the total Chl *a* during the last visit. At the stratified Norwegian Basin, Chl *a* was retained within the photic zone (Fig. 3), yet here we

observed the smallest increase in Chl *a* was observed within the mixed layer; from 0.4 to 0.6 mg Chl *a* m^{-3}. The Chl *a* fraction <10 µm comprised a major part of total integrated Chl *a*, ranging at all stations from: 47 ± 25% at the Iceland Basin; 55 ± 39% on the Shetland Shelf; and, especially dominant in the Norwegian Basin at 95 ± 7% on average during the study (Fig. 4).

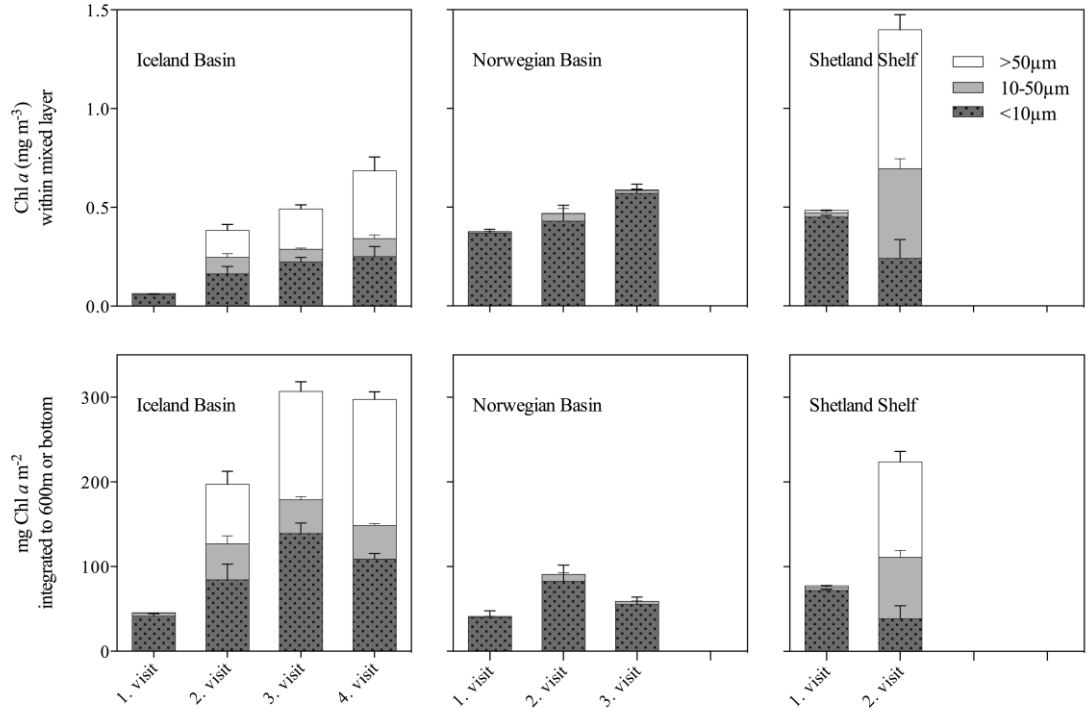

Fig. 4: Size fractionated Chl *a* at the three stations over time, shown as mean ± SD (n = 3) of three sampled profiles at each visit. In the upper panel integrated biomass of Chl *a* is divided by mixed layer depth in order to estimate the mean concentration within the mixed layer (mg Chl *a* m^{-3}). The integrated biomass (mg Chl *a* m^{-2}) to 600 m at the deep stations and to the bottom (160 m) at Shetland Shelf is shown in the lower panel.

Nutrient concentrations i.e. $NO_2^- + NO_3^-$, PO_4^{3-} and $Si(OH)_4$ (hereafter N, P, Si) were high throughout the study program and were homogeneously distributed over the mixed layers (Table 2) with slightly elevated concentrations below the mixed layer (data not shown). Increases in the >50 µm Chl *a* fraction was reflected in a slight decrease in Si from 4.7 to 4.2 µM at the Iceland Basin and from 2.8 to 1.7 µM at the Shetland Shelf, suggesting a net growth of diatoms at these locations.

At the mixed stations DOC increased during the study period, and the C:N ratio in the dissolved organic matter decreased; i.e. became more rich in N. There were no clear changes in DOC and DON at the stratified Norwegian Basin (Table 2).

Table 2. Water column characteristics during the program at the Iceland Basin and Norwegian Basin and Shetlands Shelf stations. Furthermore the estimated pico- and nanophytoplankton biomass to the measured <10 µm Chl *a* fraction (C:Chl *a*) based on linear correlation is presented as well as the DOC concentration and the DOC:DON ratio and the ratio of HNA:LNA bacteria and virus to bacteria. Data are given as mean ± SD, n, within the mixed layer, except Chl *a* for which the integrated mean within the mixed layer is presented (the mean of three integrated profiles from each visit).

Iceland Basin	**26-28 March**	**7-10 April**	**18-21 April**	**27-29 April**
Mixed layer depth (m)	618	493	492	344
Photic zone (m)	147	92	78	90
N:P:Si (µM)	13 : 0.8 : 5	12 : 0.8 : 5	12 : 0.8 : 5	12 : 0.8 : 4
Total Chl *a* (mg m^{-3})	0.06 ± 0, n =3	0.4 ± 0.1, n = 3	0.5 ± 0.1, n = 3	0.7 ± 0.2, n = 3
Chl *a* >10µm (%)	13.1 ± 5.2	81.3 ± 14.1	53.7 ± 14.6	62.2 ± 12.6
Chl *a* >50µm (%)	4.7 ± 2.8	55.5 ± 31.1	45.1 ± 19.8	49.2 ± 11.3
C: Chl *a*	47 ± 10 (p<0.005) r^2 = 0.7	21 ± 12 (p = 0.12) r^2 = 0.35	21 ± 6 (p = 0.01) r^2 = 0.6	11 ± 6 (p = 0.13) r^2 = 0.25
DOC (µM)	51.1 ± 0.4, n = 20	52.4 ± 2.2, n = 18	51.9 ± 1.4, n = 17	51.9 ± 0.6, n = 16
DOC: DON	17.2 ± 0.9, n= 6	17.4 ± 2.4, n = 19	14 ± 1.9, n = 18	15.1 ±1.3, n = 16
HNA: LNA Bacteria	2.04 ± 1.5, n = 16	2.3 ± 1.9, n = 14	4.3 ± 0.9, n = 16	3 ± 0.6, n = 6
Virus: Bacteria	8.2 ± 3.1, n = 16	6.1 ± 1.5, n = 16	2.9 ± 0.6, n = 16	2.6 ± 0.3, n = 12
Norwegian Basin	**30-31 March**	**13-14 April**	**22-25 April**	
Mixed layer depth (m)	43	37	56	
Photic zone (m)	103	105	86	
N:P:Si (µM)	12 : 0.8 : 5	13 : 0.8 : 5	12 : 0.8 : 6	
Total Chl *a* (mg m^{-3})	0.4 ± 0, n = 3	0.5 ± 0.1, n = 3	0.6 ± 0.1, n = 3	
Chl *a* >10µm (%)	2.9 ± 1.4	8.3 ± 7.6	5 ± 2.3	
Chl *a* >50µm (%)	0.2 ± 0.7	0.5 ± 0.3	1.0 ± 0.2	
C: Chl *a*	43 ± 9 (p<0.005) r^2 = 0.8	20 ± 6 (p = 0.008) r^2 = 0.6	39 ± 8 (p<0.005) r^2 = 0.7	
DOC (µM)	51.6 ± 1.4, n = 7	51.8 ± 0.8, n = 7	51.3 ± 1.5, n = 18	
DOC: DON	15.6 ± 2.6, n = 7	18.1 ± 2.2, n = 7	14.9 ± 1.5, n = 10	
HNA: LNA Bacteria	1.3 ± 1.2, n = 6	3.3 ± 1.4, n = 7	4.4 ± 1.9, n = 7	
Virus: Bacteria	4.4 ± 3.4, n = 6	3.1 ± 0.3, n = 6	2.5 ± 0.4, n = 7	
Shetland Shelf	**30-31 March**	**13-14 April**		
Mixed layer depth (m)	160	160		
Photic zone (m)	87	67		
N:P:Si (µM)	9.5 : 0.6 : 2.8	8.5 : 0.6 : 1.7		
Total Chl *a* (mg m^{-3})	0.5 ± 0, n = 3	1.4 ± 0.2, n = 3		
Chl *a* >10µm (%)	6.4 ± 1.4	55.3 ± 9.3		
Chl *a* >50µm (%)	2.3 ± 0.6	42.2 ± 6.7		
C: Chl *a*	47 ± 15 (p = 0.02) r^2 = 0.5	6 ± 1.5 (p = 0.08) r^2 = 0.8		
DOC (µM)	52.5 ± 2.3, n = 13	54.3 ± 0.8, n = 6		
DOC: DON	16.3 ± 1.9, n = 13	13.9 ± 1.2, n = 6		
HNA: LNA Bacteria	1.4 ± 0.2, n = 0.2	2.4 ± 0.2, 12		
Virus: Bacteria	71 ± 15, n = 10	148 ± 47, n = 9		

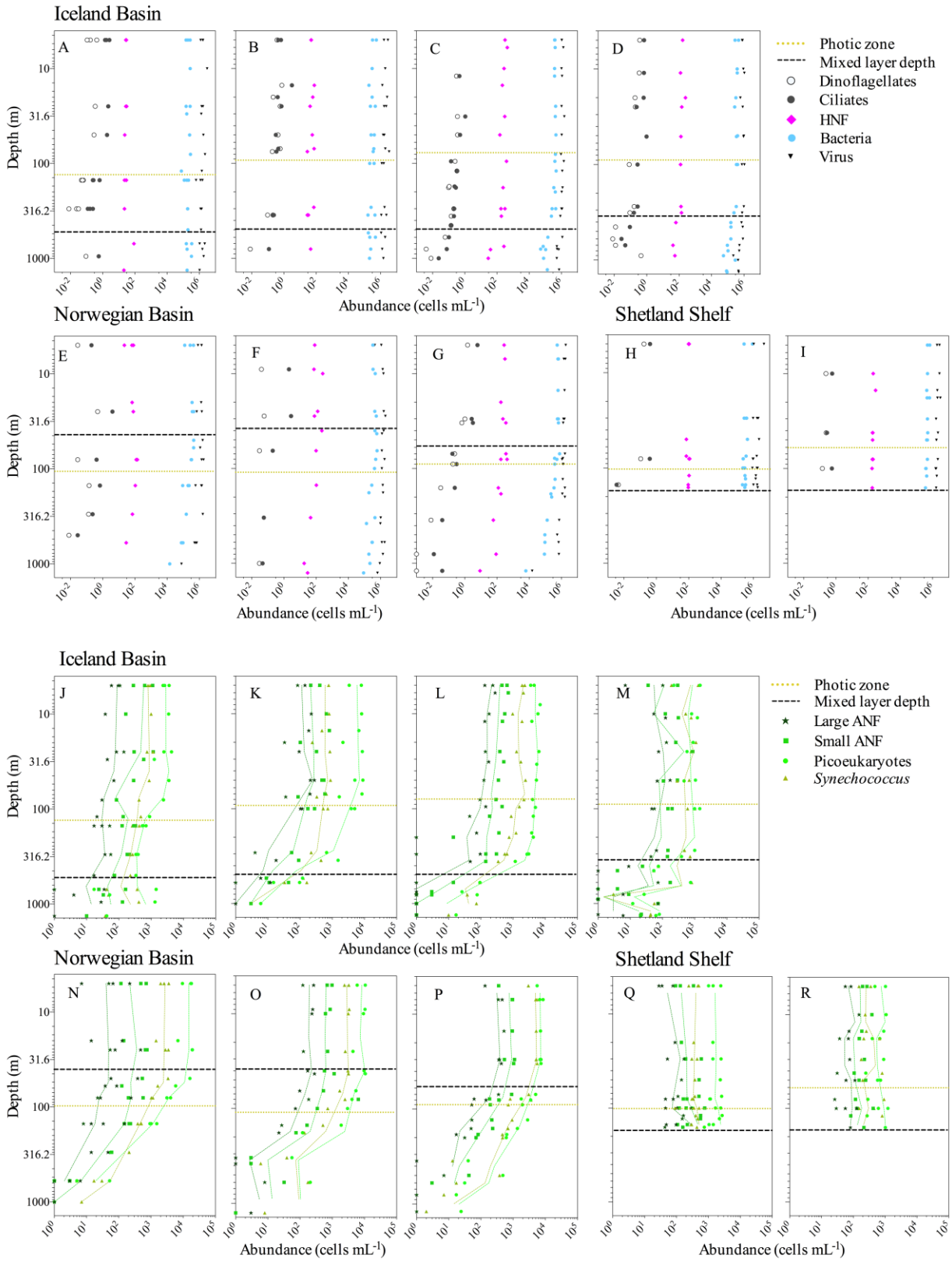

Fig. 5. Log-log scale vertical profiles showing the abundance (cells ml^{-1}) of microorganisms throughout the program (first visit to the left). Triplicate vertical profiles were performed within 20-36 h. at each visit to the stations. A-I) heterotrophic microorganisms; ciliates, dinoflagellates, HNF, bacteria and viruses. J-R) phototrophic microorganisms; *Synechococcus*, picoeukaryotes, small (>2-5 µm) and large (>5-10 µm) nanophytoplankton. The dashed line represents the mean abundance calculated within appropriate depth intervals. The horizontal black dashed line indicates the depth of the mixed layer and yellow dashed line marks the photic zone.

Sucession of phytoplankton

The picophytoplankton community (< 2 µm) was dominated by unidentified picoeukaryotes, while the prokaryotic component, dominated by *Synechococcus*, was considerably less abundant. However, the relative abundance of *Synechococcus* increased during the study program at all stations (Fig. 5). The nanophytoplankton fraction (2-10 µm) was separated into two size groups of ESD: 2-5 and 6-10 µm (Fig 3A). For conversion to biomass, the diameter of picoeukaryotes, *Synechococcus*, small and large nanophytoplankton (mean ESD ± SD, n = 7) were estimated as 1.7 ± 0.4 µm, 1.1 ± 0.4 µm, 4 ± 0.5 µm and 9 ± 0.7 µm, respectively.

Abundance of pico- and nanophytoplankton were obtained throughout the mixed layer at all stations (Fig. 5). Maximum abundance was obtained sub-surface (below 5 m) at 24 out of 27 stations, and decreased exponentially below the mixed layer. The average red fluorescence (a measure of Chl *a* content) per pico- and nanophytoplankton cell did not change with depth at the deep mixed stations, but doubled in the photic zone (± 50 m) at the stratified Norwegian Basin (Fig. 6), suggesting that phytoplankton were able to adapt their Chl *a* content to changing light conditions at the stratified station, but not at the mixed stations.

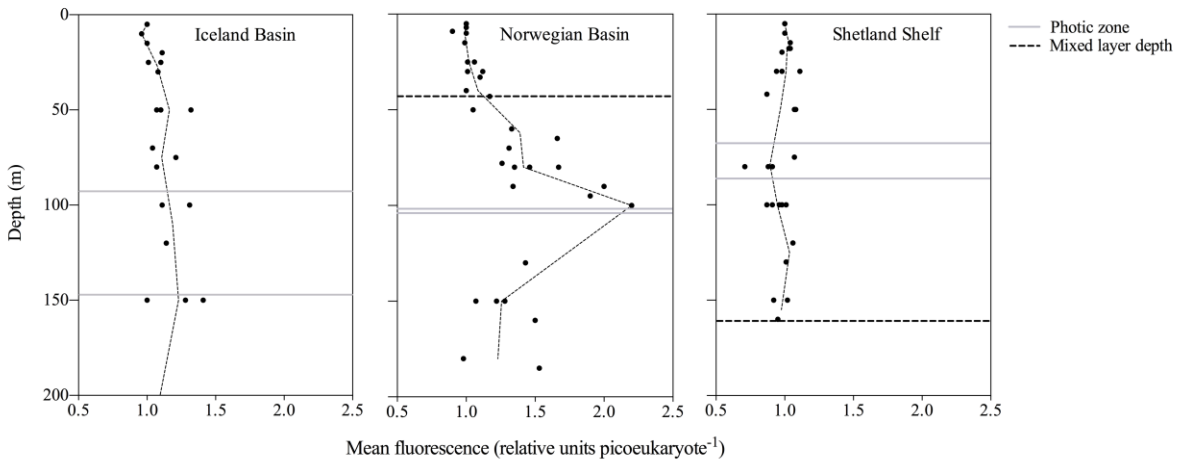

Fig 6. Changes in mean fluorescence per picoeukaryote normalized by the 5 m value shown for the first two visits to each of the three stations in the upper 200 m. The horizontal dashed black line defines the mixed layer depth, and dashed gray line the photic zone (deepest line from the first visit).

The integrated biomass of small phytoplankton was significantly correlated ($p < 0.05$) to the integrated Chl *a* fraction <10 µm. The averaged value of the slopes resulted in a Chl *a*:carbon conversion factor of 29 ± 13 (n = 7) for the Iceland Basin and the Norwegian Basin combined. Poor correlations were found for the Shetland Shelf, indicating contributions to the <10 µm Chl *a* fraction elsewhere than from the enumerated pico- and nanophytoplankton (Table 2).

During the first visit to the Norwegian Basin station picoeukaryotes were highly abundant reaching a maximum of 20×10^3 cells ml^{-1}. Hence despite their small size, this size fraction comprised up to 64 % of total phytoplankton biomass (the latter estimated from total

Chl *a* to carbon using a conversion factor of 29) (Fig. 7). During subsequent visits to the Norwegian Basin, abundance of picoeukaryotes decreased gradually to average 6×10^3 cells ml^{-1} within the mixed layer, while small nanophytoplankton increased significantly (one-way ANOVA, $p < 0.05$) and became dominant in terms of biomass. Qualitative observations from Lugol fixed samples revealed that dominant nanophytoplankton by the end of the period were of the class Cryptophyceae, with diatoms being absent from the samples. The stratified Norwegian Basin station had the highest concentration of pico- and nanophytoplankton within the mixed layer; about twice that of the Iceland Basin and triple that of the Shetland Shelf stations, as also indicated by the fractionated Chl *a* values (Fig. 4). Larger phytoplankton (>50 µm) became more dominant at the mixed stations; by the second visit to the Iceland Basin station we observed a high abundance of *Chaetoceros* spp. and a reduction in *Leptocylindricus* spp., while *Pseudo-nitzschia* spp. became more dominant during the last two visits. At the Shetland Shelf station the large phytoplankton community during the last visit was dominated by the diatoms *Thalassiosira* spp. and *Ditylum brightwellii*.

Succession of bacteria and virus

In contrast to the autotrophic plankton and the heterotrophic protists which were only distibuted evenly within the mixed layer, bacteria were homogeneously distributed throughout the entire water column, except at the Norwegian Basin station, where a 100 fold decrease in bacterial abundance was evident below 1000 m (Fig. 5). Initially, in late March and early April, the bacterial abundance was low at all stations ($2\text{-}3 \times 10^5$ cells ml^{-1}), and subsequently increased within in the upper mixed layer within 10 days at all stations and by the end of the study reached around ($6\text{-}7 \times 10^5$ cells ml^{-1}). The ratio of HNA:LNA bacteria increased significantly at all stations, and was generally lower below the mixed layer (Table 2, Fig. 8). Bacteria were the most prominent heterotrophic biomass within the mixed layer (6 ± 3 mg C m^{-3}, n = 27), while viruses comprised the lowest biomass (0.1 ± 0.04 mg C m^{-3}, n = 27). The ratio of viruses to bacteria (V:B) decreased at the Iceland and Norwegian Basin stations during the pre-bloom period, from 8.2 ± 3.1 and 4.4 ± 3.4, respectively, to 2.6 ± 0.3 and 2.5 ± 0.4 within the upper mixed layer. Below the mixed layer V:B was generally higher (Table 2, Fig. 5).

Heterotrophic nanoflagellates

The mean ESD of HNF was 3.2 ± 0.3 µm, n = 170, and did not change during the period. HNF were abundant below the mixed layer, but at depths below 1000 m they were found in relatively low concentrations (23 ± 4 cells ml^{-1}, n = 4) (Fig. 5). Within the upper mixed layer at the first visits to the Iceland Basin and Norwegian Basin stations, the abundance of HNF was low (25 and 48 cells ml^{-1}, respectively), but within 2 to 3 weeks increased rapidly 4-5 fold. At the first visit to the Shetland Shelf station, the abundance was relatively higher (97 ± 14 cells mL^{-1}) that the initial concentrations found in the Norwegian

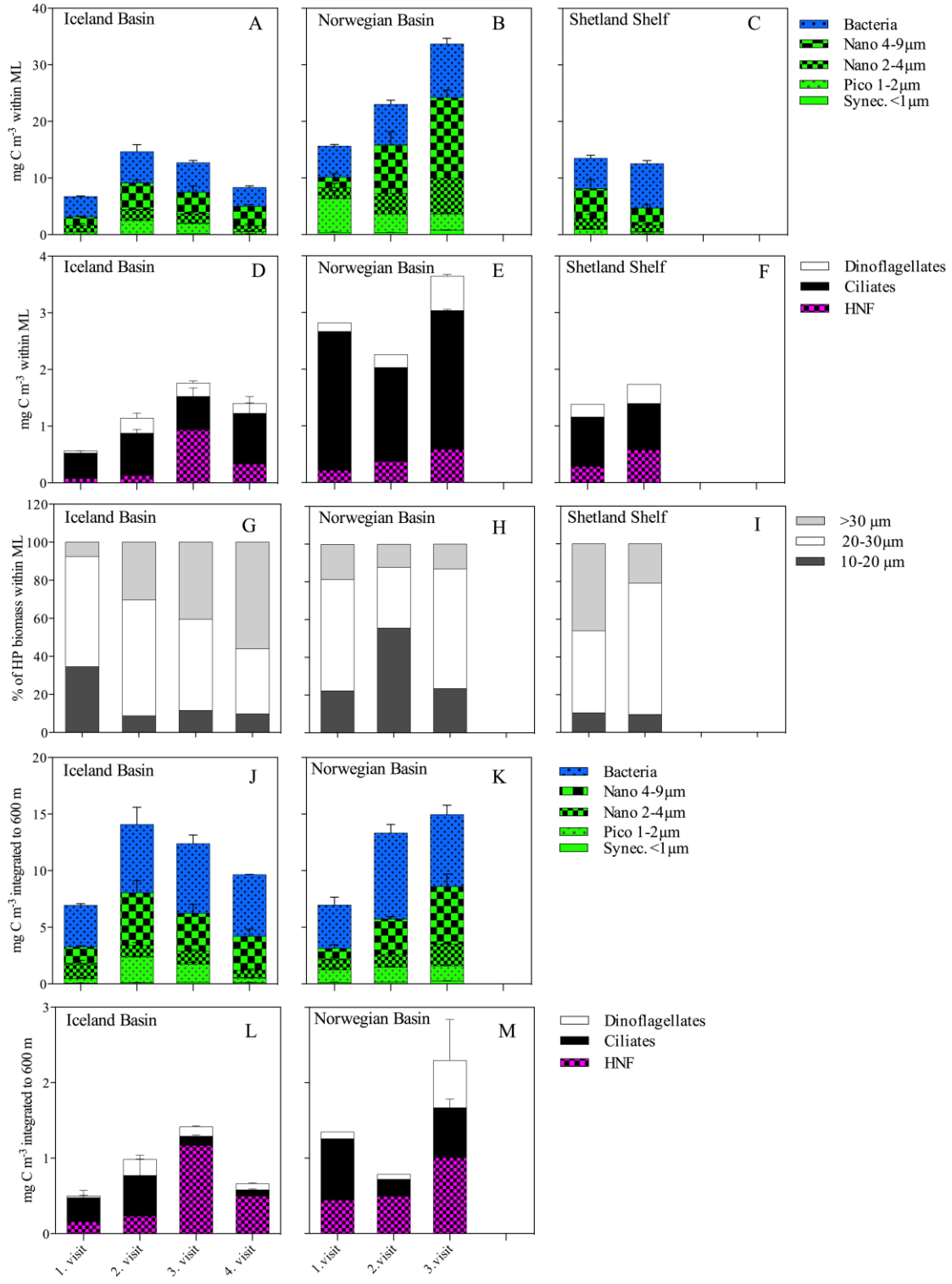

Fig.7: The development of biomass at the three stations shown as mean ± SE (n = 3) of three profiles sampled at each visit. Abundance of organisms is converted to biomass (mg C m^{-3}) using values given in Table 1 and split into panels of bacteria and autotrophs (i.e. two size fractions of nanophytoplankton, picoeukaryotes and *Synechococcus*) (A-C and J-K), and heterotrophic protists (i.e. heterotrophic nanoflagellates (HNF), ciliates and dinoflagellates (D-F and L-M). Note different y-axis. The first two panels show biomass within the mixed layer, values are obtained by integrating to the mixed layer depth (Table 2) and dividing by the depth of the mixed layer to enable comparison between stations. (G-H) show the relative size distribution of heterotrophic protist (>10 µm) within ML. The last two panels show the biomass (mg C m^{-3}) of (J-K) autotrophs and bacteria and (L-M) heterotrophic protists, when integrated to 600 m at the deep stations.

and Iceland Basins and doubled over the next 10 days (201 ± 31 cells ml^{-1}). In terms of biomass HNF equalled ~3 ± 1% of their available prey (integrated biomass of bacteria, picoeukaryotes and *Synechococcus*) averaged for the earliest visits to all stations, while later in the study the value increased to ~7 ± 3% of their prey biomass.

Microzooplankton

MZP were found throughout the mixed layer at all three stations and were evenly distributed (Fig. 5). In the Norwegian and Iceland Basin the abundance of MZP decreased with depth below the mixed layer. At all stations ciliates contributed with on average 73-91 % of the total MZP biomass, while dinoflagellates made up the remaining part of the biomass (Fig. 7). Integrated MZP biomass (mg C m^{-3}) within the mixed layer was lowest at the Iceland Basin station, slightly higher at the Shetland Shelf station and by far highest at the Norwegian Basin station (Fig. 7). At the Iceland Basin station, MZP biomass increased significantly from the first to three later visits (one-way ANOVA, $p < 0.05$). A change in MZP biomass could not be tested for the Norwegian Basin and the Shetland Shelf stations due to lack of replicates, but those samples obtained suggest there were no markedly change in MZP biomass. The MZP communities at all stations were generally composed of smaller (12-30 µm) species (Fig. 7G-I). However, at the Iceland Basin station, the fraction of larger (ESD >30 µm) species increased during the program and during the last sampling day 56% of the MZP biomass was composed of individuals with an ESD >30 µm. The Norwegian Basin station was strongly dominated by small cells (ESD <30 µm), contributing with >80 % of the MZP biomass. Ciliates were dominated by oligotrichs at all stations, but mixotrophic cyclotrichs of the genus *Mesodinium* also contributed substantially to the ciliate biomass, especially at the three later visits to the Iceland Basin station. Naked gymnodoid species dominated the dinoflagellate biomass, whereas thecate species made a minimal contribution; <5 % of the total MZP biomass (Table 3).

Table 3. Biomass contribution (%) of major groups/species of microzooplankton (dinoflagellates and ciliates) at the different visits to the three stations.

	Iceland Basin				Norwegian Basin			Shetland Shelf	
Visit	**1**	**2**	**3**	**4**	**1**	**2**	**3**	**1**	**2**
Oligotrichs	87.4	53.5	57.3	62.7	85.9	79.4	83.3	75.6	39.4
Mesodinium spp.	3.7	23.8	18.0	14.8	4.7	8.2	5.7	4.6	33.0
Tintinids	0.3	0.1	0.3	0.8	1.1	1.1	0.1	0.0	0.1
Gyrodinium spirale	1.0	4.6	5.0	4.5	0.7	1.6	0.5	0.0	1.7
Naked dinoflagellates	6.1	16.1	14.2	14.0	6.8	9.8	10.4	15.8	21.1
Thecate dinoflagellates	1.5	1.9	5.2	3.1	0.8	0.0	0.0	4.1	4.7

DISCUSSION

Deep Convective mixing enhances accumulation of phytoplankton

Our results demonstrate the quantitative importance of the pico- and small nanophytoplankton in the subarctic Atlantic winter and suggest a new role of the small-sized phytoplankton production as an important booster of the late winter microbial heterotrophic community prior to the diatom bloom. The <10 µm Chl *a* fraction dominated (in 5 of 9 sampling occasions). It is however not straight forward to draw conclusions on fractionated Chl *a*, as small phytoplankton are known to form aggregates (Barber 2007) and thus may have contributed to the larger fractions of Chl *a*. Further, we document that the stratified water enables the small phytoplankton to increase their pigment content when approaching the photic zone (Fig. 8), thereby using Chl *a* as a proxy will overestimate phytoplankton biomass at stratified stations where phytoplankton are adapted to stable light conditions when compared to the mixed stations. The following discussion it therefore strengthened by being based on both fractionated Chl *a* and the cell counts of phytoplankton (<10 µm). We found that the <10 µm Chl *a* fraction correlated significantly at all stations with the biomass of the pico- and nanophytoplankton converted from flow cytometer counts (r^2 = 0.58, p < 0.0001, n = 9, slope = 26.6), supporting dominance of the small sized phytoplankton.

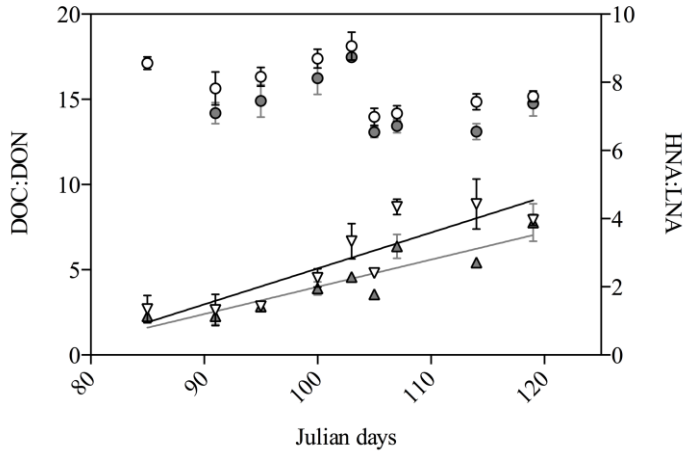

Fig 8. The C:N ratio of dissolved organic matter within the mixed layer (○) and below the mixed layer (●) and the bacteria HNA:LNA ratio within the mixed layer (▽) and below the mixed layer (△) from all three stations plotted over time (Julian days) during the entire program. Values are given as mean ± SE, n = 6-22 and represent the mean within mixed layer (ML) and below mixed layer (Deep) or in case of the Shetland Shelf below 100m. The linear regressions are given as lines straigt lines for the HNA:LNA ratio within ML; $f(x) = -7.99 + 0.11x$ (r^2=0.83, p<0.005) and for HNA:LNA ratio below the ML; $f(x) = -5.99 + 0.08x$ (r^2=0.84, p<0.005).

Backhaus et al. (2003) found presence of a winter stock of phytoplankton within the deep mixed layer of the Norwegian Basin and the Iceland Basin and suggested that the presence of phytoplankton below the euphotic zone was enabled by phytoplankton being occasionally re-entering the euphotic zone to harvest light as a result of deep convective mixing. Backhaus further documented that although the phytoplankton concentration was lower during winter within the mixed layer, the integrated phytoplankton biomass was of the

same magnitude as during the spring bloom. The present study supports the findings by Backhaus et al. (2003) and documents a similar homogeneous distribution of Chl *a* throughout the mixed layer, indicating an efficient mixing of the water column in the deep Iceland Basin station and at the shallow Shetland Shelf station. Maximum Chl *a* concentrations were low relative to spring-bloom values found in the Iceland Basin (Joint et al. 1993, Briggs et al. 2011), the Norwegian Basin (Li et al. 1993, Dale et al. 1999) and Shetland Shelf (Richardson et al. 2000, Sharples et al. 2006). However, when considering the top 600 m of the deep basins, the biomass in the mixed Iceland Basin is of the same magnitude, or even higher than the integrated Chl *a* in the surface layer during the spring bloom. Integrated Chl *a* values of the stratified Norwegian Basin were an order of magnitude lower than values reported during the Norwegian Basin spring bloom (Backhaus et al 2003,Irigoien et al. 1998). Based on the net increase in Chl *a* concentrations, the mixed stations were thus the most productive with Chl *a* increasing up to 5 fold during the course of the program. In comparison, integrated Chl *a* stayed roughly the same in the Norwegian Basin, despite an increased day length and excess nutrients (Table 2).

In contrast to Backhaus et al. (2003) who only considered total Chl *a* and counts of large phytoplankton, we also considered the community of small phytoplankton behind the Chl *a* value. In this respect we document a high contribution of pico- and nanophytoplankton, whereas large (>10 µm) phytoplankton, such as diatoms, were almost absent at all three stations during the first visits. As the spring bloom developed the relative contribution of small cells decreased at the mixed stations, while pico- and nanophytoplankton continued to dominate the phytoplankton biomass at the stratified Norwegian Sea station. This tendency suggests that convective mixing of the water column contributes to the maintenance of large cells such as diatoms in the water column, since the diatoms are otherwise subjected to high sinking losses. Similar selection has been observed in other turbulent systems (Kiørboe 1993). However it must be recognized that diatoms as in other phytoplankton groups have the ability to modify their buoyancy as a result of changes in physiology due changing growth and nutrient conditions e.g. Waite et al. (1992).

In our study, the Chl *a* fraction < 10 µm was dominated by unidentified autotrophic nanoflagellates and picoeukaryotes. The picophytoplankton community was dominated by picoeukaryote species, whereas the contribution by the prokaryotic compartment, *Synechococcus*, was minor. Numeric dominance of eukaryotic picophytoplankton relative to prokaryotes is characteristic for high latitude waters (Not et al., 2005). A picoeukaryote peak abundance of 20×10^3 cell ml^{-1} was found in the Norwegian Basin, which is comparable to peak abundances reported prior to the bloom in subarctic coastal waters (Sandaa & Larsen 2006, Bratbak et al. 2011) and in late summer in Arctic open waters (Sherr et al. 2003). The high abundance of picoeukaryotes found at all three stations during the winter-to-spring transition is in sharp contrast to the phytoplankton composition during the bloom where virtually no picoeukaryotes are found (Li et al. 1993). The integrated biomass values of nanophytoplankton was however on the lower end of those observed during the bloom (Li et al. 1993).

The success of picoeukaryotes during the late winter in high latitude systems may be explained by a high affinity for light compared to larger phytoplankton, due to the absence of a cell wall and since the small size of picophytoplankton enables an efficient packaging of

photosynthetic pigments inside the cell (Raven 1998). This high affinity for light coupled with their low sinking rates (Kiørboe 1993), position picophytoplankton to respond earlier than other groups to the increase in irradiance in the early spring. Culture experiments with the abundant picophytoplankton *Micromonas* supports this hypothesis identifying that small cells have a competitive advantage in both Arctic and subarctic regions due to their relatively high growth rate at low light and temperature conditions (Lovejoy et al. 2007).

Our observations indicate that there are surviving winter stocks of both large and small phytoplankton. The early succession suggests that picoeukaryotes have the greatest advantage earliest in the season, whereas accumulation of large phytoplankton (diatoms) rapidly follows in deep convective waters (Fig. 4), whereas nanophytoplankton remain unchanged in deep mixed waters. In the stratified Norwegian Basin station Chl *a* remained in the <10 fraction, but within this fraction there was a clear change from domination of picophytoplankton nanophytoplankton (Fig. 7). The difference in development is likely caused by both abiotic and biotic mechanisms.

Heterotrophic protists: top down control on small phytoplankton?

The heterotrophic protists (HNF and MZP) followed the same homogeneous distribution within the mixed layer as the phytoplankton (Fig 5), however whereas MZP decreased exponentially below the mixed layer, HNF showed more uniform distribution towards the bottom, resulting in a relatively higher biomass when integrated to 600 m (Fig. 7 L, M). The highest biomass of heterotrophic protists was found in the stratified Norwegian Basin where ciliates dominated the biomass (Fig. 7E). Ciliates also dominated the biomass of heterotrophic protists at the two mixed stations. However, when considering the higher growth rates of HNF relative to MZP (Hansen et al. 1997), HNF's contribution to the heterotrophic protist production may be higher than their biomass suggest. The concentrations of HNF we encountered were in general in the lower end of those observed globally (Sanders et al. 1992), but very similar to those found in Arctic marine systems during the period of winter-spring transition (Vaqué et al. 2008, Rokkan Iversen & Seuthe 2010). Peak abundances of 300 cells ml^{-1} were observed during our study period, compared to concentrations of up to 8.000 cells ml^{-1} measured in the Faroe-Shetland Channel in the summer (60-62°N) (Kuipers et al. 2003). This suggests that the increasing abundance of HNF we observed might be sustained through the spring season, thus maintaining a high grazing pressure on bacteria and picophytoplankton. The average diameter of HNF found in this study 3.2 ± 0.3 µm agrees with the ≤3 µm obtained by Jürgens & Massana (2008) for 76% of HNF across four different marine systems. HNF with a diameter of 2-5 µm have been observed to ingest 1.5-2 µm picoeukaryotes and coccoid cyanobacteria (Sherr et al. 1997). It has long been assumed that heterotrophic nanoflagellates feed on pico-sized phytoplankton (Fenchel 1982, Azam et al. 1983), yet recent studies on the grazing potential of HNF focus on quantifying bacterivory and neglect the additional portion of carbon taken up via picophytoplankton (Tanaka et al. 1997; Iriarte et al. 2008). They are, however, major grazers of picophytoplankton (Christaki et al. 2001, Sherr & Sherr 2002, Bręk-Laitinen & Ojala 2011) and for future studies resolve the importance of HNF grazing. We here would suggest splitting the group into large and small HNF to test whether the size groups have different

prey-size preferences as speculated by Sherr & Sherr (2002) and Vaqué et al. (2008). Both of these studies suggest that heterotrophic flagellates <5 µm are the main grazers on bacteria, while flagellates > 5µm select for picoeukaryotes.

The biomass (mg C m^{-3}) of dinoflagellates and ciliates was low at all sampling stations compared to biomass obtained during spring and summer in the Norwegian Sea (Verity et al. 1993). However, when integrated over the depth of the mixed layer, MZP biomasses are comparable to spring integrated biomasses (300-500 mg C m^{-2}) within the mixed layer of the Norwegian Basin and the high Arctic Kongsfjorden (Verity et al. 1993, Seuthe, Rokkan Iversen, et al. 2011) and two-three fold higher than integrated values estimated during the winter-to-spring transition in the high Arctic Disko Bay (Levinsen et al. 2000). Thus, although MZP concentrations are relatively low, their integrated biomass is significant at all stations.

Ciliates dominated the MZP biomass, with a relative increase in naked and thecate dinoflagellates at the Iceland Basin and Shetland Shelf stations as diatoms became more abundant. The positive relationship between dinoflagellates and diatoms supports the hypothesis that heterotrophic dinoflagellates are important grazers of diatoms (Sherr & Sherr 2007). The Norwegian Basin station was dominated (76-86%) by oligotrich ciliates throughout the program, which would also be expected with a phytoplankton community composed of mainly small cells. At all three stations large (>30 µm) species became increasingly important at the Iceland Basin station and mirrored the increase in large phytoplankton (>50 µm), while the smaller *Mesodinium* spp. became highly abundant at the Shetland Shelf station.

Behrenfeld (2010) and Behrenfeld and Boss (2014) suggested that the higher net-increase in the phytoplankton biomass during events of deep convection is caused by a dilution of the grazing community. Although the grazers are possibly diluted, as indicated by the homogenously vertical distribution of MZP throughout the mixed layer and a reduction in MZP biomass with increasing mixing depth (Fig. 9), a reduction in grazers will not necessarily benefit the diatoms. Based on the composition of the heterotrophic protists, which were dominated by heterotrophic nanoflagellates and ciliates, we argue that a dilution of the grazing community would mainly benefit pico- and nanophytoplankton whereas diatoms are largely unaffected; the latter because diatoms are unsuitable as prey for heterotrophic nanoflagellates and ciliates. Thus the increase in the >10 µm Chl *a* fraction at the mixed stations is more likely to be explained by reduced sinking rates due to deep convection and increased irradiance as the day length increases, rather than reduced grazing pressure from heterotrophic protists being diluted. Alternatively, dilution may reduce the grazing pressure from other grazers such as the copepods (e.g. *Oithona* sp.), which could explain the net-growth in large phytoplankton species at the mixed stations.

Controls on bacteria within the mixed layer changes from bottom-up to top-down

To our knowledge there are no previous observations of bacterial abundance during the winter-spring transition in the subarctic North Atlantic. The abundances encountered initially in late-March and early-April (2-3 × 10^5 cells ml^{-1}) are an order of magnitude lower than those obtained during the spring bloom where they have been documented to reach 2× 10^6 cells ml^{-1} (Ducklow et al. 1993), but correspond to observations found during pre-bloom

conditions elsewhere in the temperate and Arctic North Atlantic (Bratbak et al. 2011, Seuthe, Rokkan Iversen, et al. 2011). It is assumed that the growth of heterotrophic bacteria in the pre-bloom phase is substrate limited, with the increase in heterotrophic bacteria triggered by DOM excreted from spring bloom production (Lancelot & Billen 1984, Teeling et al. 2012). Here we document the pre-bloom period to be a productive period, with no accumulation of DOC in the upper mixed layer (Fig. 7, Table 2), indicating an active microbial loop (Thingstad et al. 1997). Organic carbon produced by extracellular release from phytoplankton, excretion from protist grazers, cell lysis and solubilization and bacterial transformation of organic particles (Carlson, 2002), is readily consumed by bacteria. Excretion from phytoplankton is generally a very labile carbon source. It has been suggested that smaller phytoplankton excrete relatively more, as the passive excretion is largely due to the passive diffusion of low molecular weight compounds over the cell membrane, which is proportional to the surface-to-volume ratio and therefore higher for small cells (Bjørnsen 1988), e.g. a study by Malinsky-Rushansky and Legrand (1996) found that picoeukaryotes release 30% of their primary production, while larger nano-sized cells release only 4-5%.

Our data suggest that bacteria in the deep basins initially were carbon-limited as they responded positively to the growing phytoplankton supply of labile DOC. Control by bacterivorous grazers and nutrients were assumed to be less important due to low concentrations of heterotrophic flagellate grazers and since N and P were found in excess.

The pre-bloom production resulted in an increase in bacterial abundance within the upper mixed layer between the first and second visits at all stations, from which an *in situ* net growth rate of bacteria can be estimated to be 0.08-0.10 d^{-1}. During the bloom this rate is approximately doubled as evidenced by (Ducklow et al. 1993). The bacterial carbon uptake can be estimated when the top-down control is assumed to be low; e.g. between the first and second visit within the mixed layer at the Norwegian Basin, the integrated bacterial biomass increased from 5.5 to 7.2 mg C m^{-3} within the mixed layer (Fig. 7); assuming a low growth efficiency of 15% (del Giorgio and Cole, 2000), this corresponds to a potential carbon uptake of 1.7 mg C m^{-3} / 0.15 = 11 mg C m^{-3} during 10 days. Yet, in the same period DOC increased from 462 ± 50 mg C m^{-3} to 520 ± 13 mg C m^{-3}, indicating a substantial DOC supply over the 10-day period during late winter/early spring, despite low Chl *a* values.

The C:N ratio of DOM in general decreased during the study from 17.0 to 14.5 in the upper mixed layer and from 15.7 to 13.6 below the mixed layer (Fig. 8), possibly due to grazing and loss of C by respiration of the C-rich phytoplankton primary production. Labile DOM is characterized by low C:N ratios relative to refractory DOM (Carlson, 2002) and therefore the decrease in C:N coincides (however does not correlate significantly, $p = 0.2$) with a significant ($p < 0.05$) increase in HNA:LNA bacteria ($r^2 = 0.83$ within the mixed layer, and $r^2 = 0.84$ below mixed layer), indicating a more actively growing bacterial community (Sherr et al. 2006, Martínez-garcía et al. 2013). There was however an increase in the C:N ration from first to second visit at the Norwegian Basin, this could be explained by a relatively high release of sugars from picophytoplankton, which dominated at the time (Giroldo et al. 2005).

Decreasing Virus-to-Bacteria ratio

It is generally assumed that viruses are responsible for 10-50% of the bacterial mortality in surface waters and 50-100% in environments where grazing protists are low in numbers e.g. the deep ocean (Fuhrman 1999). The higher the virus:bacteria ratio (V:B), the higher the expected bacteria mortality induced by strain specific viruses. During this study we found a significantly decreasing V:B within the upper mixed layer at all stations (one-way ANOVA, $p < 0.0001$), due to the increase in bacteria, which was not mirrored as an increase in viruses. One explanation could be that the strains of bacteria, which are the best competitors for the newly produced DOC, became dominant over the strains that dominated during the winter and the strain specific viruses have not yet evolved for the new strains of dominating bacteria or that the concentrations of bacteria were not sufficient to permit infection by virus to influence the bacterial community (i.e. a Holling type 3 or 4 reaction). This "lag-phase" by viruses gives the bacterial competition specialists a head start in the pre-bloom phase. Eventually, viruses would be expected to increase in numbers and according, to the `Killing-the-Winner' hypothesis (Thingstad 2000), become a regulating factor for the bacteria community and the V:B would increase.

By the end of pre-bloom, bacteria biomass decreased at the deep stations. As the viral abundance remained low and DOC was still produced, an assumption here is that grazing from the growing HNF population caused the reduction in bacteria numbers. This change in community structure may reflect a shift in the control of bacteria within the pre-bloom phase; from bottom-up control (and possibly top-down by virus) in the winter, to top-down control by grazers during spring.

Bacteria in the deep-water benefit from deep mixing

Bacterial abundance in deep oceans is often observed to decline exponentially with depth (Nagata 2000). In contrast, we observed a vertical distribution uniform to the bottom (1300 m) in the deep basin stations (Fig. 5). The relatively high bacterial concentrations in the deep water are potentially a consequence of the deep convective mixing, which has resulted in a homogeneous distribution of bacteria over the water column. This distribution extends below the observed convective depth at all stations suggesting that the depth of convective mixing has retreated prior to the program. Conversely, the homogeneous distribution observed in the heterotrophic properties is not evidenced in the autotrophic community at the Iceland and Norwegian Basin stations. The Shetland Shelf station, which has deep convection or mixing to the bottom during the study period, has a homogeneous distribution of all properties over the entire water column. This observation suggests that the conditions in the convective layer have the potential for a net positive growth rate although low as speculated by Backhaus et al. (2003) and Lindemann and St. John (2014). These authors have identified the role of phyto-convection (Backhaus et al. 2003) and critical turbulence resulting in surface blooms (Huisman 1999) in maintaining and fueling production in the convective mixed layer. The cell distributions we observed below the convective depth support the hypothesis of Lindemann and St. John (2014) that cells are potentially detrained from the convective mixed layer contributing to a pre-spring bloom flux of organic material to depth. However, future research is clearly necessary to test this hypothesis.

Concluding remarks

This study highlights the importance of the small fast growing phytoplankton community as the base of the food web prior to the phytoplankton spring bloom, and suggests that deep convection enhances not only phytoplankton accumulation within the mixed layer, but also feeds a growing bacterial population below the deep mixed layer. The pre-bloom production feeds a growing community of heterotrophic bacteria and heterotrophic protists, and alters the C:N ratio of DOM, without depleting the nutrient reservoirs. The subsequent succession and nutrient depletion is caused by larger phytoplankton resistant to small grazers. Our data further suggests that deep mixing reduces grazing on and thus enhances growth of >10 μm phytoplankton, but that the fast growing HNF are able to keep a tight grazing control on picophytoplankton despite deep mixing. Experimental studies are needed to further assess the coupling between picophytoplankton and their small grazers.

Acknowledgements

The research leading to these results has received funding from the European Union Seventh Framework Programme project EURO-BASIN (ENV.2010.2.2.1-1) under grant agreement n° 264933, ERC grant Microbial Network Organisation (MINOS 250254) and from the U.S. National Science Foundation (OCE-0752972). The Deep convection" cruise was funded by the Deutsche Forschunggemeinschaft in a grant to MSJ. We are very grateful to Dennis A. Hansell for supplying data on TOC and TON. We are also thankful to the crew of the RV Meteor on the Deep Convection Cruise, and especially to Françoise Morison and Chris Daniels for good teamwork and for language corrections. A special thank to Aud Larsen for steadfast flow cytometry assistance. For valuable discussions we are grateful to: Lena Seuthe, Polly G. Hill, Mary Jane Perry, Marit Reigstad, Antonio Cuevas and Mathias Middelboe.

LITTERATURE CITED

Agawin NNS, Duarte CM, Agustí S (2000) Nutrient and temperature control of the contribution of picoplankton to phytoplankton biomass and production. Limnol Oceanogr 45:591–600

Anderson LG (2002) DOC in the Arctic Ocean. In: Carlson CA, Hansell DA (eds) Biogeochemistry of Marine Dissolved Organic Matter, 1st edn. Elsevier, Oriando, Florida, p 665–681

Azam F, Fenchel T, Field JG, Gray JS, Mayer-Reil LA, Thingstad F (1983) The ecological role of water-column microbes in the sea. Mar Ecol Prog Ser 10:257–263

Barber RT (2007) Picoplankton do some heavy lifting. Science 315:777–778

Behrenfeld MJ (2010) Abandoning Sverdrup ' s Critical Depth Hypothesis on phytoplankton blooms. Ecology 91:977–989

Behrenfeld MJ, Boss ES (2014) Resurrecting the ecological underpinnings of ocean plankton blooms. Ann Rev Mar Sci 6:167–94

Bjørnsen PK (1988) Phytoplankton exudation of organic matter : Why do healthy cells do it ?'. Limnol Oceanogr 33:151–154

Blindheim J, Østerhus S (2005) The Nordic Seas, Main Oceanographic Features. Geophys Monogr Ser 158:11–37

Booth BC (1988) Size classes and major taxonomic groups of phytoplankton at two locations in the subarctic Pacific Ocean in May and August 1984. Mar Biol 97:275–286

Børsheim K, Bratbak G (1987) Cell volume to cell carbon conversion factors for a bacterivorous Monas sp. enriched from seawater. Mar Ecol Prog Ser 36:171–175

Boyer Montégut C de, Madec G, Fischer AS, Lazar A, Iudicone D (2004) Mixed layer depth over the global ocean: An examination of profile data and a profile-based climatology. J Geophys Res 109:C12003

Braarud T, Nygaard I (1978) Phytoplankton observations in offshore Norwegian coastal waters between 62°N and 69°N - I. Variation in time of the spring diatom maximum 1968-71. [Fiskeridirektoratets havforskningsinstitutt]

Bratbak G, Jacquet S, Larsen A, Pettersson LH, Sazhin AF, Thyrhaug R (2011) The plankton community in Norwegian coastal waters—abundance, composition, spatial distribution and diel variation. Cont Shelf Res 31:1500–1514

Bręk-Laitinen G, Ojala A (2011) Grazing of heterotrophic nanoflagellates on the eukaryotic picoautotroph <i>Choricystis<i/> sp. Aquat Microb Ecol 62:49–59

Briggs N, Perry MJ, Cetinić I, Lee C, D'Asaro E, Gray AM, Rehm E (2011) High-resolution observations of aggregate flux during a sub-polar North Atlantic spring bloom. Deep Sea Res Part I Oceanogr Res Pap 58:1031–1039

Christaki U, Giannakourou A, Wambeke FVAN, Grégori G (2001) Nanoflagellate predation on auto- and heterotrophic picoplankton in the oligotrophic Mediterranean Sea. J Plankton Res 23:1297–1310

Cushing DH (1959) On the nature of production in the sea. Fish Invest Lond Ser II 22:1–40

Dale T, Rey F, Heimdal BR (1999) Seasonal development of phytoplankton at a high latitude oceanic site. Sarsia 84:419–435

Dickson AG, Sabine CL, Christian JR (2007) Guide to best practices for ocean CO_2 Measurements. PICES Spec Publ 3:191

Ducklow H, Kirchman D, Quinby H, Carlson C, Dam H (1993) Stock and dynamics of bacterioplankton carbon during the spring bloom in the eastern North Atlantic Ocean. Deep Sea Res II 40:245–263

Fenchel T (1982) IV . Quantitative Occurrence and Importance as Bacterial Consumers. Mar Ecol Prog Ser 9:35–42

Fuhrman J a (1999) Marine viruses and their biogeochemical and ecological effects. Nature 399:541–548

Garside C (1985) The vertical distribution of nitrate in open ocean surfac water. Deep Sea Res 32:723–732

Giroldo D, Augusto A, Vieira H (2005) Polymeric and free sugars released by three phytoplanktonic species from a freshwater tropical eutrophic reservoir. J Plankton Res 27:695–705

Hansen PJ, Bjørnsen PK, Hansen BW (1997) Zooplankton grazing and growth : scaling within the 2-2,000-µm body size range. Limnol Oceanogr 42:687–704

Hirche H (1996) Diapause in the marine copepod, *Calanus finmarchicus* - A review. Ophelia 44:129 – 143

Huete-Stauffer T, Morán X (2012) Dynamics of heterotrophic bacteria in temperate coastal waters: similar net growth but different controls in low and high nucleic acid cells. Aquat Microb Ecol 67:211–223

Huisman J (1999) Critical depth and critical turbulence: Two different mechanisms for the development of phytoplankton blooms. Limnol Oceanogr 44:1781–1787

Iriarte A, Sarobe A, Orive E (2008) Seasonal variability in bacterial abundance, production and protistan bacterivory in the lower Urdaibai estuary, Bay of Biscay. Aquat Microb Ecol 52:273–282

Irigoien X, Flynn KJ, Harris RP (2005) Phytoplankton blooms : a " loophole " in microzooplankton grazing impact ? J Plankton Res 27:313–321

Irigoien X, Head R, Klenke U, Meyer-Harms B, Harbour D, Niehoff B, Hirche H, Harris R (1998) A high frequency time series at weathership M , Norwegian Sea , during the 1997 spring bloom : feeding of adult female *Calanus finmarchicus*. Mar Ecol Prog Ser 172:127–137

Jerlov NG (1968) Optical Oceanography. Elsevier, Amsterdam

Jespersen AM, Christoffersen K (1987) Measurements of chlorophyll-a from phytoplankton using ethanol as extraction solvent. Arch Hydrobiol 109:445–454

Joint I, Pomroy A, Savidge G, Boyd P (1993) Size-fractionated primary productivity in the northeast Atlantic in May–July 1989. Deep Sea Res II 40:423–440

Jürgens K, Massana R (2008) Protistan grazing on marine bacterioplankton. In: Kirchman D (ed) Microbial Ecology of the Oceans, Second edi. John Wiley & Sons, Inc., New York, USA, p 383–441

Kiørboe T (1993) Turbulence, phytoplankton cell size, and the structure of pelagic food webs. Adv Mar Biol 29:1–71

Koroleff F (1983) Determination of nutrients. In: Grasshoff K, Erhardt M, Kremling K (eds) Methods of seawater analysis. Verlag Chemie, Weinheim, p 125–187

Kuipers B, Witte H, Noort G Van, Gonzalez S (2003) Grazing loss-rates in pico- and nanoplankton in the Faroe-Shetland Channel and their different relations with prey density. J Sea Res 50:1–9

Lancelot C, Billen G (1984) Activity of heterotrophic bacteria and its coupling to primary production during the spring phytoplankton bloom in the southern bight of the North Sea. Limnol Oceanogr 29:721–730

Larsen A, Flaten G a. F, Sandaa R-A, Castberg T, Thyrhaug R, Erga SR, Jacquet S, Bratbak G (2004) Spring phytoplankton bloom dynamics in Norwegian coastal waters: Microbial community succession and diversity. Limnol Oceanogr 49:180–190

Lee S, Fuhrman JA (1987) Relationships between biovolume and biomass of naturally derived marine bacterioplankton. Appl Env Microbiol 53:1298–1303

Levinsen H, Nielsen T, Hansen B (2000) Annual succession of marine pelagic protozoans in Disko Bay, West Greenland, with emphasis on winter dynamics. Mar Ecol Prog Ser 206:119–134

Li WKW (1980) Primary Productivity in the Sea. In: Primary productivity on the sea. Plenum Press, New York, p 259–79

Li WKW, Dickie PM, Harrison WG, Irwin BD (1993) Biomass and production of bacteria and phytoplankton during the spring bloom in the western North Atlantic Ocean. Deep Sea Res II 40:307–327

Lindemann C, John MA St. (2014) A seasonal diary of phytoplankton in the North Atlantic. Front Mar Sci 1

Lovejoy C, Vincent WF, Bonilla S, Roy S, Martineau M-J, Terrado R, Potvin M, Massana R, Pedrós-Alió C (2007) Distribution, Phylogeny, and Growth of Cold-Adapted Picoprasinophytes in Arctic Seas. J Phycol 43:78–89

Mahadevan A, D'Asaro E, Lee C, Perry MJ (2012) Eddy-driven stratification initiates North Atlantic spring phytoplankton blooms. Science 337:54–8

Malinsky-Rushansky NZ, Legrand C (1996) Excretion of dissolved organic carbon by phytoplankton of different sizes and subsequent bacterial uptake. Mar Ecol Prog Ser 132:249–255

Marie D, Brussaard CPD, Thyrhaug R, Bratbak G, Vaulot D (1999) Enumeration of Marine Viruses in Culture and Natural Samples by Flow Cytometry. Appl Environ Microbiol 65:45–52

Martínez-garcía S, Fernández E, Valle DA, Karl DM, Teira E (2013) Experimental assessment of marine bacterial respiration. 70:189–205

Menden-Deuer S, Lessard EJ (2000) Carbon to volume relationships for dinoflagellates, diatoms, and other protist plankton. Limnol Oceanogr 45:569–579

Murphy J, Riley JP (1962) A modified single solution method for the determination of phosphate in natural waters. Anal Chim Acta 26:31–36

Pomeroy LR (1974) The ocean's food web, a changing paradigm. BioScience. Bioscience 24:499–504.

Porter KG, Feig YS (1980) The use of DAPI for identifying aquatic microfloral. Limnol Oceanogr 25:943–948

Putt M, Stoecker DK (1989) An experimentally determined carbon : volume ratio for marine from estuarine and coastal waters ciliates " oligotrichous ." Limnol Oceanogr 34:1097–1103

Raven JA (1998) Small is beautiful : the picophytoplankton. Funct Ecol 12:503–513

Richardson K, Visser AW, Pedersen FB (2000) Subsurface phytoplankton blooms fuel pelagic production in the. J Plankton Res 22:1663–1671

Rokkan Iversen K, Seuthe L (2010) Seasonal microbial processes in a high-latitude fjord (Kongsfjorden, Svalbard): I. Heterotrophic bacteria, picoplankton and nanoflagellates. Polar Biol 34:731–749

Sandaa R-A, Larsen A (2006) Seasonal variations in virus-host populations in Norwegian coastal waters: focusing on the cyanophage community infecting marine Synechococcus spp. Appl Environ Microbiol 72:4610–8

Sanders RW, Caron, David A, Berninger U-G (1992) Relationships between bacteria and heterotrophic nanoplankton in marine and fresh waters : an inter-ecosystem comparison. Mar Ecol Prog Ser 86:1–14

Seuthe L, Rokkan Iversen K, Narcy F (2011) Microbial processes in a high-latitude fjord (Kongsfjorden, Svalbard): II. Ciliates and dinoflagellates. Polar Biol 34:751–766

Seuthe L, Töpper B, Reigstad M, Thyrhaug R, Vaquer-Sunyer R (2011) Microbial communities and processes in ice-covered Arctic waters of the northwestern Fram Strait (75 to 80°N) during the vernal pre-bloom phase. Aquat Microb Ecol 64:253–266

Sharples J, Ross ON, Scott BE, Greenstreet SPR, Fraser H (2006) Inter-annual variability in the timing of stratification and the spring bloom in the North-western North Sea. Cont Shelf Res 26:733–751

Sherr EB, Sherr BF (2002) Significance of predation by protists in aquatic microbial food webs. Antonie Van Leeuwenhoek 81:293–308

Sherr E, Sherr B (2007) Heterotrophic dinoflagellates: a significant component of microzooplankton biomass and major grazers of diatoms in the sea. Mar Ecol Prog Ser 352:187–197

Sherr EB, Sherr BF, Fessenden L (1997) Heterotrophic protists in the Central Arctic Ocean. Deep Sea Res Part II 44:1665–1682

Sherr EB, Sherr BF, Longnecker K (2006) Distribution of bacterial abundance and cell-specific nucleic acid content in the Northeast Pacific Ocean. Deep Sea Res Part I Oceanogr Res Pap 53:713–725

Sherr EB, Sherr BF, Wheeler PA, Thompson K (2003) Temporal and spatial variation in stocks of autotrophic and heterotrophic microbes in the upper water column of the central Arctic Ocean. Deep Sea Res Part I Oceanogr Res Pap 50:557–571

Søndergaard M, Jensen LM, Ærtebjerg G (1991) Picoalgae in Danish coastal waters during summer stratification. Mar Ecol Prog Ser 79:139–149.

Sorokin YI (1977) The heterotrophic phase of plankton succession in the japan sea. Mar Biol 41:107–117

Steele JH (1974) The structure of marine ecosystems. Cambridge, Harvard University Press

Sverdrup H (1953) On conditions for the vernal blooming of phytoplankton. J Cons Int Explor Mer 18:287–295

Tanaka T, Fujita N, Taniguchi a (1997) Predator-prey eddy in heterotrophic nanoflagellate-bacteria relationships in a coastal marine environment: a new scheme for predator-prey associations. Aquat Microb Ecol 13:249–256

Taylor JR, Ferrari R (2011) Shutdown of turbulent convection as a new criterion for the onset of spring phytoplankton blooms. Limnol Oceanogr 56:2293–2307

Teeling H, Fuchs BM, Becher D, Klockow C, Gardebrecht A, Bennke CM, Kassabgy M, Huang S, Mann AJ, Waldmann J, Weber M, Klindworth A, Otto A, Lange J, Bernhardt J, Reinsch C, Hecker M, Peplies J, Bockelmann FD, Callies U, Gerdts G, Wichels A, Wiltshire KH, Glöckner FO, Schweder T, Amann R (2012) Substrate-controlled succession of marine bacterioplankton populations induced by a phytoplankton bloom. Science (80-) 336:608–11

Thingstad TF (2000) Elements of a theory for the mechanisms controlling abundance, diversity, and biogeochemical role of lytic bacterial viruses in aquatic systems. Limnol Oceanogr 45:1320–1328

Thingstad TF, Hagstrom A, Rassoulzadegan F (1997) Accumulation of degradable DOC in surface waters: Is it caused by a malfunctioning microbial loop? Limnol Oceanogr 42:398–404

Townsend DW, Cammen LM, Holligan PM, Campbell DE, Pettigrew NR (1994) Causes and consequences of variability in the timing of spring phytoplankton blooms. Deep Sea Res Part I Oceanogr Res Pap 41:747–765

Tremblay G, Belzile C, Gosselin M, Poulin M, Roy S, Tremblay J (2009) Late summer phytoplankton distribution along a 3500 km transect in Canadian Arctic waters: strong numerical dominance by picoeukaryotes. Aquat Microb Ecol 54:55–70

Vaqué D, Guadayol Ò, Peters F, Felipe J, Angel-Ripoll L, Terrado R, Lovejoy C, Pedrós-Alió C (2008) Seasonal changes in planktonic bacterivory rates under the ice-covered coastal Arctic Ocean. Limnol Oceanogr 53:2427–2438

Verity PG, Langdon C (1984) Relationships between lorica volume, carbon, nitrogen, and ATP content of tintinnids in Narragansett Bay. J. Plankt Res 6:859–868.

Verity PG, Stoecker DK, Sieracki ME, Nelson JR (1993) Grazing, growth and mortality of microzooplankton during the 1989 North Atlantic spring bloom at 47°N, 18°W. Deep Sea Res Part I Oceanogr Res Pap 40:1793–1814

Waite AM, Thompson P a., Harrison PJ (1992) Does energy control the sinking rates of marine diatoms? Limnol Oceanogr 37:468–477

Williams PJLB (1981) Incorporation of microheterotrophic processes into the classical paradigm of the planktonic food web. Kieler Meeresforsch Sondh 5:1–28

Wood ED, Armstrong FAJ, Rich FA (1967) Determination of nitrate in seawater by cadmium-copper reduction to nitrate. J biol Assoc UK 47:23–31

Zubkov MV, Burkill PH, Topping JN (2006) Flow cytometric enumeration of DNA-stained oceanic planktonic protists. J Plankton Res 29:79–86

Zubkov MV, Sleigh M., Tarran GA, Burkill P., Leakey RJ. (1998) Picoplanktonic community structure on an Atlantic transect from 50°N to 50°S. Deep Sea Res Part I Oceanogr Res Pap 45:1339–1355

Paper III

Submitted to Aquatic Microbial Ecology

Maria Lund Paulsen sampling on board RV Meteor. Photo: Karen Riisgaard

The North Atlantic heterotrophic protist community: Trophic links and their role in the food web

Karen Riisgaard[1], Maria Lund Paulsen[1,2], Michael St. John[1], Torkel Gissel Nielsen[1]

[1] National Institute of Aquatic Resources, DTU-Aqua, Section for Ocean Ecology & Climate, Denmark
[2] Department of Biology, Marine Microbiology Department, University of Bergen, Norway

ABSTRACT

The role of the protist community in the North Atlantic deep convective layer was studied during the winter-spring transition to assess the trophic links and their role in structuring the microbial community. In order to establish these relationships, three microcosm experiments were performed using size fractionated surface water (taken at 30 m) from the Iceland Basin (26 March, 11 April and 21 April, respectively). These experiments identified that heterotrophic nanoflagellates fed on bacteria and picophytoplankton (<2 μm) while ciliates and heterotrophic dinoflagellates controlled the heterotrophic nanoflagellate community. In general the grazing induced mortality of phytoplankton was low, however, our data suggests that autotrophic picoplankton represent important prey items for heterotrophic nanoflagellates. During the latter two experiments microzooplankton became relatively more important as grazers. The experiments illustrate the microbial succession of the community during the winter-spring transition where heterotrophic nanoflagellates are major grazers.

Furthermore, we demonstrate that reduced encounter rate between microzooplankton and phytoplankton during the period of winter deep convection could promote a build-up in phytoplankton. This reduced rate of encounter may also lead to a reduction of the top-down control of heterotrophic nanoflagellates, hereby maintaining a strong top-down control on picophytoplankton. The succession we document would consequently favor larger species, such as diatoms resistant to small grazers, which take over as dominant primary producers during the North Atlantic spring bloom. This finding has the potential to clarify, at least in part the dominance of diatoms in the North Atlantic spring bloom and brings into question the dilution recoupling hypothesis in relation to controlling the spring bloom.

KEY WORDS: Deep ocean convection, growth rate, spring bloom, microzooplankton

INTRODUCTION

The North Atlantic spring bloom is one of the largest phytoplankton blooms in the ocean and has fascinated biological oceanographers for decades (e.g. Sverdrup 1953; Cushing 1959; Siegel et al. 2002; Taylor and Ferrari 2011). The bloom is recognized as a seasonal hot spot, nourishing zooplankton and higher trophic levels and is a major driver for the global biological carbon pump (Boyd & Newton 1995). Some of the first hypotheses driving on bloom initiation were based on observations from weather station MIKE in the North Atlantic Ocean (66°N 2°E), where Sverdrup (1953) developed the Critical Depth Hypothesis. This hypothesis proposed that the bloom is initiated as the phytoplankton community is released from light limitation as day the length increases and the mixed layer shoals to a depth where phytoplankton cells are maintained in the euphotic zone and as a result net growth rates exceeds net loss rates.

Within the last two decades this classical explanation has been challenged as the North Atlantic spring bloom starts 1-2 months before establishment of the stratification (Garside & Garside 1993, Townsend et al. 1994, Dale 1999). This pre-stratification bloom is characterized by frequent mixing events due to convection as the water column losses heat. Deep convection facilitates up- and downward movements of the plankton cells within a mixed layer which can extend to 1000 m (de Boyer Montégut et al. 2004). Backhaus et al. (2003) hypothesized that there was a positive relationship between deep convection in the North Atlantic during winter and winter primary production as deep convection introduces cells to the photic zone during their circulation within the deep mixed layer allowing for growth and compensating for losses due to sinking. This hypothesis was challenged a few years later by Behrenfeld (2010) who explained the apparent net growth of phytoplankton during deep winter mixing by a reduced grazing pressure caused by the lower encounter between phytoplankton and their grazers during deep winter mixing (the dilution recoupling hypothesis). Taylor and Ferrari (2011) postulated on the other hand that the net increase in phytoplankton occur as the convective movements loss momentum (convective *shut-down*) but that stratification does not occur instantaneously herby enabling net phytoplankton growth in the surface waters despite an apparent homogeneous water column. The factors regulating the bloom are still disputed and have recently been reviewed by Lindemann & St. John (2014) who present a conceptual model where a combined effect of low grazing pressure, low community respiration and periods of convective mixing compensate for cell sinking and limited light exposure which lead to a net increase in phytoplankton biomass. However, more knowledge about the biological processes within the water column is needed to fully understand the mechanisms regulating the bloom dynamics.

Heterotrophic protists are recognized as major regulators for phytoplankton net growth during the bloom and post-bloom conditions in the North Atlantic (Verity et al. 1993; Gifford et al. 1995). However, there is at present limited knowledge on the grazing community during the winter-spring transition. Paulsen et al. (Paper II) investigated the autotrophic and heterotrophic plankton communities throughout the water column at three localities in the sub-arctic Atlantic prior to the spring bloom and documented a homogenous distribution of the plankton

communities throughout the mixed layer where deep convection occurred. Furthermore, Paulsen et al. (Paper II) and C. Daniels (pers. comm.) document that small (<10 µm) phytoplankton dominate the primary production early in the productive season, but that the relative importance of small sized phytoplankton decrease as the bloom developed. Paulsen et al. (Paper II) hypothesized that the relative decrease in picophytoplankton abundance was caused by the growing community of heterotrophic protists grazing on this size fraction.

Here, we evaluate the population dynamics of the microbial components during the winter-spring transition in the Iceland Basin. We quantify protist growth and grazing potential and test how the heterotrophic protists community influences the succession of bacteria and small-sized phytoplankton.

MATERIAL & METHODS

Location and sampling

The study was conducted from 26 March to 1 May 2012 during a cruise aboard the RV *Meteor* cruise no. 87), University of Hamburg, where a time series station (St. 1) located in the Iceland Basin (61.5°N, 11°W) was visited three times (Fig. 1). At each visit vertical profiles of temperature, salinity and PAR were obtained using a CTD Sea Bird (SBE 9 plus) with an attached rosette of 10 L Niskin bottles. The depth of the mixed layer was identified as a decrease of 0.2°C from surface (10 m) temperatures (de Boyer Montégut et al. 2004).

Sampling depths were chosen from the water column structure, and covered the full water column (bottom depth 1300m), however with the highest resolution within the mixed layer. At each visit, 3 profiles were sampled within a time frame of 20-36 h to capture the temporal variation. Water samples were collected to obtain data on chlorophyll a (Chl *a*), nutrients (N, P, Si), bacteria, autotrophic and heterotrophic flagellates and dinoflagellates and ciliates.

Concentrations of Chl *a* were estimated from triplicate water samples of 100-1000 mL and size fractionated on Whatman GF/F filters (0.7-µm pore-size), 10-µm and 50-µm mesh filters. Filters were extracted in 96% ethanol for 12-24 h (Jespersen & Christoffersen 1987). Chl *a* concentrations were measured on a TD-700 Turner fluorometer calibrated against a Chl *a* standard.

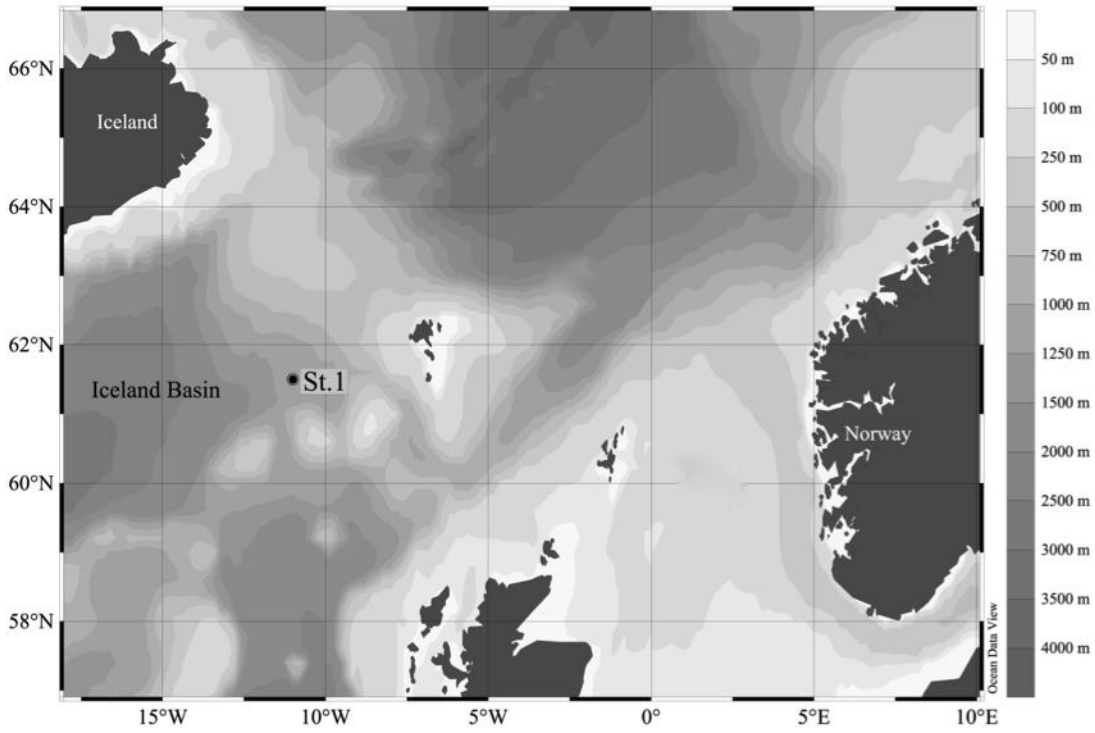

Fig. 1. Study area in the subarctic Atlantic. St.1: The 1350 m deep station in the Iceland Basin (61.5°N, 11°W).

Microcosm experiments

Growth and grazing rates of the different microbial components were obtained from three microcosm experiments. Water was collected from the photic zone at 30% surface light (~30 m) using 10 L Niskin bottles and gently siphoned into dark carboys. Prior to setup, all bottles and carboys were acid washed and then rinsed in Milli-Q® water. The experimental bottles (3.6 L) were incubated on deck in a 1000 L PVC tank with flow through water from 5 m depth, keeping temperature close to *in situ*.

Fifty L of the collected water was screened through one of three filters with different pore-sizes: 50, 10 and 0.8 µm. The treatments (hereafter Treat<0.8, Treat<10 and Treat<50) were prepared by a screening the water through either a 0.8 µm polycarbonate filter or by gently screening the water through a 10 µm or 50 µm mesh filter by reverse filtration. The three treatments aimed to remove: 1) all grazers including heterotrophic nanoflagellates (Treat<0.8), 2) all micro- and mesozooplankton (Treat<10) and 3) mesozooplankton (Treat<50). Water from each treatment was gently transferred into triplicate 2.5 L transparent polycarbonate bottles (Naglene®) by staggered filling using silicone tubing. Another 50 L of seawater was filtered through a 0.2-µm sterile Polycap filter and thereafter stored in the dark at 1°C for later addition

to the grazing experiments (max 8 days of storage). Control samples of the stored water showed no increase in the bacterial or viral abundance during the period.

The bottles were wrapped in dark nylon mesh, reducing the irradiance to ~ 30% simulating *in situ* conditions. The bottles were kept in motion by the vessel's movements and rotated daily by hand. Every other day, 260 mL subsamples (10.6% of total volume) were removed for quantification of microorganisms (virus, bacteria, small phytoplankton, HNF and MZP), Chl *a*, and nutrients (N, P, Si). After each sampling, bottles were refilled with the stored 0.2-µm filtered seawater. The experiments were terminated after 10 days.

Enumeration of microbes

Viruses, bacteria, small phytoplankton (pico- and nanophytoplankton) and HNF were enumerated using a FACS Calibur (Becton Dickinson, Oxford, UK) flow cytometer as described in Paulsen et al. (Paper II). For the enumeration of small phytoplankton (pico- and nanophytoplankton), bacteria and viruses, 2 mL samples were fixed with glutaraldehyde (final conc. 0.5%) and thereafter flash-frozen and stored in -80°C until further analysis. Small phytoplankton were discriminated on the basis of their side scatter, the pigments Chl *a* and phycoerythrin-emitting red and orange fluorescence, respectively, as in Larsen et al. (2004). Phytoplankton grouped into picoeukaryotes, *Synechococcus*, and small and large nanophytoplankton and mean red-fluorescence per cell within each group was recorded. Heterotrophs were stained with a green fluorescent nucleic-acid dye, SYBR Green I (Molecular Probes Inc., Eugene, Oregon) and discriminated on biparametric flow cytometry plots according to the recommendations of Marie et al. (1999) and Zubkov et al. (2007) for virus and bacteria, and HNF, respectively. Using this method we could not distinguish mixotrophic nanoflagellates. Bacteria were further divided into large and small based on their side scatter as in Calvo-Díaz & Morán (2006).

For enumeration and size measurements of larger protists water samples of 500 ml (*in situ*) or 50 mL (mesocosm experiments) were gently decanted from the Niskin bottle through a silicon tube into glass bottles and fixed in acidic Lugol's solution (final conc. 3%). Cells were counted and size measured using an inverted microscope. The entire sample or a minimum of 300 cells were counted. From the lugol-fixed samples, notes on the dominating phytoplankton species were made.

Size and biomass estimation of protists

Size estimations of the various groups of phytoplankton (picoeukaryotes, *Synechococcus* and small and large nanophytoplankton) were done by filtering parallel samples through 0.8, 1, 2, 5, 10-µm polycarbonate filters and counting the filtrate, hereby enumerating the percentage of

each group within the given size interval, a method modified from Zubkov et al. (1998). HNF size was estimated using epifluorescence microscopy. Samples (10 mL) were fixed with glutaraldehyde (1% final conc) for 15 min and stored at -80°C. The samples were filtered through black polycarbonate filters (pore size 0.8-µm), stained with 4,6-diamidino-2-phenylindole dihydrochloride (DAPI) DNA-specific dye (Porter & Feig 1980), and the diameters of 170 cells were measured under a UV-microscope (x1000). To ensure the measured cells were heterotrophic, each cell was crosschecked for red auto-fluorescence. For both HNF and groups of small phytoplankton the abundance within the size intervals was converted to the weighted arithmetic averaged size (Table 1). Dinoflagellates and ciliates were identified by morphology and divided into size classes covering 10-µm ranges of equatorial spherical diameter (ESD) starting with 10-20 µm. ESD and cell volume are related by: $\pi/6 \times ESD^3$= cell volume. Cell volumes were calculated using appropriate geometric shapes without including the membranelles. Biomasses of bacteria, HNF, autotrophic pico- and nanoplankton were estimated using literature values and a measured average size (Table 1), while biomass of MZP was estimated from their bio-volumes (V) converted into carbon biomass (Table 1).

Table 1. Weighted arithmetic means of measured equivalent spherical diameter (ESD) within the size fractions chosen to represent small and large autotrophic nano flagellates heterotrophic nanoflagellates, picoeukaryotes and *Synecohcocus* spp. as well as the carbon conversion factors used to convert estimates of cell abundance to biomass (pg C cell^{-1}). Dinoflagellates and ciliates are estimated from biovolumes of each individual (V) and average ESD is therefore not presented. For smaller protist groups average ESD was measured; for HNF diameter was estimated by microscopy and for small phytoplankton the weighted arithmetic mean of the diameter was calculated from the abundance within different size intervals using filtration. The biomass of viruses and bacteria are estimated using literature values.

Group	**Measured ESD (µm)**	**Carbon conversion fg C µm^{-3}**	**Conversion reference**	**Biomass pg C cell^{-1}**
Dino-flagelates		Log (pg C cell^{-1}) = -0.353 + 0.864 Log (V)	Menden-Deuer & Lessard 2000	
Aloricate ciliates		Log (pg C cell^{-1}) = -0.639 + 0.984 Log (V)	Putt and Stoecker 1989, modified by Menden-Deuer and Lessard 2000	
Loricate ciliates		Log (pg C cell^{-1}) = -0.168 + 0.841 Log (V)	Verity and Langdon 1984, Menden-Deuer and Lessard 2000	
Small ANF	4 ± 0.5	220	Booth, 1988	7.140
Large ANF	9 ± 0.7	220	Booth, 1988	58.980
HNF	3.2 ± 0.3	220	Børsheim and Bratbak, 1987	4.505
Picoeuk.	1.7 ± 0.4	220	Kana and Gilbert, 1987	0.581
Synecho.	1.1 ± 0.4	250	Booth 1988	0.191
Bacteria			Lee & Fuhrman 1987	0.020

Growth and grazing rates

Net growth rates (μ, d^{-1}) were calculated from the change in cell concentration according to:

$$\mu_n = \ln N_1 - \ln N_0 / t_1 - t_0, \quad (1)$$

where N_0 and N_1 are number of cells before dilution (t_1) and after previous dilution (t_0), respectively, and where n is the treatment type (1: Treat<0.8, 2: Treat<10 and 3: Treat<50)

Grazing mortality rates (g, d^{-1}) were estimated from the difference in growth rates of potential prey (heterotrophic nanoflagellates, phytoplankton and bacteria) between the grazing reduced treatments and the treatments with grazing (i.e. μ_1-μ_2 or μ_2-μ_3) (Verity et al. 2002).

Average prey concentration was calculated as:

$$C = (X_{t+1} - X_t) / (\text{Ln } X_{t+1} - \text{Ln } X_t), \quad (2)$$

Where t is time (d) and X is the prey concentration in subsample.

Ingestion rates (I, mg C d^{-1}) were calculated as:

$$I = g \times C, \quad (3)$$

where g is the grazing mortality and C is the average prey concentration.

RESULTS

Throughout the program (26 March to 1 May, 2012), the station was in winter-state with stormy weather and wave heights of 3-5 m. Atlantic Water (θ = 5-10.5°C, salinity = 35-35.05) was the dominating water body reaching >1000 m Blindheim and Østerhus (2005). Polar Overflow Water (θ <0.5°C, salinity = 34.88-34.93) was observed near the bottom on few occasions. The water column was initially mixed down to 600 m but the depth of the mixed layer reduced gradually to ~ 350 m during the study program. During the same period the day length increased from 11 to 15 h. The water column was sampled on 26 March, 11 April and 21 April. All sampled groups of organisms were evenly distributed throughout the mixed layer indicating active convective movements. Major nutrients (N:P:Si) were unlimited; 13:0.8:5 µmol l^{-1} and 12:0.8:4 µmol l^{-1} at first and last visit, respectively (Fig. 2).

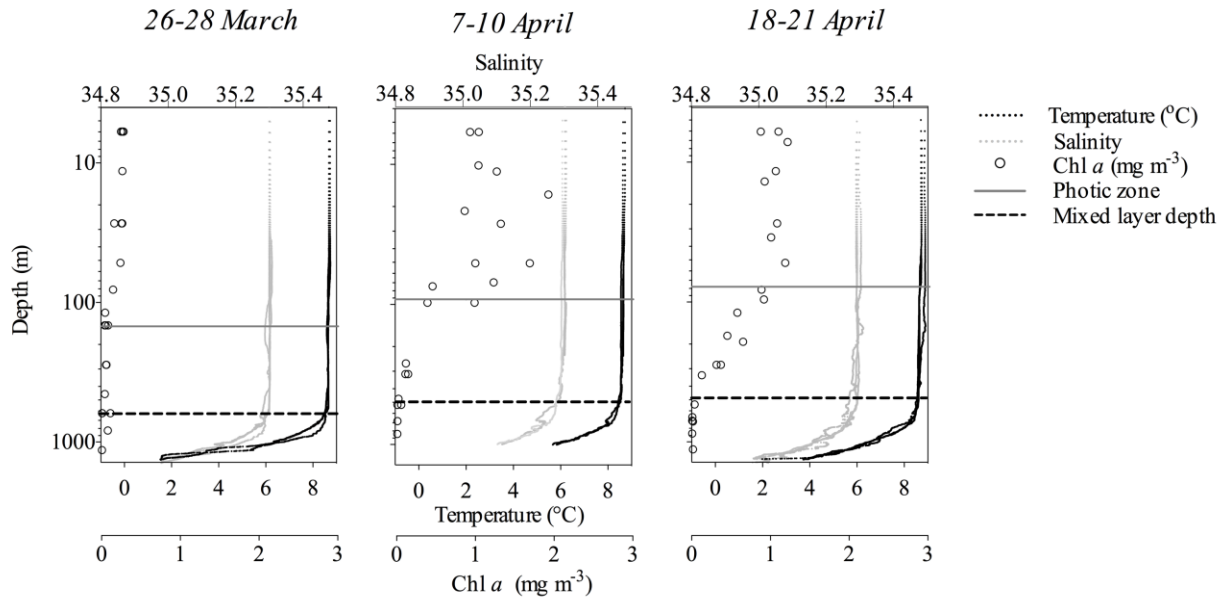

Fig. 2. Log-scaled vertical profiles of temperature (°C): ⋯⋯, salinity⋯⋯, total Chl a (mg C m^{-3}): ○. All measured three times within 20-36 h at each visit to each station (first visit to the left). Horizontal black dashed line (-----) indicates the mixed layer depth and the grey line (——) the photic zone.

Chl *a* concentrations were initially <0.2 mg Chl *a* m^{-3}, gradually increasing to 0.6 mg Chl *a* m^{-3}. The Chl *a* fraction <10 µm contributed to more than 90% of the Chl *a* on the first sampling day. On the two latter sampling days Chl *a* in the small (<10 µm) fraction was reduced but still contributed with ca. 50 % of the total phytoplankton biomass. The Chl *a* fraction <10 µm was dominated by picoeukaryotes (2-5 × 10^3 cells ml^{-1}) and nanophytoplankton (3-5×10^2 cells ml^{-1}). The average abundance of bacteria within the mixed layer ranged from 2 to 4 × 10^5 cells ml^{-1}. *Synechococcus* comprised the smallest autotrophic biomass, increasing towards the end of the study but never exceeded 0.17 mg m^{-3}. In the following we will simply use the term picophytoplankton and not distinguish between *Synechococcus* and picoeukaryotes. Bacteria biomass increased from initially 3.6 mg C m^{-3} to 5.2 mg C m^{-3} at the last sampling day (data not shown).

Heterotrophic protists were homogeneously distributed throughout the mixed layer. Heterotrophic protists <10 µm were composed by unidentified HNF with an average ESD of 3.2 µm (Table 1) which increased in abundance from 40 cells ml^{-1} at the two first sampling days to >200 cells ml^{-1} at the last sampling day. When converted to biomass HNF increased from 0.08 to 0.93 mg C m^{-3} during the program within the mixed layer (Fig. 3). In the same period MZP (heterotrophic dinoflagellates and ciliates) increased from 0.48 to 1.1 mg C m^{-3} (Fig. 3). Ciliates made up 75-91 % of the MZP biomass. Heterotrophic dinoflagellates were dominated by species of the genera *Gymnodinium, Gyrodinium* and *Protoperidinium.* Ciliates were dominated by aloricate species mainly strombilids and the mixotrophic *Mesodinium rubrum* (table 2). Biomass of both ciliates and dinoflagellates increased during the study (Fig. 3).

Table 2. Concentration (µM) of nutrients (N, P, Si) in the grazing experiments during the first 6 days of the experiments. Start values are given as mean ± SD, n = 9, while end values are given for each treatment.

		Exp. I		**Exp. II**		**Exp. III**	
		Start	End	Start	End	Start	End
N	Treat<0.8	12.3 ± 0.3	12.1 ± 0.2	12.0 ± 0.3	10.9 ± 0.1	11.6 ± 0.2	11.7 ± 0.07
	Treat<10		12.0 ± 0.3		10.2 ± 0.2		11.1 ± 0.04
	Treat<90		11.9 ± 0.1		8.4 ± 0.8		10.4 ± 0.04
PO_4	Treat<0.8	0.9 ± 0.4	1.0 ± 0.04	0.77 ±0.1	0.72 ± 0.01	0.74 ± 0.02	0.76 ± 0.01
	Treat<10		0.9 ± 0.02		0.59 ± 0.01		0.74 ± 0.01
	Treat<90		0.8 ± 0.01		0.45 ± 0.04		0.6 ± 0.03
Si	Treat<0.8	4.6 ± 0.1	4.7 ± 0.04	3.9 ± 0.1	4.1 ± 0.02	4.23 ± 0.05	4.3 ± 0.01
	Treat<10		4.7 ± 0.06		3.5 ± 0.09		4.1 ± 0.02
	Treat<90		4.6 ± 0.01		2.7 ± 0.26		3.3 ± 0.3

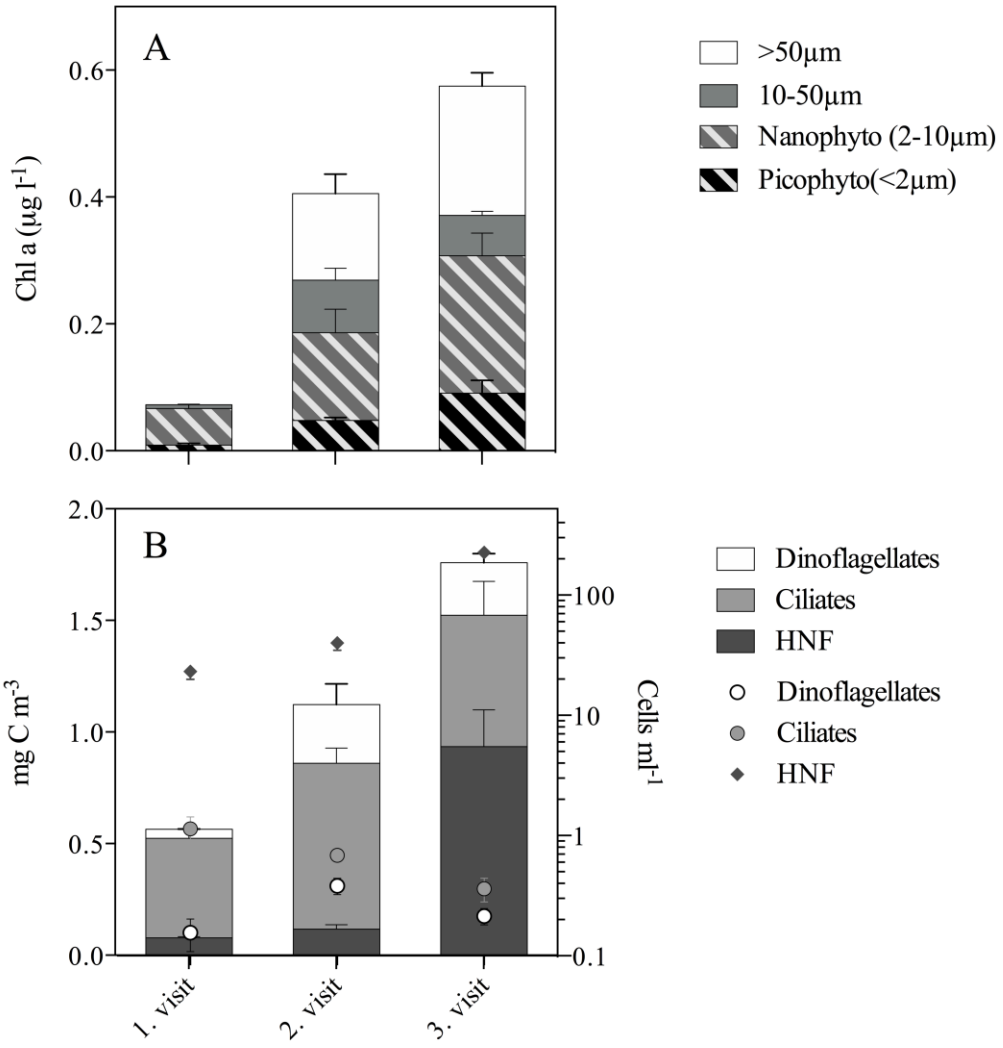

Fig. 3. Biomass and size distribution of: A) autotrophic protists and B) heterotrophic protists (HNF, dinoflagellates and ciliates) at the sampling station integrated over the mixed layer and converted into mg C m^{-3}. B) further shows the abundance of heterotrophic protists in the mixed layer (cells l^{-1}). Values are shown as mean ± SE (n = 3).

Development in abundance of functional groups

The three microcosm experiments (Exp. I, Exp. II and Exp. III) were initiated with water sampled from the Iceland Basin on 26 March, 11 April and 21 April, 2012, respectively. Exp. I represented a winter community i.e. low abundances of autotrophic and heterotrophic protists (Fig. 4). Exp. II and III were initiated with a more diverse and dense microbial community although still in the pre-bloom phase. The temperature followed approximately *in situ* sea surface temperature of 8°C (Table 2). The initial concentrations of major nutrients (N, P and Si, µmol l^{-1}) were similar for all experiments (Table 2). During the 10 days of incubation nutrients were exploited in parallel to the increase in Chl *a*, but were still replete on the last sampling day. To

ensure that nutrients were unlimited, an additional <50 µm treatment with nutrients added was conducted during Exp. I (data not shown). Since the average growth rates in total Chl *a* were similar between Treat<50 um and Treat<50+NS (One-way ANOVA, $P > 0.05$), we assumed phytoplankton growth to be nutrient unlimited under the given nutrient conditions and this additional treatment was not conducted in the two latter experiments.

The development of the autotrophic community was tracked by changes in size fractionated Chl *a* concentration and development in cell abundance of picophytoplankton and nanophytoplankton. All experiments were initiated with low Chl *a* concentrations (<1 mg Chl *a* m^{-3}, Fig. 4). Chl *a* in Treat<50 was dominated by phytoplankton <10 um in Exp. I and III and by phytoplankton >10 um (primarily diatoms identified as *Chaetoceros* spp. and *Pseudo-nitzschia* spp.) in Exp. II. The Chl *a* fraction <10 um was dominated by picophytoplankton during Exp. I and by nanophytoplankton in Exp. III.

In all experiments Chl *a* increased during the incubation period, but the relative increase was always highest in Treat<10 compared to Treat<50. Similarly, the relative increase in picophytoplankton was generally higher in Treat<0.8 compared to Treat<10. The development in picophytoplankton was characterized by a slow increase in abundance during Exp. I for all treatments. However, in Exp. II and Exp. III, the development in picophytoplankton was characterized by an initial acceleration in abundance and a sudden decrease at day 4-6 in Treat<10 and Treat<50. Abundance of picophytoplankton in Treat<0.8 increased throughout the experimental period. The development in nanophytoplankton and Chl *a* did not show the same clear succession pattern as picophytoplankton, and can best be described as an irregular increase in both Treat<10 and Treat<50.

The heterotrophic communities were composed by bacteria, HNF, ciliates and dinoflagellates. The first two days were defined as acclimation period since an initial reduction in abundance was observed. In Exp. I bacteria increased hereafter in abundance in all treatments. In Exp. II bacteria increased in all treatments but after ca. 6 days they reduced in abundance in Treat<10 and Treat<50. During the last few days of Exp. II the bacteria abundance once again increased, probably as a consequence of the increase in phytoplankton and the following excretion of labile carbon. While the succession in bacteria in Treat<10 and Treat<50 was variable within treatments, the bacterial abundance increased continuously in Treat<0.8. In Exp. III bacteria increased in abundance from day 2-4, but after day 4 they decreased exponentially in Treat<10 and Treat<50, probably as a consequence of the increase in abundance of heterotrophic protists.

The abundance of viruses were generally constant throughout all experiments, with a single high peak (>3 $\times 10^6$ ml^{-1}) in Exp. I. Apart from this single peak, which may have been caused by viral lysis, virus abundance stayed rather constant within the range 1-2 $\times 10^6$ cells ml^{-1}.

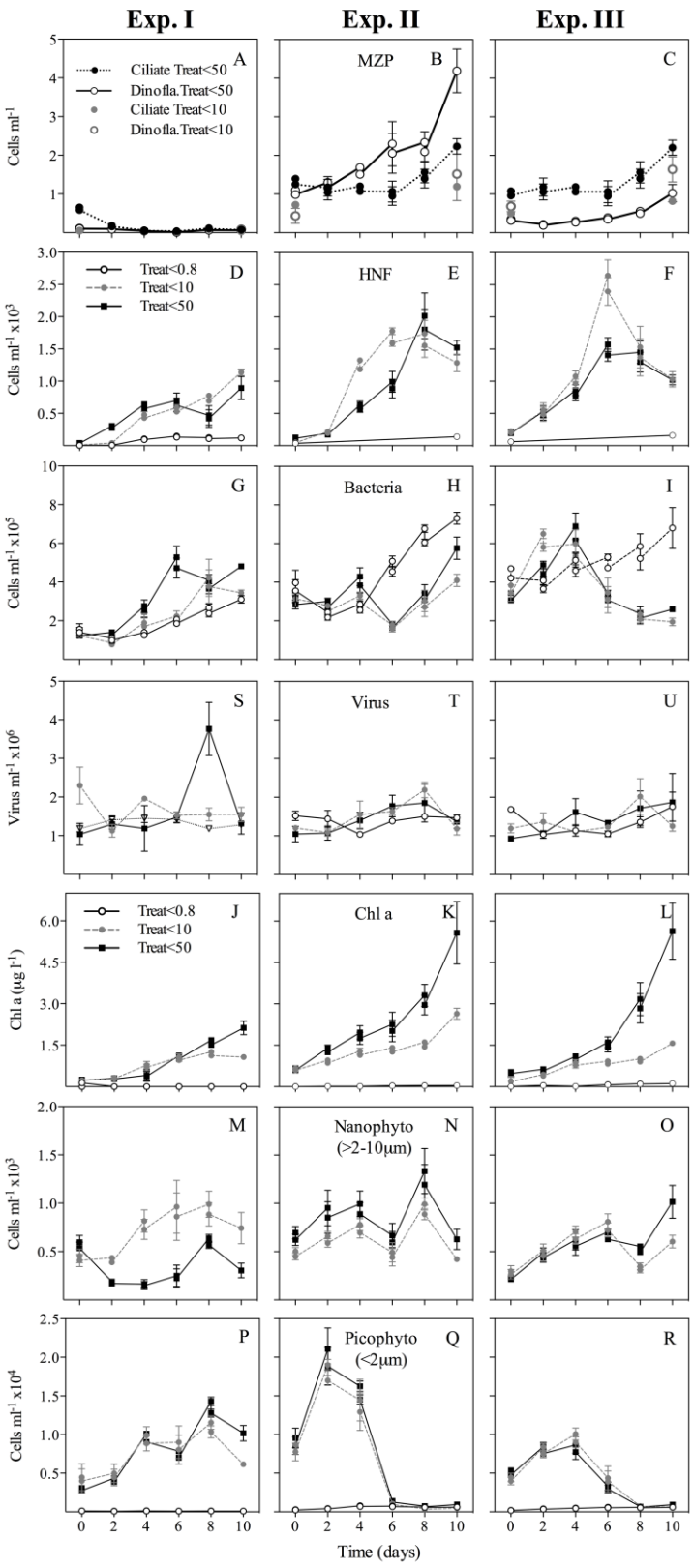

Fig. 4. Development in microorganisms in the three microcosm experiments. Cell abundance in given both before and after sampling. Values presented as mean ± SE (n = 3). Note different y-axis.

Initially, the HNF concentration was low in all the experiments, but during the experimental periods they increased. The highest increase was in Treat<10 where HNF increased from initially <100 cells ml^{-1} to >500 ml^{-1} (cumulated values up to 3000 cells ml^{-1}). During the last 3-4 days of the incubation period of Exp. II and Exp. III the abundance decreased. This decrease could be as result of a drop in abundance of phytoplankton prey the last days of the experiement, but as the relative increase was highest in Treat<10 compared to Treat<50 the decrease could also be explained by predation by the MZP.

Due to their low abundance in Treat<10, dinoflagellates and ciliates were only followed in Treat<50. All experiments were initiated with low concentrations (< 2 cells ml^{-1}) of dinoflagellates and ciliates. In Exp. I (Treat<50), the abundance remained low throughout the incubation period, whereas the abundance increased to > 5 cells ml^{-1} during in Exp. II and Exp. III. In Exp. I the major decrease in MZP abundance was caused by mortality of ciliates during the first two days of the experiment. In Exp. II and III MZP abundance increased moderately, with an average growth rates during the incubation period of 0.1 d^{-1}. Ciliates were dominated by *Mesodinium rubrum* and spirotrichs, primarily the genera *Strombidium* and *Strobilidium* (Fig. 5, left panel). In Exp. I and III, dinoflagellates were numerically dominated by small unidentified naked dinoflagellates, most likely gymnodoid species. In Exp. II, small thecate *Protoperidinium bipes* dominated along with the naked *Gymnodinium spirale* (Fig. 5, two right panels).

On the last sampling day, MZP biomass in Treat<10 µm was on average 16 ± 7 % of the biomass in Treat<50 (Table 3). Thus although MZP were present in Treat<10 their biomass was markedly reduced in Treat<10 compared to Treat<50. The MZP biomass in Treat<10 was primarily composed of dinoflagellates (*Gyrodinium spirale* and small unidentified gymnodoid species), but some small (ESD: 10-12 µm) *Mesodinium* spp. were also present in low numbers (<0.5 cells ml^{-1}). No large (>20 µm) ciliates were present in any of the Treat<10 samples.

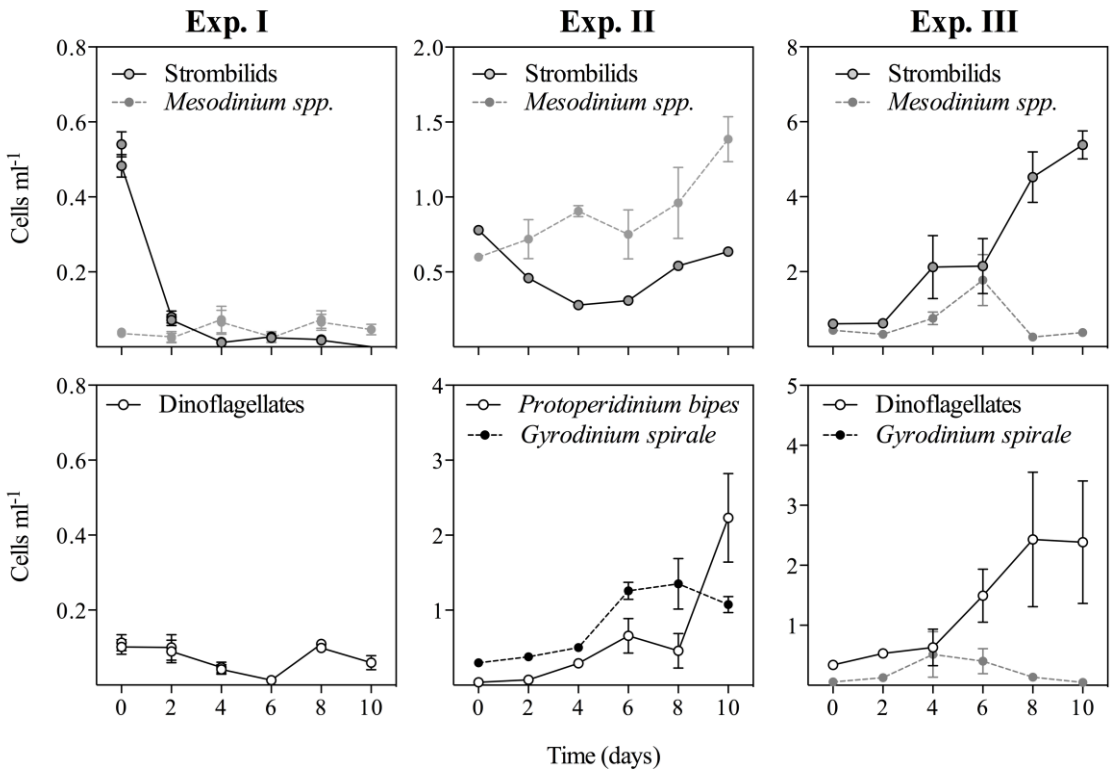

Fig. 5. Development in dinoflagellates and ciliates in the three microcosm experiments. Exp. I is shown as cell abundance before and after sampling. Exp. II and III are shown as cummulated cell abundance. Values presented as mean ± SE (n = 3). Note different y-axis.

Table 3. Abundance (cells ml^{-1}) and biomass (µg C l^{-1}) of microorganisms in the microcosm experiments. Values are given as mean during the first 4 days incubation (6 days in Exp. I) with standard deviation (in brackets). ND = no data available. *Estimated assuming exponential growth between start and end of the experiment.´

		Exp. I			Exp. II			Exp. III		
Treatment		<0.8	<10	<50	<0.8	<10	<50	<0.8	<10	<50
Ciliates	Cells ml^{-1}	ND	0.05 (0.10)	0.21 (0.24)	ND	*0.80 (0.37)	1.14 (0.25)	ND	*0.56 (0.05)	1.51 (0.53)
	mg C m^{-3}	ND	0.006 (0.002)	0.19 (0.21)	ND	*0.33 (0.11)	1.31 (0.36)	ND	*0.14 (0.001)	2.38 (1.91)
Dinofl.	Cells ml^{-1}	ND	0.09 (0.07)	0.09 (0.05)	ND	*0.43 (0.28)	1.34 (0.30)	ND	*0.84 (0.24)	0.90 (0.25)
	mg C m^{-3}	ND	0.01 (0.008)	0.08 (0.05)	ND	*0.24 (0.14)	0.98 (0.35)	ND	*0.23 (0.03)	0.53 (0.20)
HNF	Cells ml^{-1}	ND	232 (202)	396 (215)	ND	351 (237)	354 (104)	ND	538 (207)	490 (168)
	mg C m^{-3}	ND	1.2 (1.1)	2.1 (1.1)	ND	1.9 (1.3)	1.3 (0.6)	ND	2.8 (1.1)	2.6 (0.9)
Nanophyto	Cells ml^{-1}	ND	605 (197)	229 (95)	ND	472 (112)	628 (217)	ND	439 (104)	395 (80)
	mg C m^{-3}	ND	2.5 (0.82)	0.95 (0.40)	ND	9.5 (2.5)	11.3 (4.2)	ND	11.3 (2.7)	10.5 (2.0)
Picophyto	Cells $ml^{-1} \times 10^4$	0.10 (0.03)	0.68 (0.25)	0.62 (0.20)	0.44 (0.12)	1.41 (0.24)	1.57 (0.29)	0.34 (0.073)	0.73 (0.16)	0.72 (0.99)
	mg C m^{-3}	0.05 (0.01)	3.4 (1.4)	3.2 (1.1)	0.24 (0.7)	8.0 (1.3)	8.8 (1.7)	0.17 (0.045)	3.3 (0.76)	3.3 (0.50)
Bacteria	Cells $ml^{-1} \times 10^5$	1.5 (0.37)	14.0 (0.51)	23.0 (1.1)	2.6 (0.19)	29.1 (0.21)	3.2 (0.39)	4.5 (0.26)	54.6 (0.68)	5.0 (0.93)
	mg C m^{-3}	2.9 (0.73)	2.8 (1.0)	4.6 (2.1)	5.2 (0.39)	5.8 (0.41)	6.3 (0.77)	9.0 (0.52)	10.9 (1.4)	9.9 (1.9)

Table 4. Net growth rates (μ, d^{-1}) of microorganism obtained from day 0-6 (Exp. I, n=9) and day 0-4 (Exp. 2 and Exp. 3, n=6) in Treat<0.8, Treat<10 and Treat<50. Values are given as mean and standard deviation (in brackets).

	Exp. I			**Exp. II**			**Exp. III**		
Organisms	**<0.8 (μ_1)**	**<10 (μ_2)**	**<50 (μ_3)**	**<0.8 (μ_1)**	**<10 (μ_2)**	**<50 (μ_3)**	**<0.8 (μ_1)**	**<10 (μ_2)**	**<50 (μ_3)**
Ciliates			-0.81 (0.24)			-0.01 (0.21)			0.08 (0.14)
Dinofl.			-0.21 (0.54)			0.16 (0.10)			0.20 (0.20)
HNF		0.43 (0.28)	0.30 (0.24)		0.84 (0.13)	0.43 (0.25)		0.45 (0.19)	0.40 (0.15)
Nanophyto.		0.17 (0.22)	-0.12 (0.38)		0.22 (0.33)	0.31 (0.32)		0.23 (0.10)	0.23 (0.17)
Chl *a* <10 µm					0.14 (0.03)	0.17 (0.05)		0.36 (0.06)	0.22 (0.05)
Chl *a*		0.23 (0.19)	0.23 (0.14)		0.17 (0.05)	-0.004 (0.19)		0.34 (0.07)	0.19 (0.09)
Picophyto.	0.10 (0.37)	0.17 (0.27)	0.19 (0.23)	0.32 (0.08)	0.18 (0.30)	0.19 (0.27)	0.25 (0.14)	0.23 (0.10)	0.14 (0.11)
Bacteria	0.22 (0.10)	0.29 (0.23)	0.38 (0.08)	0.13 (0.02)	-0.05 (0.09)	0.23 (0.03)	0.17 (0.06)	0.14 (0.06)	0.23 (0.03)

Growth and grazing mortality

Growth rates were calculated from the changes in the concentration during the first few days of incubation: i.e. day 0-6 in Exp. I and day 0-4 in Exp. II and III. One exception was bacteria in which growth rate was estimated from day 2-4 for all three experiments, due to a small reduction in abundance during day 0-2. Cell abundances and estimated biomass of the microbes are summarized in Table 3, while growth rates are summarized in Table 4. The highest growth rates of bacteria were obtained in incubations where abundance of grazers was low: i.e. in Exp. I (Treat<50) and in the the ungrazed treatments (Treat<0.8) of Exp. II (Table 4).

Growth rates of picophytoplankton in the ungrazed treatments (Treat<0.8) ranged from 0.10 to 0.37 d^{-1} (mean: 0.22 d^{-1}). In the treatment with reduced MZP abundance (Treat<10) nanophytoplankton grew at a similar rate as picophytoplankton ranging between 0.17-0.23 d^{-1} (mean: 0.22 d^{-1}) and HNF were growing with rates in the range 0.45 to 0.84 d^{-1}. In the treatments with high MZP abundance (Treat<50), HNF were growing with at rates ranging between 0.40-0.50 d^{-1}.

Thus, growth rates were generally higher for picophytoplankton and bacteria in Treat<0.8 um than Treat<10 um and growth rates of Chl *a* and HNF were higher in Treat<10 µm than Treat<50 µm. The difference in growth rates between the different fractions indicates grazing mortality by the protist community (Table 5). In Exp. I and II mortality of HNF could be

observed corresponding to 30 % and 48 % d^{-1} of their ungrazed growth rate, respectively. In Exp. II and III apparent grazing mortality on picophytoplankton was observed, whereas grazing mortality on nanophytoplankton was only observed in Exp. I. Grazing on Chl *a* in the fraction <10 µm was generally low ranging from near 0 (Exp. I and II) to 0.14 d^{-1} for Chl *a* <10 µm in Exp. III (Table 5). Grazing mortality for large sized phytoplankton (Chl *a* >10 µm) was only obtained for Exp. II and III where it was 0.03 d^{-1} and 0.18 d^{-1}, respectively.

Table 5. Grazing mortality rates (*g*, d^{-1}) of microorganism calculated as difference in growth rates (μ_n, table 4) obtained in the fractionation treatments (Treat<0.8: μ_1, Treat<10: μ_2 and treat<50: μ_3). Values are given as mean and standard deviation (in brackets) during day 0-6 (Exp. I) and day 0-4 (Exp. II and III).

	Exp. I		**Exp. II**		**Exp. III**	
Organims	**μ_1-μ_2**	**μ_2-μ_3**	**μ_1-μ_2**	**μ_2-μ_3**	**μ_1-μ_2**	**μ_2-μ_3**
HNF		0.13		0.41		-0.03
		(0.29)		(0.16)		(0.29)
Nanophyto.		0.29		-0.08		-0.01
		(0.39)		(0.11)		(0.12)
Chl a <10 µm				-0.03		0.14
				(0.05)		(0.05)
Chl a		0.01		0.28		0.06
		(0.11)		(0.34)		(0.02)
Picophyto.	-0.08	0.07	0.20	0.07	0.02	0.09
	(0.29)	(0.24)	(0.28)	(0.21)	(0.13)	(0.05)
Bacteria	-0.07	-0.09	0.19	-0.28	0.03	-0.09
	(0.25)	(0.14)	(0.09)	(0.03)	(0.05)	(0.03)

Regression analysis

To estimate growth of heterotrophic protists and grazing mortality of picophytoplankton, nanophytoplankton and HNF due to grazing by MZP during the spring bloom transition phase more accurate, data from Exp. II and Exp. III were used for regression analysis. Data from Exp. I was not considered since this experiment was still in the winter state with low initial concentrations of microbial components and consequently low accuracy of the estimated growth rates and high mortality of ciliates. HNF growth rate was significantly correlated to picophytoplankton biomass (mg C m^{-3}) increasing linearly with a rate of 0.12 mg C m^{-3} (r^2 = 0.80, $p < 0.0001$, Fig. 6A). No growth saturation for HNF growth was found within the range of picophytoplankton biomass (0.2-10 mg C m^{-3}). Morality rate of picophytoplankton due to HNF grazing was estimated from the slope of a linear regression fitted to data on HNF biomass (mg C

m^{-3}) as a function of picophytoplankton growth rate (d^{-1}). The regression resulted in a significant relationship (r^2= 0.49, p <0.0001, Fig. 6B) and a loss rate due to grazing of 0.12 d^{-1}.

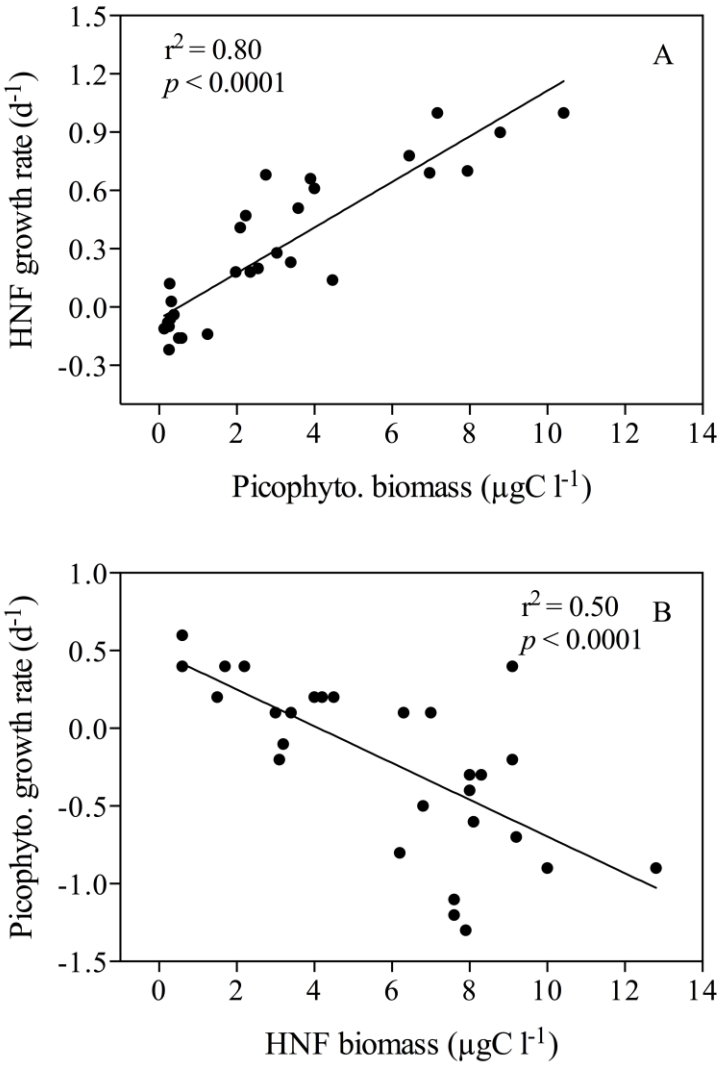

Fig. 6. A) Growth rates (d^{-1}) of heterotrophic nanoflagellates (HNF) as a function of picophytoplankton and B) Growth rates of picophytoplankton as a function of HNF biomass (mg C m^{-3}). Values are estimated from the Exp. II and Exp. III (Treat<10). The linear regressions are given as black lines: A) $f(x) = -0.059 + 0.12x$, and B) $f(x) = 0.47 - 0.12x$.

The nanoplankton (HNF and nanophytoplankton) were assumed to be grazed mainly by ciliates, and to evaluate the importance of ciliates as grazers nanophytoplankton and HNF growth rates

estimated from Exp. II and III (Treat >50) were plotted against ciliate biomass. There was no significant relationship between nanophytoplankton biomass and ciliate growth rate (r^2 = 0.004, p = 0.76) or between ciliate biomass and nanophytoplankton growth rate (r^2 = 0.006, P = 0.71). However, a significant relationship was found between HNF biomass and ciliate growth rate (r^2 = 0.26, p = 0.0063, Fig. 7A). The hypothesis of ciliates being major grazers on HNF was only supported by a weak correlation between ciliate biomass and HNF growth rate (r^2 = 0.28, p = 0.0046, Fig. 7B), where the slope indicate an average specific HNF mortality of 0.12 d^{-1}.

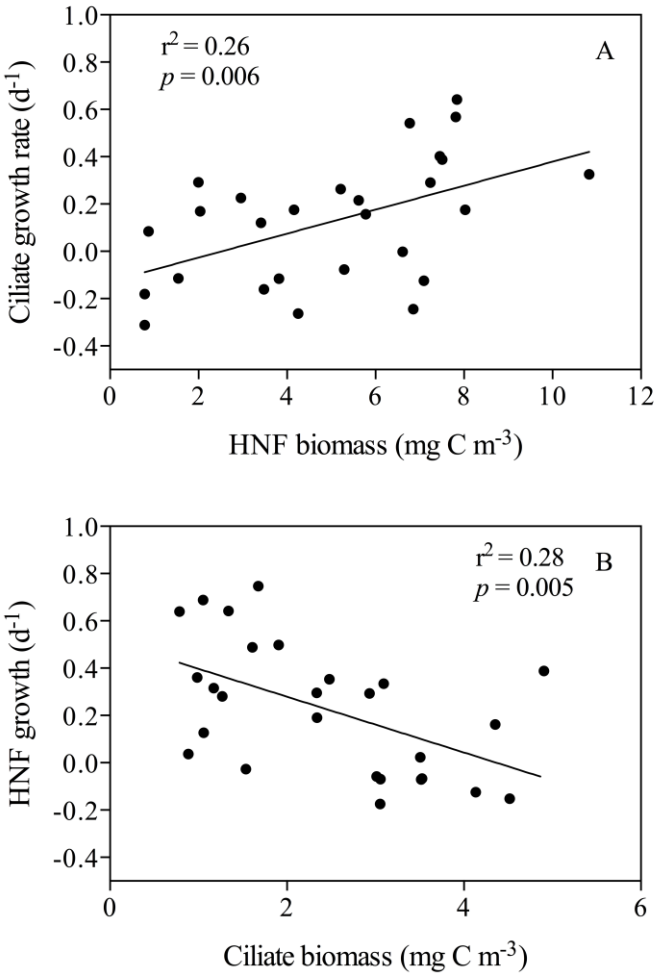

Fig. 7. A) Growth rates (d^{-1}) of ciliates (d^{-1}) as a function of heterotrophic nanoflagellate (HNF) biomass (mg C m^{-3}) and B) Growth rates of HNF as a function of ciliate biomass (mg C m^{-3}). Values are estimated from the Exp. II and Exp. III (Treat<50). The linear regressions are given as black lines: A) $f(x)$ = 0.051x-0.13, and B) $f(x)$ = 0.52 -0.12x.

DISCUSSION

Microbial communities have been studied during North Atlantic spring bloom; e.g. the North Atlantic bloom experiment of 1989 in the open Atlantic (Ducklow et al. 1993, Li et al. 1993, Verity et al. 1993). However, knowledge on the microbial plankton communities during the winter-spring transition is very limited, primarily because the spring bloom is assumed to initiate the productive cycle. Paulsen et al. (Paper II) and the present study documents the presence of an active microbial community within the deep convective mixed layer of the Iceland Basin prior to the spring bloom. Production was initially driven by pico- and nano-sized components but as the bloom progressed nano- and microplankton became increasingly more important. Observations such as these are essential for our understanding of the biological processes regulating bloom-development in the North Atlantic. Furthermore, the data underlines the importance of pico- and nano-sized phytoplankton for sustaining bacterial production and the heterotrophic protist communities dominated by HNF and ciliates.

Technical Limitations

Before discussing the results any further we will discuss the limitations of our approach. First of all, the fractionation technique used in the present study does not capture grazing impact on cells larger than the filters used for fractionation (in our case cells >10 µm). Secondly, the filters do not screen functional groups and they do not separate organisms of the intended size, especially elongated dinoflagellates >10 µm may end up in the <10 µm fractions. This generally leads to an underestimation of the grazing rates (Verity et al. 1993), but based on the estimated MZP biomass in the <10 µm treatments, that was on average 80% smaller than in Treat<50 µm, we assume that the underestimation is minor. Finally, the screening process may damage the cells and increase the concentration of dissolved organic matter (DOM). One could argue that a higher release of labile DOM will result in a higher bacterial growth in the treatments where screening has been done using fine mesh filters compared to the treatments where coarse mesh filters are used. However, labile DOM is usually assimilated within hours to days (Hansell 2013), and since bacterial growth was first positive after ca. 2 days, this indicates that bacteria growth was not supported by labile DOM. Further, the fractionation technique was also used by Christaki et al. (2001) to estimate HNF bacteriovory with these authors finding no difference in grazing rates on pico-sized organisms obtained by the fractionation technique compared and those obtained by fluorescence labeled bacteria as traces. Another argument is that picophytoplankton, which in the <0.8 µm treatment, similar to bacteria had higher growth rates relative to the <10 µm treatments. Since autotrophic picoplankton did not benefit from released DOM in the 0.8 µm treatment it is reasonable to believe that the higher growth rate of bacteria and picophytoplankton was caused by the reduced grazing pressure in these treatments rather than enhanced DOM concentration. Thus, although the fractionation technique has potential limitations we find the technique appropriate for studying dilute systems dominated by small phytoplankton.

Importance of heterotrophic nanoflagellates (HNF) as grazers

Of the investigated microbes HNF maintained the highest growth rates. Thus although HNF did not contribute substantially to the biomass of heterotrophic protists during the first days of the trials their production-rates exceed the production of MZP. The high growth rates of HNF further suggests a high grazing potential by HNF during the winter-spring-transition.

The average ingestion rate of HNF was 4 bacteria and 0.2 picophytoplankton h^{-1}. This is within the range obtained in other studies (Bjørnsen et al., 1988; Christaki et al., 2001; Vaqué et al., 2008), while the estimated grazing impact on picophytoplankton is within an order of magnitude of those reported by Christaki et al. (2005).

The linear regression of HNF community growth rate vs. picophytoplankton biomass suggests a HNF community growth rate of 0.21 d^{-1} (Fig. 6) when the biomass of picophytoplankton is 2.2 mg C m^{-3} (*in situ* average at visit 2 and 3). This equals a HNF production rate of 1.3 pg C d^{-1} given a cell carbon content of 4.5 pgC $cells^{-1}$ (Børsheim & Bratbak 1987) At 30% growth efficiency (Fenchel, 1982) this gives a carbon demand of 4.4 pg C d^{-1}, which equals 9 bacteria h^{-1} assuming a carbon content of 20 fg $bacteria^{-1}$ (Lee and Fuhrman 1987). Given our estimated ingestion rate of bacteria (max. 4 bacteria h^{-1}), consumption of bacteria would only satisfy around 1/3 of the carbon demand. The remaining carbon demand would equal ingestion of 0.24 picophytoplankton h^{-1}, which is close to the HNF ingestion rate we found experimentally of 0.21 picophytoplankton h^{-1} (average of Exp. II and Exp. III), confirming that the carbon demand of HNF was satisfied by bacteria and to a high degree picophytoplankton, grazing up to 65 % picophytoplankton production d^{-1} (1.6 mg C m^{-3}).

To evaluate if HNF influence the size distribution of bacteria, the bacterial population in the incubations was split into two distinct groups based on their side scatter (SSC) which is an approximation to cell size (Calvo-Díaz & Morán 2006). The tendency for larger bacterial cells to become more abundant in the absence of HNF grazing has previously been documented in similar fractionation experiments, where the development in bacterial population cell size was determined (Simek & Chrzanowski 1992) and later studied with molecular methods revealing that flagellate grazing select for bacterial species of relatively large size. Though we have no actual size measurements in current study, our results indicate that heterotrophic protists have a preference for larger bacteria (Fig. 8 A-C).

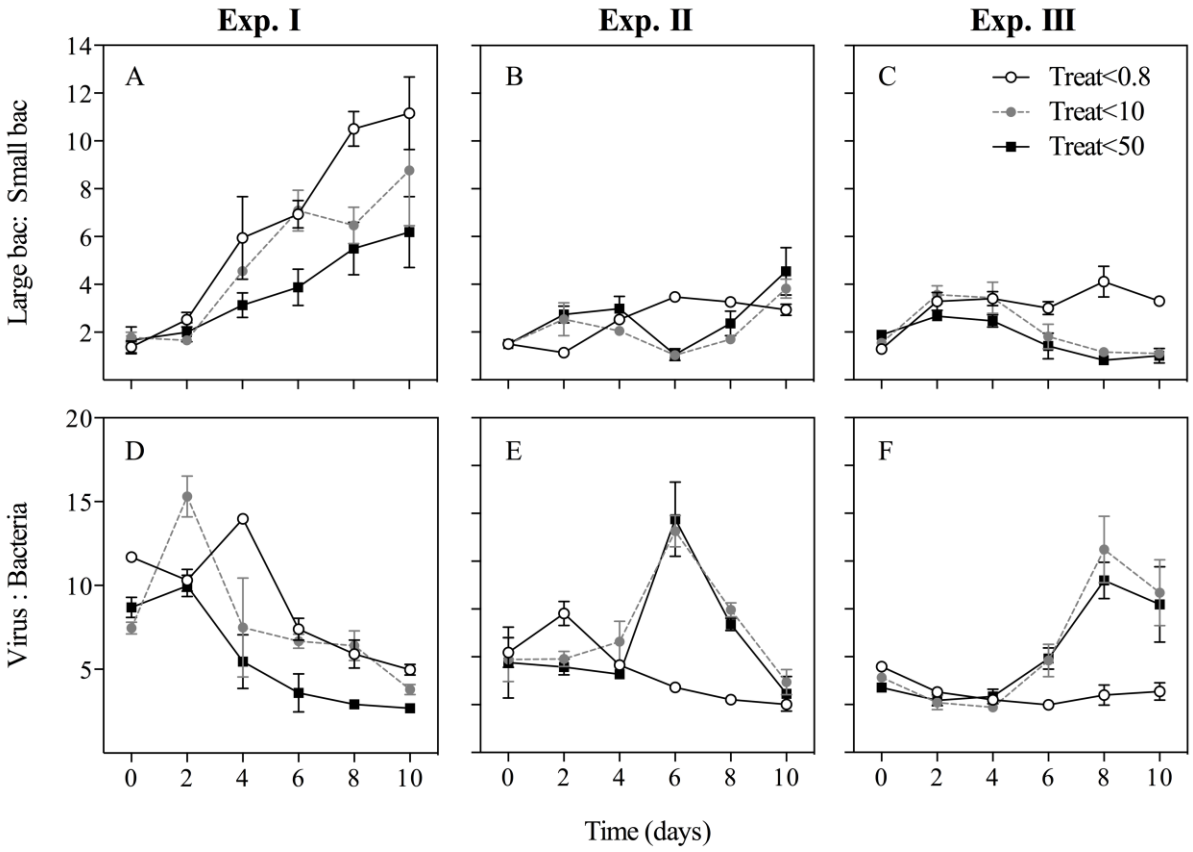

Fig. 8. Development in A-C) the ratio between large and small bacteria based on side scatter measurements (Large:Small bacteria), D-F) ratio between virus and bacteria abundance (Virus:Bacteria) and H-J). Values are given as mean and SE (n=3).

Ecological role of microzooplankton (MZP) in the deep convective layer

The biomass of MZP in the Iceland Basin ranged between 0.5 to 1.0 mg C m^{-3}, which is relatively low compared to their average biomass of 8.1 mg C m^{-3} (2-27 mg C m^{-3}) in oligotrophic waters (<0.5 mg Chl *a* m^{-3}) (Sherr & Sherr 2007). Although it is impossible to make a clear distinction between prey preference of heterotrophic dinoflagellates and ciliates we assume that dinoflagellates prefer prey equal or half to their own size (Jakobsen & Hansen 1997, Sherr & Sherr 2007, Jeong et al. 2011), i.e. nano- and microplankton, whereas ciliates prefer prey 1/10 of their own size (Bernard & Rassoulzadegan 1990), i.e. pico- and nanoplankton. Ciliates dominated the MZP biomass in the Iceland Basin, which would be expected given the relatively high concentration of small sized prey during the study period. Ciliates have also occasionally been reported to dominate the grazing community during the North Atlantic spring bloom (Gifford 1995) although dinoflagellates are generally more abundant during this period when the abundance of diatoms is higher (Verity et al. 1993, Sherr & Sherr 2007).

Verity et al. (1993) estimated grazing coefficients for heterotrophic protists using the same technique as in our study and found grazing coefficients for Chl a < 10 µm in the order 0.21-1.09 d^{-1}. Using the dilution technique (Landry & Hassett 1982) Gifford et al. (1995) found similar high grazing coefficients (average: 0.95 d^{-1}) on the < 20 µm Chl *a* fraction, during the phytoplankton bloom in the Norwegian Basin (59°N, 21°W). In comparison, grazing coefficients on Chl *a* obtained in present study ranged between -0.03 and 0.13 d^{-1}. The low grazing impact on Chl a <10 µm was further supported by low estimated grazing rates on picophytoplankton and nanophytoplankton. In this study, picophytoplankton was the primary pathway of carbon to the MZP community in Exp. III, while HNF were the major carbon source during Exp. I and II. Consumption of HNF by MZP was proposed by Azam et al. (1983) as an important pathway of the microbial loop, but is rarely considered. An example of significant consumption of HNF by MZP is the study of Solic & Krstulovic (1994) in the Adriatic Sea, where grazing of HNF by ciliates ranged between 0.3 and 17 mg C m^{-3} d^{-1} (3 to 163 cells ml^{-1} h^{-1}). In comparison, HNF were grazed at a rate of 0.5 and 0.3 mg C m^{-3} d^{-1} in Exp. I and II respectively (7 and 2 cells ml^{-1} h^{-1}). This apparent grazing within the heterotrophic protist community suggests that picophytoplankton and HNF represent important carbon sources for sustaining a winter community of MZP and possibly transferring energy up the food web despite low phytoplankton production.

Top-down control of bacteria by HNF

During the North Atlantic spring bloom the bacteria population dynamics are characterized by rapid cycles of blooms and bust responding to short term increases in primary production (Ducklow et al. 1993). Our microcosm experiments demonstrate that similar cycles are present prior to the bloom. Bacteria specific growth rate as estimated during the ungrazed treatments were comparable to rates obtained during the North Atlantic bloom experiment (45°N) (Li et al. 1993). *In situ* bacteria biomass was lower during present study compared to values obtained during the bloom (Ducklow et al. 1993). However, if we consider the rates to be valid for the entire mixed layer, production rates estimated from the growth rates and the *in situ* biomasses reveal that integrated production throughout the mixed layer are comparable to those obtained during the bloom (~0.3 g C m^{-2} d^{-1}) (Ducklow et al. 1993).

Our fractionated microcosm experiments indicate that the bacteria community was primarily controlled by HNF grazing. However, viruses may also have regulated bacteria abundance and diversity. As described in Paulsen et al. (Paper II) the ratio of virus to bacteria (V:B) decreased during the winter-spring transition due to an increase in bacterial abundance, while virus numbers remained unchanged. Similarly, the initial V:B ratio was higher in the first experimental period and subsequently declined (Fig. 8D-F). The average V:B ratio in marine surface waters of the North Atlantic is around 10, but can reach up to 40 (Parada et al. 2007, Suttle 2007). Thus the encounter rate (i.e. chance of viral infection) was relatively low in our

incubations. Despite the low initial concentration of viruses in our study, virus lysis could have caused mortality of autotrophic pico- and nanoplankton during the last part of the incubation period, where virus abundance increased in some of the treatments indicating bacteria lysis. However, virus abundance never increased drastically and we thus prescribe the main decreases in pico- and nanoplankton to be caused by grazing.

Does deep mixing of heterotrophic protists play a role in initiating the bloom?

Paulsen et al. (Paper II) and present study imply that deep winter mixing greatly impacts the vertical distribution and concentration of heterotrophic protists. In addition we show that HNF are major grazers on the picophytoplankton and bacteria prior to the bloom, succeeded by MZP later in the season when the bloom is dominated by larger species.

The dilution-recoupling hypothesis (Behrenfeld 2010) proposes that grazers are diluted due to mixed layer deepening, which may explain part of the net increase in large sized phytoplankton biomass. However, mixed layer deepening has a cascading effect on the heterotrophic nanoflagellates which may in fact benefit from the dilution since their predators (ciliates) are being diluted accordingly. Consequently the grazing pressure on nanophytoplankton and diatoms is relaxed and grazing pressure on the picophytoplankton may remain unchanged due to the high turnover rates of picophytoplankton and their small grazers (HNF).

Our data suggest that deep winter mixing greatly influences the relative abundance and encounter of all microbial components and thus plays a central role for the carbon flow and community composition during this period. Thus part of the high net increase in diatom biomass may result from a lower grazing pressure in deep mixed waters (the dilution-recoupling hypothesis). How important this biological response is compared to a direct physical response to deep convection as proposed by e.g. Backhaus et al. (2003), requires more research to resolve.

Acknowledgements

The research leading to these results has received funding from the European Union Seventh Framework Programme project EURO-BASIN (ENV.2010.2.2.1-1) under grant agreement n° 264933, ERC grant Microbial Network Organisation (MINOS 250254) and from the U.S. National Science Foundation (OCE-0752972). The Deep convection" cruise was funded by the Deutsche Forschunggemeinschaft in a grant to MSJ. Thanks to Mario Esposito for kindly measuring nutrients during the cruise and to Aud Larsen for flow cytometry assistance. We also thank the crew of the RV *Meteor* on the Deep Convection Cruise.

LITTERATURE CITED

Backhaus J, Hegseth E, Wehde H, Irigoien X, Hatten K, Logemann K (2003) Convection and primary production in winter. Mar Ecol Prog Ser 251:1–14

Behrenfeld MJ (2010) Abandoning Sverdrup ' s Critical Depth Hypothesis on phytoplankton blooms. Ecology 91:977–989

Bernard C, Rassoulzadegan F (1990) Bacteria or microflagellates as a major food source for marine ciliates: possible implications for the microzooplankton. Mar Ecol Prog Ser 64:147–155

Blindheim J, Østerhus S (2005) The Nordic Seas, Main Oceanographic Features. Geophys Monogr Ser 158:11–37

Booth BC (1988) Size classes and major taxonomic groups of phytoplankton at two locations in the subarctic Pacific Ocean in May and August 1984. Mar Biol 97:275–286

Børsheim K, Bratbak G (1987) Cell volume to cell carbon conversion factors for a bacterivorous Monas sp. enriched from seawater. Mar Ecol Prog Ser 36:171–175

Boyd P, Newton P (1995) Evidence of the potential influence of planktonic community structure on the interannual variability of particulate organic carbon flux. Deep Sea Res Part I Oceanogr Res Pap 42:619–639

Boyer Montégut C de, Madec G, Fischer AS, Lazar A, Iudicone D (2004) Mixed layer depth over the global ocean: An examination of profile data and a profile-based climatology. J Geophys Res 109:C12003

Calvo-Díaz a, Morán X (2006) Seasonal dynamics of picoplankton in shelf waters of the southern Bay of Biscay. Aquat Microb Ecol 42:159–174

Cushing DH (1959) On the nature of production in the sea. Fish Invest Lond Ser II 22:1–40

Dale T (1999) Seasonal development of phytoplankton at a high latitude oceanic site. Sarsia 84:419–435

Ducklow H, Kirchman D, Quinby H, Carlson C, Dam H (1993) Stock and dynamics of bacterioplankton carbon during the spring bloom in the eastern North Atlantic Ocean. Deep Sea Res II 40:245–263

Garside C, Garside JC (1993) The "f-ratio" on 20°W during the North Atlantic Bloom Experiment. Deep Sea Res Part II Top Stud Oceanogr 40:75–90

Gifford DJ, Fessenden LM, Garrahan PR, Martin E (1995) Grazing by microzooplankton and mesozooplankton in the high-latitude North Atlantic Ocean: Spring versus summer dynamics. J Geophys Res 100:6665–6675

Hansell D a (2013) Recalcitrant dissolved organic carbon fractions. Ann Rev Mar Sci 5:421–45

Jakobsen H, Hansen P (1997) Prey size selection, grazing and growth response of the small heterotrophic dinoflagellate *Gymnodinium* sp. and the ciliate *Balanion comatum* -a comparative study. Mar Ecol Prog Ser 158:75–86

Jeong HJ, Lee KH, Yoo Y Du, Kang NS, Lee K (2011) Feeding by the newly described, nematocyst-bearing heterotrophic dinoflagellate *Gyrodiniellum shiwhaense*. J Eukaryot Microbiol 58:511–24

Jespersen AM, Christoffersen K (1987) Measurements of chlorophyll-a from phytoplankton using ethanol as extraction solvent. Arch Hydrobiol 109:445–454

Landry MR, Hassett RP (1982) Estimating the grazing impact of marine micro-zooplankton. Mar Biol 67:283–288

Larsen A, Flaten G a. F, Sandaa R-A, Castberg T, Thyrhaug R, Erga SR, Jacquet S, Bratbak G (2004) Spring phytoplankton bloom dynamics in Norwegian coastal waters: Microbial community succession and diversity. Limnol Oceanogr 49:180–190

Lee S, Fuhrman JA (1987) Relationships between biovolume and biomass of naturally derived marine bacterioplankton. Appl Env Microbiol 53:1298–1303

Li WKW, Dickie PM, Harrison WG, Irwin BD (1993) Biomass and production of bacteria and phytoplankton during the spring bloom in the western North Atlantic Ocean. Deep Sea Res II 40:307–327

Lindemann C, John MA St. (2014) A seasonal diary of phytoplankton in the North Atlantic. Front Mar Sci 1

Marie D, Brussaard CPD, Thyrhaug R, Bratbak G, Vaulot D (1999) Enumeration of Marine Viruses in Culture and Natural Samples by Flow Cytometry. Appl Environ Microbiol 65:45–52

Menden-Deuer S, Lessard EJ (2000) Carbon to volume relationships for dinoflagellates, diatoms, and other protist plankton. Limnol Oceanogr 45:569–579

Parada V, Sintes E, Aken HM van, Weinbauer MG, Herndl GJ (2007) Viral abundance, decay, and diversity in the meso- and bathypelagic waters of the north atlantic. Appl Environ Microbiol 73:4429–38

Porter KG, Feig YS (1980) The use of DAPI for identifying aquatic microfloral. Limnol Oceanogr 25:943–948

Putt M, Stoecker DK (1989) An experimentally determined carbon : volume ratio for marine from estuarine and coastal waters ciliates " oligotrichous ." Limnol Oceanogr 34:1097–1103

Sherr EB, Sherr BF (2007) Heterotrophic dinoflagellates: a significant component of microzooplankton biomass and major grazers of diatoms in the sea. Mar Ecol Prog Ser 352:187–197

Siegel DA, Doney SC, Yoder JA (2002) The North Atlantic spring phytoplankton bloom and Sverdrup's critical depth hypothesis. Science (80-) 296:730–733

Simek K, Chrzanowski T (1992) Direct and indirect evidence of size-selective grazing on pelagic bacteria by fresh-water nanoflagellates. Appl Environ Microbiol 58:3715–3720

Solic M, Krstulovic N (1994) Role of predation in controlling bacterial and heterotrophic nanoflagellate standing stocks in the coastal Adriatic Sea : seasonal patterns. Mar Ecol Prog Ser 114:219–235

Suttle CA (2007) Marine viruses-major players in the global ecosystem. Nat Rev Microbiol 5:801–12

Sverdrup H (1953) On conditions for the vernal blooming of phytoplankton. J Cons Int Explor Mer 18:287–295

Taylor JR, Ferrari R (2011) Shutdown of turbulent convection as a new criterion for the onset of spring phytoplankton blooms. Limnol Oceanogr 56:2293–2307

Townsend DW, Cammen LM, Holligan PM, Campbell DE, Pettigrew NR (1994) Causes and consequences of variability in the timing of spring phytoplankton blooms. Deep Sea Res Part I Oceanogr Res Pap 41:747–765

Verity PG, Langdon C (1984) Relationships between lorica volume, carbon, nitrogen, and ATP content of tintinnids in Narragansett Bay. J. Plankt Res 6:859–868.

Verity PG, Stoecker DK, Sieracki ME, Nelson JR (1993) Grazing, growth and mortality of microzooplankton during the 1989 North Atlantic spring bloom at 47°N, 18°W. Deep Sea Res Part I Oceanogr Res Pap 40:1793–1814

Verity PG, Wassmann P, Frischer ME, Howard-Jones MH, Allen AE (2002) Grazing of phytoplankton by microzooplankton in the Barents Sea during early summer. J Mar Syst 38:109–123

Zubkov MV, Burkill PH, Topping JN (2006) Flow cytometric enumeration of DNA-stained oceanic planktonic protists. J Plankton Res 29:79–86

Paper III

Zubkov MV, Sleigh M., Tarran GA, Burkill P., Leakey RJ. (1998) Picoplanktonic community structure on an Atlantic transect from 50°N to 50°S. Deep Sea Res Part I Oceanogr Res Pap 45:1339–1355

Paper IV

Submitted to Marine Ecology Progress Series

Disko Island
Photo: Karen Riisgaard

Impact of elevated pH on succession of the Arctic spring bloom

Karen Riisgaard[1], Torkel Gissel Nielsen[1,2] Per Juel Hansen[3]

[1]National Institute of Aquatic Resources, DTU Aqua, Section for Oceanography and Climate, Kavalergården 6, 2920 Charlottenlund, Denmark
[2]Greenland Climate Research Centre, Greenland Institute of Natural Resources, PO Box 570, 3900 Nuuk, Greenland
[3] Centre for Ocean Life, University of Copenhagen, Department of Biology, Section of Marine Biology, Strandpromenaden 5, DK-3000, Helsingør, Denmark

ABSTRACT

Development in pH during the spring bloom in 2011 and 2012 in Disko Bay, West Greenland was investigated. The phytoplankton spring bloom led to pH values as high as 8.5 at the peak of the bloom. Subsequently, the pH decreased to 7.5. Microcosm experiments were carried out on natural assemblages sampled at the initiation of the spring bloom each year and manipulated to cover pH levels in the range of 8.0-9.5 to test the immediate tolerance of Arctic protist plankton to elevated pH under nutrient limiting (2011) and nutrient replete conditions (2012). The most pronounced effect of elevated pH was found for heterotrophic protists, whereas phytoplankton proved to be more robust. Two out of three heterotophic protist species were significantly affected when pH was increased above 8.5 and at pH 9.5 all heterotrophic protists had disappeared. Based on Chl *a* measurements from the two set of experiments, phytoplankton community growth was significantly reduced at pH 9.5 during nutrient replete conditions, while pH had little impact on nutrient limited phytoplankton growth. The results were supported by cell counts which revealed that phytoplankton growth during nutrient replete conditions was significantly reduced from an average of 0.49 d^{-1} at pH 8.0 to an average of 0.27 d^{-1} at pH 9.5. In comparison only one out of four tested phytoplankton species were significantly affected by elevated pH under nutrient limited conditions. Sudden pH fluctuations, like those occurring during phytoplankton blooms are likely to favor pH tolerant species such as diatoms. The data presented here suggest that the effect of elevated pH on phytoplankton growth will be most pronounced when phytoplankton grow at their maximum rate; i.e. in the initial phase of the bloom when nutrients are replete. However, elevated pH may also indirectly affect the phytoplankton bloom succession since the grazing community may be decoupled from the phytoplankton succession during short term periods of elevated pH.

KEY WORDS: pH, Arctic phytoplankton, spring bloom, growth rates, *Phaeocystis pouchetii*, heterotrophic protists

INTRODUCTION

The phytoplankton spring bloom is a key event in Arctic marine ecosystems where it plays a central role for the fixation and sequestering of carbon dioxide during the otherwise short productive season (Pabi et al. 2008). When dissolved in water, carbon dioxide is a weak acid and any reductions in the concentrations of inorganic carbon will be compensated by a shift in the chemical equilibrium making the water more alkaline. Seawater contains high amounts of bicarbonate ions which acts as buffers against changes in pH and pH in the open ocean is consequently relatively stable (Skirrow 1975). However, in brackish coastal waters where the buffer capacity is lower and phytoplankton blooms are more intense, pH may be highly variable (Hansen 2002, Hinga 2002, Provoost et al. 2010, Brutemark et al. 2011) and affect phytoplankton growth and species succession (Hinga 2002, Hansen 2002, Pedersen & Hansen 2003a, Pedersen & Hansen 2003b, Søderberg & Hansen 2007). There are only few studies on the role of pH in Arctic marine ecosystems and these indicate that pH may also play a central role for plankton dynamics in these high latitude ecosystems (Charalampopoulou et al. 2011, Søgaard et al. 2011, Silyakova et al. 2013).

The Disko Bay is an important fishing and hunting area in Greenland located just south of the Arctic winter sea ice border. The sea ice cover in the bay shows huge inter-annual variability (Hansen et al. 2006), and most of the new primary production is confined to a 2-4 week long phytoplankton bloom occurring in spring (Dünweber et al. 2010). The fate of the bloom, due to grazing by the dominating heterotrophs, has been investigated during the last two decades (Levinsen et al. 1999, Madsen et al. 2001), but the role of pH as a regulating factor has not yet been investigated. Heterotrophic dinoflagellates and ciliates are major grazers in Disko Bay during spring and their gross growth rates are coupled to the phytoplankton biomass (Levinsen et al. 1999). However, heterotrophic protists may be more sensitive to changes in pH than the dominating phytoplankton species (Pedersen & Hansen 2003a, Pedersen & Hansen 2003b) and in this way sudden changes in pH may uncouple the grazers from the succession. This tendency could be strengthened by high tolerance of ice-algae that are known to thrive in brine channels where pH can reach 10.0 (Gleitz et al. 1995) .

We hypothesize that both phytoplankton and heterotrophic protists are sensitive to changes in pH and that pH may play a role for protists growth rate and thus the succession of the Arctic spring bloom. The aim of our study was to study fluctuations in pH during before and after the phytoplankton spring bloom in Disko Bay, Greenland. In addition we wanted to investigate the impact of elevated pH on growth and succession of the phytoplankton and heterotrophic protist community. Since nutrient concentration is likely to affect the pH tolerance and growth of the organisms (Li et al. 2012), two independent microcosm experiments were carried out under controlled laboratory conditions. In the first set of experiments (2011) the response of a pre-bloom plankton assemblage, was studied as the phytoplankton depleted the nutrients during the course of the experiment at different levels of pH. In the second set of experiments (2012), frequent dilutions with filtered pre-bloom water adjusted to different pH levels allowed us to

study the growth response of a natural pre-bloom phytoplankton assemblage to elevated pH under nutrient rich conditions. We hypothesized that growth rates of the phytoplankton and heterotrophic protists would decrease with increasing pH and that the relative change in growth between pH treatments and controls would be the same regardless of the nutrient level.

MATERIAL & METHODS

Sampling and hydrography

The study was conducted from April to May 2011 and 2012 in the Disko Bay, West Greenland (experiments were carried out at Arctic Station, Copenhagen University). Water was collected from the RV Porsild (Copenhagen University) at a 300 m deep monitoring station, approximately 1 nautical mile off the coast (69° 14' N, 53° 23' W), using a 30 L Niskin bottle. Water samples for inorganic carbon, Chl *a*, nutrients and pH measurements were taken from the fluorescence maximum (15-20 m, measured with a seabird CTD, SBE25-01) and from 7 additional depths (1, 50, 75, 100, 150, 200, 250 m) throughout the investigated period at intervals of 2-7 days.

Chl *a* was estimated from 50-200 ml sub-samples which were filtered on GF/F filters. The filters were extracted in 5 ml 96 % ethanol in darkness for 12-24 h and measured fluorometrically before and after HCl (1 M) addition on a Turner fluorometer (TD-700) calibrated against a Chl *a* standard.

30 ml samples for measuring inorganic nutrients were kept frozen (-18 °C) for later analysis on a Skalar autoanalyser (Breda, Netherlands), following the procedures of Hansen & Koroleff (1999). The precision (analytical reproducibility) of the nutrient analyses was 0.06, 0.1, and 0.2 µM for phosphate, nitrate, and silicate, respectively.

Samples for measuring pH *in situ* were transferred to 50 ml airtight plastic bottles, which were kept cold and dark until pH was measured immediately after or a few hours later, using either a Hanna pH-meter or a WtW 3210i, both with detection level of 0.01. The pH-meters were calibrated using a two point calibration (NBS-scale) with NIST buffers 7.01 and 10.01.

Experimental conditions

Two experiments were carried out in the thermo-regulated shipping container at Arctic Station. The first set of experiments (Exp. 1) was initiated on April 23th 2011 and the second set of experiments (Exp. 2) on April 15th 2012. Water for the experiments was collected at 3-5 m depth and gently siphoned into dark carboys. Additional water for dilution between the sampling events was collected from the photic zone and below the pycnocline at 200 m depth since there

was no phytoplankton at this depth and pH was close to 8.0. This water was filtered through a 0.45 µm polycap filter and hereafter stored cold (4 °C) and dark.

12 transparent 2.5 L polycarbonate bottles (Exp. 1) or 15 transparent 1.2 L bottles (Exp. 2) were filled with sea water via silicon tube equipped with a 250 µm mesh to remove mesozooplankton. Two additional bottles were filled under same procedures and water samples were taken from these bottles as the experiment was initiated (Day 0). The rest of the experimental bottles were incubated on a plankton wheel (1 rpm) and exposed to 12:12 h light circle of cool white fluorescence of 100 µMol photons m^{-2} s^{-1}, corresponding to the light intensity from where the water was collected. Average temperatures during incubation were 3.5 °C (Exp. 1) and 3.0 °C (Exp. 2).

The pH was adjusted in the bottles by gradually adding 0.1 M NaOH. The increase in pH was ≤ 0.5 pH units per 12 h. Three or four pH treatments (pH 8.5, 8.8, 9.0 and 9.5) were maintained during the experimental period. Treatment bottles were accompanied by control bottles it which pH was not manipulated but stayed around 8.0. Controls and treatments were run in triplicate.

During Exp.1 (2011) the effect of high pH under late bloom conditions was investigated; i.e. nutrient limited growth conditions for the phytoplankton and sufficient phytoplankton for their heterotrophic grazers. These conditions were assured by replacing 20 % of the bottle volume at each sampling event (every 2-3 day) with 0.45 µm filtered surface seawater pre-adjusted to pH. In Exp.2 (2012) an early bloom situation was simulated to investigate the effect of elevated pH on maximum growth rates of Arctic phytoplankton. Nutrient rich conditions were enabled by replacing approximately 50 % of the cultures with 0.45 µm filtered nutrient rich deep water pre-adjusted to pH at each sampling event (every 24 h). The appropriate dilution of the cultures after each sampling event was ensured by keeping Chl *a* in the range 5-8 µg l^{-1} after dilution. Duration of the experiments was 8-14 d.

In both set of experiments, bottles were sampled prior to the dilution for inorganic nutrients, Chl *a* and pH (using the same procedures as described above). Sub-samples for counting phytoplankton and heterotrophic protists were fixed in acetic Lugol's solution in a final concentration of 2 %. Samples were kept cold and dark until examination; 1-2 months after the experiment. Depending on the density of the cultures, 10-50 ml samples were settled for 24 h in Üthermöhl-Chambers (Hydro-Bios). Phytoplankton and heterotrophic protists were counted on an inverted microscope at ×100 or ×200 magnifications. Five transects or a minimum of 400 cells were counted for each of the investigated species. For the prymnesiophyte *Phaeocystis pouchetii* only cells in colonies were counted (a colony was defined as ≥4 cells grouped together).

Growth rates (µ, d^{-1}) were calculated as the increase in cell concentration according to:

$$\mu\,(d^{-1}) = \frac{Ln\,N_1 - Ln\,N_0}{t_1 - t_o}, \qquad (1)$$

where N_0 and N_1 are number of cells before dilution (t_1) and after previous dilution (t_0), respectively.

Cumulated cell and Chl *a* concentration (N_{cum}) was estimated according to:

$$N_{cum}(cells\ l^{-1}) = N_{t-1} \times e^{\mu(t_1 - t_0)}, \quad (2)$$

Growth rates in treatments and controls were calculated as the slope of the logarithmic N_{cum} as a function of time during day 2-8 (2011) and day 4-9 (2012); i.e. 4 and 5 sampling events respectively. The changes in logarithmic cumulated concentration (Ln N_{cum}) for each replicate were fitted a linear regression. The slope of the regressions was accepted as significant when $p < 0.05$.

Dissolved inorganic carbon (DIC)

Dissolved inorganic carbon (DIC) was only measured in Exp. where it was measured twice in each of the treatments and controls. 10 ml subsamples were taken from each experimental bottle and fixed with 100 µL Hg_2Cl_2 in airtight glass vials (12 ml) not allowing any headspace to avoid CO_2 from leaking out of the water phase. Samples were stored dark and cold (ca. 5 ^oC) until analysis one month later. DIC concentrations of triplicate 60 µL sub-samples were measured on an IRGA (infrared gas analyzer) following the procedures of Nielsen et al. (2007). Data was analysed with the computer program Prologger® and concentrations of DIC, depending on pH, temperature and salinity, were calculated into the carbon speciation (HCO_3^-, CO_3^{2-} and CO_2) using the program CO_2Sys EXCEL Makro (Lewis & Wallace 1998), with the following available inputs. *Set of constants*: K_1, K_2 from Mehrbach et al. (1973) refit by Dickson and Millero (1987); *$KHSO_4$*: Dickson (1990); *pH scale*: NBS-scale (mol/kg-SW).

RESULTS

In situ variation in pH and other environmental parameters during the spring blooms

At the onset of the sampling period sea ice covered 15 % and 90 % of the bay in 2011 and 2012, respectively (Fig. 1 A-B). The bay was ice-free from May 4th 2011 and from May 28th 2012. The water column was stratified in both years and depth of the mixed layer remained relatively constant throughout the study periods. A sub-surface fluorescence maximum was observed at 15-40 m depths throughout the study period in both years. By late April a phytoplankton bloom had built up with Chl *a* concentrations reaching 14 and 18 µg Chl *a* l^{-1} in 2011 and 2012, respectively (fig. 1C-D). At the depth of the fluorescence maximum pH ranged from 7.9 to 8.3 in 2011 and from 7.6 to 8.3 in 2012 (Fig. 1E-F). Peak values coincided with the phytoplankton spring bloom on May 19th, 2011 and May 2nd, 2012. In 2011 the highest pH (pH 8.5) was measured in the

surface waters at 1 m depth, while the highest pH in 2012 was found at 10 m depth (Fig. 2). Lowest values were measured at 250 depths in both years, reaching values of 7.9 and 7.5 on May 9th, 2011 and May 8th, 2012 respectively (Fig. 2). The pH values were generally higher in 2011 than 2012, possibly due to the lower % ice cover. The succession of heterotrophic protists in 2011 followed the development in Chl *a*, reaching a maximum on May 12th with 7560 cells l^{-1} (ciliates and heterotrophic dinoflagellates contributed equally) (Fig 1G). The ciliates were dominated by oligotrich species; primarily *Strombidium* spp., *Strobilidium* spp., *Strobilidium oviformis* and *Mesodinium rubrum.* The dinoflagellates were dominated by the thecate *Protoperidinium bipes* and naked gymnodinid species including *Gyrodinium spirale*.

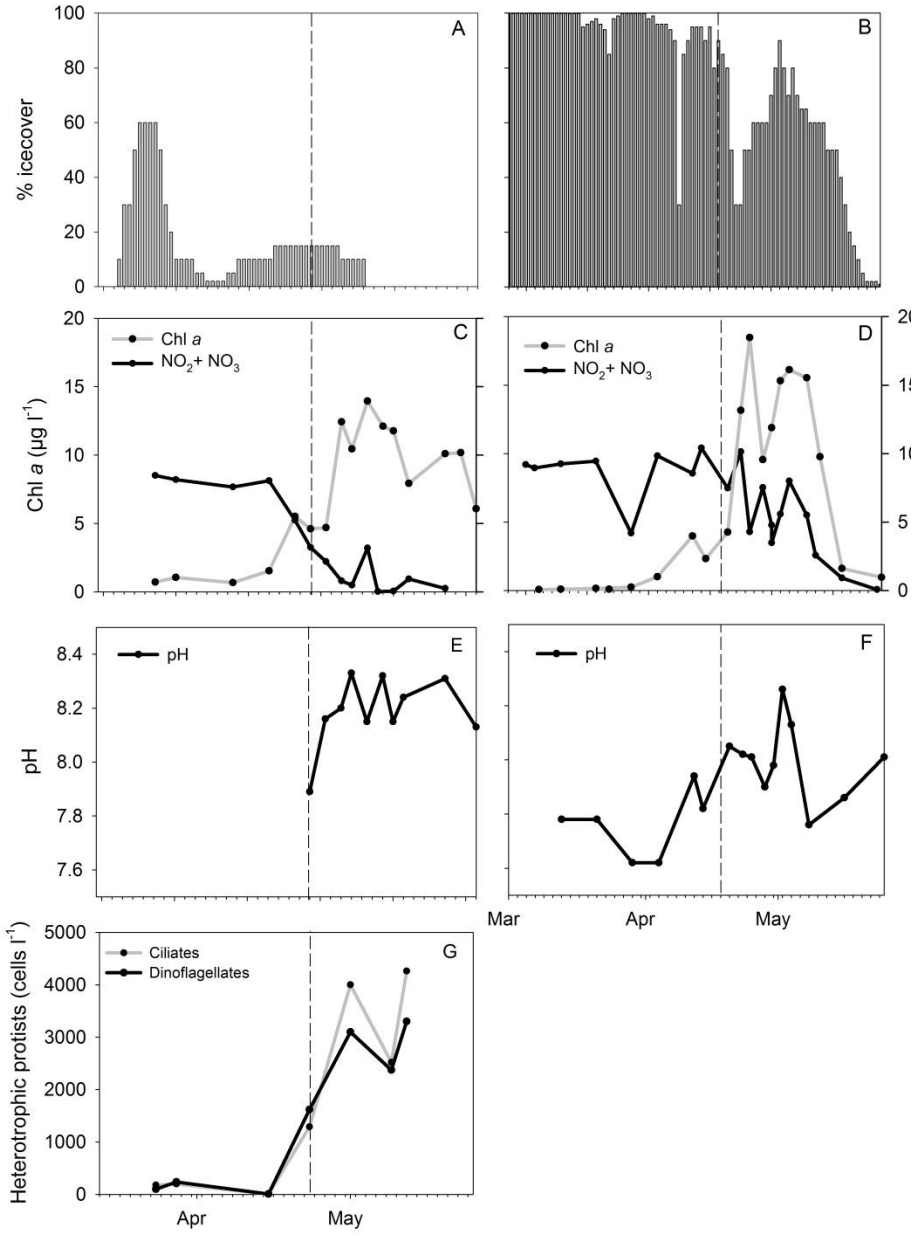

Fig. 1. *In situ* data from water collected at fluorescence maximum in 2011 (left panel) and 2012 (right panel). A-B: % ice-cover, C-D: Chl a (µg l^{-1}) and NO_2+NO_3 (µM), E-F: pH, G: Abundance of heterotrophic protists (cells l^{-1}). Dashed line marks when water for the experiments was collected.

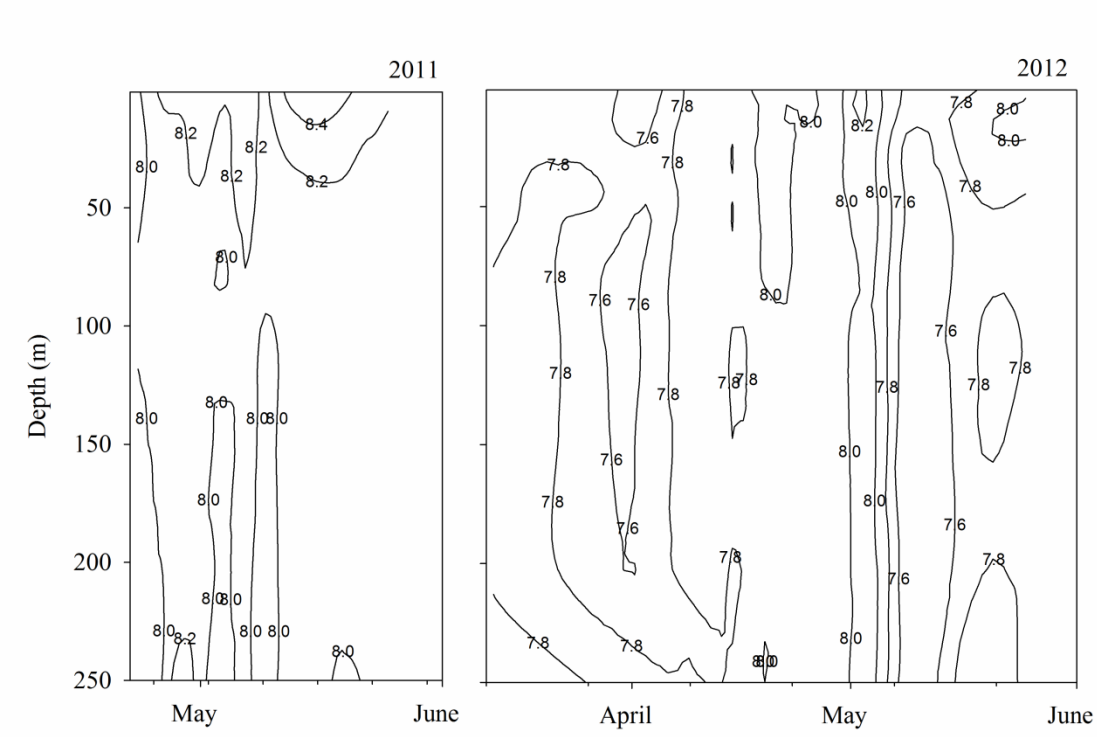

Fig. 2. Vertical distribution of *in situ* pH in 2011 (left panel) and 2012 (right panel).

First set of experiments - 2011: the response of a protist community to elevated pH under nutrient limitation

In the first set of experiments Chl *a* was allowed to reach a maximum of 22 µg Chl a l^{-1} in the experimental bottles, corresponding to the Chl *a* concentration during a spring bloom (Fig. 3). During the following days, Chl *a* declined but remained within a narrow range (5-12 µg Chl *a* l^{-1}) the rest of the period (Table 1). Chl *a* growth rates were generally low (< 0.05 d^{-1}; Fig. 4) and the slopes of the linear regressions in logarithmic cumulated Chl *a* were not significantly different from zero ($p > 0.10$). Furthermore, there was no significant difference between treatments and controls (Table 2).

The nitrate and phosphorous concentrations (N and P) were low but remained relatively stable throughout the experimental period (table 1). Silicate (Si) concentrations increased as NaOH was added. This was an artifact caused by the storage of NaOH in a glassbottle, since glass contains Si. However, according to the Si:C:N ratio of diatoms of 15:106:16 (Brezezinski 1985), N was the limiting nutrient in treatment and controls.

Table 1. Concentrations of Chl *a* and nutrient (N, P, Si) during the experimental periods for controls and pH treatments (Mean ± SD, n=15-18).

	pH	Chl *a* (µg l^{-1})	N (µM)	P (µM)	Si (µM)
Exp. 1 (2011)	8.00 ± 0.02	7.46 ± 2.53	0.05 ± 0.03	0.49 ± 0.20	1.38 ± 0.72
Nutrient limited	8.50 ± 0.01	8.23 ± 1.81	0.09 ± 0.07	0.38 ± 0.12	3.68 ± 1.98
conditions	9.00 ± 0.01	8.26 ± 2.11	0.08 ± 0.13	0.38 ± 0.17	15.8 ± 4.34
	9.52 ± 0.03	6.84 ± 2.07	0.16 ± 0.22	0.32 ± 0.18	39.6 ± 5.76
Exp. 2 (2012)	8.00 ± 0.02	7.12 ± 3.88	8.16 ± 1.57	0.72 ± 0.13	10.0 ± 1.12
Nutrient replete	8.50 ± 0.02	7.27 ± 3.29	8.36 ± 1.75	0.75 ± 0.18	16.5 ± 4.49
conditions	8.77 ± 0.05	6.59 ± 2.96	8.72 ± 1.74	0.73 ± 0.15	16.7 ± 5.04
	9.03 ± 0.05	6.60 ± 3.06	9.26 ± 0.75	0.75 ± 0.14	20.4 ± 7.73
	9.51 ± 0.06	1.74 ± 0.39	11.4 ± 0.43	0.88 ± 0.08	49.6 ± 6.92

The increase in logarithmic cumulated phytoplankton cell abundance fitted a significant linear regression for controls ($p < 0.05$), but not for the pH treatments ($p > 0.05$). The enumeration of the specific dominant phytoplankton species revealed that the growth rates of the tested phytoplankton species were only significantly reduced for *Skeletonema* sp. (Fig. 5, Table 2).

The logarithmic cumulated cell abundance of all three species of heterotrophic protists as a function of time (day 2-12) fitted an increasing linear regression ($p <0.05$) An exception was pH treatment 9.5, where no heterotrophic protists were found after the 4 days acclimation period. The growth rates of *G. spirale* and *P. bipes* were significantly affected by pH in the range from 8.0 to 9.0, and growth rates had changed from 0.30 to 0.07 d^{-1} and 0.31 to 0.12 d^{-1} for *G. spirale* and *P. bipes*, respectively (Holm-Sidak, $p < 0.05$, Table 2, Fig. 6). The growth rate of *Strobilidium oviformis* was not significant from pH 8.0 to pH 9.0 (Holm-Sidak, $p > 0.05$, Table 2, Fig. 6), but no *S. oviformis* were found in the pH 9.5 treatment after 2 days of incubation under the given pH.

Table 2. Results of one-way ANOVA (Holm-Sidak) for effect of elevated pH on growth rates (μ, d^{-1}). Significant effects are marked for 99 % (**) or 95 % (*) confidence levels. Not significant is marked with the symbol: NS = Non-significant.

	Nutrient level	8.0 vs. 8.5	8.0 vs. 8.7	8.0 vs. 9.0	8.0 vs. 9.5	8.5 vs. 8.7	8.5 vs. 9.0	8.5 vs. 9.5	8.7 vs. 9.0	8.7 vs. 9.5	9.0 vs. 9.5
Phytoplankton											
Chaetoceros socialis	Low	NS	NS	NS	NS	NS	NS	NS	NS	NS	NS
Chaetoceros socialis	High	NS	NS	NS	NS	NS	NS	NS	NS	NS	NS
Fragilariopsis sp. 1	High	NS	NS	NS	NS	NS	NS	NS	NS	NS	NS
Fragilariopsis sp. 2	High	NS	NS	NS	NS	NS	NS	*	NS	NS	NS
Navicula sp.	High	NS	NS	NS	NS	NS	NS	NS	NS	NS	NS
Phaerocystis pouchetii	Low	NS	NS	NS	NS	NS	NS	NS	NS	NS	NS
Phaerocystis poucheti	High	NS	NS	**	**	NS	NS	*	NS	NS	NS
Skeletonema sp.	Low	NS	NS	NS	**	NS	NS	*	NS	NS	*
Thalassiosira spp.	Low	NS	NS	NS	NS	NS	NS	NS	NS	NS	NS
Thalassiosira spp.	High	NS	NS	NS	**	NS	NS	**	NS	*	**
Total phytoplankton	Low	NS	NS	NS	NS	NS	NS	NS	NS	NS	NS
Total phytoplankton	High	NS	NS	NS	**	NS	NS	**	NS	**	**
Heterotrophic protists											
Protoperidinium bipes	Low	NS	ND	*	ND	ND	*	ND	ND	ND	ND
Gyrodinium spirale	Low	NS	ND	*	ND	ND	*	ND	ND	ND	ND
Strobilidium oviformis	Low	NS	ND	NS	ND	ND	NS	ND	ND	ND	ND

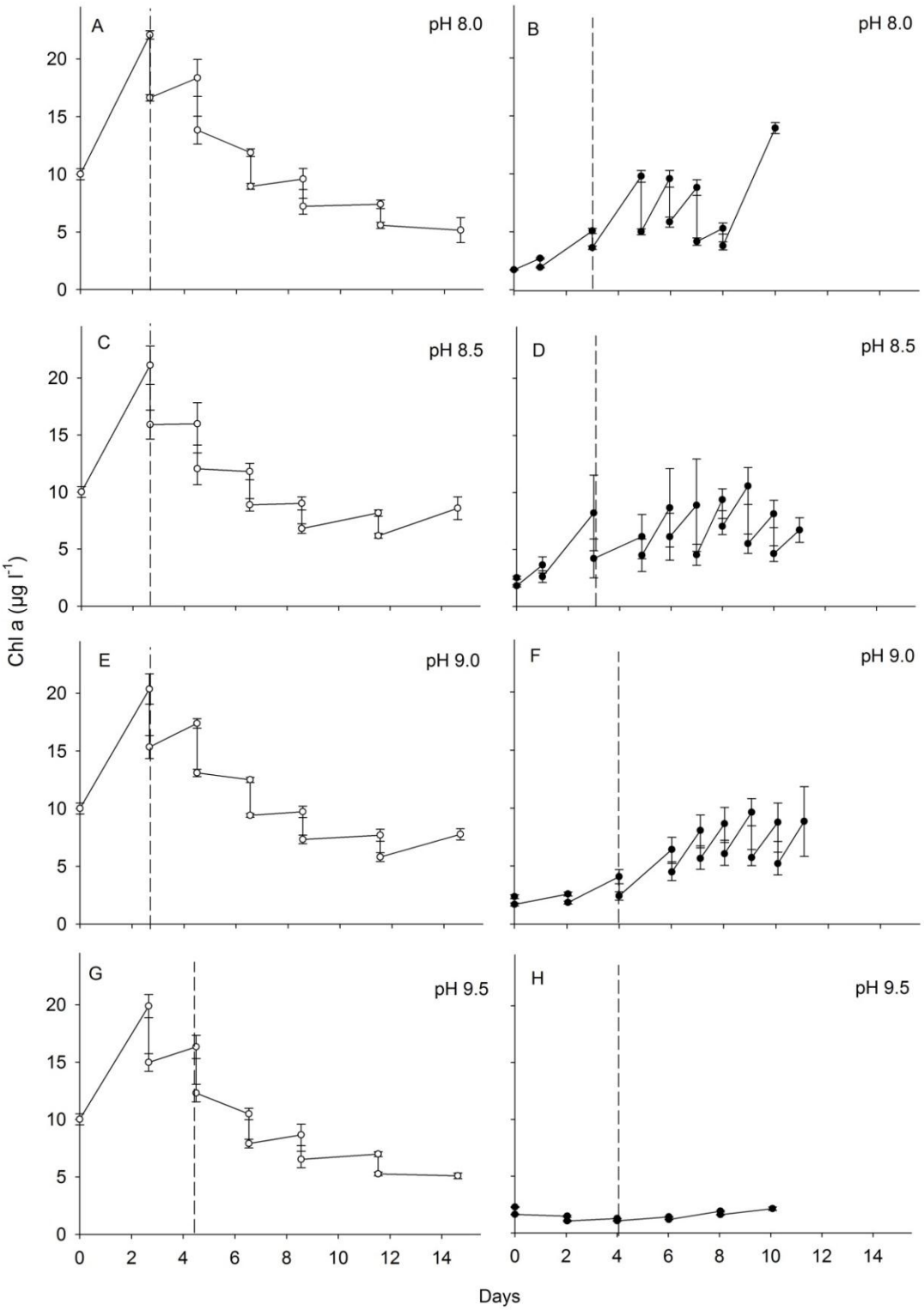

Fig. 3. Development in Chl *a* during Exp.1 (left panel) and Exp.2 (right panel) in controls (pH 8.0) and three pH treatments (pH 8.5, 9.0 and 9.5) before and after dilution of the cultures. Values represent mean ± SD (n = 3).

Second set of experiments - 2012: the response of a protist community to elevated pH under nutrient replete conditions

The second set of experiments (Exp. 2) were carried out under nutrient replete conditions, which due to the high dilution rates, included very low concentrations of heterotrophic grazers throughout the experiment (<0.4 cells ml^{-1}). The high dilution rate kept the Chl *a* level in all treatments and controls in the range 3-12 µg Chl *a* l^{-1} throughout the experimental period (Fig. 3, right panel). The increase in logarithmic cumulated Chl *a* concentrations as a function of time almost all fitted a linear regression ($p < 0.05$). An exception was the pH 9.5 treatment, where a significant reduction in Chl *a* occurred as soon as the flasks had been adjusted to pH 9.5. There was hereafter no significant increase in logarithmic cumulated Chl *a* concentration (linear regression, $p > 0.10$).

The phytoplankton community growth rates (based on Chl *a*) were higher than in the first set of experiments reaching ~0.4 d^{-1} and Chl *a* concentrations were unaffected by pH in the range of pH 8.0-9.0 (Holm-Sidak, $p > 0.05$, Table 2, Fig. 4). However, at pH 9.5 the total phytoplankton growth rate dropped to 0.06 d^{-1}. When considering the individual phytoplankton species, the trends were the same as for the community growth rates (Fig. 5) with significant linear increase in logarithmic cumulated cell abundance for all replicates in controls and pH treatments 8.5, 8.7 and pH 9.0 ($p < 0.05$). Logarithmic cumulated cell abundance in treatment 9.5 did not fit a linear regression ($p > 0.10$). Average growth rates dropped from 0.49 d^{-1} at pH 8.0 to 0.27 d^{-1} at pH 9.5. Four out of the six phytoplankton species studied were significantly negatively affected when pH was elevated to 9.5 (Holm-Sidak, $p <0.05$, Table 2), and 5 out of 6 species had maximum growth at pH 8.0 and followed a trend towards lower growth rate with increasing pH (Fig. 5).

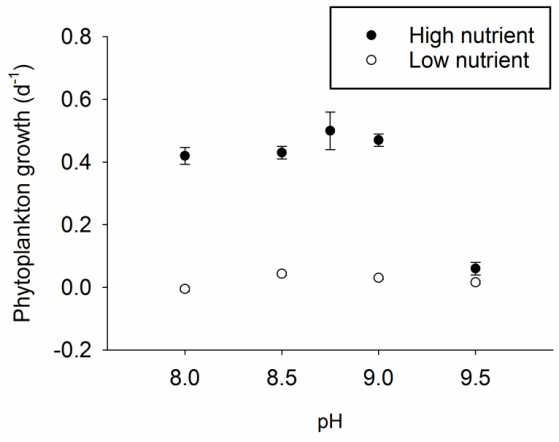

Fig. 4. Growth rate as a function of pH for the total phytoplankton community (Chl *a*) when grown under nutrient-replete (●) and nutrient-limited (○) conditions. Data points represent means ± SD (n = 3).

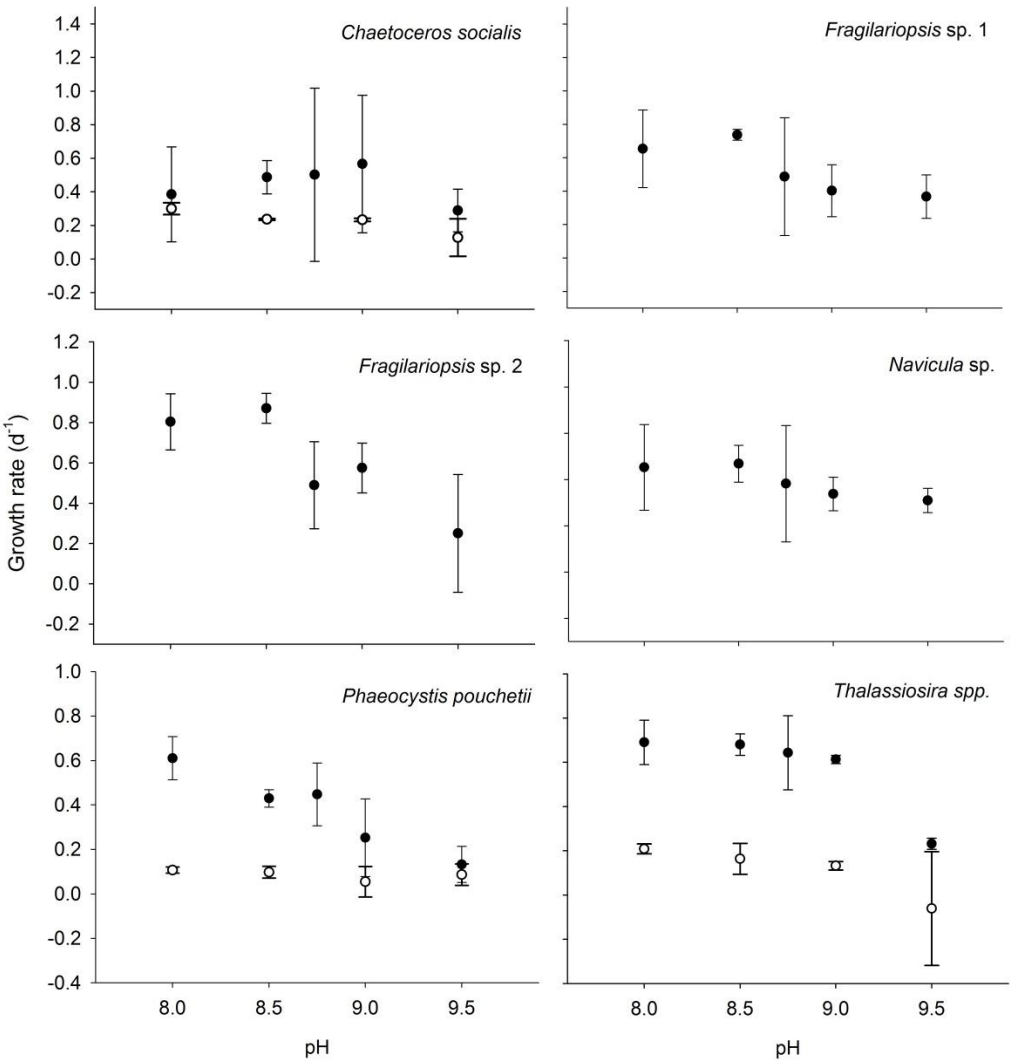

Fig. 5. Growth rate as a function of pH shown for different phytoplankton species cultured under nutrient-replete (●) and nutrient-limited (○) conditions. Data points represent means ± SD (n=3).

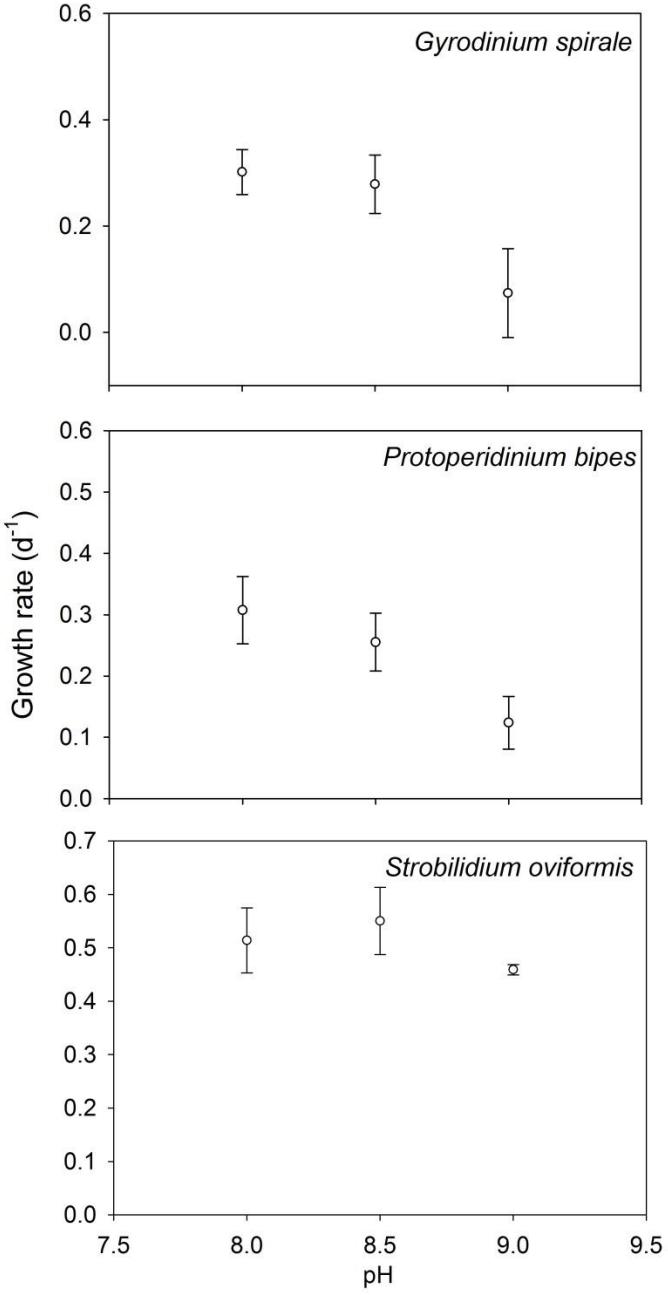

Fig. 6. Growth rate as a function of pH for three heterotrophic protists. Values are given as means ± SD (n = 3).

DIC was measured twice for each treatment/controls; at the start and end of the experiment, respectively (Fig. 7). DIC level stayed close to 2 mM at pH 8.0, 8.5, 8.7 and 9.0, and was not significantly different between start and end of the experiment (Holm-Sidak, $p > 0.05$, Table 2). The DIC pool was dominated by HCO_3^- at pH 8.0, but changed towards a higher proportion of CO_3^{2-} relative to HCO_3^- as pH was elevated. CO_2 contributed with <1% in treatments as well as controls: <0.01mM and 0.03 mM for treatments and controls respectively.

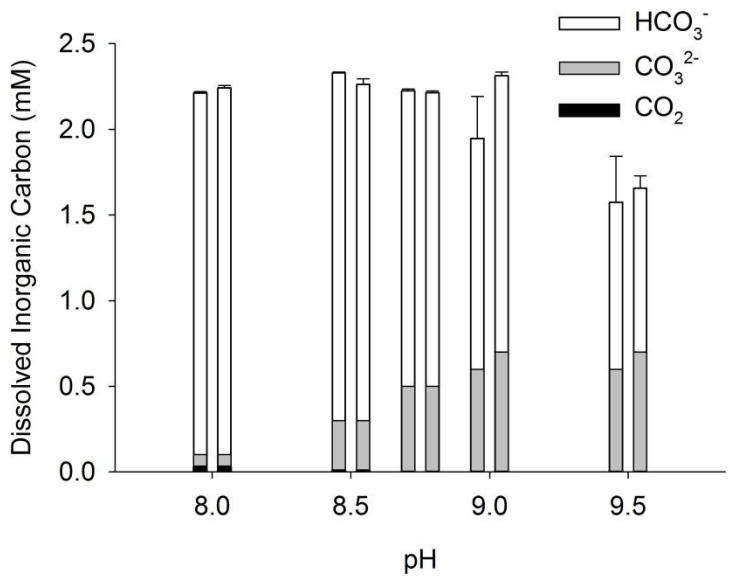

Fig. 7. Concentrations of DIC species (mM) in the second set of experiments. Bars are arranged pairwise and present concentrations at day 7 (left bars) and day 11 (right bars) respectively. Values are shown as mean ± SD (n=3).

Impact of nutrients and elevated pH on community composition

Phaeocystis pouchetii and *Thalassiosira* spp. dominated the phytoplankton community in both years. The ratio between the cell concentrations of the two species (*P. poucheti*: *Thalassiosira*) was initially around 11:1 and 13:1 in year 2011 and 2012, respectively. At the termination of the first set of experiments carried out in 2011 under nutrient limiting growth conditions, the ratio had changed to around 2:1 in treatments and controls (Holm-Sidak, $p < 0.05$). The ratio between controls and the treatments by the end of the experiment were not significantly different (Holm-Sidak, $p > 0.05$, Table 2, Fig. 8A).

In the second set of experiments conducted under nutrient replete conditions, the ratio between the two species remained unchanged at pH 8.0 (Fig. 8B). However, as pH was elevated towards pH 9.0 a relative dominance of *Thalassiosira* spp. was apparent and the ratio shifted to 2:1 (Holm-Sidak, $p < 0.05$, Fig. 8B). At pH 9.5 *Thalassiosira* spp. was so affected by the elevated

pH that the abundance dropped to <10 % at pH 8.0, resulting in a ratio on 18:1. This shift in species composition with increasing pH was not only observed between *P. pouchetii* and *Thalassiosira* spp., but also between *P. pouchetii* and the other diatoms species. A possible explanation for this sudden shift in the ratio could be caused by a high pH optimum for *Thalassiosira*, but that the population collapses when the threshold is reached.

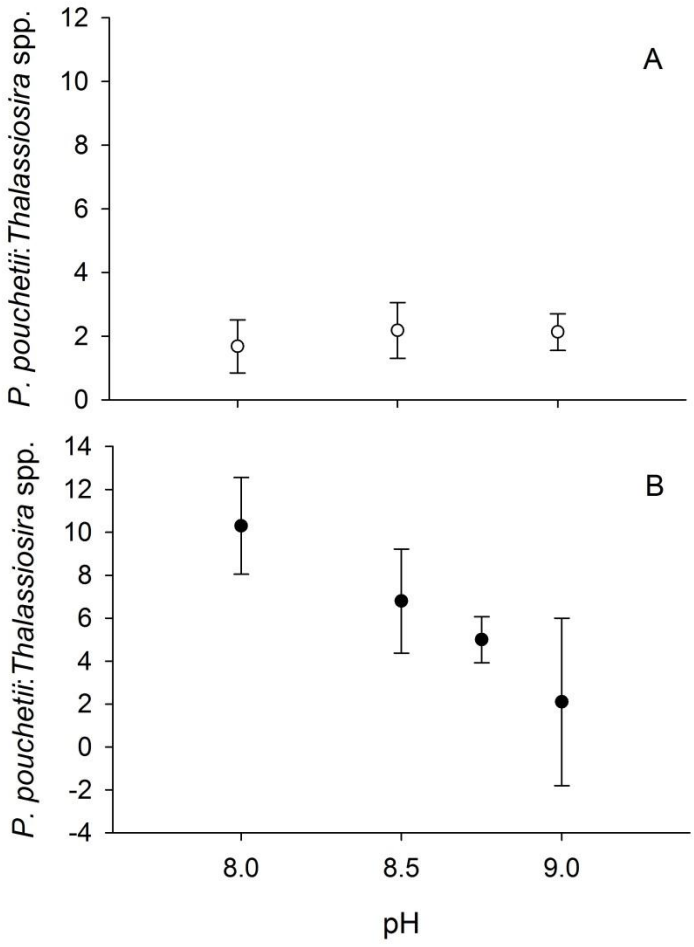

Fig. 8. Ratio between abundance of *Phaeocystis pouchetii* and *Thalassiosira* spp. as a function of pH. Ratios are estimated after 6 days of incubation under nutrient-limited (A) and nutrient-replete (B) conditions. Data points show means ± SD (n = 3).

.

DISCUSSION

Fluctuations of pH in Arctic coastal waters

The temporal fluctuations in pH in Arctic waters are primarily caused by high respiration rates during the dark Arctic winter and high primary production rates as the day length increases and sea ice cover disappears during spring. During the spring bloom in Disko Bay in 2011 and 2012, pH ranged from 7.6 to 8.5. This range in pH is similar to what has been observed in many temperate and tropical coastal waters (Provoost et al. 2010, Brutemark et al. 2011, Praveena & Aris 2013) and is consistent with the few existing measurements from the Arctic and Antarctic waters (Charalampopoulou et al. 2011, Yakushev & Sørensen 2013, Björk et al. 2014). Although pH did not exceed 8.5 in the Disko Bay, pH may exceed this value in other parts of the Arctic region where high accumulation of phytoplankton biomass occur; e.g. during intense phytoplankton blooms, which periodically develop under sea-ice/pack-ice (Gradinger 1996, Spilling 2007, Arrigo et al. 2012), inside sea-ice (Legendre et al. 1992) or in marginal ice zones (Falk-Petersen et al. 2000). In the Arctic region Sea ice primary productivity is estimated to account for 7.5 % of the primary production (Dupont 2012), and since pH has been reported to reach 9.0 under sea-ice (Spilling 2007) and 10.0 in sea-ice brine channels (Gleitz et al. 1995), elevated pH may especially an important controlling factor within these habitats. For the same reason we chose to include treatments where pH was elevated as high as pH 9.5, although pH values exceeding 8.5 must be considered rare in the Arctic marine environment.

Does nitrate affect phytoplankton tolerance to elevated pH?

The phytoplankton spring bloom in Disko Bay is characterized by a peak in phytoplankton biomass accompanied by a reduction in nitrate as the phytoplankton depletes the surface water of nutrients (Dünweber et al. 2010). In Exp. 1, nitrate levels were close to the level found as the bloom descends. The low phytoplankton concentration during the experiments in 2011was most likely a result of the low nitrate levels although grazing also played a role. In order to evaluate if latter had a major impact on the low growth rates, we inspected the logarithmic cumulated cell abundances as a function of time and experiments were terminated when the logarithmic cumulated cell abundance were no longer increasing (data not shown). For all phytoplankton species in the controls the increase followed a significant linear until day 8 (linear regression, $p < 0.05$), and based on this grazing mortality was assumed to stay relatively constant despite an increasing number of grazers.

Based on changes in Chl *a* measurements from the two experiments, community phytoplankton growth was only affected when pH was raised to 9.5 under nutrient replete conditions. Although growth rates were low under nutrient limited conditions we could have expected the same

proportional decrease in growth rate as was seen for the phytoplankton growth under nutrient replete conditions –i.e. growth rates would have been close to zero or even negative. This scenario would have been even more profound if the impact of nutrient limitation and pH sensitivity were interacting: e.g. Li et al (2012) documented that elevated CO_2 increased the photosynthetic capacity in a diatom when cultured under N-replete conditions, but not when cultured under N-limited. Other factors such as UV radiation and nutrients have also been shown to interact and hereby modulated phytoplankton sensitivity to changes of these factors (Beardall et al. 2009)

The Arctic coastal waters are generally nutrient limited during the summer period. However, climate related changes in water mass exchange is expected to increase the nutrient input in the Arctic Ocean: e.g. input of nutrient rich water into the euphotic coastal zones is expected to increase as a consequence of intensified runoffs from glacial melting and increased upwelling of nutrient rich water due to a retreating ice cover on the continental shelves. In addition, increased human activities may lead to eutrophication in certain areas of the Arctic. Our data suggest that a higher nutrient level trigger diatom growth despite elevations in pH.

Impact of elevated pH on plankton community composition

The microcosm experiments demonstrated the heterotrophic protists are tolerant to changes in pH within the natural pH range 8.0-8.5. This is in accordance with previously studies, demonstrating that heterotrophic protists are robust to 0.5 unit reductions in pH relative to *in situ* pH of 8.33 (Aberle et al. 2013). Yet, the heterotrophic protists were generally more sensitive to elevated pH than the diatoms. Two out of three heterotrophic protists were significantly affected at pH >8.5 and none of the heterotrophic protists survived at pH 9.5. The upper growth limit for heterotrophic protists is in accordance with previously published data showing that heterotrophic protists from temperate marine waters are negatively affected when pH exceeds 9.0 (Pedersen & Hansen 2003a, Pedersen & Hansen 2003b). In comparison, diatoms have be shown to maintain their growth even at pH 10 (Spilling et al. 2013). All species responded to the elevated pH within the first 24-48 h, hereafter the growth rate was rather constant. However, since different species respond differently, short term elevations in pH may favor some species rather than others. We could e.g. expect to see a decoupling of heterotrophic protists from the succession, thus expanding the length and increasing magnitude of the bloom.

Unfortunately we could not test the pH tolerance of heterotrophic protists grown under high nutrient conditions due to their lower growth rates compared to the phytoplankton, which meant that they were outgrown by the fast growing phytoplankton. For this reason we cannot conclude whether the higher sensitivity of heterotrophic protists were caused by “cascading” trophic effects (e.g. due to poor food quality and/or less food availability as pH increased) or whether the effect was caused directly by elevated pH.

The tolerance to elevated pH of the tested phytoplankton species revealed huge inter-specific variations. *Thalassiosira* spp. were unaffected by modest elevations in pH, while *Phaeocystis pouchetii* reduced its relative abundance with approximately 66% at pH 8.5 after only 6 days of incubation. The tendency towards higher ratios of diatoms with elevated pH is in contrast to what has been found in the Equatorial Pacific, where the abundance of colony forming *P. pouchetii* increased relative to diatoms when CO_2 was reduced from 750 ppm (pH ~7.9) to 150 ppm (pH ~8.5) (Tortell et al. 2002). Since *P. pouchetii* and *Thalassiosira* spp. are both important components of Northern temperate and Arctic phytoplankton blooms (Schoemann et al. 2005, Dünweber et al. 2010, Degerlund & Eilertsen 2010) even small changes in pH will affect the succession of the bloom. It should be noted that only *P. pouchetii* cells in colony was counted and the impact of pH could thus potentially have affected the ability to form colonies and not cell growth.

Among the most tolerant species was *Navicula* sp. which grew at 66% of its maximum growth rate at pH 9.5. This pennate diatom is an ice alga and one hypothesis could be that ice-algae are more tolerant to high pH than true pelagic species. The hypothesis is supported by Søgaard et al. (2011) who found similar high tolerances to elevated pH for three cultivated ice-algae species (*Fragilariopsis nana*, *Fragilariopsis* sp. and *Clamydomonas* sp.). Despite these few exceptions, almost all phytoplankton species were affected at pH 9.5. Physical stress was also evident from the morphology of the cell; many of the Lugol stained cells became darker, colonies reduced in size and the cell structures changed. These morphological changes were most evident for *P. pouchetii*, *Fragelariopsis* spp and. *Thalassiosira* spp.

Is inorganic carbon limiting phytoplankton growth?

In the present study we manipulated the carbon system by adding NaOH to a plankton assemblage with minor CO_2 exchange. By manipulating the carbon system in this way, pH and total alkalinity (TA) increases whereas DIC concentrations remain largely unchanged. The DIC levels in present study were therefore higher than would be expected during a natural bloom, where DIC concentrations decrease (e.g. Hansen et al 2007). It is possible that the phytoplankton become carbon limited during a natural phytoplankton bloom situation as CO_2 is depleted from the surface. We argue that this was not the case in present study since bloom forming phytoplankton species have been demonstrated to be limited by pH rather than CO_2 at pH levels up to 9.0 (Hansen et al. 2007). Moreover, most marine phytoplankton species have evolved highly effective CO_2 concentration mechanisms (CCMs) to avoid carbon limitation (Johnston and Raven 1996; Korb et al. 1997; Price et al. 2004; Nakajima et al. 2013). The efficiency of CCMs is species specific, but it is generally high for marine species including diatoms and *Phaeocystis* spp. (Tortell et al. 1997, Trimborn et al. 2013). In fact, even at DIC concentrations as low as 1.6 mM diatoms have been shown to maintain >90% of their growth rate relative to natural seawater DIC of 2 mM (Clark & Flynn 2000). Major CCMs in diatoms are HCO_3^-

transporters in the cell plasma membrane which enables the cell to directly or indirectly use the high amounts of HCO_3^- in seawater for their production (Nakajima et al. 2013). Other mechanisms include direct CO_2 transporters, which have also been found to increase intracellular CO_2 levels of some diatoms (Hopkinson 2013).

Although carbon is generally not limiting growth of marine phytoplankton, this might be different at extreme pH levels where the DIC speciation changes drastically. The relative percentage of CO_2 to total DIC dropped from 1.1 % at pH 8.0 to 0.08 % at pH 9.0. Thus the phytoplankton would almost certainly be limited by CO_2 at pH >9.0. However, at pH ≤ 9.0 the phytoplankton have theoretically had sufficient HCO_3^- and were most likely limited directly by pH rather than by carbon. How exactly autotrophic and heterotrophic protists are affected by pH is still unknown, but intracellular changes in pH could e.g. affect nutrient uptake, ion-transport or enzyme functioning. The cells could also be affected indirectly by changes in the solubility/precipitation of metals, nutrients or other vital elements that are known to be affected by pH.

pH of Arctic coastal waters in the future

Over the past three decades the Arctic perennial sea-ice extent has declined with a rate of ~12 % per decade (Comiso 2012). The shrinking ice-cover has resulted in increased annual primary production in large parts of the Arctic along with significant increases in annual net CO_2-fixation rates (Pabi et al. 2008, Arrigo et al. 2008, Slagstad et al. 2011). Changes in seawater carbon chemistry is known to affect natural plankton communities, but until now most studies in the polar regions have focused on the impact of CO_2 enrichment (ocean acidification) caused by increased atmospheric pCO_2 (Aberle et al. 2013, Björk et al. 2014, Trimborn et al. 2013Rost et al. 2008,). By the end of 2100 surface water pH in the Arctic region is predicted to decrease from an average of ~8.2 at present to ~7.6 (IPCC). However, we have to be aware that pH regulation in coastal ecosystems is largely disconnected from the open ocean (Duarte et al. 2013) and that the reductions in pH in the coastal areas is also regulated by other drivers than atmospheric pCO_2 such as processes affecting input of nutrients, terrestrial organic matter and freshwater discharge.

It is unknown how increased human activities in the Arctic will impact pH, but human activities have historically resulted in eutrofication. On a global scale nitrogen has e.g. increased > 3 fold since 1860 due to human activities (Passow & Carlson 2012). In temperate coastal waters, this has resulted higher photosynthetic rates and increased pH (Hansen 2012). Since predicted estimates of net primary production in the Arctic also suggest an increase (Arrigo & van Dijken 2011), we suggest that biologically related changes in pH will exceed the impact caused by elevated atmospheric CO_2 and that particular coastal zones will be associated with temporal increases in pH.

This and previous studies demonstrate that a wide range of protist species respond negatively when pH is elevated during algal blooms. However, some species, including many diatoms, are tolerant to temporal elevations in pH, which gives them a competitive advantage to more sensitive species during phytoplankton blooms. Higher frequencies in bloom events will thus favor species tolerant to elevated pH like the diatoms. On the other hand could ocean acidification reduce the pH maximum reached during the blooms thus changing the succession towards less tolerant species including heterotrophic protists and non-diatom phytoplankton species such as *Phaeocystis pouchetii*.

LITERATURE CITED

Aberle N, Schulz KG, Stuhr A, Malzahn AM, Ludwig A, Riebesell U (2013) High tolerance of microzooplankton to ocean acidification in an arctic coastal plankton community. Biogeosciences 10:1471-1481

Arrigo KR, van Dijken GL (2011) Secular trends in arctic ocean net primary production. J Geophys Res -Oceans 116:C09011

Arrigo KR, van Dijken G, Pabi S (2008) Impact of a shrinking arctic ice cover on marine primary production. Geophys Res Lett 35:L19603

Arrigo KR, Perovich DK, Pickart RS, Brown ZW, van Dijken GL, Lowry KE, Mills MM, Palmer MA, Balch WM, Bahr F, and others (2012) Massive phytoplankton blooms under Arctic sea ice. Science 336:1408-1408

Beardall J, Mukerji D, Glover HE, Morris I (1976) The path of carbon in photosynthesis by marine phytoplankton. J Phycol 12:409-417

Beardall J, Sobrino C, Stojkovic S (2009) Interactions between the impacts of ultraviolet radiation, elevated CO_2, and nutrient limitation on marine primary producers. Photochem. Photobiol. Sci. 8: 1257–65.

Björk MM, Fransson A, Torstensson A, Chierici M (2014) Ocean acidification state in western Antarctic surface waters: controls and interannual variability. Biogeoscience 11(1):57-73

Brezezinski MA (1985) The Si:C:N ratio of marine diatoms: interspecific variability and the effect of some environmental variables. J Phycol 21: 347–357

Brutemark A, Engstrom-Ost J, Vehmaa A (2011) Long-term monitoring data reveal pH dynamics, trends and variability in the western Gulf of Finland. Oceanol Hydrobiol Stud 40:91-94

Caldeira K,Wickett M (2003) Anthropogenic carbon and ocean pH. Nature 425:365-365

Charalampopoulou A, Poulton AJ, Tyrrell T, Lucas MI (2011) Irradiance and pH affect coccolithophore community composition on a transect between the North Sea and the Arctic Ocean. Mar Ecol Prog Ser 431:25-43

Clark D, Flynn K (2000) The relationship between the dissolved inorganic carbon concentration and growth rate in marine phytoplankton. Proc R Soc B-Biol Sci 267:953-959

Colman B, Rotatore C (1995) Photosynthetic inorganic carbon uptake and accumulation in 2 marine diatoms. Plant Cell Environ 18:919-924

Comiso JC (2012) Large decadal decline of the Arctic multiyear ice cover. J Clim 25:1176-1193

Degerlund M, Eilertsen HC (2010) Main species characteristics of phytoplankton spring blooms in NE Atlantic and Arctic waters (68-80 °N). Estuaries Coasts 33:242-269

Dickson AG, Millero F (1987) A comparison of the equilibrium-constants for the dissociation of carbonic-acid in seawater media. Deep-Sea Research Part A-Oceanographic Research Papers 34:1733-1743

Dickson AG (1990) Standard potential of the reaction: , and and the standard acidity constant of the ion HSO_4^- in synthetic sea water from 273.15 to 318.15 K. J Chemical Thermodynamics, 22:113-127

Duarte CM, Hendriks IE, Moore TS, Olsen YS, Steckbauer A, Ramajo L, Carstensen J, Trotter JA, McCulloch M (2013) Is ocean acidification an open-ocean syndrome? understanding anthropogenic impacts on seawater pH. Estuaries Coasts 36:221-236

Dünweber M, Swalethorp R, Kjellerup S, Nielsen TG, Arendt KE, Hjorth M, Tönnesson K, Møller EF (2010) Succession and fate of the spring diatom bloom in Disko Bay, Western Greenland. Mar Ecol Prog Ser 419:11-29

Dupont, F (2012) Impact of sea-ice biology on overall primary production in a biophysical model of the pan-Arctic Ocean.J Geophys Res 117, C00D17

Falk-Petersen S, Hop H, Budgell WP, Hegseth EN, Korsnes R, Loyning TB, Orbaek JB, Kawamura T, Shirasawa K (2000) Physical and ecological processes in the marginal ice zone of the northern barents sea during the summer melt period. J Mar Syst 27:131-159

Gleitz M, Vonderloeff M, Thomas D, Dieckmann G, Millero F (1995) Comparison of summer and winter inorganic carbon, oxygen and nutrient concentrations in Antarctic sea-ice brine. Mar Chem 51:81-91

Gradinger R (1996) Occurrence of an algal bloom under Arctic pack ice. Mar Ecol Prog Ser 131:301-305

Hansen B, Elberling O, Humlum O, Nielsen N (2006) Meteorological trends (1991–2004) at Artic Station central west Greenland (69°15' N) in a 130 years perspective. Danish J Geogr 106:45-55

Hansen H, Koroleff F (eds) (1999) Determination of nutrients. in: Grasshoff K, Kremling K, Erhardt M (eds) Methods of seawater analysis.

Hansen PJ (2002) Effect of high pH on the growth and survival of marine phytoplankton: Implications for species succession. Aquat Microb Ecol 28:279-288

Hansen PJ, Lundholm N, Rost B (2007) Growth limitation in marine red-tide dinoflagellates: Effects of pH versus inorganic carbon availability. Mar Ecol Prog Ser 334:63-71

Hansen W (2012) Marine områder 2011 NOVANA. Scientific Repport from Aahus University DCE National Center for Environment and Energy 34

Hinga K (2002) Effects of pH on coastal marine phytoplankton. Mar Ecol Prog Ser 238:281-300

Hopkinson BM (2014) A chloroplast pump model for the CO_2 concentrating mechanism in the diatom *Phaeodactylum tricornutum.* Photosynth Res 121:223-233

Johnston AM, Raven JA (1996) Inorganic carbon accumulation by the marine diatom *Phaeodactylum tricornutum*. Eur J Phycol 31:285–290.

Korb RE, Saville PJ, Johnston AM, Raven JA (1997) Sources of inorganic carbon for photosynthesis by three species of marine diatoms. J Phycol 33:433–440.

Legendre L, Ackley S, Dieckmann G, Gulliksen B, Horner R, Hoshiai T, Melnikov I, Reeburgh W, Spindler M, Sullivan C (1992) Ecology of sea ice biota. 2. Global significance. Polar Biol 12:429-444

Levinsen H, Nielsen TG, Hansen BW (1999) Plankton community structure and carbon cycling on the western coast of Greenland during the stratified summer situation. II. Heterotrophic dinoflagellates and ciliates. Aquat Microb Ecol 16(3): 217-232

Lewis E,Wallace D (1998) Program developed for CO_2 system calculations. Department of Applied Science. Brookhaven National Laboratory, Upton NY.

Li W, Gao K, Beardall J (2012) Interactive effects of ocean acidification and nitrogen-limitation on the diatom *Phaeodactylum tricornutum*. PLoS One **7**: e51590.

Madsen SD, Nielsen TG, Hansen BW (2001) Annual population development and production by *Calanus finmarchicus, C. glacialis* and *C. hyperboreus* in Disko Bay, western Greenland. Mar Biol 139:75-93

Mehrbach C, Culberso C, Hawley J, Pytkowic R (1973) Measurement of apparent dissociation-constants of carbonic-acid in seawater at atmospheric-pressure. Limnol Oceanogr 18:897-907

Nakajima K, Tanaka A, Matsuda Y (2013) SLC4 family transporters in a marine diatom directly pump bicarbonate from seawater. Proc. Natl. Acad. Sci. U. S. A. **110**: 1767–72.

Nielsen LT, Lundholm N, Hansen PJ (2007) Does irradiance influence the tolerance of marine phytoplankton to high pH? Mar Biol Res 3:446-453

Pabi S, van Dijken GL, Arrigo KR (2008) Primary production in the Arctic Ocean, 1998-2006. J Geophys Res Oceans 113:C08005

Passow U and Carlson CA (2012) The biological pump in a high CO_2 world. Mar Ecol Prog Ser 470:249-271

Pedersen M, Hansen P (2003a) Effects of high pH on a natural marine planktonic community. Mar Ecol Prog Ser 260:19-31

Pedersen M, Hansen P (2003b) Effects of high pH on the growth and survival of six marine heterotrophic protists. Mar Ecol Prog Ser 260:33-41

Praveena SM, Aris AZ (2013) A baseline study of tropical coastal water quality in Port Dickson, Strait of Malacca, Malaysia. Mar Pollut Bull 67:196-199

Price GD, Woodger FJ, Badger MR, Howitt SM, Tucker L (2004) Identification of a SulP-type bicarbonate transporter in marine cyanobacteria. Proc. Natl. Acad. Sci. U. S. A. 101: 18228–33

Provoost P, van Heuven S, Soetaert K, Laane RWPM, Middelburg JJ (2010) Seasonal and long-term changes in pH in the Dutch coastal zone. Biogeosciences 7: 3869-3878

Rost B, Zondervan I, Wolf-Gladrow D (2008) Sensitivity of phytoplankton to future changes in ocean carbonate chemistry: Current knowledge, contradictions and research directions. Mar Ecol Prog Ser 373:227-237

Schoemann V, Becquevort S, Stefels J, Rousseau W, Lancelot C (2005) *Phaeocystis* blooms in the global ocean and their controlling mechanisms: A review. J Sea Res 53:43-66

Silyakova A, Bellerby RGJ, Schulz KG, Czerny J, Tanaka T, Nondal G, Riebesell U, Engel A, De Lange T, Ludvig A (2013) Pelagic community production and carbon-nutrient stoichiometry under variable ocean acidification in an Arctic fjord. Biogeosciences 10:4847-4859

Skirrow G (1975) The dissolved gases—carbon dioxide. Riley JP, Skirrow G (Eds) Chemical Oceanography Academic Press, New York

Slagstad D, Ellingsen IH, Wassmann P (2011) Evaluating primary and secondary production in an Arctic Ocean void of summer sea ice: An experimental simulation approach. Prog Oceanogr 90: 117-131

Spilling K (2007) Dense sub-ice bloom of dinoflagellates in the Baltic Sea, potentially limited by high pH. J Plankton Res 29(10): 895-901

Spilling K, Brynjólfsdóttir Á, Enss D, Rischer H, Svavarsson HG (2013) The effect of high pH on structural lipids in diatoms. J Appl Phycol 25: 1435–1439

Søderberg LM, Hansen PJ (2007) Growth limitation due to high pH and low inorganic carbon concentrations in temperate species of the dinoflagellate genus *Ceratium*. Mar Ecol Prog Ser 351:103-112

Søgaard DH, Hansen PJ, Rysgaard S, Glud RN (2011) Growth limitation of three Arctic sea ice algal species: Effects of salinity, pH, and inorganic carbon availability. Polar Biol 34: 1157-1165

Tortell P, Reinfelder J, Morel F (1997) Active uptake of bicarbonate by diatoms. Nature 390:243-244

Tortell P, DiTullio G, Sigman D, Morel F (2002) CO_2 effects on taxonomic composition and nutrient utilization in an equatorial pacific phytoplankton assemblage. Mar Ecol Prog Ser 236:37-43

Paper IV

Trimborn S, Brenneis T, Sweet E, Rost B (2013) Sensitivity of Antarctic phytoplankton species to ocean acidification: Growth, carbon acquisition, and species interaction. Limnol Oceanogr 58:997-1007

Yakushev E, Sørensen K (2013) On seasonal changes of the carbonate system in the Barents Sea: observations and modeling. Mar Biol Res 9(9):822-830

Paper V

Published in Marine Ecology Progress Series

The Godthåbsfjord
Photo: Karen Riisgaard

Vol. 500: 67–82, 2014
doi: 10.3354/meps10706

MARINE ECOLOGY PROGRESS SERIES
Mar Ecol Prog Ser

Published March 17

Trophic role and top-down control of a subarctic protozooplankton community

Karen Riisgaard[1], Rasmus Swalethorp[1], Sanne Kjellerup[1,2], Thomas Juul-Pedersen[2], Torkel Gissel Nielsen[1,2,*]

[1]National Institute of Aquatic Resources, DTU Aqua, Section for Oceanography and Climate, Kavalergården 6, 2920 Charlottenlund, Denmark

[2]Greenland Climate Research Centre, Greenland Institute of Natural Resources, PO Box 570, 3900 Nuuk, Greenland

ABSTRACT: Plankton succession was investigated in the subarctic Godthåbsfjord, Western Greenland, from March to August 2010. The trophic role of protozooplankton (ciliates and heterotrophic dinoflagellates) was evaluated with emphasis on their seasonal succession and as prey for the copepod community. The integrated protozooplankton biomass ranged between 0.1 and 4.0 g C m^{-2}, and was dominated by ciliates. Over the 6 mo study period, maximum potential ingestion rates of the protozooplankton ranged from 0.02 to 1.2 g C m^{-2} d^{-1}, corresponding to 30 to 194% of primary production d^{-1} or 0.5 to 37% of phytoplankton biomass d^{-1}. The highest copepod biomass (24 g C m^{-2}) occurred in spring, with *Metridia longa* alone contributing up to 92% of the biomass. A grazing experiment with *M. longa* feeding on a natural plankton assemblage confirmed that this species cleared cells in the size range 10 to 60 µm with an average clearance rate of 2.4 ml µg C^{-1} d^{-1}. The copepod community, dominated by the genera *Calanus, Metridia, Pseudocalanus, Oithona, Microsetella* and *Triconia/Oncaea,* accounted for 72 to 93% of the copepod biomass in the spring. After the large calanoid copepod species left the surface layer, the protozooplankton increased numerically and were the most important grazers for some weeks until a late summer copepod community, dominated by cyclopoids *Oithona* spp., controlled the protist community. Our study indicated that protozooplankton succession is regulated by copepod grazing during most of the season, and that these protists provide an essential source of nutrition for the copepod populations.

KEY WORDS: Protozooplankton · Subarctic · Grazing · *Metridia longa*

INTRODUCTION

Greenlandic fjords support rich and diverse wildlife communities and are highly valuable ecosystems for commercial as well as cultural fishing (Hamilton et al. 2000). Climate models for the Arctic predict significant increases in temperatures, declines in the sea ice cover and acceleration of glacial melting (Stroeve et al. 2007, Comiso et al. 2008, Holland et al. 2008, Motyka et al. 2011). The Greenland fjords are major outlets of glacial runoff, and thus climate changes are likely to affect the hydrography, and possibly the food web structures, within these ecosystems (Mortensen et al. 2011). Therefore, baseline studies of the key plankton components in these areas are essential to understand climate-mediated changes in pelagic food web structure and productivity.

The Godthåbsfjord is a subarctic fjord system located next to Nuuk, the capital of Greenland. It is one of the largest fjord systems in Greenland, harbouring large populations of capelin and Atlantic cod (Smidt 1979, Storr-Paulsen et al. 2004, Bergstrøm & Vilhjalmsson 2008). The copepod community is numerically dominated by *Pseudocalanus* spp.,

*Corresponding author: tgin@aqua.dtu.dk

Microsetella spp., *Oithona* spp. and *Metridia longa* (Arendt et al. 2010, 2012, Tang et al. 2011), which is in contrast to most other Arctic regions where copepods of the genus *Calanus* are the most numerous species (Digby 1953, Nielsen and Hansen 1995, Rysgaard et al. 1999, Seuthe et al. 2011).

Metridia longa has not previously been recognized as an important component in the Arctic food web (e.g. Madsen et al. 2001), principally because sampling has often been conducted during the daytime, when *M. longa* is absent from the upper portion of the water column (Hays 1995, Falkenhaug et al. 1997, Daase et al. 2008). Recent studies show that *M. longa* is highly abundant during the productive season in the Godthåbsfjord (Arendt et al. 2010, 2012, Tang et al. 2011), where its high lipid content (Hopkins et al. 1984) makes this species a high quality prey item for planktivores (Pedersen & Fossheim 2008). *M. longa* is considered an omnivore, feeding selectively on protozooplankton and zooplankton in the size range 5 to 300 µm (Haq 1967), even when phytoplankton within this size range are available (Campbell et al. 2009).

We investigated seasonal plankton dynamics in a side branch of the Godthåbsfjord, Kapisigdlit Fjord, with emphasis on the role of protozooplankton in the food web, and the interaction between the protozooplankton and the copepod community. The latter was evaluated from maximum potential production and clearance rates given in Hansen et al. (1997) and Møller et al. (2006). Estimates of maximum potential clearance rates by *Metridia longa* were supported by a grazing experiment with *M. longa* feeding on a natural plankton assemblage.

MATERIALS AND METHODS

Locality and sampling

Sampling was conducted at Stn K4 (64° 25′ N, 50° 22′ W; Fig. 1) on 15 occasions from 24 March to 5 August 2010, in the Kapisigdlit Fjord branch of the inner part of the Godthåbsfjord system, West Greenland. All sampling was conducted while on board the RV 'Lille Masik', except 16 to 18 June, when sampling was conducted from the RV 'Dana' (National Institute for Aquatic Resources, Denmark).

Vertical profiles of water temperature, salinity and density were obtained from the surface to ca. 10 m above the bottom using a CTD profiler (SBE 19 plus or 911 plus, SeaCat, and a SBE 25 SM, MicroCat). The CTD profiles were calibrated against each other, and salinity samples (collected on 24 May and 6 July 2010), were analysed on a Portosal salinometer. Water samples were collected at 1, 10, 20, 50, 75, 100, 150 and 250 m depths using a 5 l Niskin bottle. Inorganic nutrient samples (dissolved phosphate, nitrate, nitrite, ammonium and silicate) were immediately frozen (–20°C) for later analysis on a Skalar autoanalyser following the procedures of Hansen & Koroleff (1999). The precision (analytical reproducibility) of the nutrient analyses was 0.06, 0.1, and 0.2 µM for phosphate, nitrate, and silicate, respectively. Water for chlorophyll *a* (chl *a*) was stored cold and dark in 10 l containers until it was processed. On most occasions, the samples were filtered on board immediately after sampling. However on 3 occasions, samples were brought to the laboratory and filtered the following morning (i.e. after 12 h). Since the chl *a*

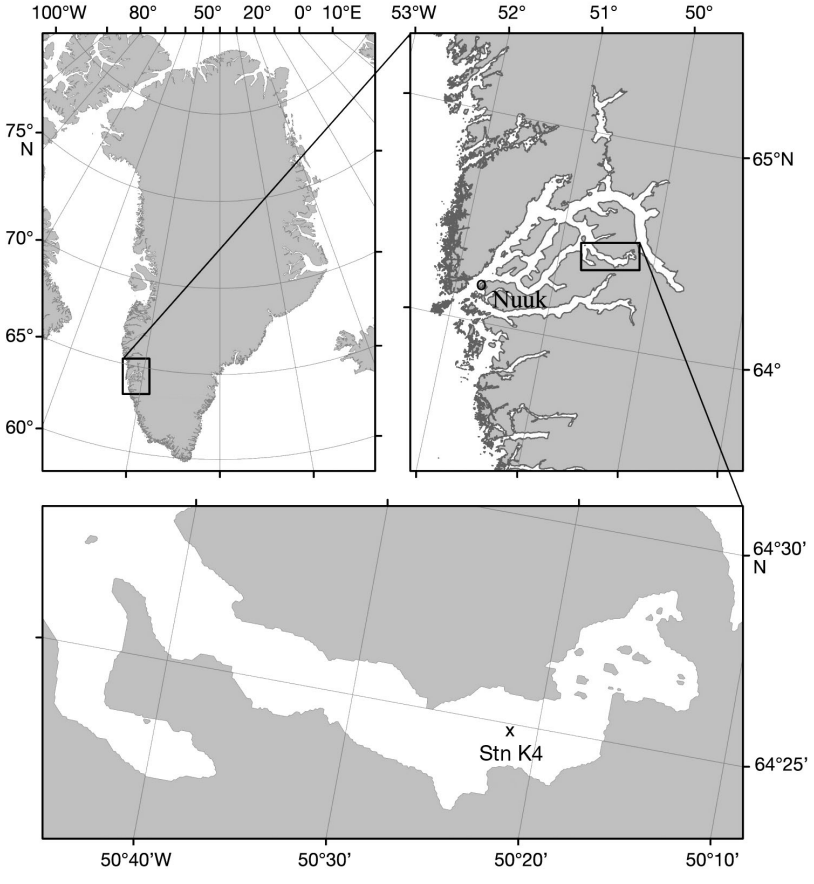

Fig. 1. Study area in West Greenland showing the location of the sampling station

concentration was relatively stable between sampling events (i.e. the average chl *a* concentration in the upper 10 m across all samplings was 0.9 ± 0.3 mg l^{-1}), we assume that this storage did not impact the chl *a* concentration.

Phytoplankton

Chl *a* concentration was determined from triplicate subsamples of 100 to 500 ml seawater, and size fractionated on Whatman GF/F filters (0.7 µm pore size, total phytoplankton biomass) and 10 µm mesh filters (from 1, 10, 20, 50 and 100 m depths). Filters were extracted in 96% ethanol for 12 to 24 h (Jespersen & Christoffersen 1987), and then either analyzed immediately or stored at −20°C for a maximum of 2 mo. Chl *a* was measured on a TD-700 Turner fluorometer calibrated against a chl *a* standard before and after acidification (Yentsch & Menzel 1963) and converted into µg C using a conversion factor of 42.7 (Juul-Pedersen et al. 2006).

Primary production was measured on 6 occasions using the ^{14}C incubation method (Steemann-Nielsen 1958) with a free-drifting array. Water samples from 5, 10, 20, 30 and 40 m depths were incubated at *in situ* depths for ca. 4 h during the day in 100 ml Winkler glass bottles (1 dark and 2 light bottles at each depth); following incubation, 200 µl $NaH^{14}CO_3$ (20 µCi ml^{-1}; DHI Denmark) was added to each of the bottles. After recovery, the samples were kept completely dark until filtration on Whatman GF/C filters. The filters were then treated with 100 µl 1M HCl, and left to fumigate for ca. 12 h to remove any remaining ^{14}C on the filter. Scintillation liquid (PerkinElmer Ultima Gold) was added and the sample was mixed and left for ca. 24 h before analyses on a TriCarb 2800 TR liquid scintillation analyzer (PerkinElmer). *In situ* dissolved inorganic carbon (DIC) concentrations, measured with a CM5012 CO2 Coulometer according to Rysgaard & Glud (2004), were applied for the calculation of primary production using the specific activity of each ^{14}C batch (DHI Denmark). The dark bottle value from each depth was subtracted from the light bottle value in order to correct for uptake of ^{14}C in the dark. *In situ* incoming irradiance, as photosynthetically active radiation (PAR; supplied by ASIAQ) during the deployment versus the entire day, was used to calculate the daily primary production. Primary production was integrated vertically from 0 to 45 m, covering the euphotic zone. The influence of the different filter types used, i.e. chl *a* (GF/F) and primary production (GF/C), has previously been examined in the Godthåbsfjord, and no significant difference was detected between these filter types (T. Juul-Pedersen unpubl. data).

Protozooplankton

Biomass, abundance and taxonomic composition of protozooplankton were determined at 5 depths: 1, 10, 20, 50/60 and 100 m. Water samples of 250 to 300 ml were collected with a 5 l Niskin bottle at each depth, gently decanted through a silicon tube into brown glass bottles and fixed in acidic Lugol's solution (final concentration of 2%). Samples were kept cool and dark until analyses (max. of 6 mo). Depending on the cell concentration, 50 to 100 ml subsamples were allowed to settle for 24 h in sedimentation chambers. All (or a minimum of 300) cells were counted using an inverted microscope (Nikon K18). Protozooplankton depth profiles were determined 9 times during the investigated period.

Protozooplankton were identified to genus level when possible. Ciliates were categorized as heterotrophic/mixotrophic. The dinoflagellates were dominated by the large heterotrophic *Gyrodinium spirale* (mean = 46% of the dinoflagellate biomass; range = 0 to 98%) and the small heterotrophic *G. glaucum* (mean = 22% of the dinoflagellate biomass; range = 8 to 78%). In general, all dinoflagellates >10 µm were classified as heterotrophic/mixotrophic (Hansen 2011). Cell volumes were calculated using appropriate geometric shapes without including the membranelles. To compensate for cell shrinkage due to Lugol's solution preservation, cell volumes were increased by a factor of 1.3 (Stoecker et al. 1994). The bio-volumes (V) were converted to carbon (pg C) using the volume-to-carbon conversion factors given in Table 1.

Table 1. Volume (V) to carbon (pg C $cell^{-1}$) conversion factors used for heterotrophic protists

	Conversion factor	Source
Aloricate ciliates	$\log(\text{pg C cell}^{-1}) = -0.639 + 0.984 \log(V)$	Putt & Stoecker (1989), modified by Menden-Deuer & Lessard (2000)
Loricate ciliates	$\log(\text{pg C cell}^{-1}) = -0.168 + 0.841 \log(V)$	Verity & Langdon (1984), Menden-Deuer & Lessard (2000)
Dinoflagellates	$\log(\text{pg C cell}^{-1}) = -0.353 + 0.864 \log(V)$	Menden-Deuer & Lessard (2000)

Identification of ciliates and dinoflagellates to species, genus or morphotypes was based on Nielsen & Hansen (1999). During enumeration, ciliates and dinoflagellates were identified to lowest taxonomic level possible and divided into size classes covering 10 µm ranges of equatorial spherical diameter (ESD) starting with 10 to 20 µm. ESD and cell volume are related by: cell volume = $\pi/6 \times \mathrm{ESD}^3$.

Rates of protozooplankton maximum potential clearance rates were calculated according to the equation in Hansen et al. (1997) for ciliates:

$$\log(C_{\max}) = 1.491 - 0.23\log(P_{\mathrm{vol}}) \quad (1)$$

and for heterotrophic dinoflagellates:

$$\log(C_{\max}) = 0.851 - 0.23\log(P_{\mathrm{vol}}) \quad (2)$$

where $C_{\max}$ is the maximum potential clearance rate, and P_{vol} is the cell volume in µm^3. $C_{\max}$ was normalized to *in situ* temperatures (ranging between 0.5 and 13°C) by using a Q_{10} factor of 2.8 (reviewed in Hansen et al. 1997). Maximum potential ingestion rate, I (µg C cell^{-1} d^{-1}) was calculated from size-specific maximum potential clearance rates and the *in situ* chl *a* concentration:

$$I = C_{\max} \times d \quad (3)$$

where d (µg C l^{-1}) is the phytoplankton density. Ciliates were assumed to graze on the chl *a* fraction <10 µm, while heterotrophic dinoflagellates were assumed to graze on the chl *a* fraction >10 µm (Jakobsen & Hansen 1997). Production (µg C l^{-1} d^{-1} or g C m^{-2} d^{-1}) of ciliates and dinoflagellates was estimated from I using an average gross growth efficiency of 0.33 (Hansen et al. 1997, 2000).

Copepod biomass

Copepods were collected in 5 depth strata (0 to 50, 50 to 100, 100 to 150, 150 to 200, and 200 to 235 m) with a Multinet (50 µm mesh, Hydrobios type mini). The nets were hauled at a speed of 0.2 to 0.3 m s^{-1}, and samples were immediately preserved in buffered formalin (4% final concentration). Sampling was conducted around 18:00 h local time. Samples containing high numbers of copepods were split by volumes into subsamples. In each sample and subsample, all nauplii and copepodite stages were identified to species or genus level, and length was measured for up to 10 individuals of each stage. Biomass of the different copepod species was calculated based on measurements of prosome length, and length/carbon relationships from the literature (Table 2).

Metridia longa grazing experiment

Seawater was collected on 28 July 2010 from 20 m depth with a 30 l Niskin bottle and transferred gently via a silicon tube into a 25 l dark carboy. The carboy was stirred gently, nutrients were added (15 µM

Table 2. Length (L) to carbon (mg C) conversion factors used for copepod nauplii (N1–N6) and copepodites (C1–C6)

Taxon	a	b	Source	Stage	Units (L)
Acartia spp.[a]	1.11×10^{-11}	2.92	Berggreen et al. (1988)	C1–C6	µm
Calanus finmarchicu[a]	4.8×10^{-3}	3.5687	Madsen et al. (2001)	C1–C6	mm
Calanus glacialis[a]	4.8×10^{-3}	3.5687	Madsen et al. (2001)	C1–C6	mm
Calanus hyperboreus[a]	1.4×10^{-3}	3.3899	Hirche & Mumm (1992)	C1–C6	mm
Centropages spp.[b]	1.78×10^{-2}	2.45	Klein Breteler et al. (1982)	C1–C6	mm
Centropages spp.[b]	1.45×10^{-2}	2.24	Klein Breteler et al. (1982)	N1–N6	mm
Metridia spp.[a]	6.05×10^{-3}	3.0167	Hirche & Mumm (1992)	C1–C6	mm
Microcalanus spp.[a]	9.47×10^{-10}	2.16	Sabatini & Kiørboe (1994)	C1–C6	µm
Microsetella spp.[a]	2.65×10^{-9}	1.95	Uye et al. (2002)	N1–C6	µm
Oithona spp.[a]	9.47×10^{-10}	2.16	Sabatini & Kiørboe (1994)	C1–C6	µm
Oithona spp.[a]	5.545×10^{-11}	2.71	Sabatini & Kiørboe (1994)	N1–N6	µm
Oncaea spp.[a]	2.51×10^{-11}	2.9	Satapoomin (1999)	C1–C6	µm
Paraeuchaeta spp.[c]	3.1107	1.8633	K. Tönnesson unpubl. data	N1–C6	mm
Pseudocalanus spp.[a]	6.12×10^{-11}	2.7302	Klein Breteler et al. (1982)	C1–C6	µm
Calanus spp. and *Metridia* spp.[a]	4.29×10^{-9}	2.05	Hygum et al. (2000)	N1–N6	µm
Other nauplii[a]	3.18×10^{-12}	3.31	Berggreen et al. (1988)	N1–N6	µm

[a]Calculated from the following equation: $a \times L^b$
[b]Calculated from the following equation: $a \times L^b$, multiplied with 0.45 to convert into carbon
[c]Calculated ash free dry weight from the following equation: $10^{(a \times \mathrm{Log}(L) - b)}$, multiplied with 0.45 to convert into carbon

NH_4Cl and 1 µM Na_2HPO_4), and seawater was inverse filtered via a silicon tube through 200 µm mesh to remove mesozooplankton, and to fill 42 transparent 600 ml polycarbonate bottles.

Metridia longa were collected using a 200 µm WP2 net. One actively swimming adult female *M. longa* was added to each of the 28 polycarbonate bottles. Fourteen additional bottles without copepods were used as controls. To ensure that copepods cleared on average <30% of the prey, half of the experimental and control bottles were incubated for 12 h, and the other half for 24 h. Bottles were incubated in darkness at 5°C (*in situ* temperature was 3.2°C) and rotated by hand every 6 h. Dark incubation was chosen since *M. longa* undergo diel vertical migrations and feed during the night (Hays 1995). As soon as the experiment was terminated, triplicate subsamples of 100 ml were removed from the bottles for determination of chl *a* concentration. For protozooplankton analyses, 100 ml subsamples were fixed in acidic Lugol's solution in a final concentration of 2%.

Metridia longa clearance rates (ml µg C^{-1} d^{-1}) were calculated from Frost (1972) when prey growth rates differed significantly from the controls (*t*-test, $p < 0.05$). Clearance rate on protozooplankton was calculated for 4 size classes of ciliates, 1 size class of dinoflagellates and 2 size classes of nanoflagellates (Table 3). A minimum of 450 cells were measured for each size class. Clearance rate on phytoplankton was calculated using chl *a* as a proxy. Clearance rates were converted to *in situ* temperatures by using a Q_{10} factor of 2.8 (Hansen et al. 1997, 2000).

Copepod community grazing

Clearance capacity of the copepod community was estimated from maximum specific clearance rates, assuming that the copepod population was not food-saturated. Maximum specific clearance rate (F) of *Metridia longa* was estimated according to Hansen et al. (1997, 2000):

$$\log(F) \times 10^5 = \log(1.5753) - 0.23\log(V) \quad (4)$$

where V is the copepod body volume in µm^3. Since *M. longa* undertake pronounced diel vertical migration and only visit the surface at night, *M. longa* maximum potential clearance capacity is only realized in the upper 50 m for 6 h per day, i.e. around midnight (S. Kjellerup unpubl. data). Maximum potential clearance was converted to *in situ* temperatures in the upper 50 m of the water column using a Q_{10} factor of 2.8 (Hansen et al. 1997, 2000).

Table 3. Average equatorial spherical diameter (ESD; µm), range, standard deviation (SD) and number of cells (n) measured within the different size classes of the grazing experiment

	Average ESD (µm)	ESD range (µm)	SD (µm)	n
Ciliates	11.7	7–15	1.8	1975
	21.2	15–30	4.4	2375
	34.9	30–40	2.8	634
	50.3	40–60	5.7	917
Dinoflagellates	33.3	25–50	5.6	865
Nanoflagellates	3.5	3–4	0.4	455
	5.4	5–6	0.2	483

Protozooplankton

The maximum potential clearance rates of *Calanus* spp. and other copepods (i.e. *Pseudocalanus*, *Oithona*, *Centropages* and *Microcalanus*) were estimated according to Møller et al. (2006):

$$\log(F) = 1.16 - 0.45\log(W),\ r^2 = 0.73 \quad (5)$$

where W is the copepod biomass (µg C), assuming that they were distributed evenly throughout the water column. Maximum potential clearance rates were converted to *in situ* temperatures using a Q_{10} factor of 2.8 (Hansen et al. 1997, 2000). From March until breakup of ice in the Kapisigdlit River around 20 June 2010, Q_{10} was calculated in the 0 to 100 m depth stratum. Thereafter, *Calanus* spp. and other copepods were distributed below the warm and fresh surface water and thus Q_{10} was calculated in the 20 to 100 m depth stratum. The small copepods *Microsetella* spp. and *Triconia*/*Oncaea* spp. were not included in the grazing estimates since they both have morphologies and feeding strategies suited for solid substrata such as marine snow (Koski et al. 2007).

RESULTS

Hydrography

Sampling was initiated in March when the water column was well-mixed with cold, saline, nutrient-rich water throughout the euphotic zone (Fig. 2, Table 4). The chl *a* concentration was low (0.5 to 1 µg l^{-1}) and evenly distributed in the upper 40 m (Fig. 2C). In late April, a weak halocline was established (Fig. 2B) and additional heat was trapped in the surface layer (Fig. 2A). The stratification stimu-

lated phytoplankton growth, which then quickly depleted the nitrate to below 0.5 µM in association with the peak of the first phytoplankton bloom of 3 µg chl *a* l^{-1} (Fig. 2C).

In May, melt water was added to the surface layer as runoff from land, and culminated in the seasonal pulse of fresh water following the breakup of ice in the Kapisigdlit River around 20 June 2010. Thereafter, the surface salinity rapidly decreased from 31 to 16 by the beginning of August. The melt water established a strong halocline, strengthened by a thermocline due to warming of the freshwater surface plume to above 13°C on the last sampling day (5 August 2010). After the depletion of nitrate above the pycnocline, a subsurface bloom developed with a peak value of 12 µg chl *a* l^{-1} on 26 June 2010 (Fig. 2).

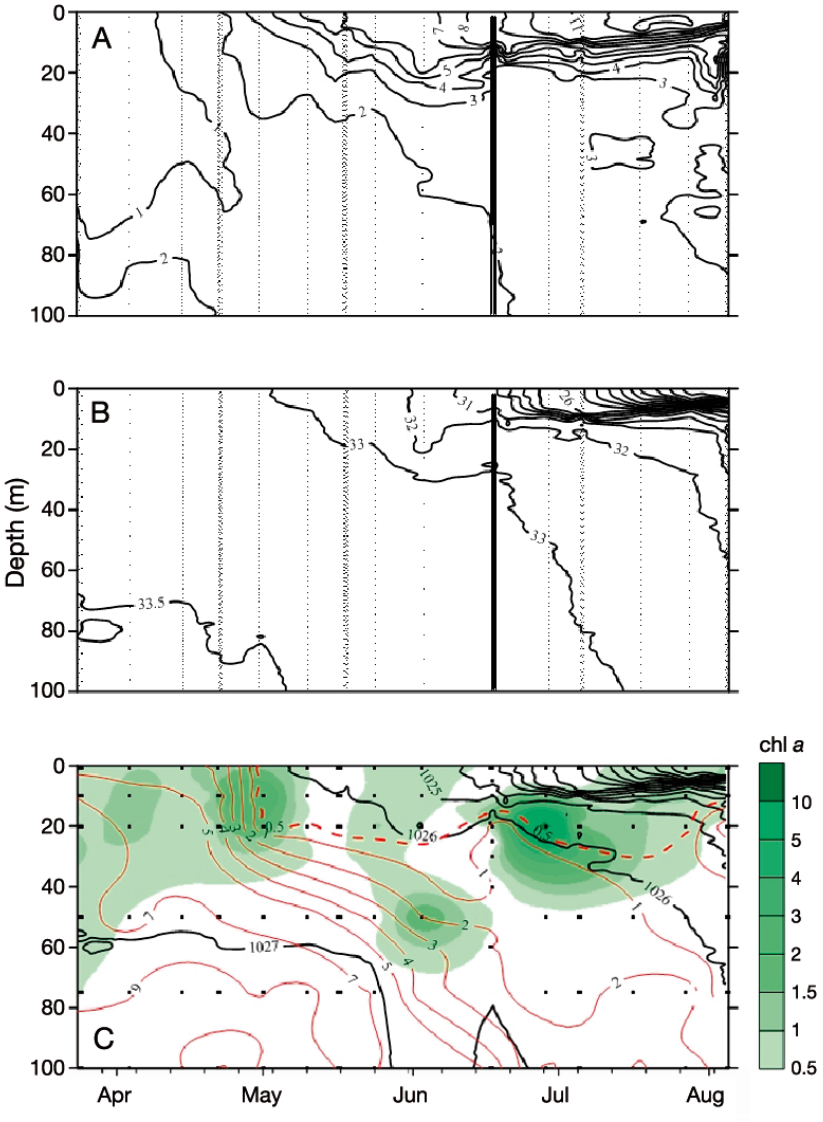

Fig. 2. Water column characteristics over the investigation period. (A) Temperature (°C), (B) salinity and (C) density (kg m^{-3}) overlaid with chl *a* concentrations (µg l^{-1}, green shading) and concentrations of the limiting nutrient, nitrate (µM), displayed as red isolines (detection limit 0.5 µM, red dashed line). Points represent sampling depths. The vertical black line indicates breakup of the ice in the fjord

Nutrients

High concentrations of nutrients (i.e. phosphorus, nitrate and silicate) were measured in the upper 100 m of the water column at the initiation of the investigation (data not shown). During the first part of the investigation, the average nitrate concentration in the upper 50 m stratum decreased from 6.8 ± 0.3 µM to 0.5 ± 0.3 µM as a result of increased stratification and the developing phytoplankton bloom (Fig. 2C). The overall phosphorus and silicate distributions (Table 4) and succession mirrored that illustrated by nitrate (Fig. 2C), but were not fully depleted in the euphotic zone. In association with the breakup of ice in the Kapisigdlit River, a

Table 4. Concentrations (µM) of nutrients (mean ± SE), in the freshwater plume (1 to 5 m depth) after the breakup of ice in the Kapisigdlit River (20 June), and in subsequent 50 m strata; n = number of samples, BD = below detection level

Strata (n)	NO_3	SiO	PO_4	NO_2	NH_3
Plume (20)	BD	5.09 ± 0.36	0.038 ± 0.003	BD	0.20 ± 0.002
0–50 m (47)	1.70 ± 0.05	2.07 ± 0.03	0.22 ± 0.01	0.03 ± 0.001	1.12 ± 0.02
50–100 m (30)	4.67 ± 0.10	3.15 ± 0.07	0.47 ± 0.01	0.129 ± 0.003	1.28 ± 0.03
100–150 m (16)	5.92± 1.50	5.92 ± 0.99	0.56 ± 0.08	0.18 ± 0.08	1.36 ± 0.50
150–200 m (17)	7.21 ± 1.25	4.43 ± 0.98	0.65 ± 0.08	0.24 ± 0.05	2.02 ± 1.16
>200 m (18)	11.47 ± 1.23	7.31 ± 0.58	0.94 ± 0.14	0.05 ± 0.03	0.68 ± 0.39

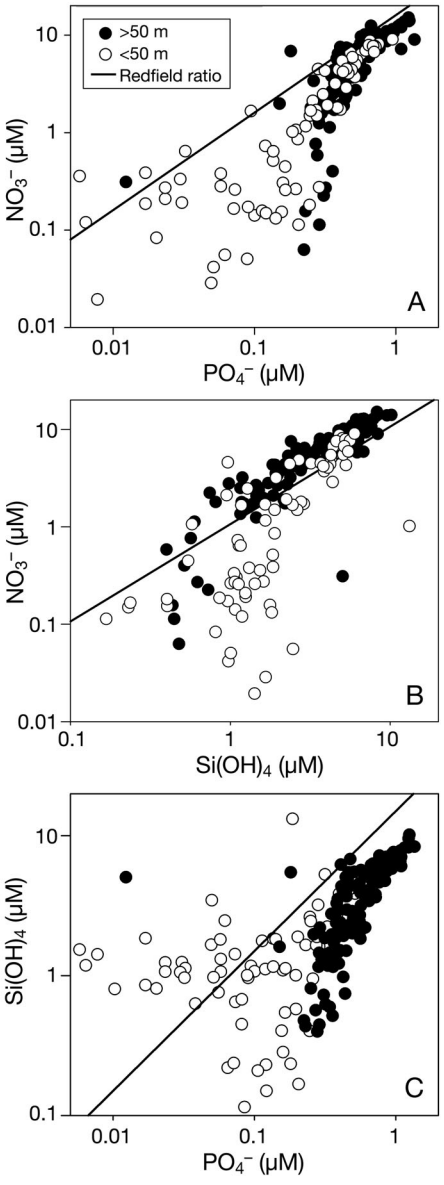

Fig. 3. Relationship between (A) phosphorus and nitrate, (B) silicate and nitrate and (C) phosphorus and silicate. ● = samples taken below the euphotic zone (i.e. deeper than 50 m); ○ = surface samples taken above 50 m. Data from the freshwater plume after the breakup of ice in the river is not included, but shown in Table 4. Lines indicate the Redfield-Brzezinski ratios of the nutrients

freshwater plume overlaid the fjord water, characterized by a very high concentration of silicate (Table 4).

Comparisons of the major nutrient types (Fig. 3A–C) suggest nitrate limitation of the primary producers, since nitrate concentration in the upper 50 m became depleted relative to the Redfield-Brzezinski nutrient ratios with respect to phosphorus (Fig. 3A) and silicate (Fig. 3B).

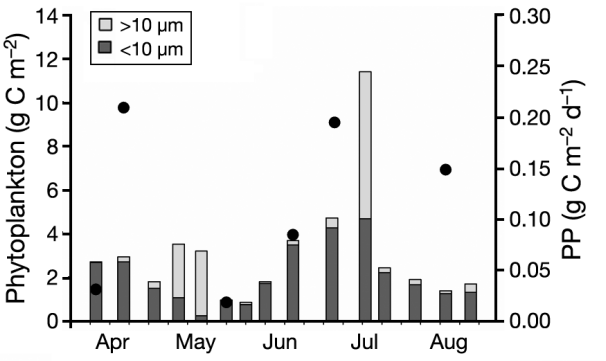

Fig. 4. Seasonal succession in phytoplankton. Bars = integrated biomass, phytoplankton (g C m^{-2}); ● = integrated primary production, PP (g C m^{-2} d^{-1}). Integration depth: 250 m for phytoplankton and 45 m for PP

Phytoplankton

The integrated phytoplankton biomass averaged 3.0 ± 2.4 g C m^{-2} over the study period with peak values of 3.5 and 11.4 g C m^{-2} during the spring and summer blooms, respectively (Fig. 4). The phytoplankton spring bloom was initially composed of small phytoplankton cells (<10 µm), which progressed into a phase dominated by larger cells (>10 µm). Within a few weeks, nitrate was depleted in the euphotic zone, and the total phytoplankton biomass and relative proportion of large phytoplankton cells decreased. As the ice in the Kapisigdlit River broke up in mid-June, a freshwater plume resulted in a temporary upwelling of nutrients into the euphotic zone (Fig. 2), causing a summer bloom to form and the relative proportion of large cells to increase. Nutrients once again became depleted in the stratified water column and the relative proportion of small cells increased (Fig. 4).

Average integrated primary production (PP) for the investigated period was 0.11 g C m^{-2} d^{-1} (n = 6) with a maximum of 0.21 g C m^{-2} d^{-1} in early spring (Fig. 4). The phytoplankton community was dominated by chain-forming diatoms (mainly *Thalassiosira* spp.) during the 2 blooms. In the non-bloom periods, the phytoplankton biomass was mostly composed of small (<10 µm) unidentified flagellates, primarily cryptophytes and solitary haptophytes (probably *Phaeocystis*).

Protozooplankton

At the onset of the investigation, the abundance of protozooplankton was low (<10^3 cells l^{-1}), but throughout June and July a diverse protozooplankton community developed in the upper 50 m, with cell concentrations as high as 3 × 10^4 cells l^{-1}

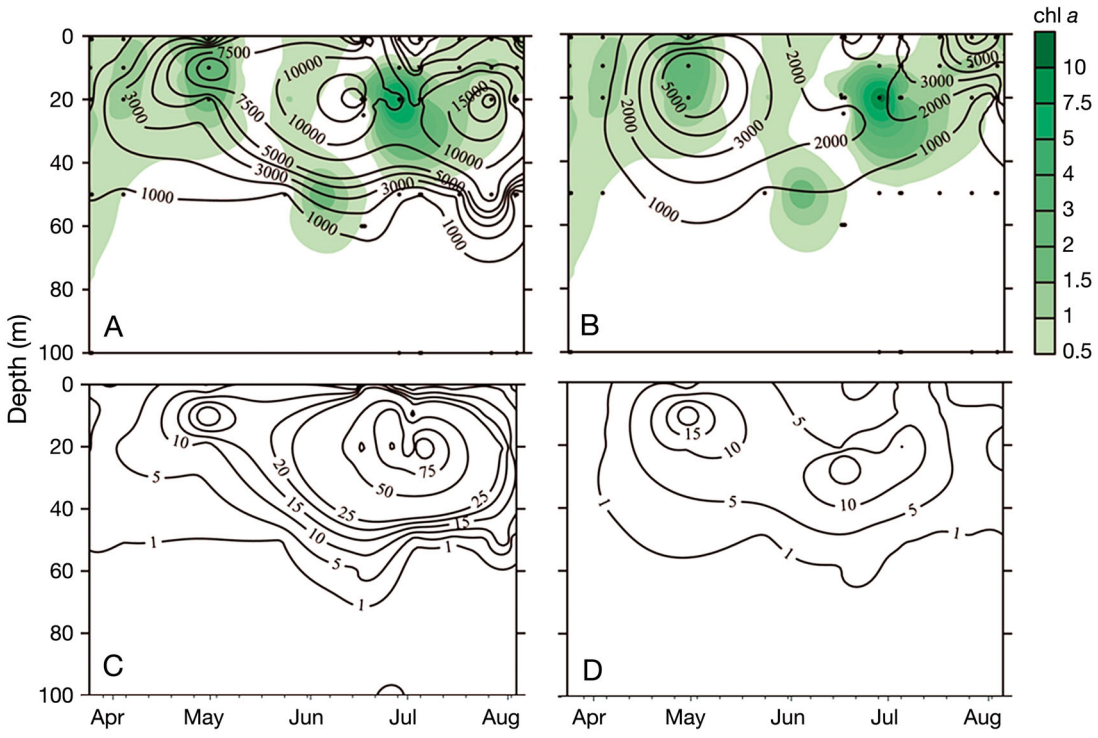

Fig. 5. Seasonal development in the abundance (cells l^{-1}) of (A) ciliates and (B) heterotrophic dinoflagellates superimposed on the chl *a* concentration (green shading, µg l^{-1}) and (C,D) seasonal succession in the biomass (µg C l^{-1}) of (C) ciliates and (D) heterotrophic dinoflagellates. Points represent sampling depths

(Fig. 5A,B). Ciliates dominated the protozooplankton community (Fig. 5A), while dinoflagellates were less abundant (Fig. 5B). The protozooplankton biomass mirrored the phytoplankton biomass with maximum biomass associated with the chl *a* maximum at a depth of 19 ± 3 m (mean ± SD). Protozooplankton biomass peaked on July 6 at 155 µg C l^{-1} (Fig. 5C,D).

The main contributors to the protozooplankton biomass were *Strombidium* spp. and *Gyrodinium spirale* during spring, while *Mesodinium* spp., *Strobilidium* spp., *Strombidium* spp., *Laboea strobila* and *G. spirale* dominated during the summer (Fig. 6). Numerically, small (<20 µm) ciliates dominated the protozooplankton community (Fig. 6).

The integrated biomass of protozooplankton ranged between 0.1 and 4.0 g C m^{-2} (Figs. 7A,B & 8A). Initially, and by the termination of the investigated period, the protozooplankton community was composed of small ciliates and dinoflagellates. However, during the bloom period, the relative amount of large cells increased. Thus, in June, 45 to 98% of the integrated protozooplankton biomass was composed of large (>40 µm) specimens (mainly ciliates; Fig. 7A).

The estimated protozooplankton production ranged between 0.01 and 0.42 g C m^{-2} d^{-1} (Fig. 7C,D). For ciliates, the seasonal variation mirrored the integrated biomass, with small ciliates being the most productive during spring and large ciliates being most productive during the summer (Fig. 7C).

Assuming that ciliates only feed on phytoplankton <10 µm, and dinoflagellates only feed on phytoplankton >10 µm (Hansen et al. 1994), the protozooplankton maximum potential ingestion rates ranged between 0.01 and 1.2 g C m^{-2} d^{-1}, corresponding to 26 to 196% of the primary production d^{-1} (data not shown) or 0.5 to 50% of phytoplankton biomass d^{-1} (Fig. 7E,F). The highest maximum potential ingestion rates were achieved in the summer after the disappearance of the copepod *Metridia longa*.

Copepod succession

The copepod community was dominated by the genera *Calanus, Pseudocalanus, Oithona, Microsetella* and *Triconia/Oncaea. Metridia longa* accounted for 72 to 93% of the copepod biomass in the spring. The integrated biomass of copepods showed a maximum of 24 g C m^{-2} in early March (Fig. 8B), but decreased after 3 June when the community changed towards dominance by smaller species such as *Pseudocalanus* spp., *Microsetella norvegica* and *Oithona similis*. The copepod biomass remained low (<6 g C m^{-2}) throughout the rest of the study period.

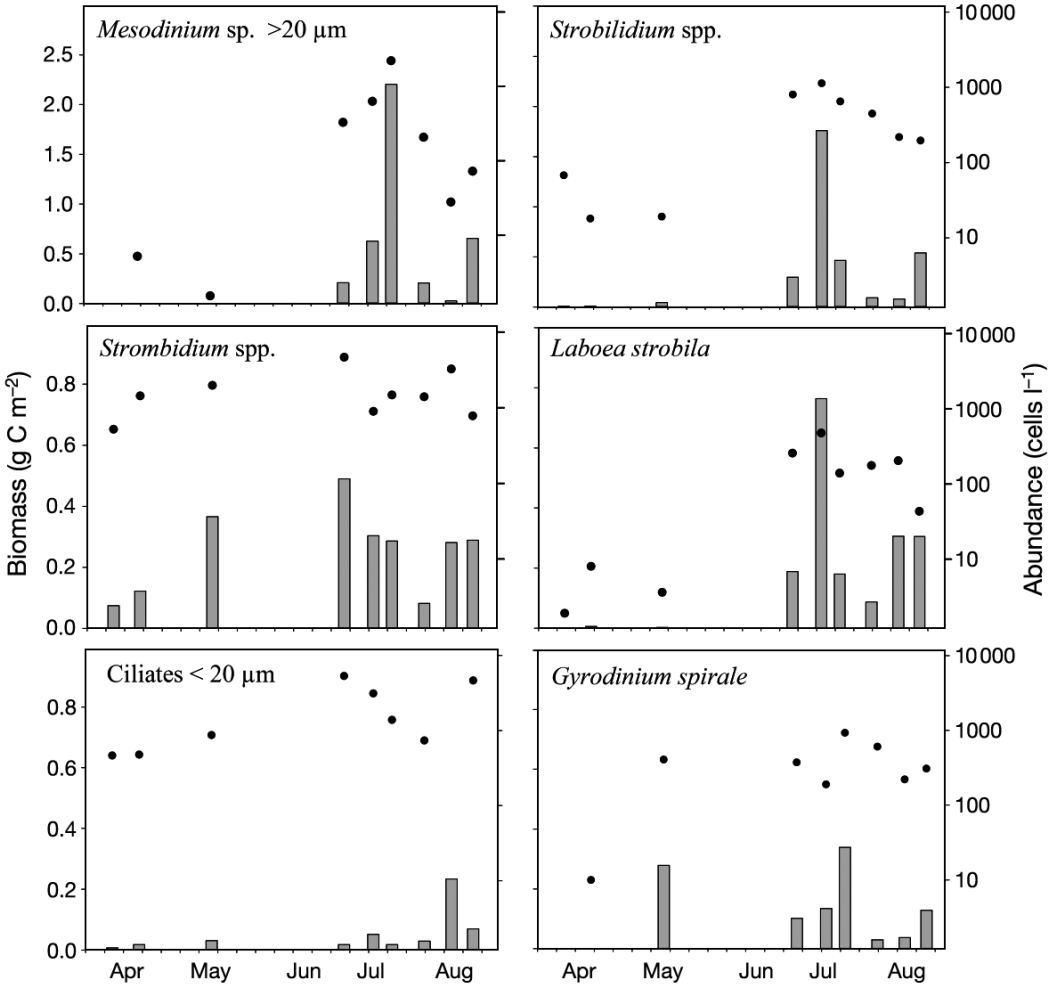

Fig. 6. Seasonal development in selected protozooplankton specimens. Bars = integrated biomass (g C m^{-2}); ● = abundance (cells l^{-1}). Integration depth: 100 m. Note different *y*-axis scales

A pairwise correlation between the integrated protozooplankton biomass and the grazing part of the copepod biomass (i.e. *Acartia* spp., *Calanus* spp., *Metridia longa*, *Microcalanus* spp., *Oithona* spp. and *Pseudocalanus* spp.) revealed a significant relationship between the 2 zooplankton groups, with protozooplankton biomass being inversely proportional to copepod biomass ($r^2 = 0.89$, $p < 0.01$; Fig. 9). A similar trend was found between chl *a* and copepod biomass ($r^2 = 0.22$, $p = 0.08$; Fig. 9). No significant correlation was found between protozooplankton biomass and chl *a*.

Grazing impact by *Metridia longa*

The *Metridia longa* grazing experiment was initiated with a phytoplankton biomass of 22 µg C l^{-1}. Phytoplankton cells in the small size fraction (0.7 to 10 µm) contributed 95% of the total phytoplankton biomass. *M. longa* clearance rate on the large chl *a* fraction (>10 µm) was estimated at 2.1 ± 0.5 ml µg C^{-1} d^{-1} (mean ± SE, n = 23), while there was negative clearance (−1.5 ± 0.6 ml µg C^{-1} d^{-1}, mean ± SE, n = 23) on the small chl *a* fraction (<10 µm). The lower threshold of clearance was corroborated from the Lugol's sample counts, where no significant clearance was found on particles in the size range 3 to 6 µm (Fig. 10; *t*-test, $p > 0.05$). We cannot conclude whether *M. longa* in fact consumed these small sized prey items or if the non-significant clearance rates on small sized particles are due to a bottle-generated cascade effect caused by removal of protozooplankton in the experimental bottles. This condition may have caused a significant underestimation of the grazing rates (Nejstgaard et al. 1997, 2001). On a global average, copepod grazing on phytoplankton is underestimated by 20 to 30% in this kind of grazing

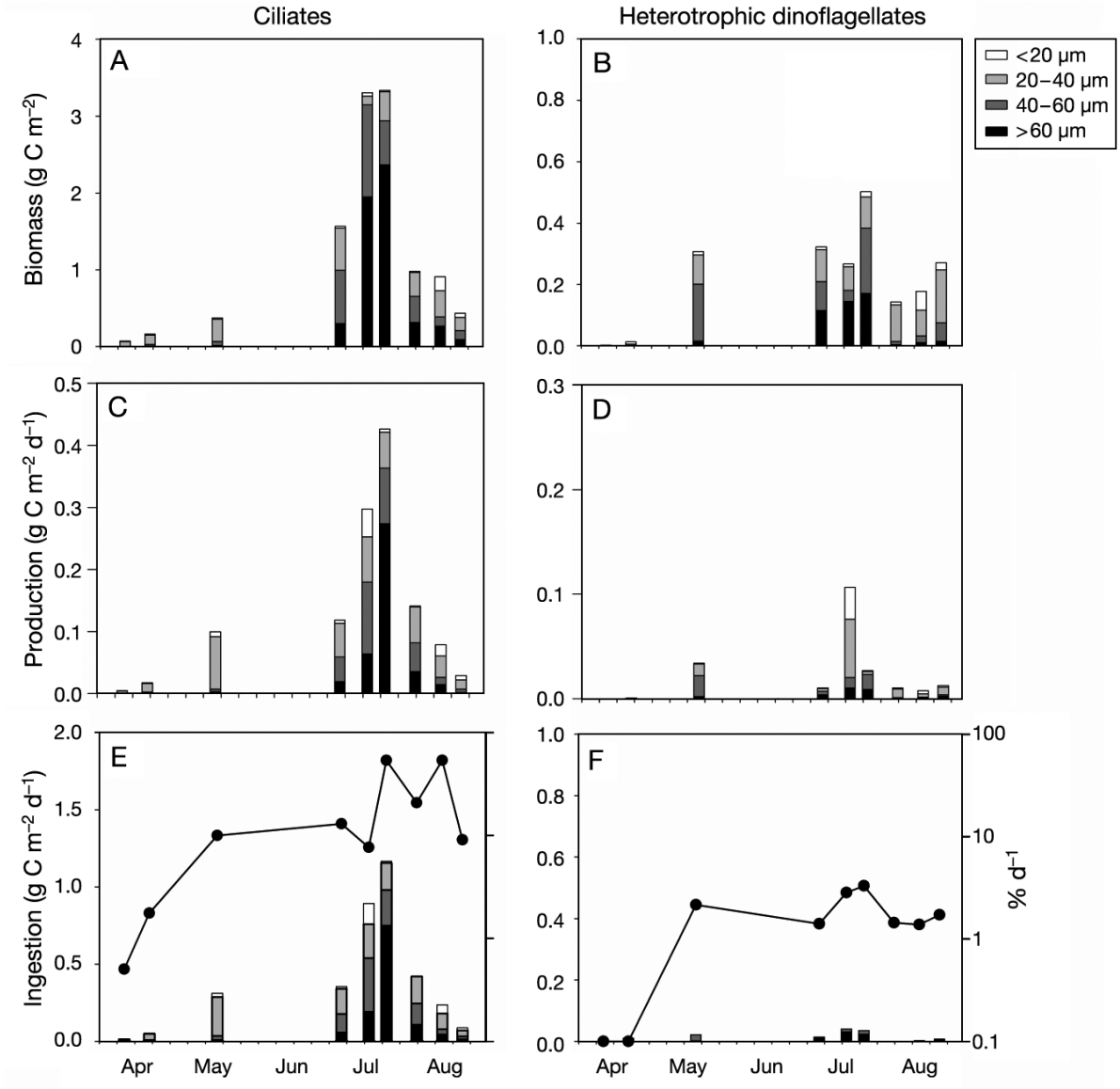

Fig. 7. (A,B) Integrated biomass (g C m^{-2}), (C,D) estimated production (g C m^{-2} d^{-1}) calculated from (E,F) estimated maximal potential ingestion rates (g C m^{-2} d^{-1}) of ciliates and heterotrophic dinoflagellates. The color codes represent the fraction of each protozooplankton size class. Size is given in equatorial spherical diameter (ESD). (E,F) ● = phytoplankton biomass ingested per day (% d^{-1}). Integration depth: 100 m. Note different *y*-axis scales

experiment (Saiz & Calbet 2011). The protozooplankton concentration in the experimental bottles was $21 \pm 5 \times 10^3$ l^{-1}, corresponding to an average biomass of 14 ± 2 µg C l^{-1}. The protozooplankton community was dominated by *Mesodinium* spp., *Strombidium* spp., *Gyrodinium spirale*, *Laboea strobila* and *Strobilidium oviformis*. *M. longa* cleared cells in the size range of 10 to 60 µm, with an average clearance rate of 2.4 ± 0.2 ml µg C^{-1} d^{-1} (mean ± SE, n = 26) (Fig. 10A). While clearance rate was positively correlated to prey size ($r^2 = 0.90$, $p = 0.06$), no clear relationship was found between biomass of the prey size classes and the clearance rate (Fig. 10B).

Copepod community grazing

The maximum potential grazing rates of the copepod community was highest from March to late May, when the copepod community cleared 16 ± 7 % of the water column per day. *Metridia longa* alone accounted for >90 % of the maximum potential copepod community clearance (Fig. 11A).

As the *Metridia longa* population disappeared from the water column, the maximum potential clearance capacity was reduced, and remained low (7 ± 2 % water column d^{-1}) throughout the summer period (Fig. 11A). Generally, our maximum poten-

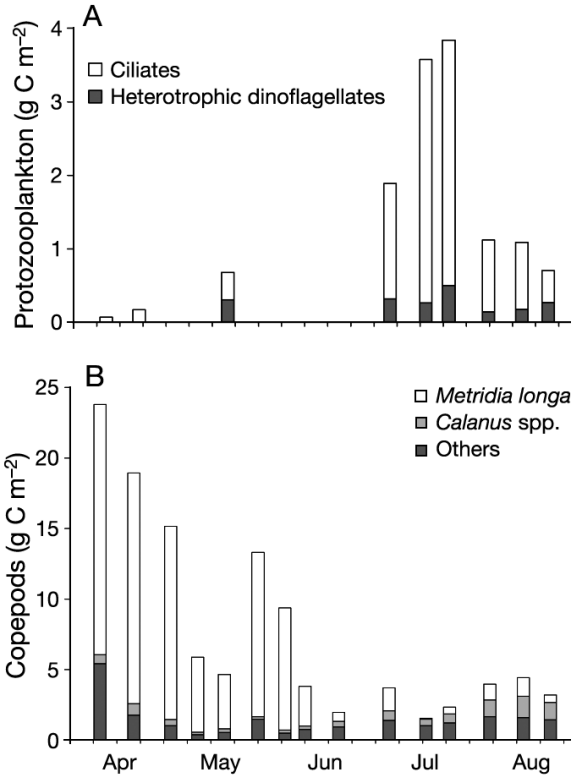

Fig. 8. (A) Integrated protozooplankton biomass (g C m^{-2}), (B) integrated copepod biomass (g C m^{-2}). Integration depth: 100 m for protozooplankton and 250 m for copepod biomass

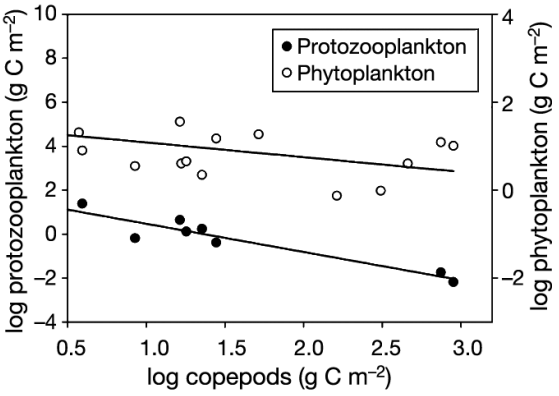

Fig. 9. Relationship between integrated copepod biomass and integrated phytoplankton and protozooplankton biomass. White dots indicate regression between copepods and phytoplankton (r^2 = 0.22, p = 0.08). Black dots indicate regression between copepods and protozooplankton (r^2 = 0.89, p < 0.01)

tial grazing estimates suggest that *M. longa* was able to control the protozooplankton community during spring, grazing >100% of the protozooplankton production every day (Fig. 11B). From June to August, the predation pressure declined and there was an intense buildup of protozooplankton biomass in response to the reduction in *M. longa* grazing pressure.

DISCUSSION

Hydrography and plankton characteristics

Fjords are important environments of the coastal zone of Greenland. They are the first components of the marine regime to be impacted by increased melt water from land, and are therefore suitable proxies to determine how open marine environments may respond in a warmer future. In this sense, the freshwater-impacted Kapisigdlit Fjord branch represents an ideal test site to develop an understanding of the potential impact of increased freshwater input and water-column stratification on the pelagic community.

The Kapisigdlit Fjord is a seasonally oligotrophic, stratified subarctic ecosystem controlled by nitrate during the productive season. The fjord shows strong seasonality in chl *a* concentrations, but is character-

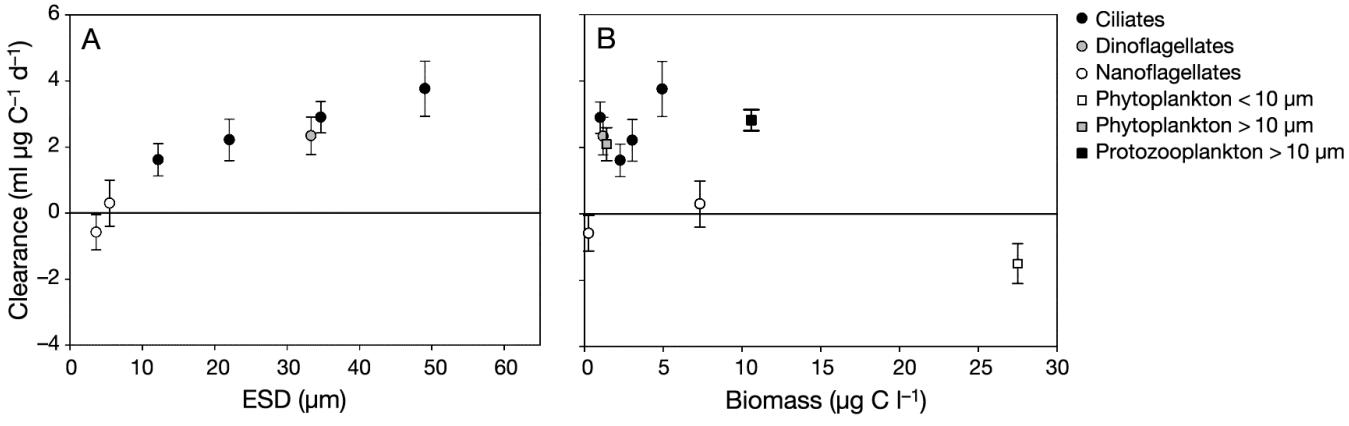

Fig. 10. *Metridia longa.* Specific clearance rate (ml µg C^{-1} d^{-1}) at 3°C of different (A) size classes and (B) biomass classes of ciliates, dinoflagellates, nanoflagellates and phytoplankton. ESD: equatorial spherical diameter. Error bars indicate mean ± SE (n = 23)

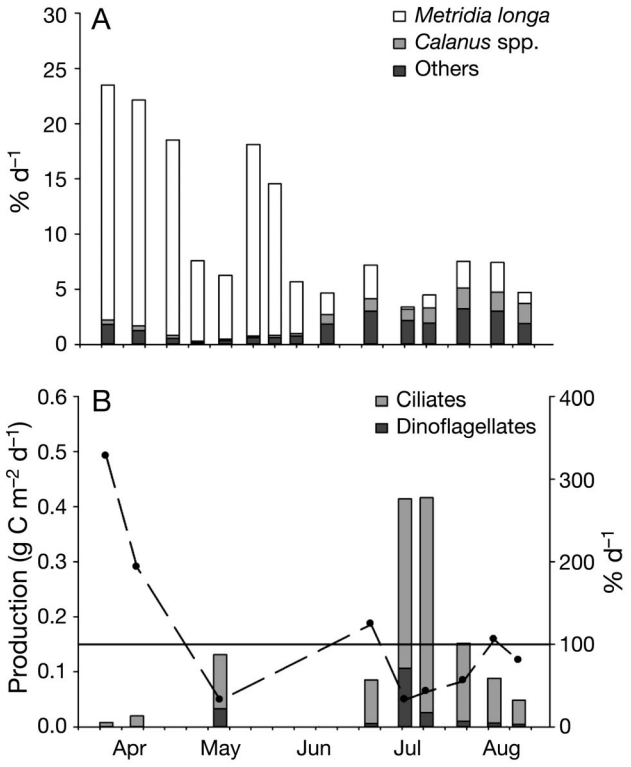

Fig. 11. Seasonal development in copepod grazing impact. (A) Water column cleared for cells in the size range 10 to 60 µm by the copepod community (% d^{-1}); (B) bars = integrated protozooplankton production (g C m^{-2} d^{-1}) and ● = fraction of protozooplankton production cleared by the copepod community (% d^{-1}). 'Others' represent copepods dominated by *Pseudocalanus* spp., *Oithona* spp., *Centropages* spp. and *Microcalanus* spp.

ized by lower concentrations than reported from other subarctic and Arctic regions, where the surface chl *a* generally exceeds 1.5 µg l^{-1} during the productive season (Pabi et al. 2008). The freshwater runoff in the Kapisigdlit Fjord creates a more stratified water column—which prevents mixing of nutrients upward into the euphotic zone, as shown by the low chl *a* concentrations, the low primary production rates and the high proportions of nanophytoplankton and protozooplankton.

Few attempts have been made to investigate the role of protozooplankton in subarctic and Arctic ecosystems, and most studies have focused on the high-productive regions dominated by diatoms and *Calanus* spp. (Verity et al. 2002, Sherr & Sherr 2007, Seuthe et al. 2011). This research documented that subarctic fjords may support rich and diverse protozooplankton communities, and that their abundances are comparable to levels found in temperate waters (Sherr & Sherr 2007, Saiz & Calbet 2011).

Compared to existing data from subarctic and Arctic regions, the protozooplankton biomass in the Godthåbsfjord (including Kapisigdlit Fjord) is remarkably high (Poulsen & Reuss 2002, Arendt et al. 2010, this study). Maximum integrated protozooplankton biomasses in coastal Arctic and subarctic waters such as Kongsfjorden (Svalbard), Disko Bay (West Greenland), Young Sound (Northeast Greenland), Fyllas Banke (off West Greenland), the Barents Sea and the subarctic Pacific Ocean have been reported in the range 0.2 to 1.7 g C m^{-2} (Strom et al. 1993, Rysgaard et al. 1999, Levinsen et al. 2000, Rat'kova & Wassmann 2002, Seuthe et al. 2011). In comparison, the maximum integrated protozooplankton biomass in the Kapisigdlit Fjord was 4.0 g C m^{-2}.

In contrast to studies at Fyllas Banke, Kongsfjorden, Disko Bay and Young Sound, where dinoflagellates dominated the protozooplankton community (Levinsen & Nielsen 2002, Poulsen & Reuss 2002, Sherr et al. 2009, Seuthe et al. 2011), ciliates contributed 82% of the total protozooplankton biomass in our study. A similar community structure has been observed in the Barents Sea (Rat'kova & Wassmann 2002) and in the subarctic Pacific Ocean (Strom et al. 1993). The difference in the relative composition of the protozooplankton community can be explained by the different feeding strategies of ciliates and dinoflagellates. While ciliates generally prefer small particles (~2 to 10 µm), heterotrophic dinoflagellates feed on diatoms and other large particles (>10 µm) (Hansen et al. 1994). The Kapisigdlit Fjord represents a seasonally stratified and oligotrophic ecosystem supporting a phytoplankton community of small flagellates, and accordingly, ciliates as the dominant protozooplankton grazers. Ciliates feeding on nanoflagellates could not be distinguished from potential predatory ciliates feeding on other ciliates and dinoflagellates. However, predatory ciliates such as *Didinium* spp. or *Favella ehrenbergii* (Berger 1980, Stoecker et al. 1981) were rare in the samples, and thus predatory ciliates were not considered important for the trophic role of the protozooplankton community.

The estimated maximum potential grazing impact of protozooplankton on phytoplankton was highly variable, but generally exceeded 100% of the primary production during the summer months. This high grazing impact of protozooplankton is consistent with data from Calbet et al. (2011) who, based on dilution experiments, estimated grazing rates corresponding to 128% of the primary production consumed per day in June. In comparison, grazing rates estimated from dilution experiments in other regions of Arctic seas have been in the range of 26 to 77% of the primary production per day (Verity et al. 2002, Sherr et al. 2009). Although the maximum potential

grazing impact may be slightly overestimated due to inclusion of mixotrophic species such as *Mesodinium rubrum, Laboea strobila* and *Strombidium cornicum*, the results emphasize the need to consider protozooplankton as key grazers in high latitude ecosystems.

Protozooplankton as prey for copepods

It is well documented that *Calanus* can exploit protozooplankton (Ohman & Runge 1994, Levinsen et al. 2000, Turner et al. 2001). Knowledge of *Metridia* feeding biology indicates this species consumes diatoms, nauplii and copepod eggs (Haq 1967, Sell et al. 2001, Campbell et al. 2009, Kjellerup & Kiørboe 2012). In contrast to typical suspension-feeding copepods (e.g. *Calanus*) which generate a feeding current to capture prey, *Metridia longa* feeds by cruising through the water, capturing prey by remote detection (Kjellerup & Kiørboe 2012). The cruising behavior of *Metridia* may be an advantage in environments in which prey concentrations are low, or when the prey tries to escape the feeding current (e.g. ciliates such as *Mesodinium rubrum;* Jonsson & Tiselius 1990, Fenchel & Hansen 2006). Haq (1967) demonstrated that *M. longa* was able to capture prey in the size range 5 to 300 µm, with clearance rates in the range of 3 to 7 ml ind.$^{-1}$ d^{-1}. Our study indicates that particles <60 µm are efficiently consumed by adult *M. longa* females, but in comparison to Haq (1967), the average clearance rate was higher: 222 ± 36 ml ind.$^{-1}$ d^{-1} (mean ± SE, n = 26) for protozooplankton in the size range 10 to 60 µm. The estimated grazing rates obtained from the grazing experiment are close to maximum potential clearance rates estimated from empirical relations in Hansen et al. (1997, 2000) and Møller et al. (2006) (Fig. 12). The low clearance rates presented in Haq (1967) could be explained by the limited variability in offered prey, since *M. longa* was only exposed to phytoplankton cells, small flagellates and *Artemia* nauplii. Our data suggest that *M. longa* has a high affinity for protozooplankton prey. Similarly, Haq (1967) demonstrated that *M. longa* feed more rapidly on animal prey than on phytoplankton. Due to the size composition of the plankton community and the possible cascading effects within the phytoplankton community in the grazing experiment, we did not find upper and lower prey size thresholds for *M. longa*. However, the relative optimal size range of prey for copepods is surprisingly constant between species, suggesting that adult copepods of similar size to *M. longa* have an optimal prey size range of ~10 to 70 µm (Berggreen et al. 1988, Hansen et al. 1994, Levinsen et al. 2000).

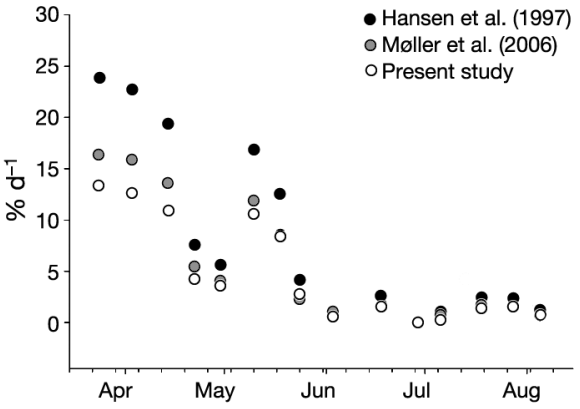

Fig. 12. Water column cleared for cells in the size range 10 to 60 µm by *Metridia longa* (% d^{-1}). Values are estimated using maximum potential clearance rates from Hansen et al. (1997) and Møller et al. (2006), or by using the average clearance rate generated from the grazing experiment with *M. longa* (present study)

Since the *in situ* size composition of the phytoplankton in the Kapisigdlit Fjord was dominated by small cells (<10 µm), we presume that only a small fraction of the phytoplankton community is available to adult *Metridia longa,* and that survival of this species to a large extent is dependent on prey items such as microzooplankton. During the study period, ciliates and dinoflagellates accounted for 55% (10–81%) and 10% (2–25%) respectively, of the carbon available for the copepods, assuming that copepods primarily feed on phytoplankton and protozooplankton >10 µm. This proportion is within the same magnitude as found in global oligotrophic ecosystems (<50 µg C l^{-1}), where ciliates and dinoflagellates on average account for 43 and 19% of the copepod carbon consumption, respectively (Saiz & Calbet 2011). Although *M. longa* is known to consume nauplii (Haq 1967, Kjellerup & Kiørboe 2012), nauplii only contributed 11% (1–40%) of the microzooplankton biomass (calculated as the sum of ciliate, dinoflagellate and nauplii biomass). Prey preference and clearance rate will likely vary depending on the copepod community composition and prey availability. However, throughout the study period, adult females and copepodites in the CV stage constituted 78 ± 9% (55–89%) of the entire *M. longa* biomass (i.e. all copepod stages including nauplii, copepodites and males), indicating that the rates estimated from our grazing experiment are within a realistic range. Thus, the present study indicates that protozooplankton, especially ciliates, are an essential source of food for the copepod community in subarctic oligotrophic systems, such as the Kapisigdlit Fjord.

Correcting grazing impact to *in situ* temperature using Q_{10}

The *in situ* temperature throughout the study period ranged between 0.5 and 13°C. Literature Q_{10} values for maximum potential clearance, ingestion and production rates of protozooplankton and copepods (reviewed in Hansen et al. 1997) range between 1.5 and 4.0 (average 2.8) within the temperature range 5 to 25°C. Since there are no consistent differences in Q_{10} between temperatures, a universal Q_{10} of 2.8 was applied to all temperatures when estimating maximum grazing potential. By using Q_{10} within the range of 1.5 to 4.0, the overall conclusions of the study would be unchanged. For example, using a Q_{10} of 4.0 at temperatures <5°C, maximum potential clearance, ingestion and production rates for protozooplankton would have been 28% lower than when using a Q_{10} of 2.8 for all temperatures.

Regulation of protozooplankton

The late summer peak of protozooplankton observed in the Kapisigdlit Fjord is a result of the disappearance of large copepods, a condition that reduces the grazing pressure on the protozooplankton community. A similar seasonal succession has been observed in Disko Bay (Levinsen & Nielsen 2002), where a 'regulation window' is created by the phytoplankton spring bloom. During the spring bloom, *Calanus* becomes food-saturated and thereby decreases the grazing pressure on the protozooplankton. In Disko Bay, a second 'window' is created when the adult *Calanus* leave the surface layer in the late summer. In the Kapisigdlit Fjord, the 'regulation window' is established as the predation pressure from *Metridia longa* is reduced when leaving the surface layer. This 'regulation window' stays 'open' a few weeks during the summer period until a high grazing pressure is reestablished by a late summer community of small copepods; mainly *Oithona* spp. (Figs. 8 & 11). In high-Arctic regions such as Young Sound, 'regulation windows' are usually absent due to the brief open water period. In these systems, copepods are able to consume most of the primary production, meaning that copepods control both the phytoplankton and protozooplankton during the entire productive season (Rysgaard et al. 1999, Nielsen et al. 2007).

Climate changes are probably the largest ecological threats facing the Arctic marine environment in the future. More detailed knowledge about trophic dynamics in subarctic marine ecosystems will provide a basis for predicting the consequences of regime shifts in high latitudes. In some areas of the Arctic, increased temperatures may reduce the sea-ice cover and expand the productive season (Tremblay & Gagnon 2009, Slagstad et al. 2011), allowing more complex plankton communities to develop (Rysgaard et al. 1999). Intensified precipitation and glacial melting may strengthen water column stratification, which would favor the development of small-sized phytoplankton populations (Ardyna et al. 2011) and position ciliates as key grazers. According to this scenario, the zooplankton community would change from dominance by copepods towards a more bimodal grazer succession, with a peak of large calanoid copepods in the spring succeeded by a late summer peak of protozooplankton and small copepod species, as illustrated in Disko Bay (Levinsen & Nielsen 2002) and the present study.

Acknowledgements. The research leading to these results was funded by the European Commission FP7 EUROBASIN (Grant Agreement: 264 933) and the Greenland Climate Research Centre (Project 6505). We acknowledge the marine sub-program of the Greenland Ecosystem Monitoring program for assistance in equipment and primary production estimates. We thank the captains and crew for excellent help during sampling on RVs 'Lille Masik' and 'Dana'. We also thank S. Zamora-Terol, B. Søborg, T. Krogh, K. Kreutzmann, H. Philipsen and J. Mortensen for help with logistics and equipment.

LITERATURE CITED

Ardyna M, Gosselin M, Michel C, Poulin M, Tremblay J (2011) Environmental forcing of phytoplankton community structure and function in the Canadian High Arctic: contrasting oligotrophic and eutrophic regions. Mar Ecol Prog Ser 442:37–57

Arendt KE, Nielsen TG, Rysgaard S, Tönnesson K (2010) Differences in plankton community structure along the Godthåbsfjord, from the Greenland Ice Sheet to offshore waters. Mar Ecol Prog Ser 401:49–62

Arendt KE, Juul-Pedersen T, Mortensen J, Blicher ME, Rysgaard S (2012) A 5-year study of seasonal patterns in mesozooplankton community structure in a sub-Arctic fjord reveals dominance of *Microsetellanorvegica* (Crustacea, Copepoda). J Plankton Res 35:105–120

Berger J (1980) Feeding-behavior of *Didinium nasutum* on *Paramecium bursaria* with normal or apochlorotic zoochlorellae. J Gen Microbiol 118:397–404

Berggreen U, Hansen B, Kiørboe T (1988) Food size spectra, ingestion and growth of the copepod *Acartia tonsa* during development: implications for determination of copepod production. Mar Biol 99:341–352

Bergstrøm B, Vilhajalmsson H (2008) Cruise report and preliminary results of the acoustic/pelagic trawl survey off West Greenland for capelin and polar cod 2005. Technical Report No. 66, Greenland Institute of Natural Resources, Nuuk

Calbet A, Riisgaard K, Saiz E, Zamora S, Stedmon C, Nielsen TG (2011) Phytoplankton growth and microzooplankton grazing along a sub-Arctic fjord (Godthåbsfjord, west Greenland). Mar Ecol Prog Ser 442:11–22

Campbell RG, Sherr EB, Ashjian CJ, Plourde S, Sherr BF, Hill V, Stockwell DA (2009) Mesozooplankton prey preference and grazing impact in the Western Arctic Ocean. Deep-Sea Res II 56:1274–1289

Comiso JC, Parkinson CL, Gersten R, Stock L (2008) Accelerated decline in the Arctic sea ice cover. Geophys Res Lett 35:L01703, doi:10.1029/2007GL031972

Daase M, Eiane K, Aksnes DL, Vogedes D (2008) Vertical distribution of *Calanus* spp. and *Metridia longa* at four Arctic locations. Mar Biol Res 4:193–207

Digby PSB (1953) Plankton production in Scoresby Sound, East Greenland. J Anim Ecol 22:289–322

Falkenhaug T, Tande KS, Semenova T (1997) Diel, seasonal and ontogenetic variations in the vertical distributions of four marine copepods. Mar Ecol Prog Ser 149:105–119

Fenchel T, Hansen PJ (2006) Motile behaviour of the bloom-forming ciliate *Mesodinium rubrum.* Mar Biol Res 2: 33–40

Frost BW (1972) Effects of size and concentration of food particles on feeding behavior of marine planktonic copepod *Calanus pacificus.* Limnol Oceanogr 17:805–815

Hamilton L, Lyster P, Otterstad O (2000) Social change, ecology and climate in 20th-century Greenland. Clim Change 47:193–211

Hansen PJ (2011) The role of photosynthesis and food uptake for the growth of marine mixotrophic dinoflagellates. J Eukaryot Microbiol 58:203–214

Hansen H, Koroleff F (1999) Determination of nutrients. In: Grasshoff K, Kremling K, Ehrhardt M (eds) Methods of seawater analysis, 3rd edn. Wiley-VCH, Weinheim, p 159–228

Hansen B, Bjørnsen PK, Hansen PJ (1994) The size ratio between planktonic predators and their prey. Limnol Oceanogr 39:395–403

Hansen PJ, Bjørnsen PK, Hansen BW (1997) Zooplankton grazing and growth: scaling within the 2–2000-µm body size range. Limnol Oceanogr 42:687–704

Hansen PJ, Bjørnsen PK, Hansen BW (2000) Zooplankton grazing and growth: Scaling within the 2–2000-µm body size range. Limnol Oceanogr 45:1891 [Erratum to Limnol Oceanogr 42:687–704]

Haq SM (1967) Nutritional physiology of *Metridia lucens* and *M. longa* from Gulf of Maine. Limnol Oceanogr 12: 40–51

Hays GC (1995) Ontogenetic and seasonal variation in the diel vertical migration of the copepods *Metridia lucens* and *Metridia longa.* Limnol Oceanogr 40:1461–1465

Hirche HJ, Mumm N (1992) Distribution of dominant copepods in the Nansen Basin, Arctic-Ocean, in summer. Deep-Sea Res A 39:S485–S505

Holland DM, Thomas RH, De Young B, Ribergaard MH, Lyberth B (2008) Acceleration of Jakobshavn Isbræ triggered by warm subsurface ocean waters. Nat Geosci 1:659–664

Hopkins CCE, Tande KS, Grønvik S, Sargent JR (1984) Ecological investigations of the zooplankton community of Balsfjorden, Northern Norway: an analysis of growth and overwintering tactics in relation to niche and environment in *Metridia longa* (Lubbock), *Calanus finmarchicus* (Gunnerus), *Thysanoessa inermis* (Krøyer) and *Thysanoessa raschi* (M. Sars). J Exp Mar Biol Ecol 82:77–99

Hygum BH, Rey C, Hansen BW, Tande K (2000) Importance of food quantity to structural growth rate and neutral lipid reserves accumulated in *Calanus finmarchicus*. Mar Biol 136:1057–1073

Jakobsen HH, Hansen PJ (1997) Prey size selection, grazing and growth response of the small heterotrophic dinoflagellate *Gymnodinium* sp. and the ciliate *Balanion comatum* — a comparative study. Mar Ecol Prog Ser 158: 75–86

Jespersen AM, Christoffersen K (1987) Measurements of chlorophyll-a from phytoplankton using ethanol as extraction solvent. Arch Hydrobiol 109:445–454

Jonsson PR, Tiselius P (1990) Feeding-behavior, prey detection and capture efficiency of the copepod *Acartia tonsa* feeding on planktonic ciliates. Mar Ecol Prog Ser 60: 35–44

Juul-Pedersen T, Nielsen TG, Michel C, Møller EF and others (2006) Sedimentation following the spring bloom in Disko Bay, West Greenland, with special emphasis on the role of copepods. Mar Ecol Prog Ser 314:239–255

Kjellerup S, Kiørboe T (2012) Prey detection in a cruising copepod. Biol Lett 8:438–441

Klein Breteler WCM, Fransz HG, Gonzalez SR (1982) Growth and development of four calanoid copepod species under experimental and natural conditions. Neth J Sea Res 16:195–207

Koski M, Møller EF, Maar M, Visser AW (2007) The fate of discarded appendicularian houses: degradation by the copepod, *Microsetella norvegica*, and other agents. J Plankton Res 29:641–654

Levinsen H, Nielsen TG (2002) The trophic role of marine pelagic ciliates and heterotrophic dinoflagellates in arctic and temperate coastal ecosystems: a cross-latitude comparison. Limnol Oceanogr 47:427–439

Levinsen H, Turner JT, Nielsen TG, Hansen BW (2000) On the trophic coupling between protists and copepods in arctic marine ecosystems. Mar Ecol Prog Ser 204:65–77

Madsen SD, Nielsen TG, Hansen BW (2001) Annual population development and production by *Calanus finmarchicus, C. glacialis* and *C. hyperboreus* in Disko Bay, western Greenland. Mar Biol 139:75–93

Menden-Deuer S, Lessard EJ (2000) Carbon to volume relationships for dinoflagellates, diatoms, and other protist plankton. Limnol Oceanogr 45:569–579

Møller EF, Nielsen TG, Richardson K (2006) The zooplankton community in the Greenland Sea: composition and role in carbon turnover. Deep-Sea Res I 53:76–93

Mortensen J, Lennert K, Bendtsen J, Rysgaard S (2011) Heat sources for glacial melt in a sub-Arctic fjord (Godthåbsfjord) in contact with the Greenland Ice Sheet. J Geophys Res 116:C01013, doi:10.1029/2010JC006528

Motyka RJ, Truffer M, Fahnestock M, Mortensen J, Rysgaard S (2011) Submarine melting of the 1985 Jakobshavn Isbræ floating tongue and the triggering of the current retreat. J Geophys Res 116:F01007, doi:10.1029/2009JF001632

Nejstgaard JC, Gismervik I, Solberg PT (1997) Feeding and reproduction by *Calanus finmarchicus*, and microzooplankton grazing during mesocosm blooms of diatoms and the coccolithophore *Emiliania huxleyi.* Mar Ecol Prog Ser 147:197–217

Nejstgaard JC, Naustvoll JL, Sazhin A (2001) Correcting for underestimation of microzooplankton grazing in bottle incubation experiments with mesozooplankton. Mar Ecol Prog Ser 221:59–75

Nielsen TG, Hansen B (1995) Plankton community structure and carbon cycling on the western coast of Greenland during and after the sedimentation of a diatom bloom. Mar Ecol Prog Ser 125:239–257

Nielsen TG, Hansen PJ (1999) Dyreplankton i danske farvande. Danmarks Miljøundersøgelser. TEMA-rapport fra DMU, Miljø- og Energiministeriet, No. 28/1999, Roskilde

Nielsen TG, Ottosen LD, Hansen BW (2007). Structure and function of the pelagic ecosystem in an ice covered arctic fjord. In: Rysgaard S, Glud RN (Eds.) Carbon cycling in Arctic marine ecosystems: case study Young Sound. Meddr Greenland, Bioscience Special Issue p 88–107

Ohman MD, Runge JA (1994) Sustained fecundity when phytoplankton resources are in short supply: omnivory by *Calanus finmarchicus* in the Gulf of St. Lawrence. Limnol Oceanogr 39:21–36

Pabi S, van Dijken GL, Arrigo KR (2008) Primary production in the Arctic Ocean, 1998-2006. J Geophys Res 113: C08005, doi:10.1029/2007JC004578

Pedersen T, Fossheim M (2008) Diet of 0-group stages of capelin (*Mallotus villosus*), herring (*Clupea harengus*) and cod (*Gadus morhua*) during spring and summer in the Barents Sea. Mar Biol 153:1037–1046

Poulsen LK, Reuss N (2002) The plankton community on Sukkertop and Fylla Banks off West Greenland during a spring bloom and post-bloom period: hydrography, phytoplankton and protozooplankton. Ophelia 56:69–85

Putt M, Stoecker DK (1989) An experimentally determined carbon-volume ratio for marine oligotrichous ciliates from estuarine and coastal waters. Limnol Oceanogr 34: 1097–1103

Rat'kova TN, Wassmann P (2002) Seasonal variation and spatial distribution of phyto- and protozooplankton in the central Barents Sea. J Mar Syst 38:47–75

Rysgaard S, Glud RN (2004) Anaerobic N_2 production in Arctic sea ice. Limnol Oceangr 49(1):86–94

Rysgaard S, Nielsen TG, Hansen BW (1999) Seasonal variation in nutrients, pelagic primary production and grazing in a high-Arctic coastal marine ecosystem, Young Sound, Northeast Greenland. Mar Ecol Prog Ser 179:13–25

Sabatini M, Kiørboe T (1994) Egg production, growth and development of cyclopoid copepod *Oithona similis*. J Plankton Res 16: 1329–1351

Saiz E, Calbet A (2011) Copepod feeding in the ocean: scaling patterns, composition of their diet and the bias of estimates due to microzooplankton grazing during incubations. Hydrobiologia 666:181–196

Satapoomin S (1999) Carbon content of some common tropical Andaman Sea copepods. J Plankton Res 21:2117–2123

Sell AF, van Keuren D, Madin LP (2001) Predation by omnivorous copepods on early developmental stages of *Calanus finmarchicus* and *Pseudocalanus* spp. Limnol Oceanogr 46:953–959

Seuthe L, Iversen KR, Narcy F (2011) Microbial processes in a high-latitude fjord (Kongsfjorden, Svalbard): II. Ciliates and dinoflagellates. Polar Biol 34:751–766

Sherr EB, Sherr BF (2007) Heterotrophic dinoflagellates: a significant component of microzooplankton biomass and major grazers of diatoms in the sea. Mar Ecol Prog Ser 352:187–197

Sherr EB, Sherr BF, Hartz AJ (2009) Microzooplankton grazing impact in the western Arctic Ocean. Deep-Sea Res II 56:1264–1273

Slagstad D, Ellingsen IH, Wassmann P (2011) Evaluating primary and secondary production in an Arctic Ocean void of summer sea ice: an experimental simulation approach. Prog Oceanogr 90:117–131

Smidt ELB (1979) Annual cycles of primary production and of zooplankton at southwest Greenland. Greenl Biosci 1:1–56

Steemann-Nielsen E (1958) A survey of recent Danish measurements of the organic productivity in the sea. Rapp Cons Int Explor Mer 144:92–95

Stoecker D, Guillard RRL, Kavee RM (1981) Selective predation by *Favella ehrenbergii* (Tintinnia) on and among dinoflagellates. Biol Bull 160:136–145

Stoecker DK, Gifford DJ, Putt M (1994) Preservation of marine planktonic ciliates: losses and cell shrinkage during fixation. Mar Ecol Prog Ser 110:293–299

Storr-Paulsen M, Wieland K, Hovgard H, Ratz HJ (2004) Stock structure of Atlantic cod (*Gadus morhua*) in West Greenland waters: implications of transport and migration. ICES J Mar Sci 61:972–982

Stroeve J, Holland MM, Meier W, Scambos T, Serreze M (2007) Arctic sea ice decline: faster than forecast. Geophys Res Lett 34:L09501, doi:10.1029/2007GL029703

Strom SL, Postel JR, Booth BC (1993) Abundance, variability, and potential grazing impact of planktonic ciliates in the open sub-Arctic Pacific Ocean. Prog Oceanogr 32: 185–203

Tang KW, Nielsen TG, Munk P, Mortensen J and others (2011) Metazooplankton community structure, feeding rate estimates, and hydrography in a meltwater-influenced Greenlandic fjord. Mar Ecol Prog Ser 434: 77–90

Tremblay JE, Gagnon J (2009) The effects of irradiance and nutrient supply on the productivity of Arctic waters: a perspective on climate change. In: Nihoul JCJ, Kostianoy AG (eds) Influence of climate change on the changing Arctic and Sub-Arctic conditions. NATO Science for Peace and Security Series C: Environmental Security. Springer, Houten, p 73–93

Turner J, Levinsen H, Nielsen TG, Hansen BW (2001) Zooplankton feeding ecology: grazing on phytoplankton and predation on protozoans by copepod and barnacle nauplii in Disko Bay, West Greenland. Mar Ecol Prog Ser 221:209–219

Uye S, Aoto I, Onbé T (2002) Seasonal population dynamics and production of *Microsetella norvegica*, a widely distributed but little-studied marine planktonic harpacticoid copepod. J Plankt Res 24:143–153

Verity PG Langdon C (1984) Relationships between lorica volume, carbon, nitrogen, and ATP content of tintinnids in Narragansett Bay. J Plankton Res 6:859–868

Verity PG, Wassmann P, Frischer ME, Howard-Jones MH, Allen AE (2002) Grazing of phytoplankton by microzooplankton in the Barents Sea during early summer. J Mar Syst 38:109–123

Yentsch CS, Menzel DW (1963) A method for the determination of phytoplankton chlorophyll and phaeophytin by fluorescence. Deep-Sea Res 10:221–231

Editorial responsibility: Marsh Youngbluth, Fort Pierce, Florida, USA

Submitted: September 26, 2012; Accepted: December 17, 2013
Proofs received from author(s): February 26, 2014

Paper VI

Published in Marine Ecology Progress Series

Midnight sun in the Godthåbsfjord
Photo: Karen Riisgaard

Vol. 442: 11–22, 2011
doi: 10.3354/meps09343

MARINE ECOLOGY PROGRESS SERIES
Mar Ecol Prog Ser

Published December 5

Phytoplankton growth and microzooplankton grazing along a sub-Arctic fjord (Godthåbsfjord, west Greenland)

Albert Calbet[1,*], Karen Riisgaard[2], Enric Saiz[1], Sara Zamora[1], Colin Stedmon[3,5], Torkel Gissel Nielsen[2,4]

[1]Institut de Ciències del Mar (CSIC), Passeig Marítim de la Barceloneta 37–49, 08003 Barcelona, Spain

[2]National Institute of Aquatic Resources, DTU Aqua, Section for Ocean Ecology and Climate, Technical University of Denmark, Kavalergården 6, 2920 Charlottenlund, Denmark

[3]National Environmental Research Institute, Department of Marine Ecology, Aarhus University, Frederiksborgvej 399, 4000 Roskilde, Denmark

[4]Greenland Climate Research Center, Greenland Institute of Natural Resources, Kivioq 2, PO Box 570, 3900 Nuuk, Greenland

[5]*Present address:* National Institute of Aquatic Resources, DTU Aqua, Section for Ocean Ecology and Climate, Technical University of Denmark, Kavalergården 6, 2920 Charlottenlund, Denmark

ABSTRACT: We evaluated the role of microzooplankton (sensu latto, grazers <500 µm) in determining the fate of phytoplankton production (PP) along a glacier-to-open sea transect in the Greenland subarctic fjord, Godthåbfjord. Based on the distribution of size fractionated chlorophyll *a* (chl *a*) concentrations we established 4 zones: (1) Fyllas Bank, characterized by deep chl *a* maxima (ca. 30 to 40 m) consisting of large cells, (2) the mouth and main branch of the fjord, where phytoplankton was relatively homogeneously distributed in the upper 30 m layer, (3) inner waters influenced by glacial melt water and upwelling, with high chl *a* concentrations (up to 12 µg l^{-1}) in the >10 µm fraction within a narrow (2 m) subsurface layer, and (4) the Kapisigdlit branch of the fjord, ice-free, and characterized with a thick and deep chl *a* maximum layer. Overall, microzooplankton grazing impact on primary production was variable and seldom significant in the Fyllas Bank and mouth of the fjord, quite intensive (up to >100% potential PP consumed daily) in the middle part of the main and Kapisigdlit branches of the fjord , and rather low and unable to control the fast growing phytoplankton population inhabiting the nutrient rich waters in the upwelling area in the vicinity of the glacier. Most of the grazing impact was on the <10 µm phytoplankton fraction, and the major grazers of the system seem to be >20 µm microzooplankton, as deducted from additional dilution experiments removing this size fraction. Overall, little or no export of phytoplankton out of the fjord to the Fyllas Bank can be determined from our data.

KEY WORDS: West Greenland coast · Sub-Arctic fjord · Plankton community structure · Microzooplankton · Grazing

INTRODUCTION

The fragility of high latitude ecosystems, their dependence on ice-cover and extreme seasonality in irradiance and temperature make them a major focus of the studies on global change (e.g. Cavalieri et al. 2003, Johannessen et al. 2004, Smetacek & Nicol 2005). In this regard, west Greenland waters are particularly relevant, not only because they fit into the category of endangered ecosystems but for the potential socioeconomical implications of any change in the pelagic food web. The west Greenland marine ecosystem is very productive and sustains commercial and recreational fishing and hunting, which largely contribute to Greenland's total export income. A disruption in the lower levels of the food web,

*Email: acalbet@icm.csic.es

induced for example by climate change, will likely propagate to higher levels in the food chain and threaten the sustainable harvesting of marine resources. For instance, large calanoid copepods are the preferred food source of cod and other commercial fish larvae in west Greenland waters (Bainbridge & McKay 1968). The copepods feed on microzooplankton and phytoplankton (Barthel 1988, Levinsen et al. 2000a, Saiz & Calbet 2011) and are vulnerable to changes in their biomass and distributions. In most marine systems, microzooplankton are the major grazers of phytoplankton and very important secondary producers (Levinsen et al. 2000b, Sherr & Sherr 2002, Calbet & Landry 2004, Landry & Calbet 2004). Consequently, the early life and recruitment of many commercially exploited fish stocks ultimately depends on primary production and on how it is channeled to higher trophic levels by microzooplankton and copepods (Levinsen et al. 2000b). It is therefore essential to understand the structure and functioning of the planktonic food web so that potential abrupt changes, which can have considerable economic and ecological impact, can be modeled and possibly predicted as the Greenland climate changes and anthropogenic activities in the region increase.

The Godthåbsfjord area is of great importance for the local fisheries (Storr-Paulsen et al. 2004) and is among the largest fjord systems in the world. Surprisingly, it is understudied, and the majority of research carried out on the plankton ecology of the system has focused on copepods and fish larvae (Munk et al. 2003, Pedersen et al. 2005, Simonsen et al. 2006, Tang et al. 2011). To our knowledge, there are a limited number of studies detailing the microbial food web in these waters and none of them quantify rates of microzooplankton grazing and growth, instead largely inferring microzooplankton grazing from community biomass and equations from the literature (Poulsen & Reuss 2002, Pedersen et al. 2005, Arendt et al. 2010). This study stands to rectify this and present novel insight into the plankton dynamics and flow of energy through the microzooplankton of this important system.

Here, we focus on the interaction between phytoplankton and microzooplankton with the goal of determining how much of the primary production (PP) is consumed by the microzooplankton (Sherr & Sherr 2002, Levinsen & Nielsen 2002, Calbet & Landry 2004, Calbet 2008). We define the group microzooplankton as all the grazers <500 µm, which in our study was mostly protozoans. The area investigated encompasses 2 important spawning areas for the Greenland cod *Gadus morhua*: the Fyllas Bank and Godthåbsfjord (Storr-Paulsen et al. 2004). Along the fjord we expected to traverse very contrasting trophic scenarios. Offshore, Fyllas Bank is highly influenced by the oceanography of the west Greenland Shelf and Davis Strait. The entrance and main body of Godthåbsfjord experience extensive tidal mixing and water exchange (Mortensen et al. 2011), leading to enhanced production of phytoplankton (Arendt et al. 2010). The inner part of the Godthåbsfjord is influenced by glacial nutrient-rich melt water and characterized by high phytoplankton abundances (Mortensen et al. 2011, Tang et al. 2011). Finally, the Kapisigdlit branch of the fjord is mostly unaffected by direct glacial melt water and is a known area of spawning for cod (Storr-Paulsen et al. 2004).

MATERIALS AND METHODS

This study was part of the Biological Oceanography of Fyllas Bank–Godthåbsfjord (BOFYGO) cruise that was conducted with RV 'Dana' from June 6 to 24, 2010. The sampling area spanned the Fyllas Bank, off southwestern Greenland, to the inner part of the Godthåbsfjord (Table 1, Fig. 1). At each station salinity, temperature, and chlorophyll *a* fluorescence profiles were recorded during the early morning using a CTD (SBE 19plus, SeaCat) and a Turner Designs fluorometer (Cyclops 7). Water samples for the determination of inorganic nutrients and chlorophyll *a* concentrations (hereafter chl *a*) were obtained using a rosette with twelve 10 l Niskin bottles. Dissolved inorganic nutrient samples (phosphate, nitrate, and silicate) were immediately frozen (–20°C) for later analysis on a Skalar autoanalyser (Breda, Netherlands), following the procedures of Hansen & Koroleff (1999). The precision (analytical reproducibility) of the nutrient analyses was 0.06, 0.1, and 0.2 µM for phosphate, nitrate, and silicate, respectively.

We also estimated the phytoplankton growth and the microzooplankton grazing rates using the dilution technique (Landry & Hassett 1982) at each station on total (GF/F filtered) and >10 µm chl *a*. The water for the experiments was collected at the fluorescence maximum (Table 1) using 30 l Niskin bottles. We gravity-filtered a portion of the water through a Pall Acropak 0.8/0.2 500 capsule (0.2 µm final pore size) that, together with its tubing, was flushed previously with diluted HCl and rinsed thoroughly afterwards with deionized water. We then poured measured volumes into a series of 2.3 l acid-washed polycarbonate bottles for each dilution treatment. At stations in which the fluorescence profile

showed very high values at the maximum, we sampled and filtered water from just below the fluorescence maximum to avoid filter clogging. The remaining volume of the bottles was filled to the top with 500 µm nylon-mesh reverse-filtered natural seawater from the selected depth to produce the following dilution series: 12.5, 25, 50, 75, and 100% of natural water. Visual examination after the filling of the bottles revealed no significant numbers of copepods in them. Moreover, an examination of 2 l of the initial water filtered through 40 µm mesh did not show many copepods either (maximum 1 to 2 small *Oithona* spp.). All handling and filtration was carried out under dim light conditions to avoid cell light-damage. To fulfill the assumptions of the method, instantaneous phytoplankton growth should be the same in all the dilution bottles. To ensure this, each bottle was amended with 10 µM of ammonium (NH_4Cl), 0.7 µM of phosphate (Na_2HPO_4), and 1 to 2 µM of silicate (Na_2SiO_3). The added nitrogen was in the form of ammonium because it is more readily taken up by algae than nitrate (Dortch et al. 1991). We also added silicate to promote constant growth of diatoms. In addition, 2 extra 100% (i.e. undiluted) bottles were prepared without nutrients to assess the natural growth of the algae and to serve as initial samples. Each 2.3 l bottle was used to sequentially fill (gentle siphoning) 2 replicated dilution incubation bottles (1 l acid-washed polycarbonate).

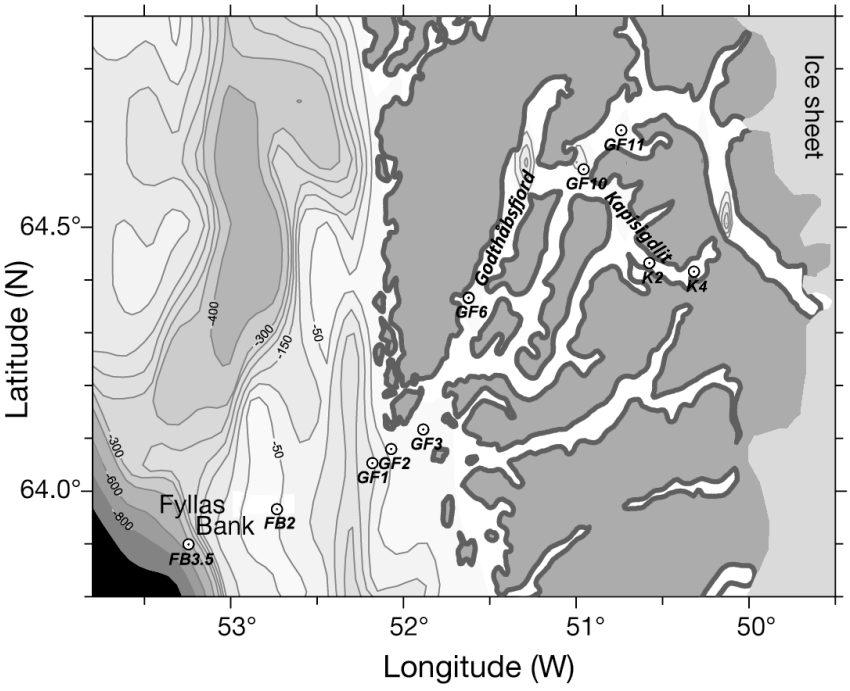

Fig. 1. Study area in and near Godthåbsfjord, west Greenland indicating the locations of the sampled stations (⊙). FB: Fyllas Bank; GF: Godthåbsfjord; K: Kapisigdlit branch

At Stns GF6, GF11 and K2 we carried out an additional dilution grazing experiment in which we reverse filtered the natural water through a 20 µm sieve. Otherwise, these bottles were treated as above. The aim of this experiment was to investigate whether grazing of phytoplankton was due to small zooplankton (<20 µm) or large ones (20 to 500 µm). By removing the >20 µm fraction, the food chain is

Table 1. Locations of the sampling stations and chlorophyll *a* concentrations of samples collected at each station during June 2010. Stations were located along a transect beginning offshore at Fyllas Bank, heading inland and ending in the inner fjord. Water depth indicates depth at which sample was collected. Incubation temperature, initial concentration of chlorophyll *a* (Total = GFF filtered duplicated samples), and proportion of >10 µm chl *a* relate to the experimental conditions and results. SE of 2 chl *a* replicated samples

Area	Stn	Day of month	Latitude (N)	Longitude (W)	Incubation temp. (°C)	Water depth (m)	Total chl *a* (±SE, µg l^{-1})	% chl *a* >10 µm
Fyllas Bank	FB3.5	8	63° 53.9′	53° 14.7′	4.9	20	1.46 ± 0.096	64.8
Fyllas Bank	FB2	10	63° 58.0′	52° 44.0′	5.2	30	1.24 ± 0.012	91.3
Outer fjord	GF1	12	64° 03.2′	52° 10.9′	3.6	10	2.21 ± 0.038	10.6
Outer fjord	GF2	13	64° 04.8′	52° 04.2′	3.7	30	0.70 ± 0.006	22.6
Outer fjord	GF3	11	64° 07.0′	51° 53.0′	3.6	25	1.07 ± 0.012	26.2
Inner fjord	GF6	15	64° 22.0′	51° 37.4′	4.3	25	2.70 ± 0.046	16.6
Near glacier	GF10	16	64° 36.6′	50° 57.5′	5.6	12	4.87 ± 0.166	92.7
Near glacier	GF10bis	21	64° 36.6′	50° 57.5′	6.6	15	7.23 ± 0.019	83.5
Near glacier	GF11	20	64° 41.0′	50° 44.4′	2.6	18	12.2 ± 0.238	86.9
Kapisigdlit	K2	17	64° 25.1′	50° 34.5′	8.0	20	1.33 ± 0.043	42.1
Kapisigdlit	K4	18	64° 24.6′	50° 19.1′	7.3	25	1.10 ± 0.013	20.4

disrupted and grazers <20 µm are favoured, as their predators are absent. Therefore, if <20 µm grazers were responsible for most of the grazing activity on phytoplankton, these fractionated experiments should show either equal or higher grazing coefficients than the standard dilution experiments conducted with the same water. Conversely, if major grazers were >20 µm, the grazing detected in these bottles should be severely diminished.

We incubated all the bottles in a 600 l opaque PVC incubator with open-circuit water running from a 5 m depth at a temperature about the same as that *in situ*. To guarantee similar light intensities to that at the fluorescence maximum we dimmed the natural sunlight with an appropriate dark plastic mesh (reduction of 80 to 90% of surface light, depending on the station). The bottles were gently mixed by repeated turning and repositioned in the incubator at least 4 times per day. The incubations were terminated after 25 to 30 h, and samples for the quantification of total and >10 µm chl *a* concentrations were taken. For <20 µm treatments, only the total chl *a* was measured.

To determine total chl *a*, we filtered 100 to 200 ml of water (depending on the dilution level) under low vacuum pressure (<100 mm Hg) through Whatmann glass fibre filters (GF/F, 25 mm diameter). For the >10 µm fraction, we filtered 150 to 300 ml through 10 µm polycarbonate filters (25 mm diameter, Osmonics). After filtration, the filters were stored frozen at −20°C until analysis and then extracted in 96% ethanol at room temperature for 12 to 18 h (Jespersen & Christoffersen 1987). Fluorescence was then measured before and after acidification, on a fluorometer (TD-700, Turner Designs) calibrated with a pure chl *a* standard. The fluorescence signal measured by the fluorometer deployed with the CTD was calibrated with extracted chl *a* measurements from the entire vertical profile using a linear regression. A separate regression was carried out for each station as the relationship was found to vary across the transect. The calibrated fluorescence profiles are used here to only reveal the relative vertical distribution of the phytoplankton biomass and its links to water column structure. For calculations, only the laboratory measured chl *a* concentrations are used.

Acid Lugol preserved samples (1% final concentration) were taken to characterize the initial microplankton concentration. Unfortunately, the commercial Lugol used was inappropriate to preserve microzooplankton, and samples were lost, except for Stns GF10bis, GF11, K2, and K4 that were preserved with self-made Lugol (Throndsen 1978). Although these samples do not provide a comprehensive view of the microplankton distribution along the fjord, they are presented to have a better understanding of these sites. The samples were processed by settling 100 ml in Utermöhl chambers for at least 48 h prior to counting them using an inverted microscope (XSB-1A). The whole chamber, or a fraction of it for the smallest and more abundant organisms, was counted at 100, 250, and 400× magnification, depending on the group. Fifty to 100 cells per group were sized, adjusted to their closest geometric shape, and converted into carbon using the equations of Menden-Deuer & Lessard (2000).

Phytoplankton mortality rates (m; d^{-1}) were computed as the slope of the linear regression between net growth rate of chl *a* and the dilution factor for the nutrient-amended bottles (Landry & Hassett 1982). Instantaneous phytoplankton growth rates (µ; d^{-1}) in the dilution grazing experiments were obtained by adding the net growth in the unamended bottles (K_o; d^{-1}; no nutrients added) to the mortality rate of microzooplankton from dilution experiments when the latter was significant ($\mu = K_o + m$). Potential primary production (pPP; µg chl *a* l^{-1} d^{-1}) was obtained according to Landry et al. (2000) by multiplying µ by the average concentration of chl *a* during the incubation (C_m; $C_m = C_o\,[e^{(\mu-m)t} - 1]/(\mu - m)t$), where C_o is the initial chl *a* concentration and t is the incubation time (d).

RESULTS

Physical environment

Different oceanographic regimes were observed along the transect (Figs. 1 & 2). At the Fyllas Bank stations (Stns FB3.5 and FB2) the upper 100 m of the water column consisted largely of 2 layers: a warm (>3°C) surface layer between 10 and 15 m thick with a salinity of approximately 33.1 and an underlying layer of colder (<2°C) and slightly more saline water (Fig. 2). At the region near the entrance of the fjord between the Bank and the eastern most fjord sill (Stns GF1–GF3) the water column was comparatively well mixed (Fig. 2). Further east into the main branch of the fjord and towards both the glaciers and Kapisigdlit, the water column was stratified (Stn GF6). The warmest waters were measured at the surface of the Kapisigdlit branch (Stns K2 and K4), whilst the lowest salinity surface waters were found where glacier melt water was influential (GF 10 and 11).

The regional differences in the water column structure were also mirrored in the vertical distribution of

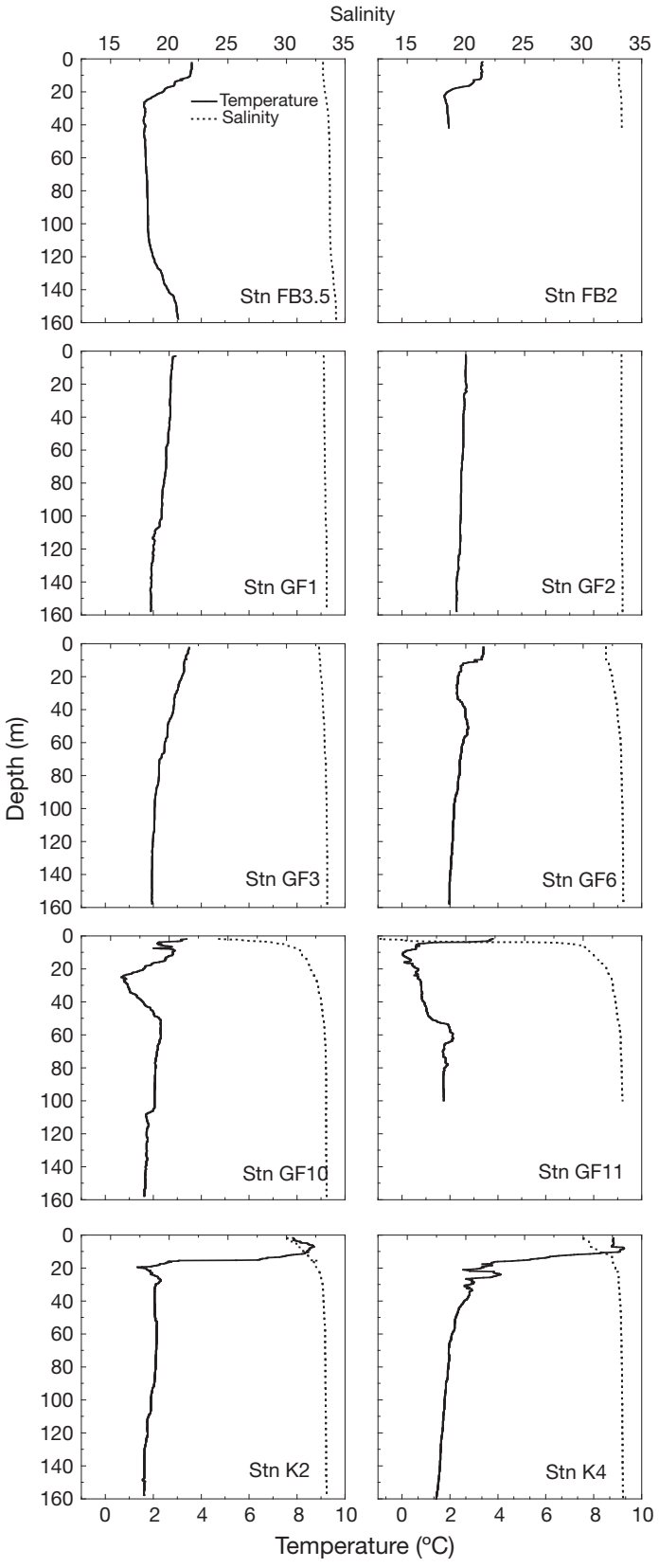

Fig. 2. Profiles of temperature and salinity at the sampled stations. See Fig. 1 for station abbreviations and locations

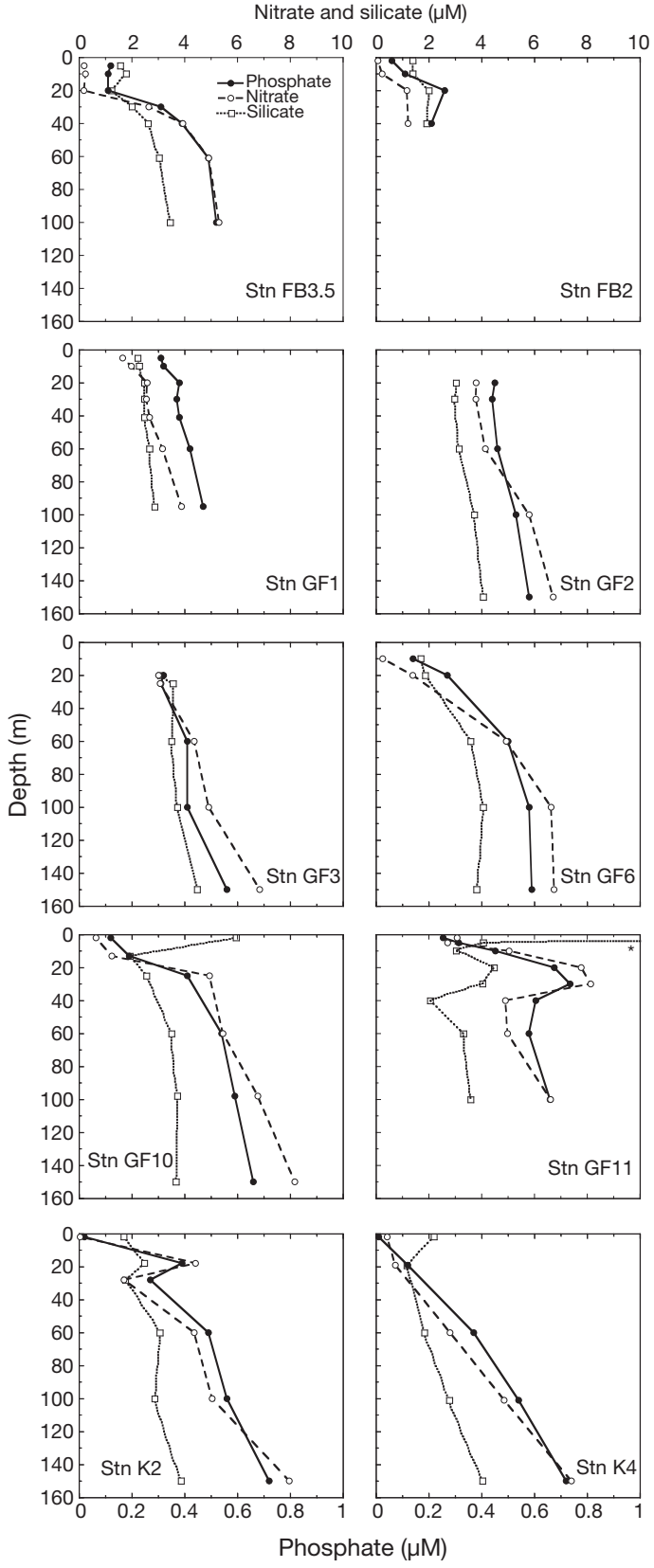

Fig. 3. Profiles of inorganic nutrient concentrations at the sampled stations. See Fig. 1 for station abbreviations and locations. *Silicate maximum concentration 23.7 µM

the major nutrients (Fig. 3). At the Fyllas Bank nutrients were depleted in the upper mixed part of the water column (Fig. 3). In the outer mixed part of the fjord (Stns GF1–GF3) high concentrations of all major nutrients were measured throughout the water column. In the Kapisigdlit branch (Stns K2 and K4) the phosphate and nitrate were close to detection limit in the upper freshwater-impacted part of the water column, from where they increased towards the bottom (Fig. 3). The highest surface concentrations of nutrients were measured at the innermost station in the Godthåbsfjord, where the freshwater outlet from the glacier resulted in subglacial circulation (Mortensen et al. 2011) that caused upwelling of nutrient rich subsurface water (Stn GF11).

Community structure

The initial concentrations of chl *a* at the fluorescence maximum for each experiment and the proportion of the total chl *a* >10 µm are presented in Table 1. Total chl *a* concentrations at the fluorescence maximum were quite similar at most stations, ranging from 0.7 to 2.7 µg chl *a* l^{-1}. However, concentrations were greater near the glacier (4.87 to 12 µg chl *a* l^{-1}; Stns GF10, GF10bis, and GF11), which mostly corresponded to >10 µm cells (diatom chains; Table 2). Small cells dominated the phytoplankton community biomass at the mouth of the main fjord and in the Kapisigdlit branch. At the latter stations (Stns K2 and K4), a very heterotrophic community was present with a clear predominance of large ciliates (Table 2).

The vertical distribution of chl *a* is presented in Fig. 4. Fyllas Bank stations showed a deep chl *a* maximum ca. 30 to 40 m (note Stn FB2 was a very shallow station on the Bank). At the mouth and sill region of Godthåbsfjord (Stn GF2), phytoplankton were relatively homogeneously distributed. In the fjord and beyond the sill region a clear subsurface chl *a* maximum was again found in a narrow and distinct layer matching the thermal stratification (Figs. 3 & 4). On the other hand, in the Kapisigdlit stations the chl *a* maximum was very wide and reached very deep layers, quite below the thermocline (Fig. 4).

Table 2. Mean (± SE) biomass (µg C l^{-1}) of protists at the stations near the glacier (GF10bis and GF11) and Kapisigdlit fjord (K2 and K4) from 2 initial bottle measurements (see 'Materials and methods' section). Biomass of dominant taxa for each station is shown in **bold**

	GF10bis		GF11		K2		K4	
	Mean	SE	Mean	SE	Mean	SE	Mean	SE
Diatoms								
Chaetoceros spp.	27.9	0.25	10.9	0.6	12.1	0.32	1.1	0.04
Pseudo-nitzschia spp.	0.03	0.004	0.01	0.001	0.01	0.002	0.004	0.001
Thalassiosira spp.	**54.3**	3.16	**147.0**	4.1	2.2	0.51	0.18	0.06
Other centric diatoms	7.6	0.79	5.4	0.15	2.8	0.14	0.40	0.05
Other pennate diatoms	0.14	0.003	0.04	0.01	0.01	0.01	0.00	0.00
Flagellates								
Dinobryon spp.	0.04	0.01	0.02	0.002	0.22	0.02	0.37	0.05
Phaeocystis sp.	0.99	0.31	0.00	0.00	0.25	0.01	0.31	0.05
Other nanoflagellates	1.0	0.05	1.35	0.33	0.57	0.02	0.59	0.004
Dinoflagellates								
Amphidinium sphenoides	0.59	0.06	0.64	0.03	0.16	0.01	0.21	0.00
Dinophysis spp.	0.05	0.05	0.00	0.00	0.90	0.75	2.0	0.05
Gyrodinium spp.	6.3	0.69	7.61	0.82	10.6	0.47	12.2	2.6
Katodinium glaucum	0.05	0.01	0.03	0.003	0.03	0.01	0.06	0.02
Protoperidinium spp.	0.24	0.09	0.24	0.02	0.79	0.00	1.17	0.11
Torodinium robustum	0.15	0.06	0.02	0.00	0.83	0.08	0.19	0.02
Other dinoflagellates (<20 µm)	0.59	0.02	0.53	0.06	2.4	0.06	0.96	0.07
Other dinoflagellates (>20 µm)	4.2	0.32	3.93	0.15	8.5	1.8	9.0	1.5
Ciliates								
Laboea strobila	0.00	0.00	0.00	0.00	4.3	0.98	18.3	0.30
Strombidium spp.	0.55	0.14	0.07	0.07	10.4	0.89	4.4	0.34
Tintinnida	0.15	0.02	0.14	0.04	0.05	0.05	0.00	0.00
Other ciliates (< 20 µm)	0.06	0.01	0.05	0.00	0.07	0.001	2.20	0.22
Other ciliates (> 20 µm)	23.0	3.09	17.5	0.15	**50.6**	7.63	**265.9**	21.9

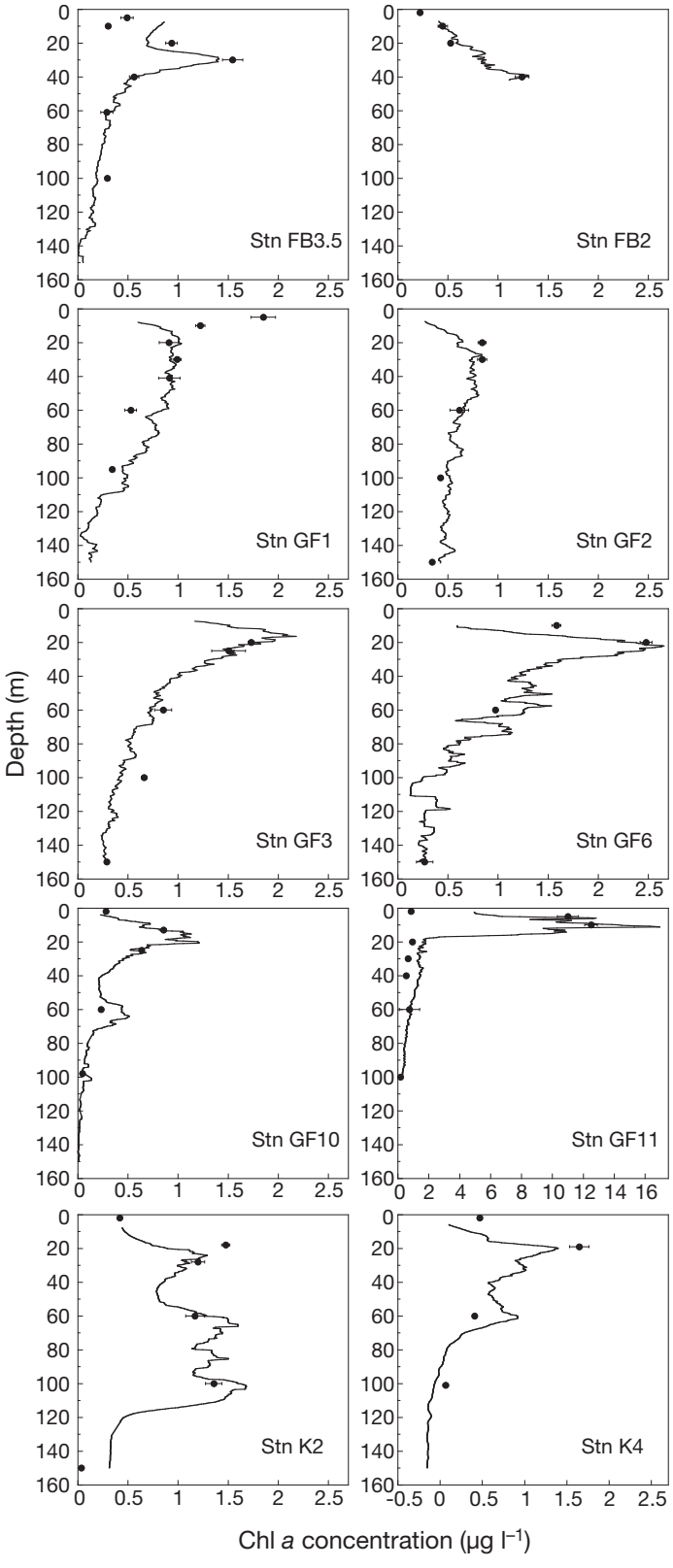

Fig. 4. Vertical distribution of chl *a* at each of the sampled stations. Continuous line indicates the calibrated fluorescence from the CTD mounted fluorometer. Dots correspond to the actual chl *a* measurements (mean ± SE, n = 3). Note the different scale at Stn GF11

Phytoplankton growth and mortality rates

The analysis of the net growth rates in the 100% bottles without added nutrients (K_o) provide a proxy for the short-term natural evolution of the community during the incubations, although it does not resolve the mechanisms behind the observed rates (phytoplankton mortality versus growth). With this in mind, the data presented in Table 3 provide evidence that for most stations the phytoplankton community was growing or was rather stable (slightly diminishing in Stns FB3.5 and K4 for total chl *a*). For the main Godthåbsfjord stations, excluding Stn GF3 (see below), net growth rates increased towards the inner fjord and glaciers. Globally, net phytoplankton growth rates (K_o) showed a significant relationship with chl *a* (Fig. 5). The comparison of the net growth rates in bottles without added nutrients (K_o) with those amended (K) reveals that the areas with lower concentrations of chl *a* showed important phytoplankton growth enhancement because of the nutrient amendment (Fig. 6). On the other hand, there was no apparent growth enhancement as a result of the addition of nutrients in the areas with higher chl *a* concentrations (Stns GF10bis and GF11; Fig. 6).

Besides the information provided by the net growth rates, further insights are obtained when these rates are analyzed together with the dilution experiments, as these provide estimates of instantaneous phytoplankton growth and mortality rates. These data show that the phytoplankton community was growing at higher instantaneous rates (0.2 to 0.4 d^{-1}) at the inner part of the main fjord and at

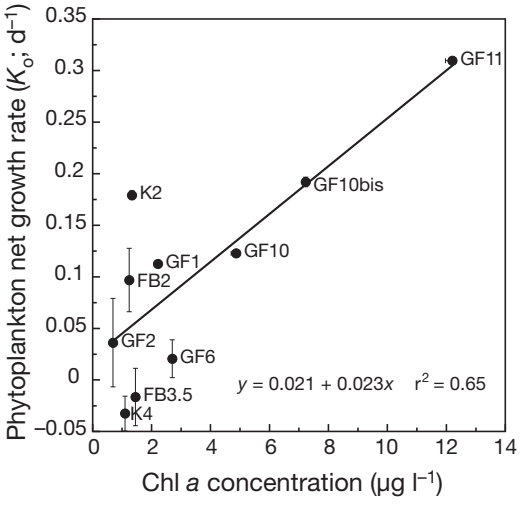

Fig. 5. Relationship between initial chl *a* concentrations and net growth rates without nutrient addition at the sampled stations. Stn GF3 was excluded from the analysis (see 'Results'). Error bars are SE of 2 replicates

Table 3. Summary of the dilution grazing experiment results for total chl *a* (GFF based) and >10 µm chl *a* at each station. The determination coefficients for the regression analyses are provided for the significant ($p < 0.05$) regressions. K_o: phytoplankton net growth rate; µ: instantaneous growth rate in the 100% bottles without nutrients ($\mu = K_o + m$); *m*: mortality rate; pPP: potential primary production; % pPP: percentage of phytoplankton potential production daily removed by grazers ($m/\mu \times 100$); ns: not significant; nd: not determined because positive slope in the regression

Stn	K_o (d^{-1})	µ (d^{-1})	*m* (d^{-1})	r^2	pPP (µg chl *a* l^{-1} d^{-1})	% pPP
Total chl *a*						
FB3.5	−0.02	0.20	0.22	0.72	0.29	110.2
FB2	0.10	0.10	ns	ns	0.14	0.0
GF1	0.11	0.11	ns	ns	0.26	0.0
GF2	0.04	0.32	0.28[a]	0.70	0.23	87.4
GF3	−0.29	−0.29	nd	0.89		0.0
GF6	0.02	0.39	0.37[a]	0.72	1.1	94.8
GF10	0.12	0.33	0.21	0.48	1.9	64.0
GF10bis	0.19	0.19	ns	ns	1.5	0.0
GF11	0.31	0.39	0.07[b]	0.48	6.0	19.9
K2	0.18	0.36	0.18	0.61	0.5	49.7
K4	−0.03	0.11	0.14	0.74	0.12	127.8
>10 µm chl *a*						
FB3.5	0.16	0.405	0.25[b]	0.59		
FB2	−0.01	−0.01	ns	ns		
GF1	0.21	0.21	ns	ns		
GF2	−0.25	−0.25	ns	ns		
GF3	0.30	0.30	ns	ns		
GF6	0.09	0.37	0.28[b]	0.60		
GF10	0.18	0.27	0.09[b]	0.59		
GF10bis	0.19	0.27	0.08	0.55		
GF11	0.42	0.42	ns	ns		
K2	0.20	0.20	ns	ns		
K4	0.14	0.14	ns	ns		

[a]Feeding saturation, 3-point method used (Gallegos 1989); [b]one outlier removed

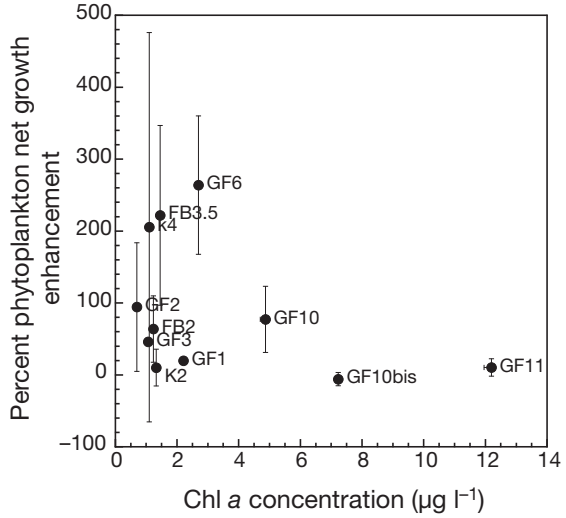

Fig. 6. Net phytoplankton growth rate enhancement due to nutrient addition in the 100% dilution experiment bottles compared to the unamended bottles at each station: $(K - K_o)/K_o \times 100$; see 'Materials and methods'. Error bars along the abscissa axis are the SE of 2 replicates. Error bars along the ordinate axis are SE and have been calculated by applying the corresponding error propagation equations

lower rates in the mouth and adjacent Fyllas Bank area (0.1 to 0.2 d^{-1}; Table 3).

The microzooplankton grazing control on phytoplankton, as a percentage of the potential primary production (pPP) consumed per day (Table 3, Fig. 7), reveals a close coupling between producers and grazers in the middle part of the fjord and Kapisigdlit branch, a globally low, although very variable, grazing pressure in the Fyllas Bank and mouth part of the fjord, and an overall low pressure in the inner part of the Godthåbsfjord near the glacier. For this analysis we excluded Stn GF3 because the positive slope of the relationship between net growth rates and dilution factor, likely a result of trophic cascades during the incubations (Calbet et al. 2011), prevents any interpretation of the data.

To better characterize the microbial food web structure of the system, we analysed the grazing activity on >10 µm phytoplankton in the standard dilution grazing experiments and on total chl *a* in the experiments without organisms >20 µm. These data provide a measure of both the microzooplankton

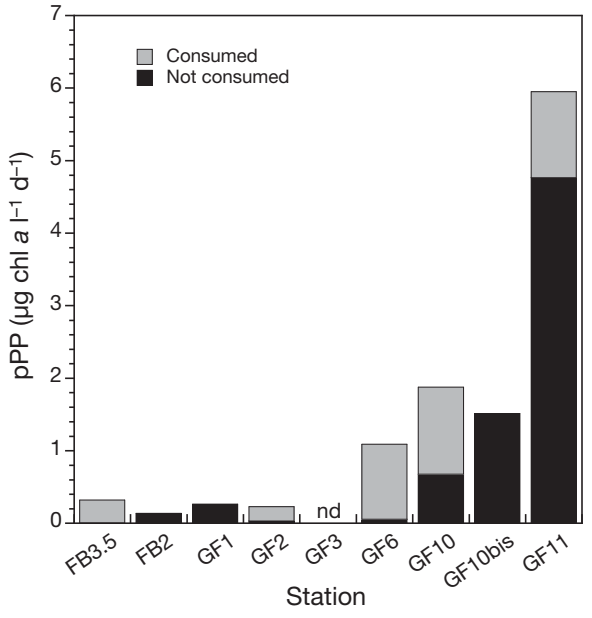

Fig. 7. Potential primary production (pPP) at stations in the main branch of Godthåbfjord (G) and the Fyllas Bank (FB) area. The proportion of the pPP grazed by microzooplankton is indicated. nd: not determined

grazing impact on large phytoplankton and further insights into the size-fractions of the major grazers of the system. The grazing activity on >10 µm cells was only significant at Stns FB3.5, GF6, and 2 visits to Stn GF10 (Table 3). In the experiments where the food web was truncated by removing organisms >20 µm (Stns GF6, GF11 and K2), we observed a clear reduction in grazing rates in 2 out of 3 stations (Table 4), which indicates that >20 µm grazers were exerting an important impact on the phytoplankton of the area.

Table 4. Mean growth and mortality rates and regression determination coefficient from the <20 µm pre-filtered dilution grazing experiments for two Godthåbsfjord stations (GF6 and GF11) and one Kapisigdlit branch station (K2). K_o: phytoplankton net growth rate without added nutrients; µ: instantaneous growth rate without nutrients; *m*: mortality rate; ns: not significant

Stn	K_o (d^{-1})	µ (d^{-1})	*m* (d^{-1})	r^2
GF6	0.03	0.03	ns	ns
GF11	0.15	0.25	0.10	0.52
K2	−0.08	−0.08	ns	ns

DISCUSSION

Main scenario

In this section we will define how the physiochemical characteristics of the area shape the distribution of phytoplankton and how this is reflected in well defined zones within the study area.

Fyllas Bank stations corresponded to coastal water, largely composed of an intermediate between subpolar mode water flowing northwards and polar water originating from the Arctic Ocean and flowing south (Mortensen et al. 2011). In summer, increased ice melt and warming often influence these surface waters (Mortensen et al. 2011). Near the entrance of the fjord the water column was homogeneous, due to the constrained bathymetry and extensive tidal mixing. Overall, stratified surface waters were depleted in nutrients, except in areas with substantial vertical mixing, such as the sill and glacier region, where nutrient-rich subsurface waters are upwelled (Mortensen et al. 2011), replenishing nutrient concentrations. From the station furthest inside the fjord moving outward to the ocean, the surface nutrient concentration gradually decreased. This characteristic distribution of inorganic nutrients matches the distribution, community size-structure, and activity of phytoplankton; high concentrations of fast-growing large cells were found near the glacier and small, less-abundant cells in the mouth of the main fjord and the Kapisigdlit branch. Whether this distribution is a characteristic of the area or a particular condition cannot be concluded at the present time as there are no previous studies on the subject in this branch of the fjord. In the open waters of the Fyllas Bank the chl *a* was mostly found in the >10 µm size fraction. These results support the findings of Arendt et al. (2010) in the same area in May 2006. According to these authors, *Thalassiosira* spp. represented the bulk of net phytoplankton near the glacier, which was corroborated by our observations, whereas other centric diatoms and prymnesiophyte *Phaeocystis* spp. largely contributed to the total abundance of phytoplankton in the rest of the fjord and adjacent coastal areas.

The differences observed in water column characteristics, chl *a* concentration and size composition allow us to establish 4 main areas in the study region: the Fyllas Bank stations, those in the mouth and sill region, the stations near the glacier, and the stations in the Kapisigdlit branch. The main biological areas established in this study based on the distribution, biomass and size structure of the phytoplankton community add further detail to the major domains described in the area according the hydrographic characteristics (Mortensen et al. 2011, Tang et al.

2011). This biological zonation of the fjord, as well as the distribution of chl *a*, coincide with previous reports from the area (Arendt et al. 2010, Tang et al. 2011) and seem to be driven by the physical and chemical characteristics, mostly resulting from the interaction of the glacier water runoff with the circulatory patterns in the fjord (Mortensen et al. 2011). Nevertheless, some additional biological traits (e.g. grazing) may affect the structure of the community of producers.

Phytoplankton growth and mortality rates

Phytoplankton instantaneous growth rates (i.e. potential growth in the absence of grazing), even considering the *in situ* temperatures, are in the lower range of the average phytoplankton growth rates gathered by Calbet & Landry (2004) for polar (mostly Antarctic) areas. However, they are close to more recent estimates in different areas of the Arctic (Strom et al. 2007, Sherr et al. 2009, Calbet et al. 2011). When grazing is taken into account, the net phytoplankton growth rates in the unamended bottles (K_o) show a significant relationship with chl *a*. Such a relationship seems to indicate a continuous nutrient supply where algae developed in dense blooms (i.e. in the vicinities of the glacier). These blooms appear not to be nutrient limited, as deducted by the null phytoplankton growth enhancement shown for the areas with higher chl *a* concentrations (Fig. 6). However, away from the direct influence of the glacier the differences between the nutrient-amended bottles and the unamended ones became, although variable, very substantial (up to ca. 250%). Some of this variability is because small differences in very low rates (some close to zero) sometimes result in a huge proportional increase, which calls for some caution when drawing general conclusions from these data. Nevertheless, our results seem to consistently indicate that in summer the majority of the nutrients supplied by fjord circulation and melt water at the glacier area are taken up and few nutrients are exported out of the fjord. This is also corroborated by the vertical profile of inorganic nutrients (Fig. 3) and coincides with the findings of Arendt et al. (2010).

The question that remains to be answered, however, is whether the grazing by the microzooplankton can control the expansion of the phytoplankton bloom out of the fjord. The percentage of the potential primary production consumed per day indicates microzooplankton (dominated by large athecate dinoflagellates inside the fjord and by >40 µm ciliates in the Fyllas Bank stations; Arendt et al. 2010) are unable to cope with the fast growing and numerous diatom chains forming the major bloom. This indicates the minor influence that microzooplankton had on very large cells (mostly diatom chains) and agrees with findings from other Arctic semi-enclosed areas (Strom et al. 2007). Consequently, most of the autotrophic biomass produced in the vicinity of the glacier likely settled, in the absence of strong mesozooplankton grazing. This seems to be the case, as the estimated copepod grazing impact on the phytoplankton of the fjord is very low (Arendt et al. 2010, Tang et al. 2011). The only available microzooplankton grazing estimates in the area are those from Arendt et al. (2010), which were obtained by converting protozoan biomass into growth using temperature-related equations and then assuming a gross growth efficiency of 33% (Hansen et al. 1997). These data are likely to be overestimations, given the assumption of an entirely autotrophic ingestion. Nevertheless, their estimate for grazing in fjord waters (37% of the pPP consumed daily) is not far from our estimates (44%, average for all Godthåbsfjord stations). On the other hand, our limited sampling in the Fyllas Bank rendered quite contrasting results (from 0 to 110% of the pPP consumed daily) to the earlier study (20%), although obviously, given the variability of our results, within the range.

A remark on the methodology used

An important aspect of our methodology is the addition of not only dissolved inorganic nitrogen and phosphorus to the dilution series, but also dissolved silicate in the form of Na_2SiO_3. The dilution technique (Landry & Hassett 1982) relies on several assumptions. A very important one is that phytoplankton growth rates should be unaffected by the dilution. If nutrients are limiting phytoplankton growth, diluting the sample may result in a higher growth in the more diluted treatments. The common way to circumvent this is to add enough nutrients to guarantee that the growth of the algae is unaffected by dilution. This necessitates the addition of a control series without nutrient addition in order to estimate the actual phytoplankton instantaneous growth rates. However, in the majority of studies using this technique the nutrients added are phosphate, nitrate and sometimes ammonium; silicate is seldom added to the experimental bottles. This omission to the nutrient pool may result in an overestimation of mor-

tality rates in these systems dominated by diatoms and under dissolved silicate deplete conditions. If one nutrient is limiting, provided that direct uptake is faster and more efficient than the uptake of regenerated nutrients, the most diluted bottles will offer a richer environment for the less abundant cells. This implies that phytoplankton net growth rates in these bottles will be proportionally higher than in the bottles where the concentration of algae is larger and where the nutrients are depleted faster, leading to an increase in the slope of the regression equation between phytoplankton growth and dilution factor. Unfortunately, if this artefact occurs, it is difficult to detect and microzooplankton grazing rates will be overestimated. We therefore recommend the addition of silicate together with ammonium and phosphate to the dilution grazing experiments conducted in areas dominated by diatoms or in those where this nutrient may be limiting.

Conclusions

Overall, little of the PP generated near the glacier is exported out of the fjord. Whether this is a result of microzooplankton grazing activity in the fjord or sedimentation in the vicinity of the glacier remains to be determined. In any case, the grazing activity of the microzooplankton serves to retain the phytoplankton carbon in the surface layer rather than accelerate the vertical flux, as does grazing by mesozooplankton (Wassmann 1998). In the inner part of the fjord, where melt water from the glacier causes subglacial circulation (Mortensen et al. 2011) and upwelling of nutrient-rich waters in front of the glacier, the growth rate of the phytoplankton is much higher than the grazing capacity of the microzooplankton; however, as the water leaves the fjord the phytoplankton deplete the nutrients and the consumption from microzooplankton balances their production. Therefore, the phytoplankton production along the fjord waters seems to be retained in the system by microzooplankton, allowing little or no direct export production to the Fyllas Bank.

Acknowledgements. This research was funded by the project BOFYGO (from the board of the Danish Centre for Marine Research, DCH) and projects Oithogreen (CTM 2010-10036-E) and PROTOS (CTM2009-08783) (funded by the Ministry of Science and Innovation) assigned to T.G.N., E.S. and A.C., respectively. We thank the Greenland Climate Centre for support and logistics, and we are indebted to the captain and crew of the RV 'Dana' and to the colleagues on board for their invaluable help and support during the cruise. B. Søborg is thanked for excellent technical assistance. P. Munk provided Fig. 1. Finally, we thank 2 anonymous reviewers for their help and efforts in improving the manuscript.

LITERATURE CITED

Arendt KE, Nielsen TG, Rysgaard S, Tönnesson K (2010) Differences in plankton community structure along the Godthåbsfjord, from the Greenland Ice Sheet to offshore waters. Mar Ecol Prog Ser 401:49–62

Bainbridge V, McKay BJ (1968) The feeding of cod and redfish larvae. ICNAF Spec Publ 7:187–217

Barthel KG (1988) Feeding of three *Calanus* species on different phytoplankton assemblages in the Greenland Sea. Meeresforsch Rep Mar Res 32:92–106

Calbet A (2008) The trophic roles of microzooplankton in marine systems. ICES J Mar Sci 65:325–331

Calbet A, Landry MR (2004) Phytoplankton growth, microzooplankton grazing, and carbon cycling in marine systems. Limnol Oceanogr 49:51–57

Calbet A, Saiz E, Almeda R, Movilla JI, Alcaraz M (2011) Low microzooplankton grazing rates in the Arctic Ocean during a *Phaeocystis pouchetii* bloom (Summer 2007): fact or artifact of the dilution technique? J Plankton Res 33:687–701

Cavalieri DJ, Parkinson CL, Vinnikov KY (2003) 30-Year satellite record reveals contrasting Arctic and Antarctic decadal sea ice variability. Geophys Res Lett 30, 1970, doi: 10.1029/2003GL018031

Dortch Q, Thompson PA, Harrison PJ (1991) Short-term interaction between nitrate and ammonium uptake in *Thalassiosira pseudonana*: effect of preconditioning nitrogen source and growth rate. Mar Biol 110:183–193

Gallegos CL (1989) Microzooplanton grazing on phytoplankton in the Rhode River, Maryland: nonlinear feeding kinetics. Mar Ecol Prog Ser 57:23–33

Hansen HP, Koroleff F (1999) Determination of nutrients. In: Grasshoff K, Kremling K, Ehrhardt M (eds) Methods of seawater analysis, 3rd edn. Wiley-VCH, Weinheim, p 159–228

Hansen PJ, Bjørnsen PK, Hansen BW (1997) Zooplankton grazing and growth: scaling within the 2-2,000-µm body size range. Limnol Oceanogr 42:687–704

Jespersen AM, Christoffersen K (1987) Measurements of chlorophyll-*a* from phytoplankton using ethanol as extraction solvent. Arch Hydrobiol 109:445–454

Johannessen OM, Bengtsson L, Miles MW, Kuzmina SI and others (2004) Arctic climate change: observed and modelled temperature and sea-ice variability. Tellus A 56: 328–341

Landry MR, Calbet A (2004) Microzooplankton production in the oceans. ICES J Mar Sci 61:501–507

Landry MR, Hassett RP (1982) Estimating the grazing impact of marine micro-zooplankton. Mar Biol 67: 283–288

Landry MR, Constantinou J, Latasa M, Brown SL, Bidigare RR, Ondrusek ME (2000) Biological response to iron fertilization in the eastern equatorial Pacific (IronEx II). III. Dynamics of phytoplankton growth and microzooplankton grazing. Mar Ecol Prog Ser 201:57–72

Levinsen H, Nielsen TG (2002) The trophic role of marine pelagic ciliates and heterotrophic dinoflagellates in arctic and temperate coastal ecosystems: a cross-latitude

comparison. Limnol Oceanogr 47:427–439
Levinsen H, Nielsen TG, Hansen BW (2000a) Annual succession of marine pelagic protozoans in Disko Bay, West Greenland, with emphasis on winter dynamics. Mar Ecol Prog Ser 206:119–134
Levinsen H, Turner JT, Nielsen TG, Hansen BW (2000b) On the trophic coupling between protists and copepods in arctic marine ecosystems. Mar Ecol Prog Ser 204:65–77
Menden-Deuer S, Lessard EJ (2000) Carbon to volume relationships for dinoflagellates, diatoms, and other protist plankton. Limnol Oceanogr 45:569–579
Mortensen J, Lennert K, Bendtsen J, Rysgaard S (2011) Heat sources for glacial melt in a sub-Arctic fjord (Godthåbsfjord) in contact with the Greenland Ice Sheet. J Geophys Res 116, C01013, doi:10.1029/2010JC006528
Munk P, Hansen BW, Nielsen TG, Thomsen HA (2003) Changes in plankton and fish larvae communities across hydrographic fronts off West Greenland. J Plankton Res 25:815–830
Pedersen SA, Ribergaard MH, Simonsen CS (2005) Micro- and mesozooplankton in Southwest Greenland waters in relation to environmental factors. J Mar Syst 56:85–112
Poulsen LK, Reuss N (2002) The plankton community on Sukkertop and Fylla Banks off West Greenland during a spring bloom and post-bloom period: hydrography, phytoplankton and protozooplankton. Ophelia 56:69–85
Saiz E, Calbet A (2011) Copepod feeding in the ocean: scaling patterns, composition of their diet and the bias of estimates due to microzooplankton grazing during incubations. Hydrobiologia 666:181–196
Sherr EB, Sherr BF (2002) Significance of predation by protists in aquatic microbial food webs. Antonie van Leeuwenhoek 81:293–308
Sherr EB, Sherr BF, Hartz AJ (2009) Microzooplankton grazing impact in the Western Arctic Ocean. Deep-Sea Res II 56:1264–1273
Simonsen CS, Munk P, Folkvord A, Pedersen SA (2006) Feeding ecology of Greenland halibut and sandeel larvae off West Greenland. Mar Biol 149:937–952
Smetacek V, Nicol S (2005) Polar ocean ecosystems in a changing world. Nature 437:362–368
Storr-Paulsen M, Wieland K, Hovgård H, Rätz H (2004) Stock structure of Atlantic cod (*Gadus morhua*) in West Greenland waters: implications of transport and migration. ICES J Mar Sci 61:972–982
Strom SL, Macri EL, Olson MB (2007) Microzooplankton grazing in the coastal Gulf of Alaska: variations in top-down control of phytoplankton. Limnol Oceanogr 52: 1480–1494
Tang KW, Nielsen TG, Munk P, Mortensen J and others (2011) Metazooplankton community structure, feeding rate estimates, and hydrography in a meltwater-influenced Greenlandic fjord. Mar Ecol Prog Ser 434:77–90
Throndsen J (1978). Preservation and storage. In: Sournia A (ed) Phytoplankton manual. UNESCO, Paris, p 69–74
Wassmann P (1998) Retention versus export food chains: processes controlling sinking loss from marine pelagic systems. Hydrobiologia 363:29–57

Editorial responsibility: Matthias Seaman, Oldendorf/Luhe, Germany

Submitted: May 9, 2011; Accepted: August 12, 2011
Proofs received from author(s): November 11, 2011